Title
Identification and characterization of genes involved in Arabidopsis thaliana cell wall acetylation

Author
de Souza, Amancio Jose

Publication Date
2014

Peer reviewed|Thesis/dissertation

Identification and characterization of genes involved in *Arabidopsis thaliana* cell wall acetylation

By

Amancio José de Souza

A dissertation submitted in partial satisfaction of the

requirements for the degree of

Doctor of Philosophy

in

Plant Biology

in the

Graduate Division

of the

University of California, Berkeley

Committee in charge:

Professor Markus Pauly, Chair
Professor Chris R. Somerville
Professor Jamie H. D. Cate

Fall 2014

Abstract

Identification and characterization of genes involved in *Arabidopsis thaliana* cell wall acetylation

by

Amancio José de Souza

Doctor of Philosophy in Plant Biology

University of California, Berkeley

Professor Markus Pauly, Chair

Most non-cellulosic plant cell wall polysaccharides including the hemicellulose xyloglucan and the pectic polysaccharides can be *O*-acetylated. This feature has direct significance in the use of these polymers in the food and biofuel industry. For example, increased pectin acetylation can reduce its gelling abilities and is hence detrimental in its application as a food thickener or emulsifier. In general, plant biomass with wall polymers with high acetate content can negatively influence biomass hydrolysis by fungal enzymes and interfere with downstream fermentation by yeasts.
Genetic and biochemical approaches were used to identify genes involved in wall polymer acetylation in the model species *Arabidopsis*. A forward genetics approach was able to identify wall acetylation differences within a population of *Arabidopsis* ecotypes in both total wall acetate and xyloglucan *O*-acetylation. One of these naturally occurring mutant alleles of a recently identified putative xyloglucan acetyltransferase (AXY4) was found in the Ty-0 ecotype. Ty-0 completely lacks xyloglucan acetyl-substituents in roots and leaves, suggesting that the lack of XyG acetylation does not compromise the fitness of the ecotype in its ecological niche. In an attempt to further characterize the AXY4 protein, and characterize peptide domains involved in cell wall polymer recognition, a functional domain swap approach was utilized without success. A biochemical approach to identify and purify a putative xyloglucan acetylesterase was attempted also without success. Another way to modulate wall acetylation is by apoplastic plant acetylesterases, which naturally remove acetyl-substituents on polymers. To characterize genes in the Pectin acetyl esterase gene family in *Arabidopsis thaliana*, reverse genetics was used and lead to the identification of two genes responsible for altering wall acetate levels of pectins. Further pectin fractionation experiments suggest that PAE8 and PAE9 act predominantly but distinctively on pectic rhamnogalacturonan I. Pectin acetylesterase activity was demonstrated *in vitro* for the proteins encoded by *PAE8* and *PAE9*. Through genetic means it is possible to increase wall acetate content, but this modification lead to a reduction in *Arabidopsis* inflorescence size giving insights about the function of acetylation of pectins.

Dedication

This work is dedicated to my wife Tais Nayanne da Costa Abreu who has endured with me all of the challenges during this journey, supporting me in the hardest times and sharing the good times. Thank you for being my partner and friend. I love you.

Table of Contents

List of abbreviations

A	deoxyadenosine monophosphate / Alanine
A. thaliana	*Arabidopsis thaliana*
A. tumefaciens	*Agrobacterium tumefaciens*
Ac	acetyl
acetyl-CoA	acetyl-coenzyme A
ASP	Aspartic acid
AXY	altered xyloglucan
bp	base pair
C	deoxycytosine monophosphate / Cysteine
cDNA	complementary deoxyribonucleic acid
CSLC	cellulose synthase like class C
CTAB	cetyltrimethylammonium bromide
dCAPS	derived cleaved amplified polymorphic sequence
D	Aspartic acid
DHB	2,5-dihydroxybenzoic acid
DNA	deoxyribonucleic acid
E	Glumatic acid
E. coli	*Escherichia coli*
EDTA	Ethylenediaminetetraacetic acid
F	Phenylalanine
Fuc	fucose
g	gram
g	gravity
G	deoxyguanosine monophosphate / Glycine
Gal	galactose
GalA	galacturonic acid
GFP	green fluorescent protein
GH	glycosyl hydrolase
Glc	glucose
GlcA	glucuronic acid
Glu	Glutamic acid
Gly	Glycine
GT	glycosyltransferase
H	Histidine
H_2O	water
HCl	hydrochloric acid
HPAEC-PAD	high-performance anion exchange chromatograph with pulsed amperometric detection
I	Isoleucine
IRX	irregular xylem
K	Lysine
kb	kilobase pairs
kDa	kilodalton

KOH	potassium hydroxide
L	Lysine
Lys	Lysine
LB	lysogeny broth
M	Methionine
m / z	mass to charge ratio
MALDI-TOF	matrix assisted laser desorption ionization time of flight
Man	mannose
Mb	megabase pairs
MES	4-Morpholineethanesulfonic acid
min	minute
mL	milliliter
MS	Murashige and Skoog
N	Asparagine
n	number of replicates / sample size
N. benthamiana	*Nicotiana benthamiana*
n.d.	not determined
NaOH	sodium hydroxide
nasturtium	*Tropaeolum majus*
nd	not detected
OD	optical density
OLIMP	oligosaccharide mass profiling
P	Proline
PCR	polymerase chain reaction
Q	Glutamine
Q RT PCR	quantitative reverse transcription polymerase chain reaction
R	Arginine
Rha	rhamnose
RNA	ribonucleic acid
S	Serine
SNP	single nucleotide polymorphism
T	Threonine
TAE	tris, acetic acid and EDTA
T-DNA	transfer DNA
TE	tris EDTA
U	unit
V	Valine
W	Tryptophan
WT	wild type
XEG	xyloglucan specific endoglucanase
XyG	xyloglucan
Xyl	xylose
Y	Tyrosine

List of figures

List of tables

1.0 Introduction

1.1 Plant cell walls

Plant cell walls have played a critical role in human development. Fire, a fundamental part of the human ability to survive in nature during the beginning of civilization was in great part fueled by carbon from plant walls. The construction of shelter in many societies has relied on wood, which is primarily constituted of cell walls. Cell wall based cotton fibers and wood pulp have been a major part of how we dress and register our knowledge. Recently, plant biomass has again been considered as one of the solutions for the growing demand for liquid fuels (Carroll and Somerville 2009). This has been particularly attractive since the carbon in this fuel source originates from the atmosphere and not from fossil carbon reserves, whose burning has been implicated in global warming (Carroll and Somerville 2009; Cox et al. 2000).

Plant cell walls were one of the first cellular structures to be observed under a microscope and provided the basis for coining the term “cell” (Hooke 1665). Many of the first studies investigating plant tissues relied on microscopy and different staining properties pertaining to different types of walls. It is known today that the differential staining of different cell wall types are based on their difference in composition (Obrien et al. 1964; Soukup 2014; Western et al. 2000), hinting that this cellular structure was more than just an inert deposit of carbon rich molecules.

The plant cell wall provides a protective outer cell layer that shapes the plant cell (Cosgrove 2005). It participates in cell-to-cell communication by producing signaling molecules (Darvill et al. 1992), and it can be a stored source of carbon energy for the developing seed of many species (Buckeridge et al. 2000).

Cell walls have been subdivided into middle lamella, and primary and secondary walls (Carpita and Gibeaut 1993). The middle lamella is rich in pectic polymers and resides between two primary walls of adjacent cells (Knox et al. 1990; Varner and Lin 1989). This structure is thought to be responsible for cell to cell adhesion. The primary wall is present in the expanding cell and can be subdivided into type I and type II (Carpita and Gibeaut 1993). Type I primary cell walls are present in dicots and non-graminaceous monocots and are enriched in pectins, the hemicellulose xyloglucan, structural proteins and cellulose (Carpita and Gibeaut 1993). In contrast, Type II primary walls, present in grasses, have less pectin and are enriched in the hemicellulose glucurono-arabinoxylan (Carpita and Gibeaut 1993). After the plant cell has ceased to expand it may synthesize a secondary wall, which consists of large amounts of crystalline cellulose, hemicellulose and lignin (Carpita and McCann 2000). These modifications impart rigidity and hydrophobicity to the wall and are often found in the vasculature and in structural tissues (Albersheim et al. 2011).

Cell wall biosynthesis takes place in distinct cellular compartments. Cellulose is synthesized at the plasma membrane (1.2), lignin monomers are synthesized in the cytosol and polymerized in the apoplast, while pectins and hemicelluloses are synthesized in the Golgi apparatus and delivered to the apoplast via exocytosis. Evidence for Golgi wall biosynthesis is provided by microscopical studies that used immunolabelling to identify hemicellulosic and pectic polymers within Golgi structures (Zhang and Staehelin 1992) as well as studies showing that isolated Golgi enriched

vesicles (microsomes) contain wall polymers (Gunl et al. 2011; Pauly and Scheller 2000). A large number of genes have been implicated in the polysaccharide biosynthesis in the Golgi and many others are involved in editing these polymers once deposited in the wall. Classes of enzymes involved in pectin and hemicellulose biosynthesis in the cell include glycosyl transferases, nucleotide sugar transporters, sugar nucleotide epimerases and isomerases, phosphatases, pyrophosphorylases, reductases and mutases (Pauly et al. 2013; Seifert 2004). Once these polymers are exported to the wall a new suite of proteins are present in the apoplast that act by editing these polymers. These proteins include glycosylhydrolases (Gunl et al. 2011; Gunl and Pauly 2011; Sampedro et al. 2012; Sampedro et al. 2001), carbohydrate esterases (Breton et al. 1996; Gou et al. 2012; Orfila et al. 2012) and endo-transglycosylases (Cosgrove 2005; Nishitani and Tominaga 1992). The polymer modifications made in the apoplast can be extensive, characterizing this cellular compartment as a highly dynamic one.

1.2 Biosynthesis and structural components of the plant cell wall

Cellulose is the dominant sugar polymer present in plant walls (Somerville 2006; Somerville et al. 2004). Second to cellulose are the hemicelluloses and pectic polymers which vary in their abundance and composition. Types of hemicelluloses identified to date include: xyloglucan, heteroxylan, heteromannans and mixed-linkage glucans (Pauly et al. 2013). Amongst the pectic polymers the following are present in the plant wall: homogalacturonan (HG), rhamnogalacturonan I (RGI), rhamnogalacturonan II (RGII); xylogalacturonan; and apiogalacturonan (Atmodjo et al. 2013; Harholt et al. 2010). Proteins also play a structural role in the wall and these include several classes, namely: arabinogalactan proteins (AGPs), hydroxyproline-rich glycoproteins (HRGPs), proline-rich proteins (PRPs) and glycine-rich proteins [GRPs; (Albersheim et al. 2011)]. Lignin is composed primarily of polyphenolic units including p-hydroxyphenyl, guaiacyl and syringyl-units (Boerjan et al. 2003)].

One of the dominant features of land plants is the formation of a cellulose microfibril (Graham et al. 2000). Cellulose is considered to be the most abundant polymer on Earth with an estimated 180 billion tons produced every year (Delmer 1999). It is made at the plasma membrane by large protein complexes termed rosettes. These structures synthesize individual chains of β-1,4-linked D-glucose from UDP-glucose, which are assembled into a larger crystalline structure, the microfibril (Mueller and Brown 1980; Somerville 2006). The microfibrils are composed of varying numbers of glucan chains (18-36), and these structures represent the major scaffolding structure of the wall (Albersheim et al. 2011; Ha et al. 1998; Herth 1983; Somerville 2006). The cellulose synthesizing genes in plants have been termed *CESA* and it has been shown that primary and secondary wall rosettes are composed by different but homologous proteins (Albersheim et al. 2011; Persson et al. 2007b; Taylor et al. 2003). In Arabidopsis three different *CESA* genes compose a rosette complex: *CESA1*, *CESA3* and *CESA6* in the primary wall (Persson et al. 2007b) and *CESA4*, *CESA7*, and *CESA8* in the secondary wall (Albersheim et al. 2011; Persson et al. 2007b; Taylor et al. 2003). Several other genes and gene families have been implicated in participating in cellulose synthesis including *KORRIGAN* (Nicol et al. 1998), *COBRA* (Roudier et al. 2005),

COBRA-LIKE (Dai et al. 2011; Liu et al. 2013) and *KOBITO* (Pagant et al. 2002). The precise role of these genes in the synthesis processes has yet to be determined.

Lignin is a polyphenolic component of the wall (Albersheim et al. 2011; Vanholme et al. 2010). It is usually deposited in the secondary wall to confer rigidity and water proof the structure. Without lignin plants would not be able to transport water from root to leaf in xylem vessels, which have to tolerate high negative water pressures (Sperry 2003). Monolignols are the subunits of lignin (Boerjan et al. 2003). These precursors are synthesized in the cytoplasm from phenylalanine via a well characterized biochemical pathway, the phenylpropanoid pathway (Boerjan et al. 2003; Vanholme et al. 2010). These molecules are transported to the wall through the plasma membrane in an ATP dependent manner (Miao and Liu 2010). Recently, an *Arabidopsis* monolignol transporter was identified advancing our knowledge of the lignin subunit transport process (Alejandro et al. 2012). Once in the wall the monolignols are oxidized to radicals by laccases and/or peroxidases (Ostergaard et al. 2000; Sterjiades et al. 1992), before they polymerize through a random non-enzymatic chemical process creating a large hydrophobic lignin complexes (Boerjan et al. 2003). Plants with reduced amounts of lignin or altered lignin structures have been produced from mutations in monolignol biosynthetic genes (Van Acker et al. 2014; Vignols et al. 1995). Reduction of lignin content and alteration of its chemical structure in walls has been associated with increased wall saccharification, a desirable trait in the production of liquid fuels from biomass (Anderson et al. 2012; Van Acker et al. 2014; Wilkerson et al. 2014).

The wall also contains proteins that play a structural role. These proteins are grouped into four distinct classes: AGPs, HRGPs, PRPs and GRPs (Carpita and McCann 2000). AGPs are highly glycosylated with arabinan and galactan side chains (up to 25 kDa), which constitute 90-99% of their mass (Albersheim et al. 2011; Seifert and Roberts 2007). These proteins are involved in cell division (Langan and Nothnagel 1997), apoptosis, and embryo development (van Hengel et al. 2001). Extensins are structural proteins, which belong to the HRGP group. These proteins can be mono- to tetra-arabinosylated (hydroxyproline) and mono-galactosylated (serine) in their amino acid repeat motif [Ser(Hyp)$_4$; (SommerKnudsen et al. 1997; Tierney and Varner 1987)]. Once deposited in the wall as monomers these proteins are crosslinked via isodityrosine ether bonds to form the extensin network (Albersheim et al. 2011; Cooper and Varner 1984). This network is thought to play a role in cell extension (Gille et al. 2009; Carpita and McCann 2000). GRPs have large stretches of glycine residues, which are thought to confer a β-pleated sheet structure to the protein (Condit and Meagher 1986; Keller 1993). GRPs can be found in vascular bundle walls and in the mucilage of root caps (Matsuyama et al. 1999; Ryser et al. 1997). PRPs are thought to act like extensins (HRGPs) contributing to a peroxide-mediated crosslinked network implicated in pathogen defense (Albersheim et al. 2011; Cassab 1998). Structural wall proteins are thought to share a common evolutionary origin based on their codon structure (Keller 1993; Showalter 1993).

Another major group of polymers present in the wall are the hemicelluloses This class of molecules can represent one third of the wall biomass (Albersheim et al. 2011). One of their major features is a backbone composed of the β-1,4 glycosidic bonds (Pauly et al. 2013). In contrast to cellulose these polymers are decorated with side chains that render them amorphous and soluble (Carpita and McCann 2000).

Hemicelluloses can be grouped into xyloglucans, heteroxylans, heteromannans, and mixed-linkage glucans (Pauly et al. 2013). There is ample diversity in structure amongst these groups of polymers, varying in tissue types (Gille et al. 2011b) and in plant species (Albersheim et al. 2011; Pauly et al. 2013; Schultink et al. 2013). Some of the more common structures are presented in Figure 1.2-1 and Figure 1.3-1.

Xylans are particularly abundant in secondary cell walls of dicots and constitute the major hemicellulose in all commelinoid monocot walls (Carpita and Gibeaut 1993). Plants with aberrant xylan structures often harbor irregular xylem (IRX) and dwarfed phenotypes, as is the case for many of the IRX mutants identified (Brown et al. 2007; Brown et al. 2009; Lee et al. 2007a; Lee et al. 2007b). Heteroxylans have a backbone of β-1,4 linked xylosyl residues, which can be substituted with (methyl-)glucuronic acid and arabinose (Figure 1.2-1). Features of the heteroxylan sidechains include: arabinosylation of the backbone at C-3 (Anders et al. 2012); methylation of the glucuronic acid at O-4 (Urbanowicz et al. 2012); xylose substitution of the α-1,3 arabinose side chains at C-2 (Chiniquy et al. 2012), acetylation of the xylose backbone at O-2 and/or O-3 (Xiong et al. 2013); feruloylation of the α-1,3 arabinose side chains residue (Faik 2010).

Mannans have been found in some algal cell walls and are thought to represent the most ancient hemicellulose (Domozych et al. 2012). These polymers are found in the secondary cell walls of dicots (Rodriguez-Gacio et al. 2012; Scheller and Ulvskov 2010), can be utilized as storage polymers in some species (Buckeridge 2010; Rodriguez-Gacio et al. 2012) and are abundant in the secondary walls of gymnosperms (Pauly and Keegstra 2008). Heteromannans can be subdivided in four groups: mannan, galactomannan, glucomannan and glucogalactomannan (Pauly et al. 2013; Scheller and Ulvskov 2010). Mannans and galactomannans have a backbone consisting of β-1,4 linked mannose while glucomannans also contain β-1,4 glucose interdispersed in its backbone (Figure 1.2-1). The *CSLA* (Dhugga et al. 2004; Gille et al. 2011a; Goubet et al. 2009; Liepman et al. 2005; Suzuki et al. 2006) and *CSLD* (Verhertbruggen et al. 2011) gene families in *Arabidopsis* are involved in the synthesis of the mannan backbone. A galactosyltransferase activity responsible for the galactosylation of mannan has been demonstrated in *Trigonella foenum-graecum* (Edwards et al. 1999). Another protein from *Trigonella foenum-graecum* and *Arabidopsis*, denominated MSR, has been implicated in mannan biosynthesis. However, its biochemical activity remains undetermined (Wang et al. 2012; Wang et al. 2013). Recently, *TBL25* and *TBL26* in *Arabidopsis* have been proposed to act as mannan acetyltransferases. This hypothesis has been put forward based on the identification of a TBL ortholog expressed in the developing corm of voodoo lily (*Amorphophallus konjac*), which deposits massive amounts of acetylated glucomannan as a storage polymer (Gille et al. 2011a).

In higher plants mixed linkage glucans (MLG) are only found in the walls of the order Poales (Sorensen et al. 2008). This polymer has also been identified in some algal species (Popper et al. 2011), in some ancient plant lineages such as bryophytes [liverworts; (Popper and Fry 2003)] and in the genus *Equisetum*. In grasses it can be highly abundant in young tissues like coleoptiles (Carpita 1996) and in the endosperm (Pauly et al. 2013) being rapidly degraded by licheninases during development (Kim et al. 2000; Pauly et al. 2013). For this reason it has been proposed that MLGs could have a role as a storage polysaccharide. Some of the MLG remains in the wall throughout the

plant life cycle which could also suggest a role as structural polymer (Gibeaut et al. 2005). MLGs are composed of β-1,3-linked cellotriosyl and cellotetraosyl subunits. This general structure can vary according to plant species; mixed linkage glucans with different ratios of cellotriosyl and cellotetraosyl subunits as well polymers containing subunits varying in their degree of polymerization from 2-12 glucoses have been described (Meikle et al. 1994; Pauly et al. 2013). Genes from the CSLF and H families have been implicated in MLG biosynthesis. Rice [CSLF; (Burton et al. 2006)] and barley [CSLH; (Doblin et al. 2009)] cDNAs, when expressed in *Arabidopsis*, are sufficient to produce MLGs, which were detected using antibodies against the polymer. Based on biochemical evidence MLGs are believed to be synthesized in the Golgi apparatus (Gibeaut et al. 2005; Pauly et al. 2013).

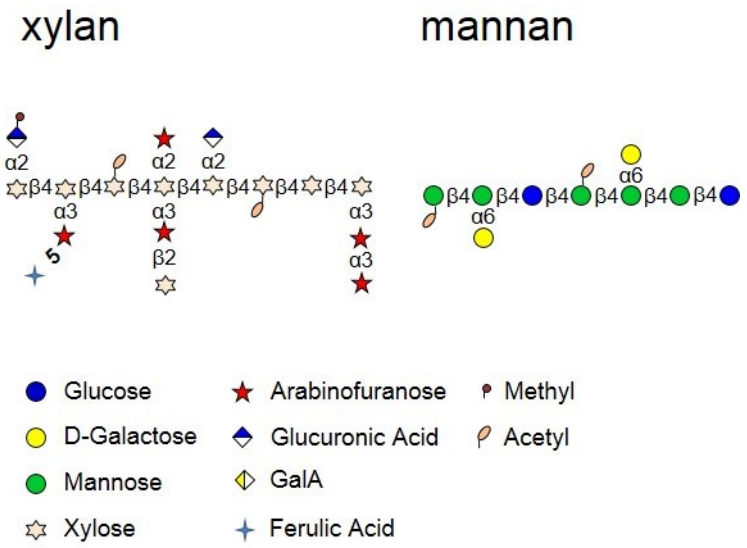

Figure 1.2-1. Heteroxylan and heteromannan polysaccharide structures. Representative structures from glucuronoarabinoxylan and galactoglucomannan, linkage is indicated between sugar residues. Hemicellulose structures reprinted with modifications from Pauly et. al. (2013).

1.3 Xyloglucan – function, structure, biosynthesis, metabolism, and applications

Xyloglucan (XyG) has been one of the most extensively studied wall polymers. It is abundant in the primary walls constituting up to 30% of its mass (Pauly et al. 2013; Scheller and Ulvskov 2010). XyGs are also used by some plant species such as Nasturtium (*Tropaeolum majus L.*) as a storage polysaccharide (Edwards et al. 1988; Meier and Reid 1982). XyG crosslinks cellulose microfibrils via hydrogen bonds in the primary wall (Carpita and Gibeaut 1993; Hayashi et al. 1994; Pauly et al. 1999a; Somerville et al. 2004). These interactions were believed to maintain the structural integrity and rigidity of the wall (Hayashi 1989) and XyG metabolism has been thought for many years to be a key element for wall extension (Nishitani 1998). This role was supported by the discovery of enzymes, which could promote cell elongation such as expansins, which have been suggested to disrupt the hydrogen bonds between XyG and cellulose causing the polymers to slide and hence promote cell elongation (Cosgrove 1998). Other enzymes capable of modifying the XyG structure *in muro* such as endo-transglycosylases also lent support to these ideas (Nishitani and Tominaga 1992; Smith and Fry 1991). In agreement with these hypotheses is the proposed role for XyG as a spacer between cellulose microfibrils, which would reduce the friction between these structures during cell elongation (Mccann et al. 1990). Recently however, the view that XyG is a critical player in wall structure and dynamics has been challenged. The discovery of mutant plants that lack detectable XyG due to mutations in key biosynthetic genes, but have close to normal plant growth and development has promoted a paradigm shift (Cavalier et al. 2008) reducing the importance of XyG in cell wall biology. In a recently revised model for the role of XyG in the primary cell wall architecture the

polymer can act as a strengthening agent together with pectins and arabinoxylans and it contributes to cell elongation facilitating growth through the action of expansins (Park and Cosgrove 2012). However, its role as a spacer between microfibrils remains challenged based on the observation that mutant cell walls that lack detectable XyG are not less extensible (Cavalier et al. 2008; Park and Cosgrove 2012).

XyG has also been implicated in growth regulation by functioning as a source of physiologically active oligosaccharides termed oligosaccharins (Darvill et al. 1992). XyG oligosaccharides containing fucose have been shown to inhibit auxin induced elongation of pea stems (York et al. 1984). In contrast, the opposite effect can be achieved when present at higher concentrations (McDougall and Fry 1990). XyG polysaccharides incorporated into the wall by endotransglycosylases have been shown to suppress cell elongation (Takeda et al. 2002). In contrast, addition of XyGOs can accelerate cell elongation (Takeda et al. 2002). These observations have substantiated the notion that this polymer is involved in fundamental cellular extension processes even though the exact mechanism remains elusive.

XyG is a highly branched polysaccharide composed primarily, in most dicots, of the sugars glucose, xylose, galactose), and fucose. As a hemicellulosic polysaccharide it has a β-1,4-linked D-glucopyranosyl backbone (Fry et al. 1993; Pauly et al. 2013). The backbone is decorated with xylosyl residues at the O-6 position; the xylosyl residue can contain a galactose substitution at O-2, which can be further substituted with a fucose at O-2 (Scheller and Ulvskov 2010). The galactose in XyG can be mono- or di-acetylated at position 2, 3 or 6. However, position 6 seems to be the predominant position of the acetyl group (Kiefer et al. 1989). This overall structure of a common oligosaccharide found in dicots containing fucogalactoxyloglucan can be seen in Figure 1.3-1 A. A nomenclature for XyG structures has been developed to standardize the description of these molecules [Figure 1.3-1 B; (Fry et al. 1993)]. To date 18 different side chain structures have been assigned to a one-letter code (Fry et al. 1993; Pauly et al. 2013; Schultink 2013). XyG present in most dicots and non-graminaceous monocots are described as the XXXG type (Pauly et al. 2013). XyG structures can vary among plant tissues and among plant species (Gille et al. 2011b; Schultink et al. 2013).

In the families poaceae (Kato et al. 2004) and solanaceae (Jia et al. 2003), as well as in some ancient plant lineages like mosses, lycophytes and liverwarts (Pena et al. 2008) XyG structures are usually described as the XXGG type and are often referred to as arabinogalactanxyloglucan (Pauly et al. 2013). In this type of XyG, xylose residues can be further substituted at O-2 with arabinofuranosyl residues (Schultink et al. 2013) and fucosyl-residues are not present (Pauly et al. 2013). The XXGG type xyloglucan can harbor acetate groups on their backbone glucosyl residues (Pauly et al. 2013).

The main genes involved in fucogalactoxyloglucan biosynthesis have been identified and characterized (Figure 1.3-1 C). The first biosynthetic gene involved in XyG biosynthesis was the XyG: fucosyltransferase. A biochemical approach was used to isolate a protein with that activity followed by sequencing for gene determination [*AtFUT1*; (Perrin et al. 1999)]. The same gene (*MUR2/AtFUT1*) was later identified in a forward genetics mutant screen, which identified mutants with altered monosaccharide composition, in the case of *mur2* a deficiency in fucose (Reiter et al. 1997; Vanzin et al. 2002). The identification of the XyG: galactosyltransferase MUR3 also arose from the same screen (Reiter et al. 1997). Utilizing pea microsomes an α-xylosyl transferase

activity towards cellooligosaccharides was established leading to the identification of the *XXT* genes in *Arabidopsis*, now established as XyG: xylosyltransferases (Faik et al. 2002). A XyG: galacturonosyltransferase (XUT1) has been identified using a reverse genetics approach and it was shown to act specifically in *Arabidopsis* root hair tissue (Pena et al. 2012). A functional complementation approach was recently used to characterize two tomato arabinosyltransferases (XST1 and XST2) members of the GT 47 family (Schultink et al. 2013). The characterization of the XyG backbone synthase (CSLC4) was achieved via a transcriptomics approach coupled to biochemical characterization and implicated genes in the CSLC family in *Arabidopsis* (Cocuron et al. 2007). Recently, two putative XyG: acetyltransferases have been identified via a combined forward and reverse genetics approach, which revealed mutants altered in XyG structure (Gille et al. 2011b). *AXY4* and *AXY4L,* when knocked out, result in complete loss of XyG acetylation in tissues, in which they are expressed (Gille et al. 2011b). AX4L acts only in seeds, while AXY4 is responsible for XyG acetylation in vegetative and root tissue (Gille et al. 2011b).

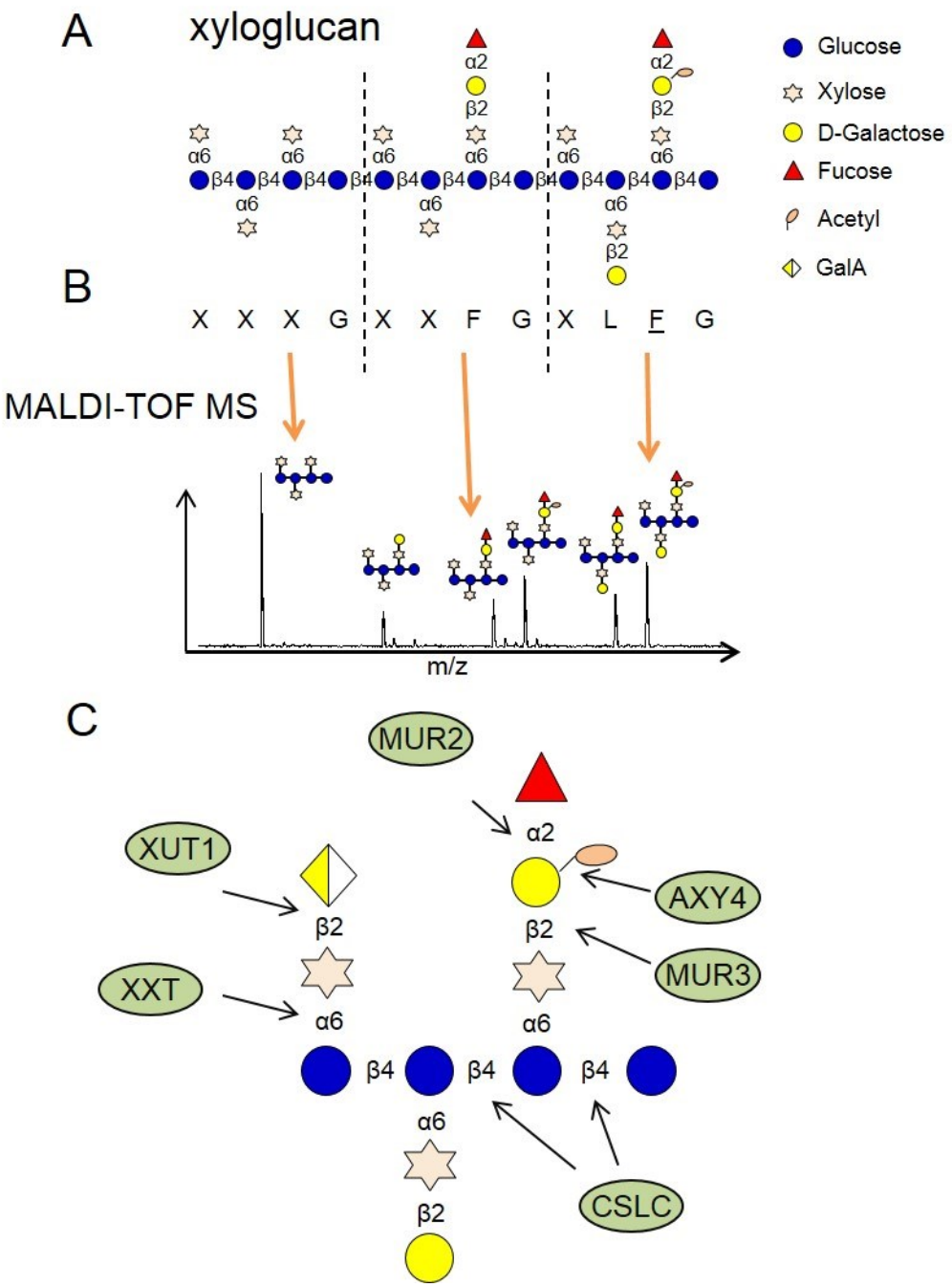

Figure 1.3-1 XyG structures and genes involved in its biosynthesis. A) Representative XyG structure with glycosidic linkages highlighted between sugar residues (Pauly et. al. 2013. B) Schematic representation of XyG oligosaccharide mass profiling: letters below XyG structure indicate one-letter code nomenclature to describe the polymer side chains (Fry et al. 1993). Dashed lines indicate sites for XyG specific endoglucanase cleavage to generate XyG oligosaccharides (Lerouxel et al. 2002). MALDI-TOF mass spectrum with distinct ion-signals representing XyG oligosaccharides released by a xyloglucan specific endoglucanase. Orange arrows point toward the different structures within the spectrum. C) Genes or groups of genes involved in the biosynthesis of XyG are indicated within the green circles. (Schultink (2013).

After being deposited in the wall XyG can be modified by apoplastic enzymes. The XTHs or XyG transglycosylase / hydrolases play key roles in this polymer editing. These enzymes are able to hydrolyze and/or re-attach XyGs to existing molecules in the wall and in this manner contribute to incorporation of polymers into the existing composite structure, rearrangements of the XyG network and/or mobilization of storage forms of XyG (Nishitani and Tominaga 1992; Pauly et al. 2013; Smith and Fry 1991; Takeda et al. 2002). In species that use XyG as a storage polymer XTHs are highly active during germination presumably channeling sugars present in XyG into catabolic cell metabolism (de Silva et al. 1993; Fanutti et al. 1993). Many apoplastic hydrolases acting on XyG have been identified. A biochemical approach was used to characterize a XyG: xylosidase [*At*XYL1/ AXY3; (Gunl and Pauly 2011; Obel et al. 2006; Sampedro et al. 2001)]. Mutations in *AtXYL1* produced plants with shorter siliques suggesting a role of the xylosidase in proper organ formation in *Arabidopsis* (Gunl and Pauly 2011). *Axy8*, a mutant exhibiting an increase in XyG fucosylation and decrease in XyG galactosylation, is impaired in a fucosidase involved in XyG turnover (Gunl et al. 2011). A reverse genetics approach coupled to biochemical characterization identified the *BGal10* gene as one of the main galactosidases acting on XyGs. Plants deficient in this protein were found to have growth defects in silliques and flowers (Sampedro et al. 2012). The plant phenotypes produced by mutant hydrolases demonstrate the extensive remodeling undertaken by XyG in the apoplast. To date no apoplastic XyG acetylesterase has been identified, however the variation in tissue acetate levels as well as the observation that overexpression of the AXY4 putative XyG acetyltransferase does not lead to complete XyG acetylation suggests that this activity could exist (Gille et al. 2011b).

The study of XyG has benefited enormously by the identification of polysaccharide specific hydrolytic enzymes. These enzymes have been used in combination with mass spectrometry techniques to digest oligosaccharides from wall polymers and establish fingerprint patterns (Lerouxel et al. 2002). One established technique is OLigosacharide Mass Profiling (OLIMP) and is based on the action of a fungal XyG specific endoglucanase (XEG), which can cleave XyG at very specific sites (Lerouxel et al. 2002; Pauly et al. 1999b). Figure 1.3-1 A, B indicates the cleavage sites for the XEG enzyme and the nomenclature of the released XyG oligosaccharides. The released oligosaccharide mixtures are then subjected to Matrix Assisted Laser Desorption/Ionization Time Of Flight (MALDI-TOF) mass spectrometry. In addition XEG released oligosaccharides can be quantified using High Performance Anion Exchange liquid Chromatography with Pulse Amperometric Detection (HPAEC-PAD), with the caveat that this technique will hydrolase the ester linkages present due to the use of alkaline mobile phases (Gunl et al. 2011). Another technique available to interrogate the structure of extracted XyG from cell walls is Polysaccharide Analysis using Carbohydrate Electrophoresis (PACE). This technique is based on the labeling of oligosaccharide mixtures with a fluorophore which can then be separated according to size in polyacrylamide gels (Goubet et al. 2002). In order to analyze XyG structures *in muro* many antibodies have been developed which will recognize specific epitopes in the XyG structure and can be labeled with fluorophores for use in microscopy experiments. Examples of these specific antibodies include: CCRC-M1 which

recognizes fucosylated XyG structures (Puhlmann et al. 1994) and LM15 which recognizes XXXG (Marcus et al. 2008).

XyG has many applications in the food, pharmaceutical and paper/textile industries. In the food industry it is used as a thickener and is classified as a soluble fiber that conveys benefits in controlling cholesterol and improving aspects of digestion (Albersheim et al. 2011; Mishra and Malhotra 2009). Coating of bacterial cellulose with XyG to yield an immune inert material for the production of artificial blood vessels is an application being considered by the pharmaceutical industry (Fink et al. 2011). XyG can also be used to functionalize the cellulose surface. By using aminoalditol XyG oligosaccharides it was shown that it is possible to attach fluorescein, biotin as well as other molecules to the oligosaccharides (Brumer et al. 2004). The modified oligosaccharides can be incorporated by XyG endotransglycosylases into high molecular weight XyG that will bind to the cellulose surface functionalizing the material (Brumer et al. 2004). This technique could be useful for the paper industry by creating high-performance paper and packaging materials and for creating biocomposites that could be functionalized for specific purposes.

1.4 Pectin –structure, function, biosynthesis, metabolism and applications

An example of a structurally very complex polysaccharide is pectin. At least 67 transferase activities are needed to account for all the linkages found in the pectic polymers (Albersheim et al. 2011). In the primary walls of dicots pectins can represent up to 35% of the mass (Carpita and Gibeaut 1993; Mohnen 2008). Pectins have been implicated in several cellular processes in plants including cell adhesion, cell growth, and pathogen perception (Anderson et al. 2012; McNeil et al. 1984; Ridley et al. 2001). Five classes of polymers constitute pectins; HG, RGI, RGII, apiogalacturonan and xylogalacturonan (Harholt et al. 2010).

The common feature that unites all of the pectic polymers is the presence of galacturonic acid in their backbone. HG, the most abundant of the pectic polymers, is composed of an α-1,4-linked galacturonic acid backbone, which can be methyl esterified at the C-6 position [Figure 1.4-1; (Atmodjo et al. 2013)]. Methyl esterification neutralizes the negative charge of a galacturonic acid (Harholt et al. 2010; Ralet et al. 2003). HG can also be *O*-acetylated at O-2 and O-3 positions (Ishii 1997; Keenan et al. 1985). RGI is the second most abundant pectic polymer (Albersheim et al. 2011). It has a more complex structure (Nakamura et al. 2002; Ridley et al. 2001; Yapo 2011). The polymer backbone is composed of the repeating disaccharide *α*-1,4-D-GalA-*α*-1,2-L-Rha [Figure 1.4-1; (Ridley et al. 2001)]. Rhamnose residues in the RGI backbone can be decorated with extensive arabinan or galactan side chains at C-4 and to a lesser extent fucosyl- and glucuronosyl-residues attached to a galactose (C-6) (Atmodjo et al. 2013; Harholt et al. 2010). It has been shown that between 25-80% of the rhamnose residues are substituted with sugars depending on tissue and species examined (Atmodjo et al. 2013). The galacturonic acid residues of the RGI backbone can be acetylated in the O-2 and O-3 positions (Ishii 1997; Komalavilas and Mort 1989). In contrast to HG, methyl esterification of the C-6 carbonyl group in RGI has not been reported (Atmodjo et al. 2013). Xylogalacturonan is composed of an HG backbone with xylose residues attached to the O-3 position (Figure 1.4-1); this polymer can be found in relatively small amounts

in *Arabidopsis* tissues (Zandleven et al. 2007). The complex structure, sugar substitutions, linkages and decorations of the RGII molecule are described in Figure 1.4-1. It has been shown that pectic polymers extracted from cell walls can be covalently attached to each other as well as with other wall polymers such as hemicelluloses and structural proteins. HG, RGI, XGA and RGII have been extracted in conjunction from cell walls of different sources and can be separated through endopolygalaturononase digest suggesting that these polymers could be covalently linked in the wall (Yapo 2011). Pectin covalently attached to XyG have also been demonstrated to exist in suspension cultures of rose cells (Thompson and Fry 2000). Recently evidence for linkages between pectins, arabinoxylans and a wall proteoglycan has been shown in *Arabidopsis* suspension cell cultures. Using a combination of biochemical characterization and NMR spectroscopy it was shown that arabinoxylan-pectin-arabinogalactan protein 1 (APAP1) can be covalently linked to arabinoxylan and RGI (Tan et al. 2013). How these linkages are produced is still unclear and the action of transglycosylases in the wall has been proposed (Atmodjo et al. 2013).

One of the major roles of pectin in the plant is cell adhesion (Bouton et al. 2002). This role is taken on by the middle lamella, which is composed predominantly by HG thought to confer the cell-to-cell adhesive force mediated by calcium and covalent crosslinks (Bouton et al. 2002; Jarvis et al. 2003; Marry et al. 2006; Zhang and Staehelin 1992). A polymer decoration, namely methylesterification, regulates pectin gel formation by controlling the number of C-6 carbonyl groups carrying negative charges in HG (Ralet et al. 2003; Ralet et al. 2008). These charged structures can bind calcium, forming junction zones which will cross link different HG molecules conferring the adhesive force (Albersheim et al. 2011). Pectins are involved in regulating the pore size of the wall in plants. *In vitro* studies have shown that by modifying the pectic network using mild enzyme treatments it is possible to alter wall porosity (Baronepel et al. 1988). Based on microscopic and *in vitro* experiments wall pore size has been estimated to vary between 4-13 nm in diameter, which could accommodate the movement of globular proteins varying from 20 to 150 kDa (Albersheim et al. 2011; Baronepel et al. 1988; Carpita et al. 1979; Odriscoll et al. 1993). RGI and RGII actively participate in regulating wall pore size due to their extensive branching patterns as well as their crosslinking capacity (Albersheim et al. 2011; Fleischer et al. 1999). Pectic derived oligosaccharides participate in signaling including cell integrity and pathogen perception (Ridley et al. 2001). A group of genes termed wall associated kinases (WAKs) were shown to bind HG derived oligosaccharides and initiate signaling cascades involved in defense responses (Brutus et al. 2010). The precise role for RGI in the wall still remains to be determined. There is accumulating evidence pointing towards a structural role in wall architecture (Harholt et al. 2010; Jones et al. 2003; Ulvskov et al. 2005). RGII also seems to play a significant role in wall architecture in particular due to its boron crosslinking capacity (Albersheim et al. 2011; Fleischer et al. 1999). Developmental aberrations are common in plants deficient for Boron (Blevins and Lukaszewski 1998), which is required for RGII crosslinking (Kaneko et al. 1997).

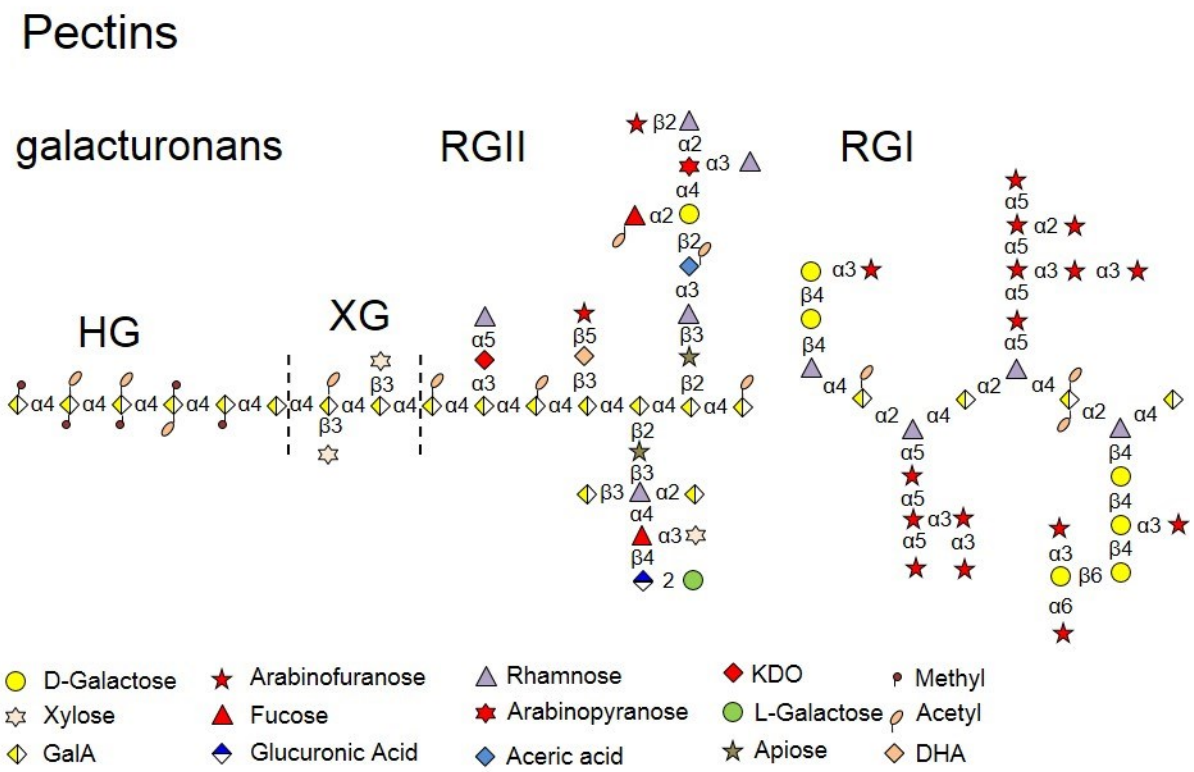

Figure 1.4-1 Pectin structures. Representative structures from homogalacturonan (HG), xylogalacturonan (XG), rhamnogalacturonan I (RGI), and rhamnogalacturonan II (RGII) are shown. Glycosidic linkages are shown between sugar residues; dashed lines delimit XG structure. Pectin structures adapted from Harholt et al. (2010), Mohnen (2008) and Schultink (2013).

Only few genes have been identified that are involved in pectin biosynthesis. There is evidence that at least four families of CAZy glycosyltransferases [GTs; (GT8; GT47; GT77; GT92)] are involved in pectin biosynthesis (Atmodjo et al. 2013; Lombard et al. 2014). The *GAUT1* gene (GT8) was identified based on a proteomics approach and has been shown biochemically to represent a HG galacturonic acid transferase (Sterling et al. 2006). The identification of GAUT1 led to the annotation of the *GAUT* and *GAUT-like* gene families in *Arabidopsis* (Sterling et al. 2006). Mutants in these families often have walls altered in galacturonic acid content (Caffall et al. 2009; Kong et al. 2011). Mutants termed QUASIMODO (for their dwarfism) have also been associated with pectin biosynthesis. *QUASIMODO1* (*QUA1*) also known as *GAUT8* is also thought to represent a HG: galacturonic acid transferase (Bouton et al. 2002). The *QUA2* gene when mutated produces plants compromised in its growth, the protein coded by this gene has been proposed to represent a methyl transferase to HG (Krupkova et al. 2007; Mouille et al. 2007). The backbone synthases for RGI remains elusive to this date. GTs involved in the sidechain decoration of RGI including arabinosyl transferases [*ARADs*; (Harholt et al. 2006)] and galactosyl transferases [*GALSs*; (Liwanag et al. 2012)] have been identified, but the only biochemical activity that has been demonstrated so far is for GALS1, a β-1,4 galactosyltransferase. The RGXT gene family has been shown to encode for α-1,3 xylosyl transferases to RGII (Egelund et al. 2006). The *RGXT4* gene,

when mutated, compromises root and pollen development leading to sterility and seedling lethality, highlighting the role of RGII in proper cell wall assembly (Liu et al. 2011). A β-1,3 xylosyl transferase activity towards xylogalacturonan has been shown for the *XGD1* gene (Jensen et al. 2008).

Multiple enzymatic activities have been isolated from primary walls, which could be involved in pectin metabolism or remodeling once deposited in the apoplast. These include β-D-galactosidase, α-L-arabinosidase, α-D-galacturonidase, methylesterase, acetylesterase and polygalacturonases as well as others (Fry 2004; Hadfield and Bennett 1998). Pectin de-methylesterification by PMEs is perhaps the best characterized apoplastic modification of pectic HG (Micheli 2001). PMEs are involved varied cellular processes including cell adhesion, stem elongation and pathogen resistance (Bethke et al. 2014; Hongo et al. 2012; Micheli 2001). HG is synthesized in highly methyl esterified forms and extensively edited by PMEs in the apoplast (Wolf et al. 2009). Not only does the *A. thaliana* genome have 67 putative PMEs (Lombard et al. 2014), it also contains PME inhibitors (Jolie et al. 2010) that presumably aid in enzymatic regulation (Jolie et al. 2010). Defects in *MUM2,* which encodes an apoplastic β-D-galactosidase, results in defective seed coat mucilage that fails to expand upon hydration (Dean et al. 2007). Pectin acetylesterases (PAE) also play a significant role in pectin remodeling *in muro* as discussed below (Gou et al. 2012; Orfila et al. 2012).

Pectins are extensively used in the food industry as thickener, texturizer, stabilizer, and emulsifier. The textile and paper industries also use pectins as a sizing and film forming agent (Albersheim et al. 2011). Pectins are estimated to be a 2 billion dollar worldwide business. Commercial sources include apple pomace, citrus peel and sugar beet cake (Thakur et al. 1997). The quality of the pectins is based on its gelling ability and thus dependent on molecular size, and degree of acetylation and methylesterification (Albersheim et al. 2011; Thakur et al. 1997; Willats et al. 2006).

1.5 Cell wall polymer *O*-acetylation

Hemicellulosic and pectic polymer *O*-acetylation occurs during synthesis in the Golgi. Studies using radiolabelled acetyl-CoA with potato microsomal preparations have demonstrated that acetyl-CoA is a donor substrate for wall polysaccharides acetylation in the Golgi (Pauly and Scheller 2000). Recently, several enzymes involved in plant polysaccharide acetylation have been identified. Advances in the knowledge of several polysaccharide acetylation systems in bacteria, fungi and mammals have been useful in plant research (Gille and Pauly 2012). Protein sequence analysis between the different taxa has revealed many similar mechanisms for polysaccharide acetylation. The first study to shed light into this field in plants was the characterization of the *rwa2* mutant (Manabe et al. 2011). The gene family in *Arabidopsis*, composed by 4 members, was identified based on protein sequence similarity to a fungal (*Cryptococcus neoformans*) protein involved in polysaccharide acetylation. Mutations in the *RWA2* gene led to *A. thaliana* leaves containing 20% less acetate in its walls (Manabe et al. 2011). The acetylation status of several polymers is affected (including pectin and XyG). Triple and quadruple *rwa* mutants exhibited severe dwarfism and abnormal tissue development including aberrant xylem cells (Manabe et al. 2013). If overexpressed in the quadruple mutant background RWA2 is able to completely rescue the acetylation chemotype

establishing the functional redundancy of these proteins (Manabe et al. 2013). Interestingly, in the different triple mutant combinations differential acetylation of wall polysaccharides suggest preference for particular substrates. The RWA2 protein is predicted to have 10 transmembrane domains and it has been proposed to represent a transporter, which delivers precursor molecules to the endomembrane system (Manabe et al. 2011).

A family of putative plant acetyltransferases has been identified in *A. thaliana* (Gille et al. 2011b). Members of the Trichome Birefringence-Like (TBL) family include proteins that had previously been associated with freeze tolerance (Bouchabke-Coussa et al. 2008; Xin and Browse 1998), pathogen resistance (Vogel et al. 2004) and cell wall biosynthesis (Bischoff et al. 2010a; Bischoff et al. 2010b; Gille et al. 2011b; Xiong et al. 2013). TBL29/ESK1 has been implicated in xylan acetylation, displaying a collapsed xylem phenotype, when mutated (Lefebvre et al. 2011; Xiong et al. 2013; Yuan et al. 2013). The *pmr5* mutant was originally identified based on a powdery mildew resistance. The capacity of *pmr5* to bind to HG suggests that the protein is involved in pectin biosynthesis (Lim 2013). In a similar manner the TBR protein, whose identification was based on light birefringence phenotypes led to the TBL family annotation, is thought to be involved in HG acetylation [Brad Dotson, Somerville Lab, Personal communication; (Bischoff et al. 2010a; Bischoff et al. 2010b)]. In Figure 1.5-1 a model is presented describing the known genes and molecules known to be involved in polysaccharide acetylation.

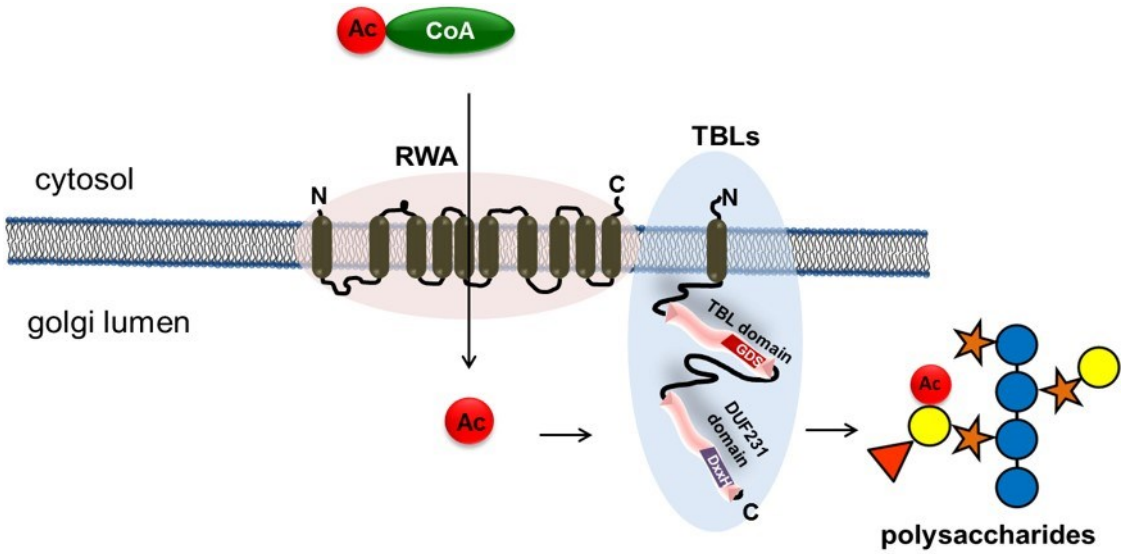

Figure 1.5-1 Model for polysaccharide acetylation in Golgi vesicles. Possible path of acetate from the donor substrate acetyl-CoA to a polysaccharide. Positions proposed for RWA and TBL proteins are shown. Adapted from Gille et al. (2011).

The biological function of wall polysaccharide *O*-acetylation is still not clear. The collapsed xylem phenotypes in several acetylation mutants suggest that wall polymer acetylation is critical for secondary wall function (Manabe et al. 2013; Schultink 2013; Xiong et al. 2013). A recent study suggests that xylan acetylation could mediate the interaction between xylan coated cellulose microfibrils and hydrophobic components of

the wall such as lignin (Busse-Wicher et al. 2014). Plants overexpressing PAEs also show aberration in tissue development and physical structure (Gou et al. 2012; Orfila et al. 2012). On the other hand some acetylation mutants have shown increased resistance to pathogens (Vogel et al. 2004). Future work will be necessary in order to dissect the biological role of acetylation in each wall polymer.

1.6 Objective

Since the completion of the *A. thaliana* genome in the year 2000 significant advances have been made in cell wall gene discovery. Components of the cell's machinery for wall polysaccharide *O*-acetylation have only recently emerged after breakthroughs in the identification of gene families involved in polymer acetylation (Gille et al. 2012) although the precise molecular mechanism remains elusive. Since the role of polysaccharide *O*-acetylation in plant growth and development is largely unknown various experimental approaches are being pursued here to reveal and characterize genes involved in this process. By studying these genes and their respective mutants it should be possible to provide insights into the biology of this cellular process and further detail its biochemistry. The identification of genes in the wall acetylation pathway can consolidate a tool box for genetic engineering of plant cell walls with altered acetylation level applicable in the food and biofuel industries.

To identify genes and mutants involved in wall acetylation, forward and reverse genetics as well as biochemical approaches are proposed. The forward genetics has the power of revealing unknown or non-obvious genes related to the process. For this purpose a collection of naturally occurring and genetically diverse *Arabidopsis* ecotypes will be explored. In a more directed fashion the reverse genetics employed should shed light on the role of a putative family of pectin acetylesterases in wall acetylation. Likewise, the specific search for the XyG acetylesterase biochemical activity, previously undescribed in plants, aims at identifying a causative gene.

2.0 Material and Methods

2.1 Plant and bacterial growth

2.1.1 Soil grown *Arabidopsis thaliana*

Seeds were stratified at 4 ^{o}C for 24h in a 0.15% agar solution and pipetted on to soil. Pots were placed in chambers maintained at 22 ^{o}C with a 170 to 190 µmol m^{-2} s^{-1} light intensity in a 16 hours light / 8 hours dark regime. Plant trays were fertilized once with Miracle Grow All-purpose Plant Food (Scotts) according to manufacturer's recommendation and watered as needed. After one week, excess plants were removed in order to obtain one plant per pot. Plant tissue was harvested at 35 days unless otherwise stated.

For the stem acetylation ecotype screen (3.2.1) plants were stratified at 4^{o}C in water for 48 hours and planted onto a pot for 2 weeks than singled out onto pots. The first two internodes of the stems were harvested when the inflorescences presented 8-14 mature siliques.

2.1.2 Soil grown *Nicotiana benthamiana*

Nicotiana benthamiana plants used for transient gene expression (6.2.3; 6.2.4) were sown directly on soil, grown for 2 weeks then transplanted into destination pots and grown for 4 weeks until use. The plants were grown under a 26 ^{o}C, 170 to 190 µmol m^{-2} s^{-1} light intensity and 16 hours light / 8 hours dark regime. Plants were fertilized once with Miracle Grow All-purpose Plant Food (Scotts) according to manufacturer's recommendation and watered as needed.

2.1.3 *Arabidopsis thaliana* seed sterilization and plate growth

Seeds were surface sterilized using a solution of 0.05% Triton-X in 70% ethanol for 10 minutes with gentle mixing. Seeds were then washed with 95% ethanol 3 times and pipetted onto filter paper for drying. When dry, seeds were sprinkled onto petri dishes containing growth media (see below). The plates were then stratified for 48 hours at 4 ^{o}C and placed into a growth chamber at 22 ^{o}C with a 170 to 190 µmol m^{-2} s^{-1} light intensity in a 16 hours light / 8 hours dark regime.

Alternatively, for the XyG acetylation ecotype screen (3.2.2) seeds were sterilized using a 70% ethanol wash followed by 15 min incubation under agitation with a 50% (v/v) house hold bleach (Chlorox) solution. After the incubation seeds were washed 4 times with sterile water and stratified for 48 hours. After stratification seeds were plated in media without sucrose and covered with aluminum foil and grown for 7 days at 22 ^{o}C. After harvest seedlings were stored in 70% ethanol at 4 ^{o}C until processing.

Plants were grown on plates containing media composed of (w/v) 0.125% MS salts, 0.06% 2-(*N*-morpholino)ethanesulfonic acid (MES) - pH 5.6 (adjusted with KOH), 0-1% sucrose, 0.8% agar. For transgenic selection the plates were complemented with the following antibiotics: kanamycin (60 µg / mL), hygromycin (50 µg / mL), or gentamycin (80 µg / mL).

2.1.4 *Arabidopsis thaliana* suspension cultured cells

Arabidopsis cell suspension cultures [5.2.1; (Parsons et al. 2012)] were grown in liquid MS media - pH 5.8 (adjusted with KOH) containing (w/v) 0.433% MS salts, 3% sucrose, 0.05 mg / L kinetin, and 0.5 mg / L 1-Naphthaleneacetic acid (NAA). Cultures were kept under constant agitation (130 rpm) at 22 ^{o}C with a 170 to 190 µmol m^{-2} s^{-1} light intensity in a 16 hours light / 8 hours dark regime. The cell cultures were re-inoculated every 7 days.

2.1.5 Bacterial growth conditions

Bacterial liquid cultures of transformed One Shot® Top10 chemically competent cells or *Agrobacterium tumefaciens* strain GV3101 were grown in LB media (w/v; 1% sodium chloride, 1% tryptone, 0.5% yeast extract, pH 7.0) supplemented with the appropriate antibiotics or S.O.C. media (w/v; 2% tryptone, 0.5% yeast extract, 10 mM NaCl, 2.5 mM KCl, 10 mM MgCl2, 10 mM MgSO4, and 20 mM glucose). Antibiotics used included kanamycin (60 µg / mL), spectinomycin (100 µg / mL), gentamycin (25 µg / mL) and/or rifampicin 10 µg / mL. Cultures were grown at 37 ^{o}C (30 ^{o}C for Agrobacterium) under constant agitation (230 rpm) in 14 mL tubes containing 5 mL of media.

2.2 Molecular Biology

2.2.1 Plant Genomic DNA extraction

2.2.1.1 CTAB DNA extraction

Genomic DNA from plants was extracted using 3 different techniques. The method consisted of grinding frozen plant tissue (liquid nitrogen) in a 1.5 mL Eppendorf tubes with 3 glass beads in a ball mill (Retsch MM 400; 25 Hz, 1min). Plant tissue was ground to a fine powder and 300 µL of a buffer containing 2% (w/v) CTAB, 1.4 M NaCl, 100 mM Tris HCl - pH 8, and 20 mM Ethylenediaminetetraacetic acid (EDTA) was added (Murray and Thompson 1980). The mixture was vortexed and incubated at 65 ^{o}C for at least 10 min. After cooling down to room temperature, 300 µL of chloroform was added and samples vortexed vigorously. To separate the aqueous phase from the organic phase samples were spun down at 21,000 *g* for 5 min. The supernatant was collected and transferred to a new tube, where an equal volume of isopropanol was added. Samples were spun down once more and the supernatant was removed by decanting. The pellet was washed with 500 µL of 70% ethanol and spun down at 21,000 *g* for 5 min. The supernatant was removed by decanting and the pellet was dried for re-suspension in 100-300 µL of TE buffer (10 mM Tris HCl, pH 8, and 1 mM EDTA).

2.2.1.2 One step DNA extraction

The “one step” method consisted of grinding plant material in 200 µL of a 10 X dilution of Edwards solution (200mM Tris HCl pH 7.5, 250 mM NaCl, 25mM EDTA, and 0.5% SDS). Plant debris was spun down at 21,000 *g* for 5 min and supernatant was directly used in PCR reactions (Kasajima et al. 2004).

2.2.1.3 One point five step DNA extraction

In a variation of the method described above, DNA was extracted by grinding frozen plant tissue (liquid nitrogen) using 3 glass beads in a ball mill (Retsch MM 400; 25 Hz, 1min) and adding 400 µL Edwards solution (Edwards et al. 1991). Mixture was spun down at 18,000 g and 300 µL of the supernatant collected and mixed with equal volume of isopropanol. This mixture was then spun down and the supernatant discarded. The pellet was dried and re-suspended in 100 µL of TE buffer.

2.2.2 Genotyping PCRs

Genotyping PCRs (see primer list Appendix 1) were performed using the JumpStart Red Taq ReadyMix (Sigma) following manufacturers recommendation. PCR reactions were done in a total volume of 20 µL. DNA in TE buffer was added to 1 µL volume (~ 150 ng / µL) and primers were added to a final concentration of 0.1 µM each . Cycling conditions were adjusted according to primer melting temperatures and amplicon sizes. PCR products were visualized in UV transluminators using 1% agarose gels in TAE buffer (40 mM Tris, 20 mM acetic acid, and 1 mM EDTA.) containing ethidium bromide (0.01 µg / mL).

2.2.3 DNA amplification for cloning

For cloning purposes DNA amplification fragments were generated using Phusion DNA Polymerase (Finnzymes). This enzyme has proof reading capabilities, which increases the sequence fidelity of the products. Manufacturer’s recommendations were followed for PCR optimization (see primer list Appendix 1). Templates for these reactions included cDNA, genomic DNA or plasmids.

2.2.4 DNA fragment cloning (conventional, TOPO® TA, Gateway, Golden Gate, Gibson Cloning)

Various techniques for cloning DNA fragments into plasmids were used. Initially TOPO® TA cloning (Invitrogen) was used to produce PCR fragments of interest into the pCR™8/GW/TOPO vector. TOPO® cloning procedures were followed according to the manufacturer’s recommendation. As with all cloning procedures generated plasmids were checked by analytical restriction digests and Sanger sequencing. Restriction digests were used to extract fragments of interest from the pCR™8/GW/TOPO vectors. Fragments of interest were subsequently ligated into other vectors using DNA ligase (T4 Ligase, Invitrogen). Alternatively the pCR™8/GW/TOPO vectors containing fragments of interest were used in Gateway Cloning (Invitrogen).

For the overexpression of PAE family members (6.2.1) Gateway Cloning was used. Coding sequences (cds) of these genes (AT1G57590.1, *PAE2*; AT2G46930.1, *PAE3*; AT3G09405 , *PAE4*; AT3G09410.1, *PAE5*; AT3G62060.1, *PAE6*; AT4G19410.1, *PAE7*; AT4G19420.1, *PAE8*; AT5G23870.1, *PAE9*; AT5G26670.1, *PAE10*; AT5G45280.1, *PAE11*; and AT3G05910.1, *PAE12*) were amplified with attB primers from cDNA or plasmids (obtained from stock centers), gel extracted, purified and recombined in a BP reaction with the pDONOR221 vector. This vector was then recombined in an LR reaction with the binary vector pORE E4 containing the enTCUP2 promotor for constitutive overexpression [Appendix 2; (Schultink 2013; Schultink et al. 2013)].

Conventional cloning, using restriction digests and ligation, was used to clone genes of interest into the tobacco expression vectors, pVKH18En6 [PAE9cds:GFP; (6.2.3); (Gunl et al. 2011)], pART7 and pART27 [protein expression of PAE9; (6.2.4); (Gleave 1992)]. The fragments of interest (cds) were excised from the pCR™8/GW/TOPO vector backbone.

Chimeric constructs of *TBL3* and *TBL26* with *TBL27* (4.2.1) were assembled using Golden Gate cloning (Engler et al. 2009). In short, multiple PCR fragments with matching sticky ends were generated and in one step were digested and ligated. These fragments were then TOPO® TA cloned into the pCR™8/GW/TOPO vector and later recombined via an LR reaction into the pGWB510 (Appendix 3) vector containing the *TBL27* promotor and a 3' FLAG tag.

Gibson cloning (Gibson et al. 2009) was used to generate plasmids for protein expression (PAE8cds:6XHIS in pART27; 6.2.4) and GFP fusions for subcellular localization [PAE9promotor:PAE9cds:GFP in pMDC107 (6.2.3); (Curtis and Grossniklaus 2003) in tobacco]. The New England Biolabs Gibson Assembly cloning kit was used according to the manufacturer's recommendation as well as the on-line tool NEBuilder™.

2.2.5 Restriction Digest of plasmids

Analytical restriction digests of plasmids were executed using enzymes from New England Biolabs. Plasmids were extracted from *E. coli* or *A. tumefaciens* using the Qiagen Miniprep kit and incubated with endonucleases for 4 - 24 hours in buffers according to enzyme requirements at 37 ^{o}C. Fragments were then visualized in UV transluminators using 1% agarose gels in TAE buffer containing ethidium bromide (0.01 µg / mL).

2.2.6 DNA Sequencing

DNA sequencing services were provided by ELIM Biopharmaceuticals. Plasmids and PCR products were Sanger sequenced. Samples were submitted with appropriate primers according to company specifications.

2.2.7 Bacterial transformation (*E. coli* and *A tumefaciens*)

Chemically competent Bacteria (One Shot ® TOP10, Invitrogen) were transformed by adding 1 µL of purified plasmids (20-100 ng) to 50 µL of cells. The mixture was kept on ice for 30 min and heat shocked at 42 ^{o}C for 30 s followed by a 2 minutes incubation on ice. S.O.C media was added (250 µL) and incubated for 1 hour at 37 ^{o}C and 230 rpm. Following incubation, 10 – 50 µL of cells were plated on LB plates (2.1.5) with desired antibiotics.

A tumefaciens was transformed using electroporation. Plasmids (1 µL) were added to 40 µL of cells in an electroporation cuvette. Current was applied using the following parameters: 1800V, 50 µF and 150 Ω. S.O.C (2.1.5) media was added (500 µL) and cells were incubated for 2.5 hours at 30 ^{o}C and 230 rpm. Cells (10-50 µL) were then plated on LB plates with the required antibiotics.

2.2.8 Genetic transformation of *Arabidopsis thaliana*

A tumefaciens containing the binary vector of interest was cultured in LB media (250 mL, with desired antibiotics) to an OD_{600} of approximately 2. Cells were pelleted (4,000 *g*, 10 min, 20 ^{o}C) and re-suspended to 0.7-0.8 OD_{600} in transformation media [3 % (w/v) sucrose and 0.05% (v/v) Silwet L-77]. Arabidopsis plants harboring developing floral structures were dipped 3 times in transformation media containing cells (Clough and Bent 1998). Plants were immersed for 0.5 to 3 minutes each time. Plants were then grown to maturity at 22 ^{o}C with a 170 to 190 µmol m^{-2} s^{-1} light intensity in a 16 hours light / 8 hours dark regime.

2.2.9 Transient gene expression in *N. benthamiana* (confocal microscopy and protein expression)

For subcellular localization experiments (6.2.3) *A. tumefaciens* was grown as described for *A. thaliana* transformation (2.2.8). Cells were pelleted and re-suspended to an OD_{600} of 0.05 in infiltration buffer (10 mM MES pH 6.0, 2mM Na_2PO_4, 0.5% (w/v) glucose and 100 µM acetoseryngone). *N. benthamiana* plants were immersed in infiltration buffer containing cells and vacuum infiltrated 3 times for 3 min each. Tobacco plants were grown for 5 days at 26 ^{o}C with a 170 to 190 µmol m^{-2} s^{-1} light intensity in a 16 hours light / 8 hours dark regime.

For protein expression (6.2.4) the infiltration buffer consisted of 10 mM MES pH 5.6, 10 mM $MgCl_2$ and 0.15 mM acetoseryngone. The *A. tumefaciens* cells were suspended to OD_{600} 1.4-2 and incubated for 3-4 hours with acetoseryngone prior to infiltration. A construct overexpressing the P19 (Voinnet et al. 2003) gene silencing suppressor was always infiltrated in conjunction with the construct of interest (final OD_{600} ratio of 1:0.7).

2.2.10 Transcriptional analysis of *A. thaliana* (Reverse Transcription - PCR and Quantitative Reverse Transcription - PCR)

Total RNA was extracted from plant tissue using the Plant RNeasy kit from Qiagen according to manufacturer's protocol. Total RNA was quantified using the Nanodrop and concentration normalized for DNase treatment.

For RT-PCR reactions (6.2.1) total RNA (3.5 µg) was treated with DNAse (Roche 04716728001) in a 20 µL reaction using 1 µL DNAse and 2 µL of 10 X buffer. The treatment was carried out at 37 ^{o}C for 15 minutes followed by a 70 ^{o}C denaturation step for 15 minutes. The Superscript III First Strand Synthesis kit (Invitrogen) was used to synthesize cDNA and non-RT controls from 250 ng of total RNA. The cDNA (2 µL) was mixed in JumpStart Red Taq ReadyMix (Sigma) as described for the genotyping PCRs (2.2.2). As an expression control the polypyrimidine tract-binding protein 1 [*PTB1*; (Gille et al. 2009)] gene was used.

DNase treatment for Q-RT-PCR (4.2.2; 6.2.1) was done using the Ambion TURBO DNA-free™ kit. Treated total RNA (200 ng) was then used for cDNA synthesis using the M-MLV Reverse Transcriptase kit (Invitrogen 28025-013) following manufacturer's instructions. The templates (1 µL) were then used for Q-RT-PCR reactions with a Thermo Scientific Maxima SYBR Green/ROX qPCR Master Mix. Primers were designed according to kit recommendations. Reactions were setup according to instructions from the manual and Q-RT-PCR reactions were run on a StepOnePlus Real-Time PCR System from applied Biosciences. Cycling conditions started with 10 minutes at 95 °C followed by 40 cycles of 95 °C for 15 s, 60 °C for 30 s, and 72 °C for 30 s. Relative abundance of transcripts was calculated by the Applied Biosciences software using the *PTB1* gene as the internal control.

2.2.11 Protein extraction

Protein extracts were produced for two purposes: activity assays and protein identification via western blotting.

For XyG acetylesterase activity assays (2.6) proteins were extracted from *Arabidopsis* suspension cells culture mass, 7 day old etiolated seedlings and leaves (5.2.1). The cell mass from suspension cultures was washed with water twice and collected for protein extraction. The protein extraction consisted of agitating ground tissue (Retsch ball mill; 30 Hz for 2 minutes) with extraction buffer (0.5 X McIlvane buffer, 1 M NaCl and 0.05 M Ascorbic Acid) using 3 metal beads in the Retsch ball mill (30 Hz, 2min). The suspension was spun down at 21,000 g for 10 min and the supernatant collected. Denaturation of proteins was achieved by incubation at 99 ^{o}C for 10 minutes.

Cell culture medium protein (5.2.1) was prepared by passing 20ml of medium through an Amicon 100000 Da column (3X, 10 min 3000 g), collecting medium and concentrating this medium in a 10000 Da column (2X 10 min, 1X 3 min and 1X 2 min at 3000 *g*). Final volume collected contained 750 µL, and approximate 6.6X concentration of the original medium.

To identify and verify activity of proteins transiently expressed in *N. benthamiana* (6.2.4) the powder of pre-ground (in mortar and pestle with liquid N_2) leaves (~ 1 mL in a 2 mL tube, 2 times) was ground again in the Retsch ball mill (25 Hz, 2.5 minutes) and extraction buffer added (1M NaCl; 50 mM Na_2PO_4, pH 8; 10 mM imidazole; 1X Halt™ Protease Inhibitor, Thermo Scientific 1861278; 2 mM β-mercaptoethanol). The mixture was incubated under gentle agitation at 4 ^{o}C for 1 hour, spun down at 21,000 *g* for 10 minutes and supernatant collected for protein purification. Protein content of the supernatant was measured using the Bradford assay [Bio-Rad Protein Assay Dye

Reagent concentrate; (Bradford 1976)] in order to normalize the protein concentration for Ni-NTA bead loading (Qiagen 1018240; 20 µL of resin per 2 mL protein extract). Beads were incubated with protein for 1 h at 4°C under gentle agitation and collected into a mini spincolumn (Pharmacia Biotech) after a 500 g, 1 minute, spin down. The beads were washed 5 times with 250 µL extraction buffer, 4 times with 250 µL washing buffer (300 mM NaCl, 50 mM Na_2PO_4, pH 8, 20 mM imidazole) and 6 times with 50 µL elution buffer (300 mM NaCl, 50 mM Na_2PO_4, pH 8, 150 mM imidazole). The eluate was buffer exchanged with 50 mM ammonium formate pH 4.5, in a 500 µL Vivaspin column (MWCO of 5000 Da, Sartorius Stedim Biotech). A final volume of ~ 200 µL was recovered which was used for activity assays and western blots.

2.2.12 Western blots

Proteins were denatured in loading buffer (NuPAGE LDS Sample Buffer 4X, Invitrogen, NP0007) at 70 °C for 10 min and 20 µL was loaded onto an SDS polyacrylamide gel. The gel was wet blotted onto nitrocellulose membranes using transfer buffer (0.075 % (v/v) ethanolamine, 0.0935 % (w/v) Glycine and 20 % (v/v) ethanol) at 100 V for 80 minutes at 4°C. The membrane was blocked overnight at 4°C in 50mM Tris HCl, 150 mM NaCl, and 0.5% Tween (TBS-T) containing 3 % (w/v) nonfat powdered milk. After the blocking step the primary antibody (mouse anti 6X HIS, Fisher 50272472) was added (1:3000, v/v) and incubated for 3 hours at room temperature. After three 10 minute washes with TBS-T, the membrane was incubated in TBS-T containing 3 % (w/v) nonfat powdered milk with the secondary HorseRadish Peroxidase (HRP) conjugated antibody (Goat Anti-mouse IgG HRP Conjugate, Invitrogen, M30102; 1:3000, v/v) for 1 hour at room temperature. After another series of TBS-T washes (3) the membrane was developed by adding chemiluminescent reagents (Genscript LumiSensor) and visualized using the Fuji LAS-4000 imager.

2.3 Confocal microscopy for protein subcellular localization

Transiently transformed *N. benthamiana* (2.2.9) or transformed *A. thaliana* plants with GFP fusion constructs (2.2.8) were imaged using one of two microscopes: a Zeiss LSM 710 laser scanning confocal microscope or a Leica SD6000 microscope attached to a Yokogawa CSU-X1 spinning disc head. In some cases leaves were infiltrated with propidium iodide (PI; 10 µL / mL) for cell wall visualization or FM 4-64 (25 µM) for plasma membrane visualization. Plasmolysis of leaves was achieved with a 1 M mannitol solution. The samples were mounted on glass slides and the abaxial plant epidermis was examined using the following lasers and filters: GFP, 488 nm laser and 525-550 nm band pass filter; PI and FM 4-64 dyes, 594nm laser and 620-660 nm band pass filters. Images were acquired using 100-400 ms exposure times and processed using the ImageJ software with standard processing conditions.

2.4 Gene and protein sequence analysis

Protein sequence alignments and trees were generated using the Seaview4 and the MUSCLE software packages. All constructions of vectors and sequence analysis were done using the ApE- A plasmid Editor v20.30.

Calculation of % identity in TBL protein alignments were done by dividing the total number of identical positions by the total number of aligned positions including gaps within a determined domain. For % similarity the total number of similar amino acids (amino acid groups utilized to determine similarity: AVLIPMFW, GSTCNQY, DE, KRH) plus the identical positions were divided by the total number of aligned positions including gaps within a determined domain. For the calculations in fragment D TBL20 was excluded since this protein is missing in great part that stretch of amino acids (Appendix 4).

2.5 Analytical methods

2.5.1 Plant cell wall preparations

2.5.1.1 Cell wall preparation for acetic acid measurements and monosacharide comoposition

Dry plant material (leaf, stem or flowers) was ground to a fine powder using the Retsch ball mill by grinding 20-40 mg of material in liquid nitrogen using 3 small metal beads in 2 mL plastic tubes (2 times at 25 Hz for 2.5 minutes). The ground powder was washed 2 times with 70 % aqueous ethanol (1.5 mL) by vortexing, pelleting of wall material (21,000 *g* for 10 minutes) and discarding the supernatant. This was followed by 3 washes with a 1:1 methanol : chloroform solution (1.5 mL) using the same pelleting conditions. The pellet was dried in a speed vacuum centrifuge at 60 ^{o}C for 15 min.

2.5.1.2 Cell wall preparations for 7 day old etiolated seedlings for OLIMP (Oligosaccharide mass profiling)

Huskless seedlings (5) were dried under vacuum. Two metal beads were added and the material ground in the Retsch ball mill with liquid nitrogen (2 times at 25 Hz for 2.5 minutes). Material was washed twice, once with 1 mL 70% ethanol and then once with 1 mL of a 1:1 methanol : chloroform solution recovering the pellet by centrifugation (12,000 *g* for 10 min) after each wash. The pellet was finally dried under vacuum and used for oligosaccharide mass profiling of the XyG (2.5.6).

2.5.1.3 Cell wall preparations for other *Arabidopsis* tissues for OLIMP

Wall preparations for OLIMP from other tissues followed protocol described for 7 day old etiolated seedlings (2.5.1.2) but included a buffer wash with 1 mL 50mM ammonium formate before drying material for OLIMP.

2.5.1.4 Cell wall preparations from *Arabidopsis* liquid culture cell mass for OLIMP

Cell mass from cell cultures were pelleted at 3220 g for 20 min in a 50 mL tube. Medium was removed and water added to 50 mL. Cell mass was pelleted at 3220 g for 10 min and supernatant was discarded. Ethanol (70%) was added to 50 mL volume and cells were gently agitated overnight on a table top orbital shaker at room temperature. Cell mass was pelletd at 3220 g for 10 min and washed once more with 50 mL 70% ethanol. Two washes with 15 mL 1:1 methanol:chloroform were performed and material was dried in the hood. This material was then processed as described in 2.5.6 for OLIMP.

2.5.1.5 Large leaf cell wall preparations for acetic acid measurements and pectin digest

For larger leaf wall preparations up to 600 mg of dried plant material was ground in large metal grinders twice (200 mg at a time; 30 Hz for 30 s). This procedure produced a fine powder, 500 mg of which was washed 4 times with 70 % ethanol (30 mL / wash) by vortexing and pelleting the walls (3220 *g* for 10 minutes). This was followed by 4 washes with a 1:1 (v/v) methanol : chloroform solution (30 mL / wash) using the same pelleting conditions. The pellet was dried at room temperature for 48 hours followed by 1 hour in the lyophilizer.

2.5.2 Enzymatic starch removal of plant cell wall preparations

The destarching reaction entailed suspending 13 mg of wall material in 1.5 mL of McIlvane buffer, pH 5. The suspension was vortexed and incubated at 80 ^{o}C for 20 minutes, then cooled on ice. The following was added to 1.5 mL of cell wall suspension: 10 µL of a 0.01 mg / mL sodium azide solution; 10 uL of a 100 µg / mL α-amylase (Sigma A-6380) in 0.5 X Mcilvane buffer, pH 5.0; 22 µL of Pullulanase M2 (Megazyme). The reaction continued with a 37 ^{o}C incubation at 230 rpm for 15 hours and was stopped by incubation at 99 ^{o}C for 10 minutes (small preparations) or 80 ^{o}C for 20 min (larger preparations). Destarched wall material was pelleted by centrifugation and the supernatant discarded. The material was washed with equal volumes of water 3 times, followed by a 70 % aqueous ethanol wash. The remaining pellet was dried at room temperature followed by vacuum treatment (at least one hour in the lyophilizer for large preparations or 30 min at 60 ^{o}C in the speed vacuum for smaller preparations).

2.5.3 Pectinase digest of de-starched cell walls

De-starched wall material was treated with pectinases in order to solubilize pectic components. The enzymatic reaction was conducted with 6 mg of destarched wall material per mL of 50 mM ammonium formate, pH 4.5, containing 0.2 µg / mL of sodium azide, 2 mU / mL of endopolygalacturononase M2 (EC3.2.1.15; Megazyme), and 0.04 mU / mL of pectin methyl esterase (EC3.1.1.11; Novozymes, Christgau et al., 1996). The digest was incubated for 17.5 h at 37 ^{o}C, 230 rpm and stopped by incubation at 80 ^{o}C for 20 min. The pellet was spun down (3220 *g* for 10 minutes) and the supernatant filtered through a 0.45 µm syringe filter (Minisart® high flow 16533, Satorius Stedin). The pellet was washed 3 times with 15 mL water before drying.

2.5.4 Pectin Fractionation using Size Exclusion Chromatography

The pectic extract (10 mL) was freeze-dried, re-suspended in 50 mM ammonium formate, pH 4.5 (1 mL), and subjected to size exclusion chromatography using a Superpose 12 10/300 GL column (Amersham Biosciences). The column was connected to the Akta Purifier Fast Protein Liquid Chromatographer (FPLC; General Electric) or the PL–GPC 50 chromatographer (Gel Permeation Chromatographer; Varian Inc.). The sample was eluted isocratically in 50 mM ammonium formate pH 4.5 using a 0.4 mL / minute flow. Samples were injected manually using a 100 µL loop with a run time of 90 min. Fractions were collected according to the scheme depicted in (Figure 6.2.2-3). The fractions were dried in a lyophilizer and re-suspended in water (100 µL) and stored for subsequent biochemical analysis. Dextran standards were used to determine the separation profile of the column.

2.5.5 Acetic acid measurements of de-starched cell walls, pectin extract and pectin fractions

Cell wall suspensions (10 mg /mL), pectin extract or purified fractions were saponified by adding an equal volume of 1 M NaOH and incubation for 1 hour at 26 ^{o}C, 600 rpm, and neutralized with an equal volume of 1 M HCl. The final mixture was spun down for 10 minutes at 21,000 *g* and aliquots of the supernatant (10-50 µL) were subjected to the Acetic Acid Kit (K-Acet, Megazyme) to determine the released acetate. The assay consisted of a scaled down version of the manufacturer's instructions. In short, water was added to the supernatant from the saponification reaction to 104 µL total volume in UV compatible 96 well plates. This was followed by the addition of 30 µL of kit solution 1 and 12 µL of kit solution 2. After 3 minutes the absorbance at 340 nm was recorded. A 10 X dilution of kit solution 3 (12 µL) was added followed by 4 minutes incubation and absorbance measurement at 340 nm. A 10 X dilution of kit solution 4 was added followed by absorbance measurement at 12 minutes. The absorbance measurements were then used to calculate the final acetic acid content based on a formula provided in the kit.

2.5.6 XyG OLIMP

A variation of the method described by Lerouxel et al. 2002 was used to analyze the XyG oligosaccharide mass profile of XyG oligosaccharides, suspension cell culture supernatant (2.5.7), cell mass from cultures (2.5.1.4), leaf walls (2.5.1.3) and etiolated seedling walls (2.5.1.2). Wall material (2.5.1.2; 2.5.1.3; 2.5.1.4; 2.5.7) was incubated overnight with 0.1 U of XEG in 25 µL of 50 mM ammonium formate. The assay was carried out at 37 ^{o}C and 230 rpm. The digest was de-salted with Biorex MSZ501 cation beads (~ 15 beads for 45 minutes) and 2 µL of the supernatant was spotted onto a MALDI-TOF plate containing pre-spotted 2,5-dihydroxybenzoic acid (DHB; 2 µL of a 10 mg / mL solution per spot). The supernatant was incubated with DHB for 3 minutes and then dried under vacuum. The plate was inserted into an AXIMA Performance MALDI-TOF mass spectrometer (Shimadzu) using an accelerating voltage of 20,000 V to record the mass spectra.

2.5.7 Purification of XyG oligosaccharides for activity assay

Cell culture medium was collected (14mL) and 96% ethanol was added until 70% ethanol was achieved. Mixture was incubated overnight at -20^{o}C. Material was pelleted by centrifugation at 3220 *g* and washed 2 times with 15 mL 70% ethanol. The pellet was dried down at room temperature and then suspended in 2 mL water. Digested 500 uL of the suspended medium polymers with XEG using same conditions as for OLIMP (2.5.6). The digest product was cleaned up using an Amicon 10000 Da cut off spin column. After adding 200 ul of digest to the column and spinning down at 20880 *g* for 3 min recovered 150 uL of flow through, which was subsequently used for enzymatic assays and OLIMP.

2.5.8 Monosaccharide analysis using HPAEC-PAD

Cell wall material, pectic extract, pectic wall residue and purified fractions were hydrolyzed in 250 µL of 2M Tri-fluoroacetic acid (TFA) heated to 121 ^{o}C for 90 minutes followed by a stream of dried air using nitrogen. The hydrolyzed samples were re-suspended in water (0.3-1 mL) and further diluted. Neutral sugars were separated via a CarboPac PA20 column, while a CarboPac PA200 was used to separate uronic acids. Three distinct programs were used to resolve the sugars of interest. Samples were run at a flow rate of 0.4 mL / min and gradients consisted of i) 2mM NaOH for 20 min followed by a 5 minute 100mM flush and subsequent 5 minutes at 2mM (neutral sugar separation 1; excludes xylose and mannose); ii) 18 mM NaOH for 15 min followed by a 5 minute 100mM flush and subsequent 7 minutes at 18 mM (neutral sugar separation 2; excludes rhamnose and arabinose); iii) 0.1 M NaOH with a gradient of 50 – 200 mM sodium acetate from 0 to 10 minutes followed by a 2 minute 200 mM sodium acetate flush returning to 50 mM for 2.9 minutes (uronic acid separation).

2.6 Activity assays of extracted proteins

Protein extracts (2.2.11) from cell mass and medium in suspension cultures etiolated seedlings and leaves were tested for esterase activity against 4-nitrophenol acetate (PNPA). The protein extract (50 µL) was incubated with 1 mM PNPA in 0.5 X McIlvane buffer, pH 7.4 (total volume of 500 µL). After 30 minutes at room temperature the absorbance at 410 nm was measured. Protein extracts (10 µL) were also incubated overnight with purified XyG oligosaccharides obtained from cell cultures (2.5.7; 10 µL) and 2 µL of this reaction was used for OLIMP.

Protein preparations from tobacco leaves (PAE9 and PAE8; 2.2.11) were used for activity against PNPA and pectic fractions (2.5.4). For activity against PNPA ~0.7 µg of protein was incubated with 1.67 mM PNPA in 150 µL of 50 mM ammonium formate for 10-45 minutes. After incubation, 125 µL of sodium phosphate buffer pH 7.4 was added to the reactions in order to visualize PNP at an absorbance of 410 nm. For activity against pectic fractions equal amounts of protein (PAE8, PAE9, and empty vector) were incubated for 18 hours with 40 µL of pectic fraction (0.039-0.078 µg acetic acid / µL) in a total volume of 60 µL containing 50 mM ammonium formate, pH 4.5, for

PAE9 and pH 5.0 for PAE8). After incubation the total released acetate was measured using the Acetic Acid Kit (K-Acet, Megazyme; 2.5.5).

2.7 Morphological measurements

Plant inflorescence heights were measured at 35 days using a common ruler. The measurements were taken from the base of the inflorescence to the highest flower.

2.8 Powdery Mildew resistance assays

Resistance to powdery mildew was assayed by inoculating 3 week old *A. thaliana* plants (2.1.1) with *Golovinomyces cichoracearum.* The inoculation was done via mechanical dispersal of fungal spores grown in curcurbits. After 10 days the plants were visually inspected for signs of resistance to the fungus.

3.0 Investigating cell wall acetylation in *A. thaliana*

3.1 Background

One commonly used approach to gain insight into a biological process is forward genetics (Alonso-Blanco and Koornneef 2000). Forward genetics consists of identifying an individual plant mutant with an altered trait and then mapping the genetic modification/s associated with that trait. The trait investigated can be controlled by one or more genes/genetic elements. Such an approach shed light into many fundamental biological processes in plants (Meinke et al. 1998). One of the first examples of a successful forward genetics approach in the plant cell wall (1.1) field was the use of monosaccharide composition analysis to reveal genes involved in polysaccharide biosynthesis and metabolism (Reiter et al. 1997). This screen uncovered previously unknown genes involved in XyG biosynthesis and nucleotide sugar synthesis. A screen that looked at altered XyG structures (AXY) revealed additional genes involved in XyG biosynthesis and metabolism (Gunl et al. 2011; Gunl and Pauly 2011). The XEG screen which utilized a chemical genetics approach by culturing mutants in liquid media containing an enzyme which attacked specific cell wall components, revealed a glycosylltransferases involved in structural protein (extensin) glycosylation in the wall (Gille et al. 2009). In another very successful forward genetics approach, the IRX screen, which explored irregular xylem patterns in mutants, revealed many genes involved in cell wall biosynthesis in particular in the synthesis of xylan and cellulose in secondary walls (Brown et al. 2007; Brown et al. 2009; Lee et al. 2007a; Persson et al. 2007a; Taylor et al. 2003; Turner and Somerville 1997).

Forward genetics can also be used to characterize quantitative trait loci (QTL), i.e. genetic loci that harbor genetic elements that contribute to a single quantitative trait. One way to identify QTLs is to explore the natural diversity present within the *Arabidopsis* population (Alonso-Blanco and Koornneef 2000). Collections of *Arabidopsis* ecotypes from around the world amount to over 7000 accessions varying in phenotype and genotype (Weigel 2012). Many resources are now available for QTL mapping in *Arabidopsis* including approximately 60 Recombinant Inbred lines populations [RILs; (Weigel 2012)]. These populations consist of lines with recombinant chromosomes containing genomic segments of multiple accessions of interest, each line with a different chromosomal region integrated, creating a patch work of genetic material which aids in determining which genomic region is responsible for controlling a specific trait. An advantage of RIL populations in *Arabidopsis* is that once established and genotyped, phenotypic studies for QTL mapping can be undertaken without the need for additional genotyping. Over 49 traits have been studied in *Arabidopsis* using the available natural accessions (Weigel 2012). A few examples include QTLs for flowering time (Clarke et al. 1995), plant longevity (Luquez et al. 2006), trichome density (Hilscher et al. 2009) and seed dormancy (Alonso-Blanco et al. 2003).

The cell wall polymer XyG (1.3) has proven to be a good model polymer for genetic studies. Alterations in XyG structure and quantity lead only to minor morphological and developmental consequences in plant growth thus avoiding extensive pleiotropic effects (Cavalier et al. 2008; Gille et al. 2011b; Gunl et al. 2011; Gunl and Pauly 2011). For example, the discovery that complete lack of XyG acetylation

by lesions in the *AXY4* gene lead to no detectable developmental phenotype in the mutant plants under the conditions grown positioned this wall polymer as a good target for forward genetics (Gille et al. 2011b). Techniques that can generate XyG fingerprints have also been developed and are able to be executed in a high throughput manner (Lerouxel et al. 2002).

The *Arabidopsis* natural accessions were explored here to map genes or QTLs involved in wall polysaccharide acetylation (total stem wall acetate and XyG OLIMP; 1.5). By utilizing a forward genetics approach we expect to find novel and/or unexpected components of the biochemical/regulatory pathway. The power of this approach lies in the observation of a phenotype related to the trait of interest, however the phenotype could be caused by an unexpected source, like an enzyme of unknown function or a regulatory protein.

3.2 Results

3.2.1 *Arabidopsis* ecotypes vary in their stem wall acetate content

A collection of 117 *Arabidopsis* ecotypes was screened for stem wall acetate content for Quantitative Trait Loci (QTL) mapping (Figure 3.2.1-1). Stem tissue was selected due to its abundance in secondary walls, which are more relevant in plant biomass to fuels related research. The first two internodes of the main inflorescence were used for wall acetate content analysis (2.5.1.1; 2.5.5; Figure 3.2.1-1).

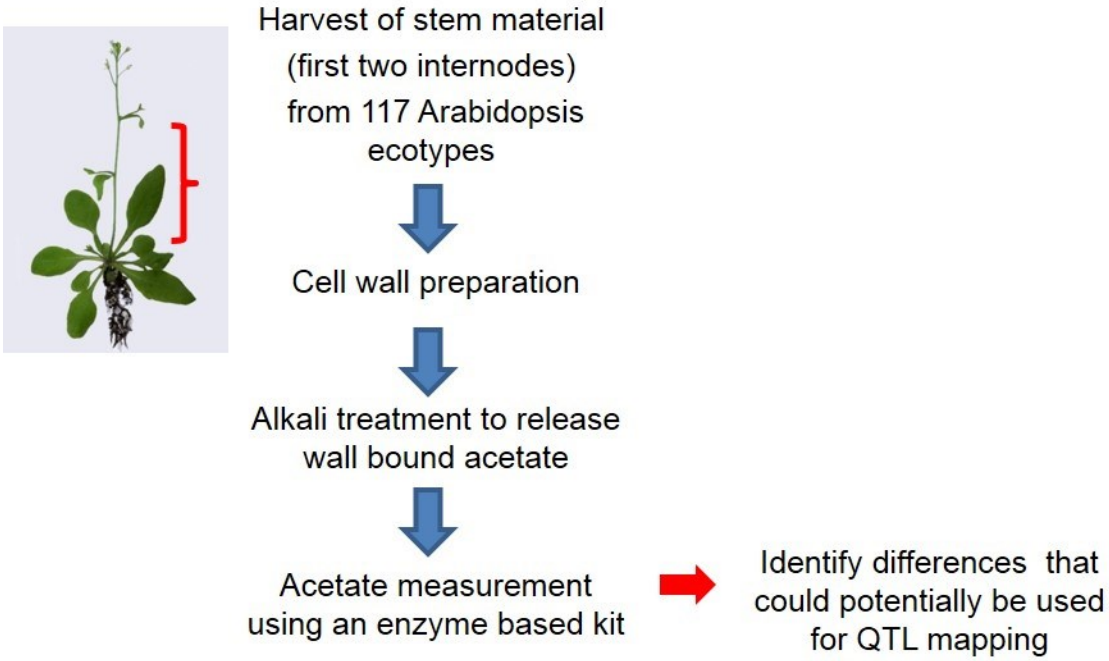

Figure 3.2.1-1 General scheme of the stem wall acetate assessment of *Arabidopsis* Ecotypes.

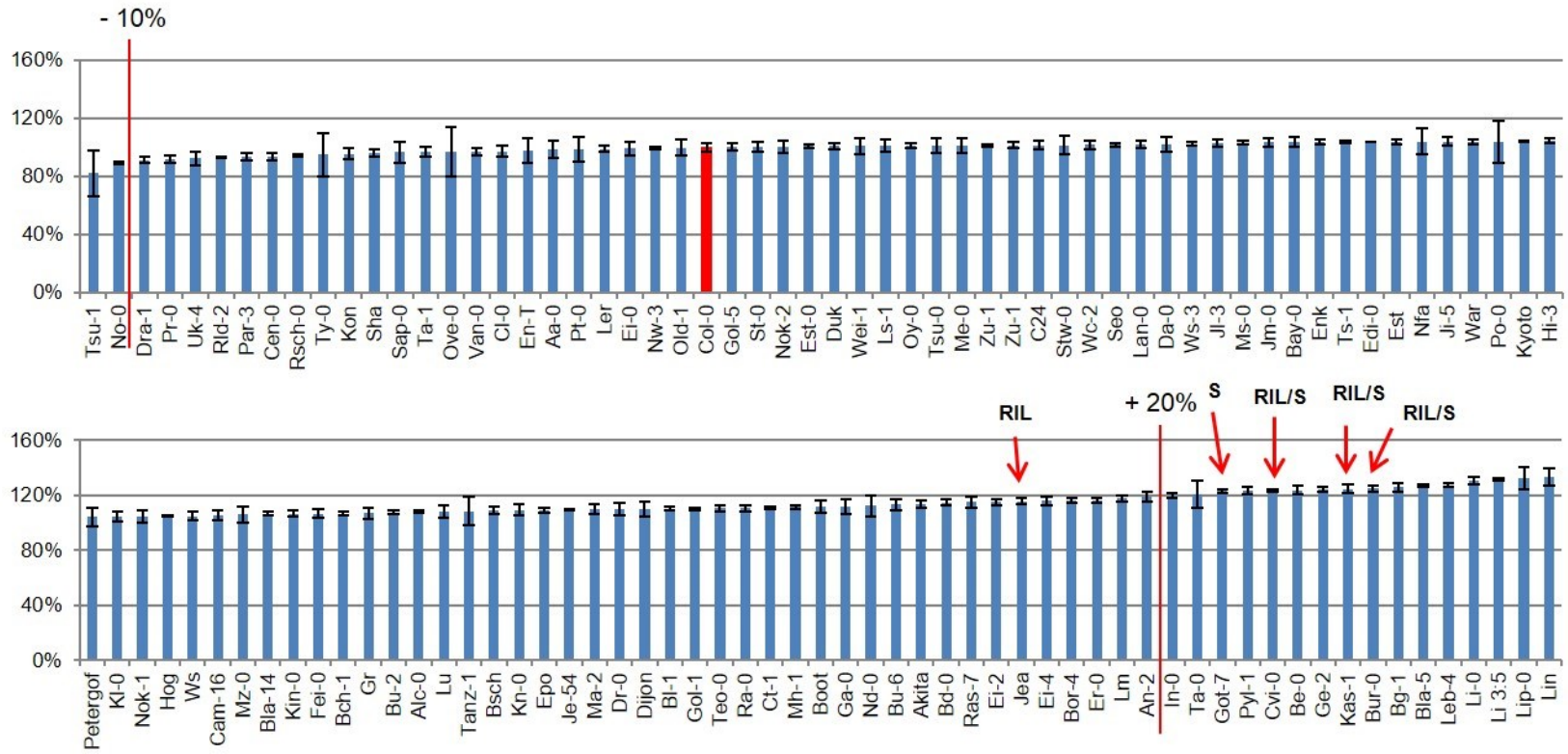

Figure 3.2.1-2 Relative acetate content of *Arabidopsis* ecotype stems. Graph indicates relative differences to Col-0 (red bar, Col-0 = 100%). Red lines indicate arbitrary limits of interest. Red arrows indicate Ecotypes that have genome sequence (S) or recombinant inbred lines available for QTL mapping (RIL). A total of 117 ecotypes are depicted. n=3.

Within the *Arabidopsis* ecotype population the stem acetate content varied from 82.1% (Tsu-1) to 133.1% (Lin) relative to Col-0 [(Col-0 = 100%); Figure 3.2.1-2]. Potentially interesting outliers were arbitrarily set at -10% and +20% from Col-0 acetate levels. On the lower end Tsu-1 (-17.9%) and No-0 (-11%) exhibited the lowest stem acetate levels. Sixteen ecotypes had acetate values greater than 20 % with Lin exhibiting the highest value (+33.1%). Based on the availability of genome sequences and recombinant inbred line populations, five ecotypes (Jea, Got-7, Cvi-0, Kas-1 and Bur-0) were selected and their increased stem acetate phenotype was confirmed in a new experiment (Figure 3.2.1-3). Hence, these ecotypes and/or their recombinant inbred lines represent a valuable resource for the potential identification of QTLs related to stem wall acetate content.

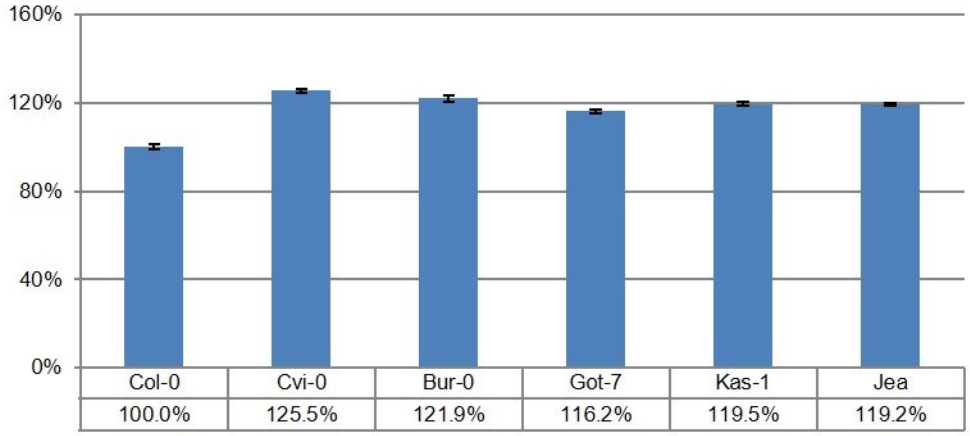

Figure 3.2.1-3 Relative wall acetate content of selected ecotype candidates for QTL mapping. Col-0 = 100%, all ecotypes shown are significantly different from wild type based on T test (p-value < 0.05). n=3.

3.2.2 Identification of XyG acetylation differences in a collection of *A. thaliana* ecotypes

Differences in XyG acetylation were assessed using the genetically diverse population of *Arabidopsis* ecotypes (Figure 3.2.2-1). OLIMP was used as a high throughput method to probe the acetylation status of XyG (2.5.1.2; 2.5.6). Etiolated seedlings where selected as tissue material due to overall uniformity, fast production, presence of acetylated XyG structures and ease of collection. Based on the XyG oligosaccharide mass spectrum the percentage of XyG acetylation was calculated using the peak area ratio of acetylated (XXLG, XXFG, XLFG) to total oligosaccharides that could be acetylated [XXLG, XXLG, XXFG, XXFG, XLFG, XLFG; Figure 3.2.2-2; 2.5.6; (Gille et al. 2011b)]. The range of percent XyG acetylation within the population varied from 12 % to 43 % (Figure 3.2.2-3). Col-0 was positioned in the top third of the data set with a 31.2 % XyG acetylation level (Figure 3.2.2-3). One notable case was Ty-0 exhibiting the lowest value observed in the screen with 12 %.

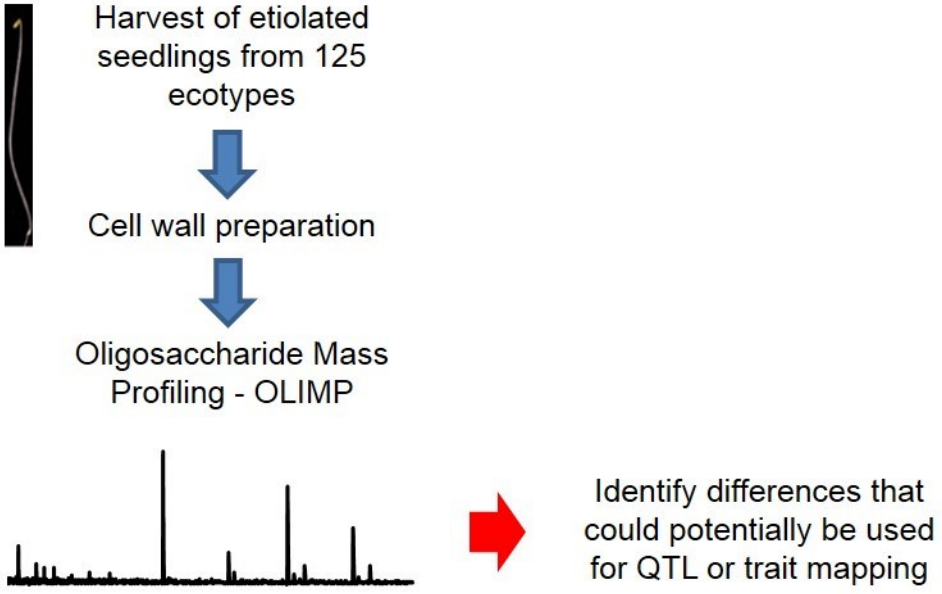

Figure 3.2.2-1 General scheme of the XyG acetylation assessment of *Arabidopsis* ecotypes.

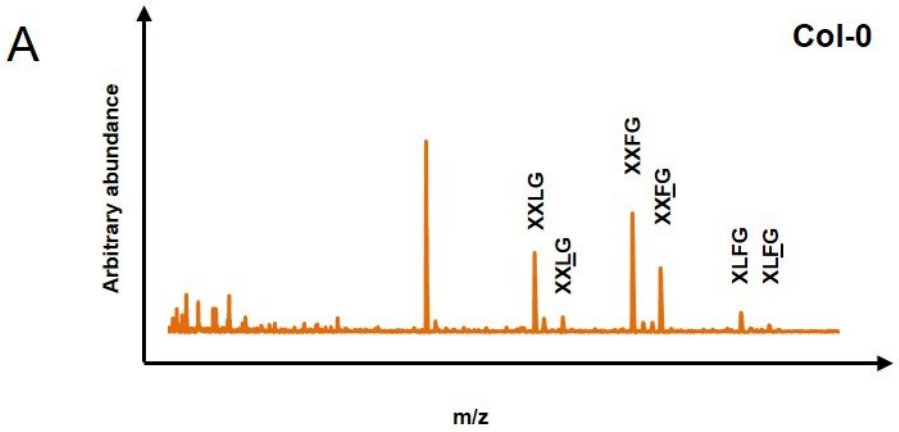

B

$$\text{Percent XyG Acetylation} = \frac{\text{XXLG + XXFG + XLFG}}{\text{XXLG + XXLG + XXFG + XXFG + XLFG + XLFG}} \times 100$$

Relative abundance of XyG oligosaccharides released by XEG digest

Figure 3.2.2-2 Example of XyG mass spectrum and calculation of the percent XyG acetylation. A) Mass spectrum of Col-0 7 day old etiolated seedling showing ion signals representing the XyG oligosaccharides used for the calculation of the percent XyG acetylation (Gille et al. 2011b). B) Percent XyG acetylation calculation; the ion signal intensity for each ion signal representing each oligosaccharide was integrated and used to calculate the relative degree of XyG acetylation. Oligosaccharides used in the calculations are indicated.

Figure 3.2.2-3 Percent xyloglucan acetylation of *Arabidopsis* Ecotypes based on OLIMP. Red arrows indicate limits of the variation found. Red bar represents the average for Col-0 over the screen independent experiments. Total of 127 Ecotypes are shown. n≥6

XyG OLIMP was performed on different tissues of the Ty-0 plant [7 day old seedlings (2.5.1.2); 3 weeks old roots, 5 weeks old leaf, and dry seed (2.5.1.3)]. The results revealed the absence of XyG acetylation in roots and leaves. However, as noted before XyG was still acetylated in 7 day old etiolated seedlings (Hypo) and seeds (Figure 3.2.2-4).

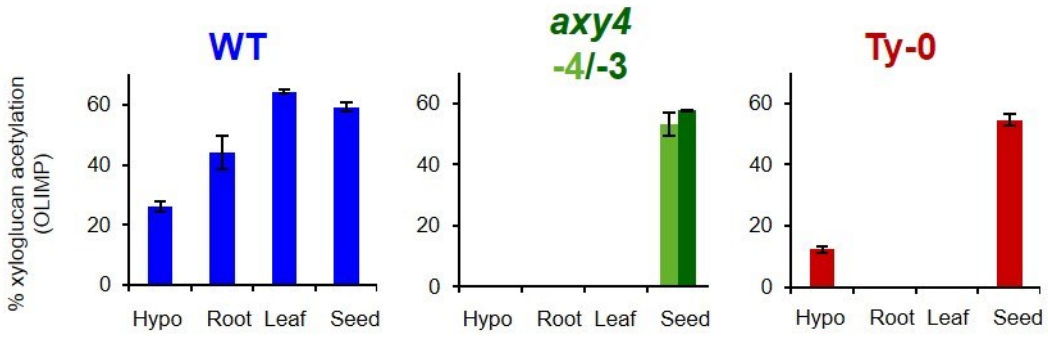

Figure 3.2.2-4 Percentage of XyG acetylation based on OLIMP in different tissues of Col-0, *axy4* alleles and Ty-0. *axy4-3*, SALK_044972; *axy4-4*, SALK_070873; Hypo = 7 day etiolated seedlings; root = 3 weeks old roots; leaf = 5 weeks old leaves; seed = dry seed. n≥5. Data adapted from (Gille et al. 2011b).

Recently, a putative XyG acetytransferase (1.3) was identified within the TBL family in *A. thaliana* (Gille et al. 2011b). A forward genetics approach (AXY screen) had led to the identification of a mutant with reduced XyG acetylation (Obel et al. 2006). The mutation causing this chemotype was mapped to the *TBL27* gene in *A. thaliana*. Knockout alleles of *AXY4*/*TBL27* were identified (*axy4-3* and *axy4-4;* Figure 3.2.2-5) from T-DNA mutant collections and exhibited complete lack of XyG acetylation [Figure 3.2.2-4 (Gille et al. 2011b)]. Interestingly, these knockout lines for *AXY4*/*TBL27* still had XyG acetylation in their seeds [Figure 3.2.2-4; (Gille et al. 2011b)]. It was later determined that another member of the TBL family (*AXY4like*/*TBL22*) was responsible for XyG acetylation in the seed tissue (Gille et al. 2011b). These two genes act on XyG. However, their expression is tightly controlled in the different tissues causing the spatial separation in XyG acetylation (Gille et al. 2011b; Winter et al. 2007). AXY4 is a type II membrane protein localized to the Golgi apparatus and it is believed to act as a XyG acetyltransferase (Gille et al. 2011b; Gille and Pauly 2012). The chemotypes observed for Ty-0 were very similar to the ones observed for AXY4, with lack of XyG acetylation in roots and leaves, suggesting that Ty-0 could harbor a natural mutation in the *AXY4* gene. Therefore, the *AXY4* genomic sequence was verified in the publically available genome sequence of Ty-0 (Salk Arabidopsis 1001 Genomes 2014) and confirmed through sequencing of the *AXY4* locus (2.2.1.1; 2.2.6; 2.4). The sequence data revealed that the *AXY4* locus in Ty-0 contains 3 single nucleotide polymorphisms that lead to 2 amino acid changes in the highly conserved DUF231 domain of the protein (Figure 3.2.2-5).

An allelism test was performed by crossing Ty-0 to *axy4-3*, an *AXY4* knockout-allele. The resulting F1 plants were analyzed for their XyG acetate content (Figure 3.2.2-6; 2.5.1.3; 2.5.6). TheTy-0 x *axy4-3* F1 plants lacked XyG O-acetyl substituents in rosette leaves (Figure 3.2.2-6), confirming that the Ty-0 *AXY4* allele is allelic to *AXY4*.

As a control, F1 plants of a cross between Col-0 and Ty-0 exhibited wild type XyG acetylation levels demonstrating the recessive nature of the Ty-0 mutation (Figure 3.2.2-6).

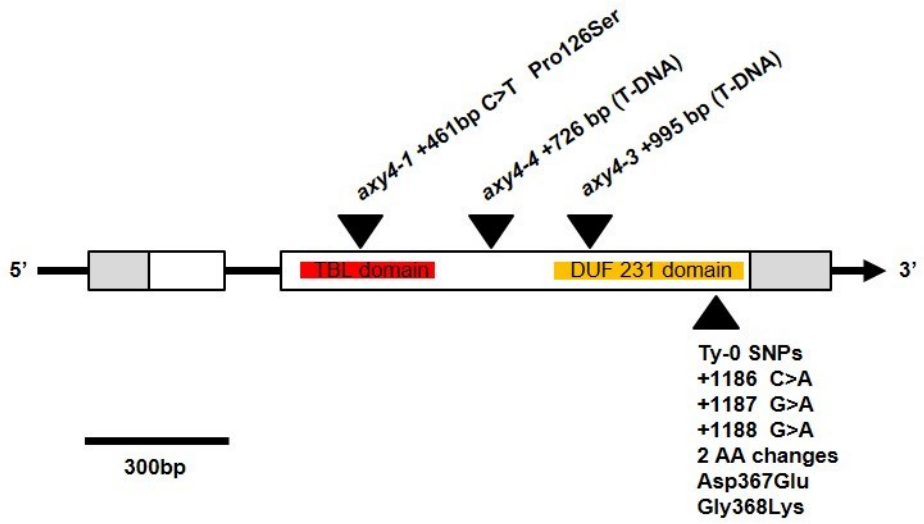

Figure 3.2.2-5 Schematic cartoon of the *AXY4* gene. Black triangles indicate lesion positions within the DNA sequence. Grey areas represent untranslated regions, white boxes represent coding sequences. Colored boxes indicate the relative position of the highly conserved protein domains TBL and DUF 231 (Bischoff et al. 2010a). *axy4-3* - SALK_044972; *axy4-4* - SALK_070873. Data adapted from (Gille et al. 2011b)

Increased XyG acetylation chemotypes were also encountered in the screen, seven ecotypes had at least 20% higher XyG acetylation levels than the reference Col-0 (Figure 3.2.2-3). The ecotypes with elevated XyG acetate represent candidates for the mapping of monogenic traits or QTLs depending on how their chemotypes segregate. Three ecotypes (Er-0, Ra-0 and Ta-0) were selected for further analysis based on the consistency of their chemotypes and availability of complete genomic sequences. Samples of mass spectra (2.5.1.2; 2.5.6) from three selected ecotypes displaying chemotypic differences are shown in Figure 3.2.2-7. The *Arabidopsis* ecotype Ra-0 has a higher degree of XyG acetylation, there is 87.5 % more acetylated XXFG in Ra-0 when compared to Col-0. The ratio between XXFG and XXFG is altered in Er-0 (1.03) and Ta-0 (0.89) when compared to Col-0 [(0.51); Figure 3.2.2-7].

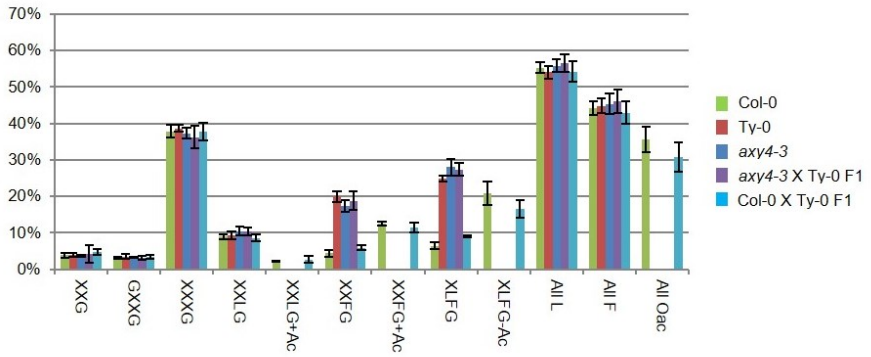

Figure 3.2.2-6 Allelism test between *axy4-3* and Ty-0. Relative abundance of XyG oligosaccharides based on mass spectra obtained by MALDI-TOF after XEG digest of 18 day old leaves of F1 plants from Col-0 x Ty-0, *axy4-3* x Ty-0, and single mutants. All L = all galactosylated oligosaccharides; All F = all fucosylated oligosaccharides; All Oac = all acetylated oligosaccharides; n=5

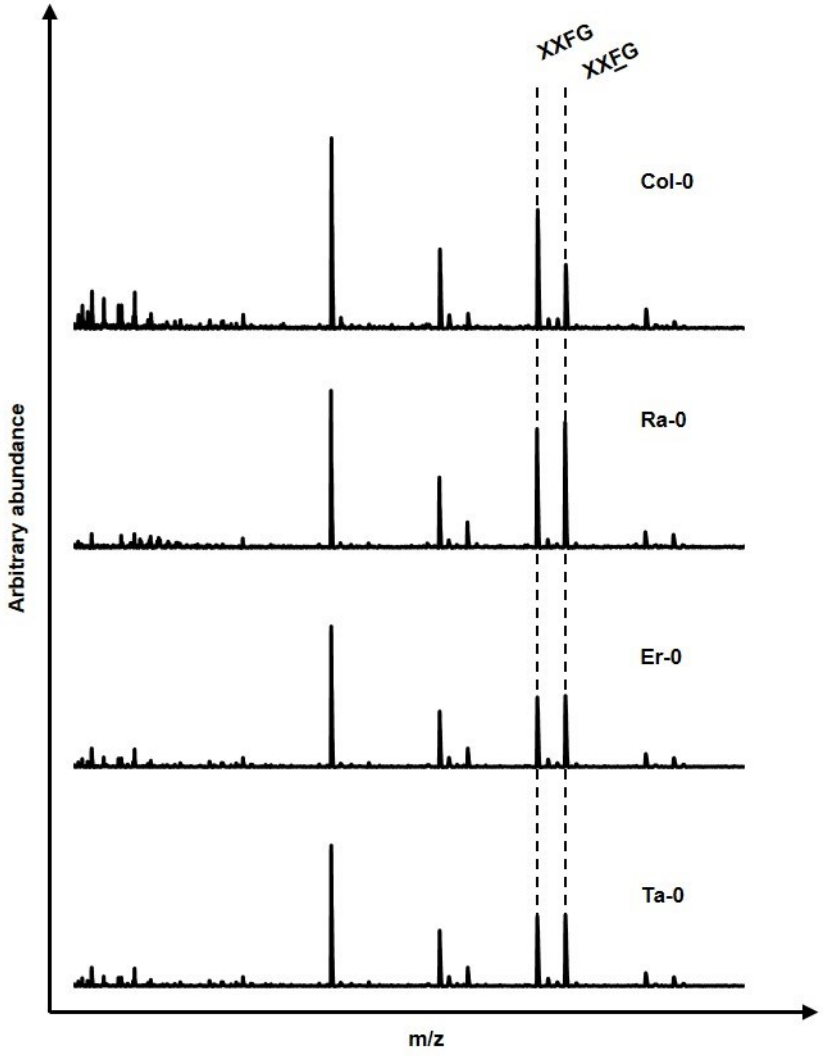

Figure 3.2.2-7 Mass spectra of XyG oligosaccharides from selected highly acetylated XyG containing ecotypes. Example of mass spectra obtained by MALDI-TOF after XEG digest of 7 day old *Arabidopsis* etiolated seedlings. Dotted lines indicate the position of the acetylated and non-acetylated XXFG oligosaccharide. The selected ecotypes exhibit an altered ratio of XXFG/XXFG (Ra-0, 1.06; Er-0, 1.03; Ta-0, 0.89; n=6) when compared to Col-0 (0.51; n=6).

In an attempt to verify if chemotypic differences in XyG acetylation amongst the high acetate ecotypes were stronger in other tissues (2.5.1.3; 2.5.6), which could facilitate the mapping efforts, leaves, flowers and roots were tested (Figure 3.2.2-8; Appendix 5). In leaves, Er-0 had a 26.5% reduction in XyG acetylation when compared to WT. Indeed the differences in the XyG of the Er-0 leaf could represent a good opportunity for mapping since this tissue can be easily collected and the acetylation differences are strong. It remains to be determined if the Er-0 leaf chemotype segregates in a monogenic manner. The biggest differences in flowers were shown for Er-0 (-26.3%) and Ta-0 (-30%). Despite these seemingly large differences observed in flowers this tissue has a low relative abundance of acetylated oligosaccharides (16% less) when compared to seedlings (Figure 3.2.2-3; Figure 3.2.2-8; Appendix 5), which could increase undesirable variation in chemotype detection. A small 10% reduction was also found for Er-0 in roots. However, the phenotypic intensity is lower than the one identified for seedlings (>20% increase in XyG acetylation; Figure 3.2.2-3). Surprisingly, the differences in XyG acetylation in other tissues of the high acetate ecotypes were reductions, which contrast directly to the increase in acetylation found in seedlings (Figure 3.2.2-3; Figure 3.2.2-8; Appendix 5). These different acetylation patterns could represent variations in gene expression and activity between ecotypes. For mapping purposes the reduced leaf chemotype of Er-0 and the increased acetylation of its seedlings could potentially be useful for the identification of novel genes involved in XyG acetylation. Of particular interest was the increase of acetylation in seedlings of this ecotype since a potential cause could be a mutation in a XyG acetylesterase (1.3, 1.5), which has not been identified.

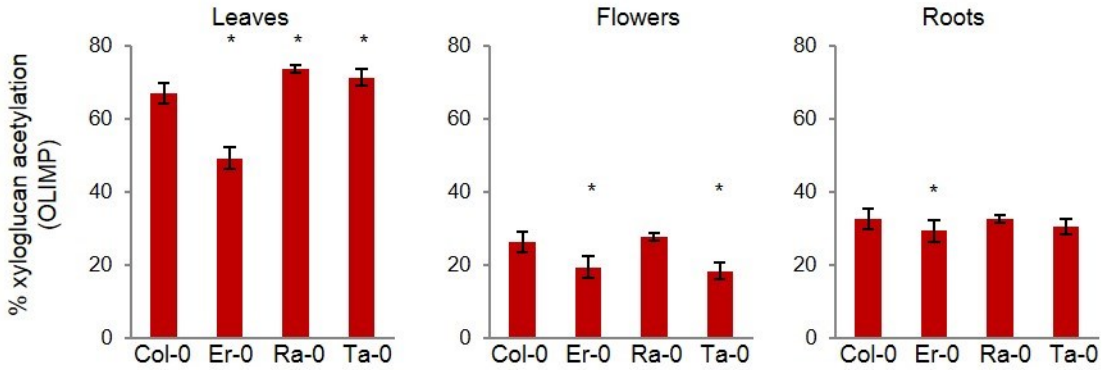

Figure 3.2.2-8 Percentage of XyG acetylation of selected high acetate ecotypes in various tissues.The figure depicts the % of acetylated oligosaccharides released after XEG digest in various tissues (leaf, 27-31 days old; flowers, 5-7 weeks old; roots, 2 weeks old). Noticeable differences were found in leaves and flowers. * indicates statistical significant differences based on T test (p-value < 0.05), n≥4.

All three ecotypes were crossed to Col-0 to verify, if the observed seedling increased acetate traits were monogenic. Only the Ta-0 chemotype seems to be segregating as a monogenic trait. The Er-0 and Ra-0 cross to Col-0 produced F2 populations with varying XyG acetylation patterns which suggest the effect of multiple genes (Appendix 5). The cross between Col-0 and Ta-0 resulted in a F2 population segregating in a monogenic manner based on the ratio between XXFG and XXFG

(Figure 3.2.2-9). Six (30%) individuals from the F2 population harbored a Col-0-like chemotype while 14 (70%) exhibited Ta-0-like phenotype (χ^2=0.26). These findings suggest that the natural variation in *Arabidopsis* has proven useful in revealing mapable XyG chemotypic differences generated by single and multiple genes. The Ta-0 hypocotyls show an increase in XyG acetylation that could be mapped as a monogenic trait and Er-0 and Ra-0 show increased XyG acetylation that could be contributed by QTLs.

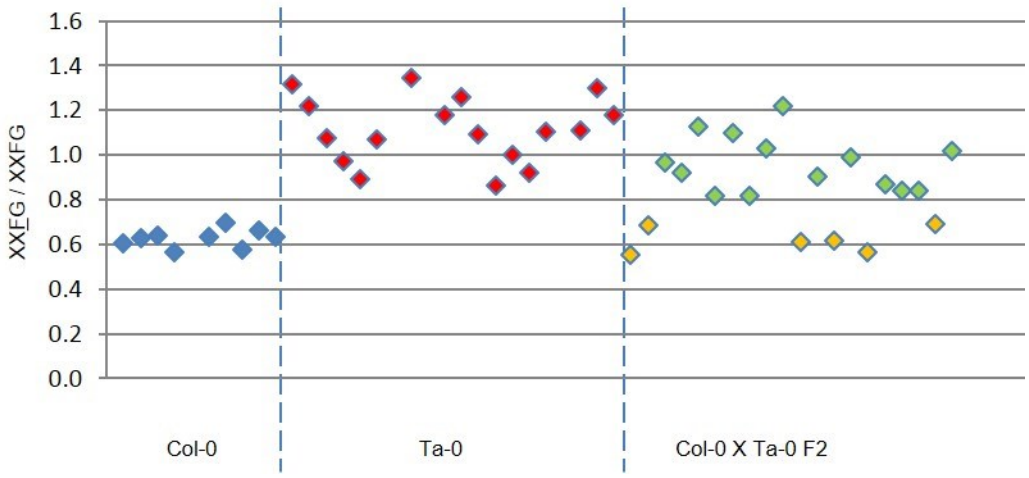

Figure 3.2.2-9 Phenotypic analysis of F2 plants from a Col-0 X to Ta-0 cross.The ratio between the XXFG / XXFG oligosacharides based on mass spectra obtained by MALDI-TOF after XEG digest of 7 day old etiolated *Arabidopsis* seedlings was determined. Blue diamonds represent Col-0; red diamonds represent Ta-0; green diamonds represent F2 plants with Ta-0 like chemotypes (14); orange diamonds represent F2 plants with Col-0 like chemotypes (6). Col-0 X Ta-0 F2 segregates in a monogenic manner.

3.3 Discussion

3.3.1 Natural variation in *Arabidopsis* is a resource for QTL mapping of total cell wall acetate in stems

There is a considerable amount of variation in wall acetylation within the *Arabidopsis* ecotype population tested (Figure 3.2.1-2). The spread of acetate content is in agreement with other data such as trichome density found for quantitative traits in *Arabidopsis* (Hilscher et al. 2009). This indicates that total stem acetate can be considered a quantitative trait.

Among the ecotypes tested a few had complete, publicly available genomic sequences [Figure 3.2.1-2; (Salk Arabidopsis 1001 Genomes 2014)]. In addition, some recombinant inbred populations were available, which could be used for QTL mapping [Figure 3.2.1-2; (Versailles Arabidopsis Stock Center 2014)]. A number of ecotypes (16) presented increases of 20% in total stem acetylation when compared to the reference accession Col-0. Col-0 served as a control in every experiment during the screen and deviates from the raw data average and median by -5.6% and -7.8%, respectively. This places this ecotype in a relatively central position within the data set. Furthermore, the majority of the RIL populations available are based on crosses with Col-0. In particular one ecotype, Cvi-0, with a wall acetate difference of +23% compared to Col-0 presented itself as a potential candidate for further studies as a RIL population with Col-0 and a full genomic sequence were available.

Mapping those QTLs could reveal genes involved in the wall polymer O-acetylation pathway. So far, the characterization of single mutants has provided insights into the proteins involved in this process (Figure 1.5-1). This same model however could still be incomplete. The recent finding of AXY9 for example, a protein of unknown function proposed to involved in intermediating acetate carriers inside the Golgi has opened new avenues of research (Schultink 2013). The biochemical activity of TBL proteins has not been demonstrated to date opening the possibility for the existence of other proteins involved in acetate transfer to wall polymers. Also the regulation of polysaccharide acetylation has not been explored. In light of this incomplete cell wall acetylation model, mapping acetylation QTLs could reveal novel players in this process.

Understanding the basic processes involved in plant cell wall acetylation could enhance the capacity to engineer or breed for plants with reduced levels of acetate in the wall. Economic models have shown that reducing acetate content in biomass will reduce costs in lignocellulosic biofuel production (Klein-Marcuschamer et al. 2010). Demonstrating that acetylation QTLs can be found in *Arabidopsis* will serve as a basis for the identification of molecular markers responsible for wall acetylation thus advancing breeding programs (Dwivedi et al. 2008). Many agronomically important crops like maize (Agrama et al. 1999), rice (You et al. 2006) and sorghum (Zou et al. 2012), which can be used in lignocellulosic biofuel production, have RIL populations that could be used to map QTLs associated with acetylation. This represents a significant tool for improving crop biomass for bioenergy related processes.

3.3.2 *Arabidopsis* ecotypes harbor differences in XyG acetylation that could be used for single gene and QTL mapping

The percentage of XyG acetylation of 7 day old etiolated seedlings showed a wide range of variability (Figure 3.2.2-3). XyG acetylation varied from 12 to 43 % among the ecotypes tested. At the low end of XyG acetylation was Ty-0, an ecotype that had approximately 40% less XyG acetylation than the reference ecotype Col-0. A forward genetics approach had led to the identification of a putative *O*-acetyltransferase, AXY4 (Gille et al. 2011b). As shown by sequencing (Figure 3.2.2-5) and through allelism tests (Figure 3.2.2-6) the Ty-0 phenotype is also caused by mutations in the *AXY4* gene. However, the Ty-0 ecotype exhibited some phenotypic differences to the *axy4* mutant. It had residual XyG acetylation in 7 day old etiolated seedlings, which is not the case for the *axy4-3* mutant (Figure 3.2.2-4). A possible explanation is that the Ty-0 allele is not entirely inactive in this particular tissue. Determination of the *in vitro* activity of the Ty-0 allele would test this possibility. Alternatively, differential regulation of gene expression might occur in the two ecotypes. AXY4LIKE is responsible for XyG O-acetylation in the seeds of Col-0 (Gille et al. 2011b) and is expressed exclusively in the seeds making it non-redundant to the *AXY4* expression pattern in Col-0 (Winter et al. 2007). The mutant phenotypes for *AXY4* and *AXY4L* exhibit clear spatial separation of XyG acetylation (*axy4* lacks leaf, root and seedling XyG acetylation while *axy4L* is only deficient in seed XyG acetylation) the same is true for the expression pattern of the genes (Winter et al. 2007). When AXY4LIKE is expressed under the control of the *AXY4* promoter in the *axy4-3* background it is able to complement the mutant phenotype (Dr. Guangyan Xiong, Pauly Lab, Personal communication) showing that this protein is involved in the acetylation of the same substrate as *AXY4*. It is possible that AXY4LIKE is not entirely transcriptionally suppressed in Ty-0 of 7 day old etiolated seedlings as it is in Col-0. When comparing the genomic sequence of Ty-0 and Col-0, at least 12 SNPs can be found in the putative promoter region (4585 bp) of *AXY4LIKE* in the Ty-0 ecotype (Salk Arabidopsis 1001 Genomes, 2014). This may hint that expression of AXY4L may be altered in these two ecotypes. Q-RT PCR analysis of the *AXY4L* transcript in seedlings of Ty-0 could reveal if the different chemotypes found are based on differential gene expression patterns.

Ty-0, a naturally occurring *Arabidopsis* ecotype found in the highlands of Scotland, lacks XyG acetylation in leaves and roots suggesting that the lack of XyG acetylation does not compromise the fitness of the ecotype at least in the ecological niche found. Indeed, small or no developmental defects have been observed in mutants harboring structural XyG alterations (Cavalier et al. 2008; Gille et al. 2011b; Gunl et al. 2011; Gunl and Pauly 2011). However, in general, *Arabidopsis* ecotypes harbor 1 SNP for every 200 bp in their genomes when compared to the reference Col-0 (Weigel 2012), not excluding the possibility that other mutations in Ty-0 could compensate for the effect of lack of XyG acetylation under natural growth conditions. Mutations in *Arabidopsis* ecotypes producing large phenotypic effects have occurred after collection from natural environments (Laitinen et al. 2010), suggesting prudence when making any evolutionary assumptions in this case.

At the increased acetylation end of the spectra there were ecotypes revealed by the screen with phenotypic differences that could be explored for single trait or QTL

mapping. This natural variation could be utilized in identifying (novel) genes involved in XyG acetylation. Such a forward genetics approach has been repeatedly applied with success to unravel novel plant biological processes [3.1; (Weigel 2012)]. Three ecotypes (Er-0, Ra-0 and Ta-0; Figure 3.2.2-3) were selected based on their XyG acetylation alterations compared to Col-0 and the availability of their complete genomic sequences. No RIL populations are available of the selected ecotypes at this point, which complicates QTL mapping (Weigel 2012). In the Ta-0 ecotype it is possible that the high XyG acetate levels are a result of mutations in a single gene. Such presumed mutations would lead to an up-regulation of the O-acetylation machinery or suppress the removal of acetates through e.g. the action of a XyG O-acetylesterase, which has not been identified to date.

XyG acetylation varies among different plant tissues (Gille et al. 2011b; Pauly et al. 2013). Leaf, flower and root tissue were examined in the selected high acetate ecotypes and surprisingly, in all examined tissues decreases in XyG acetylation were encountered (Figure 3.2.2-8). This result was in contrast to the initial increased acetate chemotype found for the 7 day old etiolated seedlings with an average of 27% increase of XyG acetate content compared to Col-0 (Figure 3.2.2-3; Figure 3.2.2-7). These results present the possibility that Col-0 can harbor a non or partially functional acetylesterase in these tissues were the acetate was higher or that differences in gene expression and activities exist in these ecotypes resulting in the observed changes.

Due to the low relative abundance of ion signals representing acetylated XyG oligosaccharides such as XXFG and XLFG in the mass spectra of flowers, the XyG acetylation chemotype in flowers of Er-0 and Ta-0 would be undesirable for mapping purposes despite being large (26.3% and 30 %, respectively). In leaves, the reduction of 26.5 % in XyG acetylation between Er-0 and Col-0 might represent a tractable phenotype for trait mapping since leaves allow for mutant selection in the F2 population without destruction of the plant allowing a concomitant genotypic assessment. Moreover, leaf tissue contains abundant acetylated XyG oligosaccharides (Figure 3.2.2-8). It remains to be determined if the leaf chemotype in Er-0 segregates in a monogenic manner. The analysis of 7 day old etiolated seedlings in the F2 population from the cross between Col-0 and Er-0 showed that the acetate chemotype is likely to be a product of multiple genes due to its ample variation (Appendix 5). The same was observed in 7 day old etiolated seedlings in the cross between Ra-0 and Col-0 (Appendix 5). In these two cases QTL mapping would be necessary instead of single trait mapping.

Analysis of 7 day old etiolated seedlings derived from the cross between Ta-0 and Col-0 suggested that the acetylation phenotype segregated in a monogenic recessive manner (χ^2=0.26; Figure 3.2.2-9). The recessive chemotype was identified as Col-0 with lower acetate. One of the impediments in mapping this trait would be the destructive nature of the etiolated seedling analysis. The F2 mapping population would have to be selected based on the F3 individuals chemotype, increasing the necessary work in the mapping process (Kraemer 2008). The large number of SNPs present between ecotypes (1 in every 200 bp on average), would represent an additional challenge for this project. Since the target gene or genetic element causing the chemotype could be unknown, it would be difficult to select candidate genes in a given genomic are with multiple SNPs per gene. After rough mapping which uses ~ 5 markers

per chromosome and 20-40 mutants from an F2 population to delimitate genomic areas in the Mbp range, a much finer mapping effort would be required in order to identify the genetic mutation causing the chemotype.

The forward genetics approach attempted in this study proved to be fruitful by uncovering a natural allele of a recently characterized putative XyG acetyltransferase and by revealing that ecotypes harbor XyG acetylation differences that could be useful in QTL mapping. While the feasibility and challenges of avenues for obtaining new insight into cell wall polymer acetylation via QTL or trait mapping are outlined these were not further pursued in this study.

4.0 Functional investigation of protein domains in the TBL gene family

4.1 Background

The notion that enzymes can be separated into modules or domains, which harbor distinct functions, has been utilized for almost 50 years. One of the first reports regarding protein modular complementation *in vitro* came from studies of the *E. coli* β–galactosidase - non-functional fragments of the protein expressed separately regained activity, when recombined *in vitro* (Ullmann et al. 1967). This ground breaking work spawned the concept that protein modules could be used independently, swapped or fused. This realization opened the field of protein engineering using available, known modules in nature. However, its main contributions have been in determining protein interactions *in vivo* using techniques such as yeast two hybrid or split ubiquitin (Fields and Song 1989; Johnsson and Varshavsky 1994).

Another development, which helped to consolidate the theme of protein module functionality, entailed the use of fluorescent protein fusions for subcellular localization. This technique demonstrated the possibility of functional fusion of a fluorescent protein to another protein of interest, with both proteins often retaining their original properties (Chalfie et al. 1994; Lippincott-Schwartz et al. 2001). Deriving from these techniques Bimolecular fluorescence complementation (BiFC) was developed which explores protein module splitting and fluorescence reconstitution, when the two modules are brought back together (Hu et al. 2002). Förster resonance energy transfer (FRET) has also been used for determining protein interactions within complexes and is based on the excitation of a fused fluorescent protein by the fluorescence of another fused fluorescent protein within 10 nm distance (Oikawa et al. 2013). Molecular fluorescent sensors have been engineered based on these concepts of protein modularity (Deuschle et al. 2005).

In mammalian cells (Sandor et al. 2003) and in Drosophila (Tauszig et al. 2000) the functions of a few transmembrane receptors (Toll like and Toll, respectively) have been determined using domain swap approaches. In plants this approach has been very successful in characterizing receptor kinases (Kaiserli et al. 2009). For example, the BRI1 brassinosteroid receptor ectodomain was characterized by using a chimeric construct with the rice *XA21* defense gene, a disease resistance receptor; the chimera initiates defense responses in rice cells when treated with brasinosteroids (He et al. 2000). The function and mode of operation of a Wall-Associated Kinase (WAK1), which is thought to be involved in cell wall damage recognition (perception of oligogalacturonides) were also studied using domain swap approaches (Brutus et al. 2010). By treatment with oligogalacturonides plants transformed with a chimeric construct containing the WAK1 ectodomain (part of the transmembrane protein that is facing the apoplast) and the EFR kinase domain it was possible to induce defense responses usually associated with EFR-mediated signaling (Brutus et al. 2010). When the domains were inversed for the two proteins the opposite effects were observed. These experiments show that the domain swap approach can be used successfully in plants to obtain insights into the function of a protein module. This domain swapping technique was used here to investigate the function of protein modules within putative acetyltransferases, the TBLs.

The TBL gene family in *A. thaliana* contains 46 genes (Figure 4.1-1) and was originally annotated as Trichome Birefringence Like (TBL) due to its protein sequence similarity to the *tbr* mutant, which lacked trichome birefringence (Bischoff et al. 2010a). Genes in the TBL family have been implicated in various cellular processes. The *TBR* and *TBL3* genes have been associated with cellulose synthesis and deposition in secondary cell walls (Bischoff et al. 2010a). Another TBL, *YLS7*, has elevated expression pattern in senescing leaves in *A. thaliana* (Yoshida et al. 2001). PMR5, which is also a member of the TBL family, was identified in a screen for resistance to powdery mildew (*Erysiphe cichoracearum* and *Erysiphe orontii*) in *A. thaliana* (Vogel et al. 2004). While the function of these proteins remained at the time speculative, recently it has been proposed that they might represent wall polymer specific O-acetyltransferases (Gille et al. 2011b). Two genes of the TBL family were shown to play an exclusive and essential role in XyG acetylation: *AXY4* (*TBL27*) and *AXY4LIKE* [*TBL22*; (Gille et al. 2011b)] as their corresponding mutants lacked O-acetyl substituents on XyG and only on XyG. TBL29 has also been proposed to represent a xylan: acetyltransferase (Xiong et al. 2013; Yuan et al. 2013).

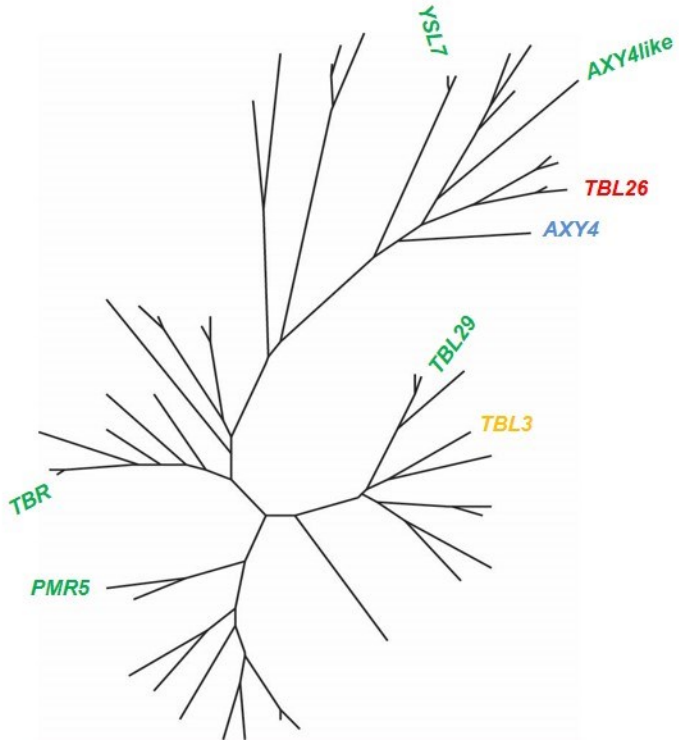

Figure 4.1-1 Phylogenetic tree of the TBL gene family. Genes labelled in green have proposed functions based on their observed phenotypes. Genes in red, blue and orange are part of the current study. Phylogenetic tree reprinted with adaptations from (Bischoff et al. 2010a)

All TBL proteins harbor a highly conserved GDS motif within the TBL domain in their N-terminal region, as well as a DxxH motif within the also highly conserved DUF231 domain located in the C-terminal region [Figure 4.1-2 A; (Bischoff et al. 2010a)]. By comparing the crystal structure of an *Aspergillus aculeatus* rhamnogalacturonan acetylesterase to the TBR protein it was proposed that the serine (S) in the GDS motif could work as a catalytic triad with the aspartate (D) and histidine (H) in the DUF231 domain (Bischoff et al. 2010b). The TBR protein however lacks extra glycine and asparagine residues thought to be used as proton donors in the catalytic site of the acetylesterases of the SGNH hydrolase family (Bischoff et al. 2010b). With the finding that TBL proteins represent putative acetyltransferases and that these motifs are largely conserved across taxa (Gille et al. 2011b; Gille and Pauly 2012) the possibility that these motifs could play a catalytic role has to be tested. To determine if the conserved amino acids in these motifs played a catalytic role a directed mutagenesis approach was conducted with the AXY4 protein. The approach consisted in modifying to alanine the GDS, the D and H in DxxH, and two conserved Ds between the TBL and DUF231 domains (Figure 4.1-2 A). The GDS conserved motif was also completely deleted in one of the constructs (Pauly Lab, Dr. Sascha Gille, personal communications). The modification to alanine or deletion would hypothetically render mutant proteins inactive and unable to fulfill their catalytic function. This would be ascertained by verifying if the mutants could complement the XyG acetylation chemotype in the *axy4-3* background which completely lacks XyG acetylation. As a control the *AXY4* cds was transformed into the same vector used for the directed mutagenesis approach and it was determined that complementation could be obtained (Figure 4.1-2 B, C). The results of this experimental approach showed that the conserved amino acids in the TBL (GDS) and DUF231 (DxxH) domains are essential for the function of AXY4 since mutations or deletion in the respective amino acids produced proteins unable to rescue the *axy4-3* chemotype. Only the two aspartates located between the two domains had no effect on protein activity when mutated (Pauly Lab, Dr. Sascha Gille, Personal communication).

The question arises, which part of the protein is responsible for polymer recognition and specificity. In order to address this question a domain swap approach was designed to shed light into the role of the different protein domains of this family.

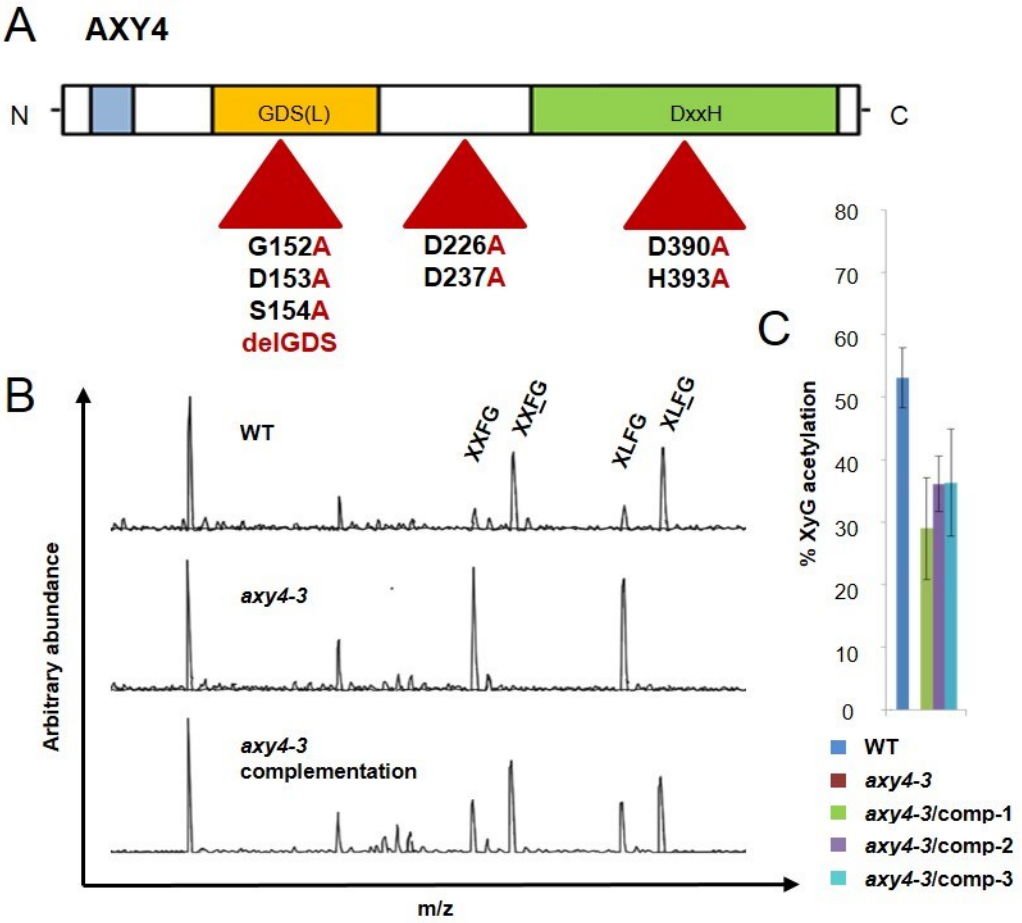

Figure 4.1-2 Directed mutagenesis approach to determine catalytic role of conserved amino acids within the TBL and DUF231 domain. A) Cartoon of the AXY4 protein, transmembrane domain is shown in blue; TBL domain is indicated in yellow and DUF231 in green. Mutated amino acids and their relative positions are indicated by red triangles, numbers indicate amino acid position. B) Sample mass spectra of 3 week old *A. thaliana* leaves, WT = Col-0; *axy4-3* complementation = *axy4-3* transformed with the *AXY4* cds in the pGWB510 vector (Appendix 3). C) Percent XyG acetylation of *axy4-3* complementation lines. Three independent lines are shown. *axy4-3*/comp = *axy4-3* transformed with the AXY4 cds in the pGWB510 vector. Data: Pauly Lab, Dr. Sascha Gille.

4.2 Results

4.2.1 Design of TBL chimeric constructs based on protein sequence analysis

In an attempt to address which protein domains are responsible for substrate recognition and enzymatic activity in a TBL, a functional complementation approach with chimeric TBL proteins was pursued (Figure 4.2.1-1). By swapping different sections of closely related and distant TBLs with the AXY4/TBL27 protein and assessing their capacity to complement the *axy4* mutant phenotype by restoring XyG acetylation it would be possible to gain insights into how certain domains are operating.

Initially, TBLs had to be identified that lend themselves to distinct domains to be swapped with AXY4. A phylogenetic tree of the TBL family was examined and two genes were selected based on relative sequence similarity and occurrence of mutant phenotypes (Figure 4.1-1). TBL3 (At1g01360) is phylogenetically distant (Figure 4.1-1) to AXY4 and is believed to act on xylan (Pauly Lab, Dr. Guangyan Xiong, personal communication). TBL26 (At4g01080) is closely related to AXY4 (Figure 4.1-1) and there is preliminary data from the Pauly lab (Dr. Monique Benz, personal communication) that suggested that it may act on mannan (Gille et al. 2011a). Since both TBLs are not thought to act on XyG placing their domains into AXY4 should give insights into which domain conveys TBL substrate specificity.

In order to establish boundaries of domains with a TBL protein, a protein alignment of members of the TBL family was produced (Appendix 4). Based on sequence conservation, four regions were selected (Figure 4.2.1-2; Appendix 4). The first fragment (A) contained the transmembrane and TBL domain in its entirety (3.49% identity and 7.53% similarity; 2.4; Figure 4.2.1-2; Appendix 4). The second fragment (B) was composed of an interdomain region, which is the less conserved stretch of the protein alignment (0% identity and 3.19% similarity; 2.4 Figure 4.2.1-2; Appendix 4). Fragments C (2.22% identity and 6.67% similarity; 2.4; Figure 4.2.1-2; Appendix 4) and D (9.16% identity and 16% similarity; 2.4; Figure 4.2.1-2; Appendix 4) were products of the DUF231 domain splitting (Appendix 4). The N-terminal part of the DUF231 domain, fragment C, is a less conserved region when compared to fragment D, thus could provide the variability necessary for recognition of the different substrates for the TBL family. The exact borders of the chosen domains are indicated in Appendix 4.

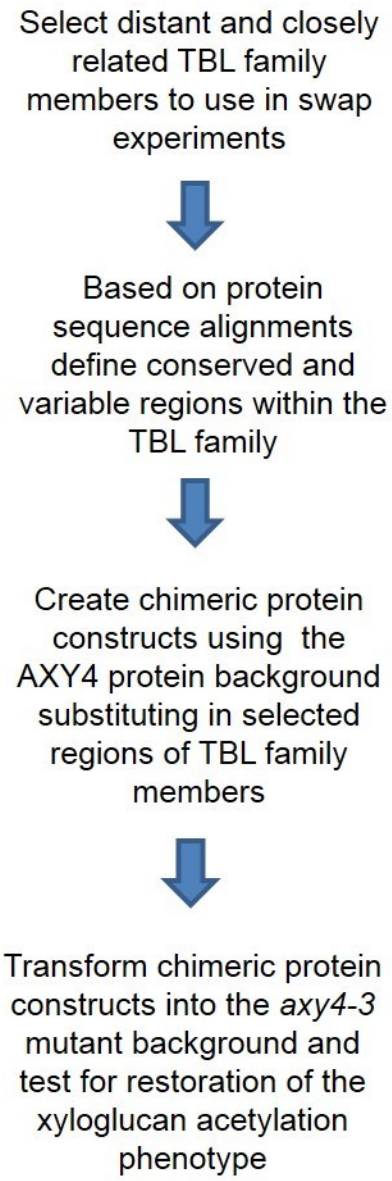

Figure 4.2.1-1 Overview of the approach used in the functional investigation of protein domains in the TBL gene family.

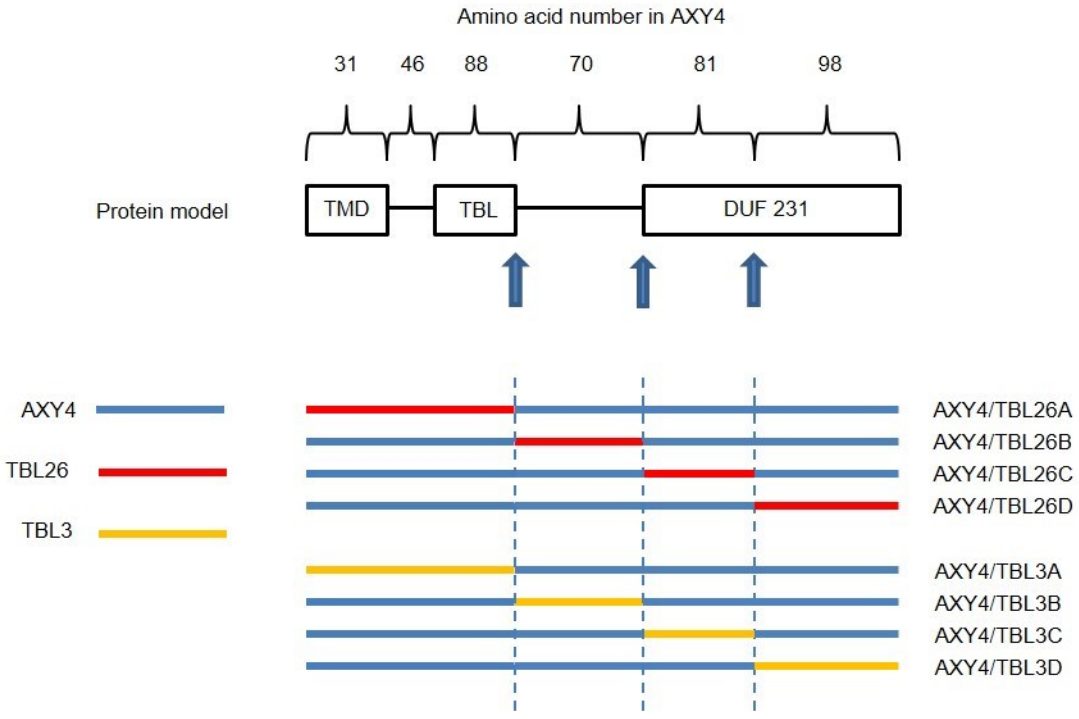

Figure 4.2.1-2 AXY4 protein model and general representation of the chimeric protein constructs generated. Protein model of AXY4 with the transmembrane domain (TMD), TBL domain and DUF231 domain (Bischoff et al. 2010a). Blue arrows indicate where the limits were established for the chimeric constructs. Number of amino acids in each fragment of the protein (AXY4) are indicated above the brackets. Colored horizontal lines represent regions of the chimeric proteins belonging to each TBL type. Letters on the right represent the chimera assembly names (A, B, C or D).

The chimeras were built using the coding sequence of each gene section for the respective protein domain and cloned into the destination vector pGWB510 (2.2.4) containing the *AXY4* promoter and a C-terminus FLAG tag for protein detection. The *AXY4* promotor was chosen in order to keep the expression of the chimeras as close as possible to the physiologically relevant expression of *AXY4*. The cloned chimeras were transformed into the *axy4-3* background and expression of the transgene and complementation of the XyG acetylation phenotype was analyzed.

4.2.2 TBL chimeric constructs fail to complement the *ax4-3* mutant phenotype

Three independent transgenic lines were generated in the *axy4-3* background for each of the chimeric constructs (Figure 4.2.1-2). The transgene expression was ascertained via Q-RT PCR (2.2.10). The transcript levels of chimeras with TBL3 domains can be seen in Figure 4.2.2-1. As a control the entire *AXY4* sequence (*axy4*/*comp*) was used. All independent transgenic lines show expression of the TBL3 chimeric transgene. The TBL26 chimeras also express the transgene as can be seen in Figure 4.2.2-2. As can be observed in Figure 4.2.2-1 and Figure 4.2.2-2 there is considerable variation in the level of expression between independent transformants of chimeric constructs of TBL3 and TBL26 swaps. There are three plausible explanations for this variation in expression. Since T-DNA insertions in *Arabidopsis* occurs randomly within the genome and different genomic regions induce variable levels of gene expression it is possible that the observed variation is a product of positional effects of transgene insertion (Matzke and Matzke 1998). The chimeric mRNAs could have different turnover rates. Another possible source in the variation of expression of the chimeric constructs is that there could exist multiple insertions of transgenes in the independent transgenic lines causing the expression level to be altered.

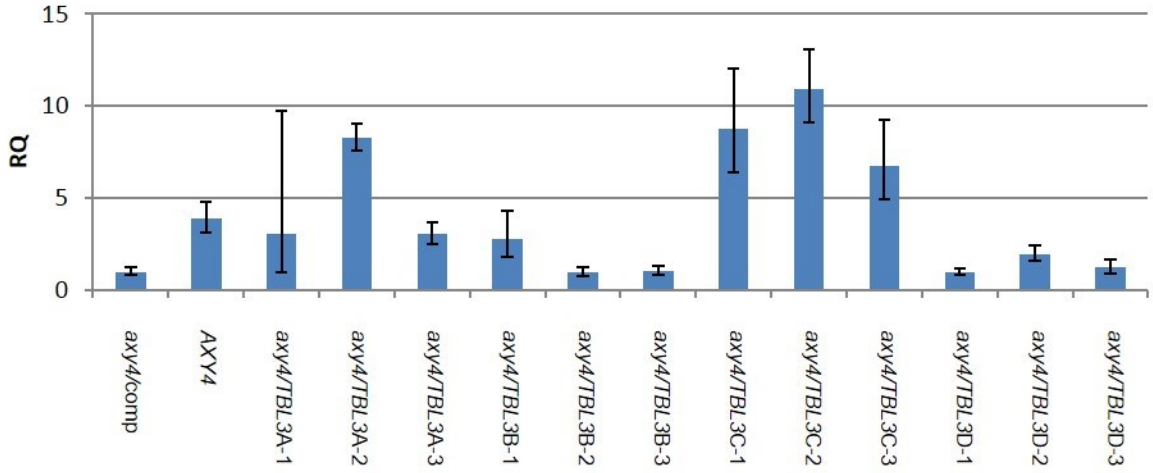

Figure 4.2.2-1 Q-RT PCR of the chimeric TBL3/AXY4 chimeric constructs. Relative quantity (RQ) of the transcripts of the chimeric constructs determined by Q-RT-PCR in 4 week old leaves of T2 lines containing the transgenic construct for the respective TBL3 fragment (A, B, C or D; Figure 4.2.1-2). *AXY4* = expression of the *AXY4* gene in the *pae9-1*/PAE9p:EV:GFP-1 line. *PTB1* gene expression was used as an internal control for normalization. *axy4* = *axy4-3.* n=3.

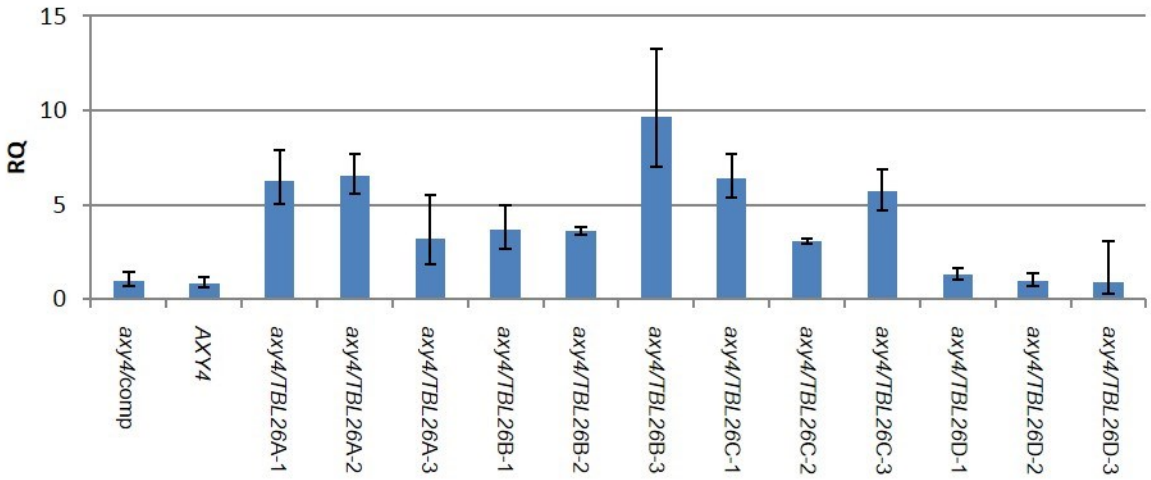

Figure 4.2.2-2 Q-RT PCR of the chimeric TBL26/AXY4 chimeric constructs. Relative quantity (RQ) of the transcripts of the chimeric constructs determined by Q-RT-PCR in 5 week old leaves of T2 lines containing the transgenic construct for the respective TBL26 fragment (A, B, C or D; Figure 4.2.1-2). *AXY4* = expression of the *AXY4* gene in the *pae9-1*/PAE9p:EV:GFP-1 line. *PTB1* gene expression was used as an internal control for normalization. *axy4* = *axy4-3.* n=3.

Since expression of the chimeric constructs was successful in all cases, the XyG profile was analyzed in those lines. As can be seen in Figure 4.2.2-3 and Figure 4.2.2-4 none of the T2 lines generated containing the transgene produced any detectable acetylated XyG oligosaccharides (2.5.1.3; 2.5.6). In essence, the XyG remains unacetylated as in the original non-transformed *axy4-3* mutant.

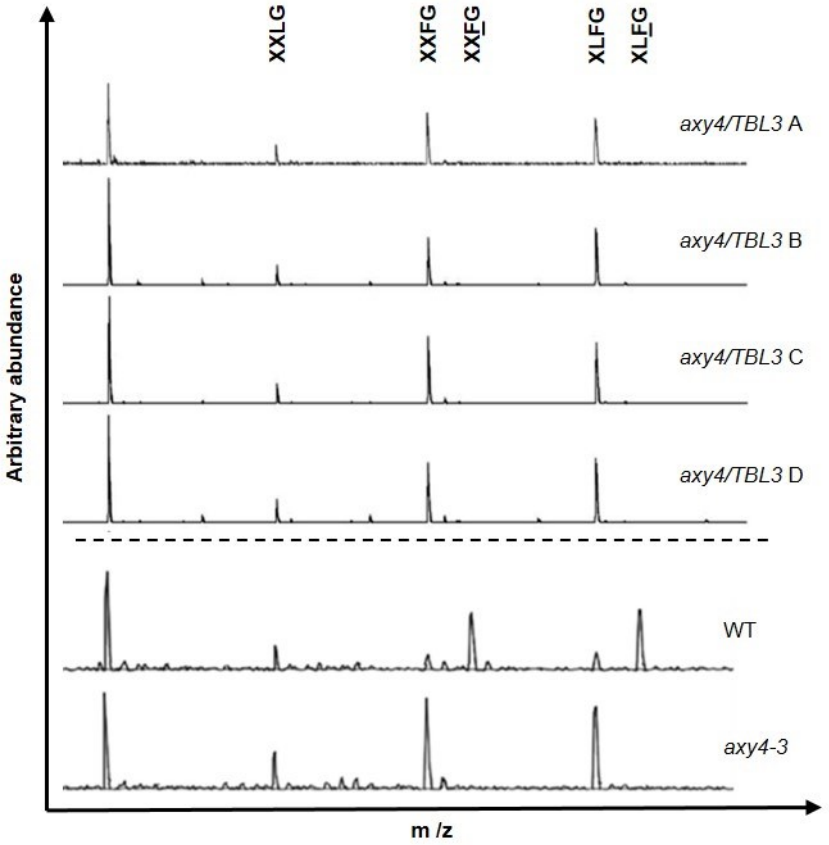

Figure 4.2.2-3 Representative mass spectra of TBL3/AXY4 chimeras. XyG oligosaccharide mass spectra after XEG digest (OLIMP). TBL chimeric constructs mass spectra are from 4 week old *A. thaliana* leaves of T2 plants containing the transgenic construct for the respective TBL3 fragment (A, B, C or D; Figure 4.2.1-2). Dashed lines separates spectra obtained in distinct experiments. WT and *axy4-3* mass spectra obtained from 3 week old plants (Data: Pauly Lab, Dr. Sascha Gille). WT = Col-0; *axy4* = *axy4-3.*

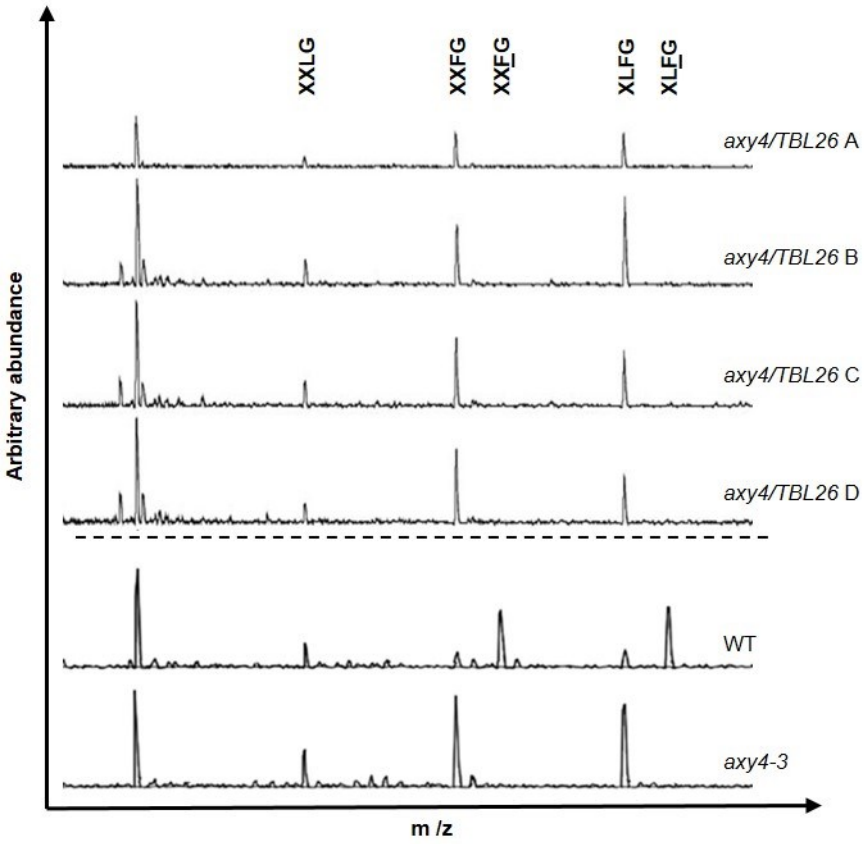

Figure 4.2.2-4 Representative mass spectra of TBL26/AXY4 chimeras. XyG oligosaccharide mass spectra after XEG digest (OLIMP). TBL chimeric constructs mass spectra are from 5 week old *A. thaliana* leaves of T2 plants containing the transgenic construct for the respective TBL26 fragment (A, B, C or D; Figure 4.2.1-2). Dashed lines separates spectra obtained in distinct experiments. WT and *axy4-3* mass spectra obtained from 3 week old plants (Data: Pauly Lab, Dr. Sascha Gille). WT = Col-0; *axy4* = *axy4-3.*

4.3 Discussion

4.3.1 Domain swap approach did not reveal insights into the functional role of TBL protein domains.

Very little is known about the mechanisms of action of TBL proteins. The conserved domains in these proteins, namely the GDS and DUF231 domains, have no demonstrated mode of action. The abundance of conserved cysteines and aromatic residues encountered within both the TBL and DUF231 domains could represent polymer binding sites (Bischoff et al. 2010a; Bischoff et al. 2010b). Alternatively, it has been proposed that together (TBL and DUF231) they could compose the catalytic site of these proteins, based on alignments to models of fungal acetylesterases, the TBL domain would contribute the S in the GDS motif and the DUF231 domain the DxxH to a catalytic triad found in some hydrolases (Bischoff et al. 2010b; Gille et al. 2011b). This idea finds support on site directed mutagenesis studies in which the above mentioned amino acids when mutated to alanine (or the GDS motif is deleted) hinder the activity of AXY4 mutants (Pauly Lab, Dr. Sascha Gille, personal communication). The domain swap approach had the goal to gain some insight into what domains contributed to the substrate specificity of the TBLs, in this case AXY4/TBL27. No chimeric construct generated between AXY4 and TBL3 or TBL26 was able to restore XyG O-acetylation (Figure 4.2.2-3; Figure 4.2.2-4) demonstrating that all domains of AXY4 participate in the reaction / substrate specificity in some form. Due to the conservation of amino acids in the domains (Appendix 4) it was expected that at least some domain swaps would not abolish activity. The chimeric constructs were tagged with a FLAG tag and when the AXY4 cds was cloned into the same vector and used for complementation of the *axy4-3* phenotype, restoration of 70% of the WT phenotype was observed (unpublished data, Pauly Lab, Dr. Sascha Gille; Figure 4.1-2 C). This indicates that the tag did not abolish activity of the protein.

The domain boundaries for the swap experiments were decided based on amino acid alignments (Appendix 4) and these sites might have affected the final 3D structures of the chimeric proteins resulting in the lack of activity. The possible catalytic site in the TBL proteins composed by amino acids in two different protein motifs (the S in the GDS motif of the TBL domain and the D and the H in the DxxH of the DUF231 domain; Figure 4.1-2) separated by 236 amino acids (in AXY4) could be particularly sensitive to folding differences imposed by the chimeras. Modifications in protein folding could affect the proper spatial arrangement of active amino acids within the catalytic site or modify the accessibility of substrate to it (Dobson 2003).

Another possible reason for lack of *axy4-3* complementation by the chimeras is potentially the lack of chimeric protein present in the cell. It is known that gene expression does not necessarily correlate with protein abundance (Vogel and Marcotte 2012). Even though the transcript level of the chimeric TBL genes was demonstrated via Q-RT PCR (Figure 4.2.2-1; Figure 4.2.2-2), there is a possibility that the chimeric proteins are present in sufficient quantities to restore the WT phenotype or are rapidly degraded. Attempts in our lab to detect AXY4:FLAG using western blotting failed even though the XyG chemotype was rescued (personal communication, Pauly Lab, Dr. Guangyan Xiong).

In summary, at this stage no new insights can be proposed for the mode of action of the TBL protein domains or the presumed O-acetylation mechanism of the proteins. Future research should be targeted towards producing crystal structures of one or more TBLs in order to gain structural insights into how the proteins are functioning.

5.0 Biochemical approach for the identification of the XyG acetylesterase

5.1 Background

Humans have been using biochemical activities from substances in nature for over 6000 years (Neelakantan et al. 1999). Cheese making might be one of the most ancient examples where enzyme activities were used intentionally. For thousands of years without knowing people have been extracting chymosin, a protease, from calf gut and using it to coagulate milk in cheese making (Guinee and Wilkinson 1992; Neelakantan et al. 1999). Eventually the protein was isolated, characterized (Moir et al. 1982) and with the advent of molecular biology it is now made in fermenters by transgenic *Aspergillus* (Neelakantan et al. 1999). This example illustrates how the classical approach of protein purification via its activity can lead to the identification of the corresponding gene and its functional characterization.

Many plant genes have been characterized through biochemical approaches, consisting of protein isolation via activity assays, protein purification, protein sequencing followed by determination of the gene involved. A pectin acetylesterase (PAE) gene family in plants was initially annotated based on such approaches to chase the causal protein (Williamson 1991; Bordenave et al. 1995; Christensen 1996). The mung bean PAE was isolated from hypocotyls, purified, and sequenced to identify the corresponding coding DNA sequence (Bordenave et al. 1995). Several XyG biosynthetic genes have been identified in a similar manner; examples include a fucosyltransferase (Perrin et al. 1999), a xylosidase (Sampedro et al. 2001) and a glucan synthase (Cocuron et al. 2007). No plant XyG acetylesterase has been identified to date and there is no gene family in plants annotated for such an activity (Lombard et al. 2014). For these reasons genomic approaches to find genes involved in XyG acetylesterase activity are not very straight forward. Due to the previous success of biochemical approaches for gene characterization this approach was used to attempt to identify the still elusive XyG acetylesterase (Gille et al. 2011b).

5.2 Results

5.2.1 XyG acetylesterase activity cannot be detected in *Arabidopsis* protein extracts

A biochemical approach was used to isolate a putative XyG acetylesterase in etiolated seedlings, leaves, and cell cultures of *Arabidopsis*. Selected tissues for protein extraction and testing included cell culture medium, cell culture cell mass extract, 7 day old etiolated seedlings and *Arabidopsis* leaves (Figure 5.2.1-1; 2.2.11). These materials are easily obtained and the XyG present in them contains some level of de-acetylated oligosaccharides (Figure 3.2.2-7; Figure 3.2.2-8; Figure 5.2.1-2), which could imply the activity of a XyG acetylesterase. As is described in Figure 5.2.1-1, the approach consisted in testing for *in vitro* acetylesterase activity (2.6) of a protein extract against an acetylated XyG model substrate (2.5.7). Since XyG in the medium of suspension cell cultures can be highly acetylated (Figure 5.2.1-2), XyG oligosaccharides were generated from cell culture medium to be used as a substrate (Figure 5.2.1-2; 2.5.7).

XyG in cell cultures contains double acetylated XXFG oligosaccharides (Figure 5.2.1-2). Differences in the oligosaccharide composition of the medium and the cell walls can be observed (Figure 5.2.1-2). XyG in the walls of the suspension cultured cells had only minor amounts of XXLG compared to the medium. Since the medium contained two kinds of acetylated oligosaccharides (XXLG and XXFG) the XyG polymer was purified through ethanol precipitation (2.5.7).

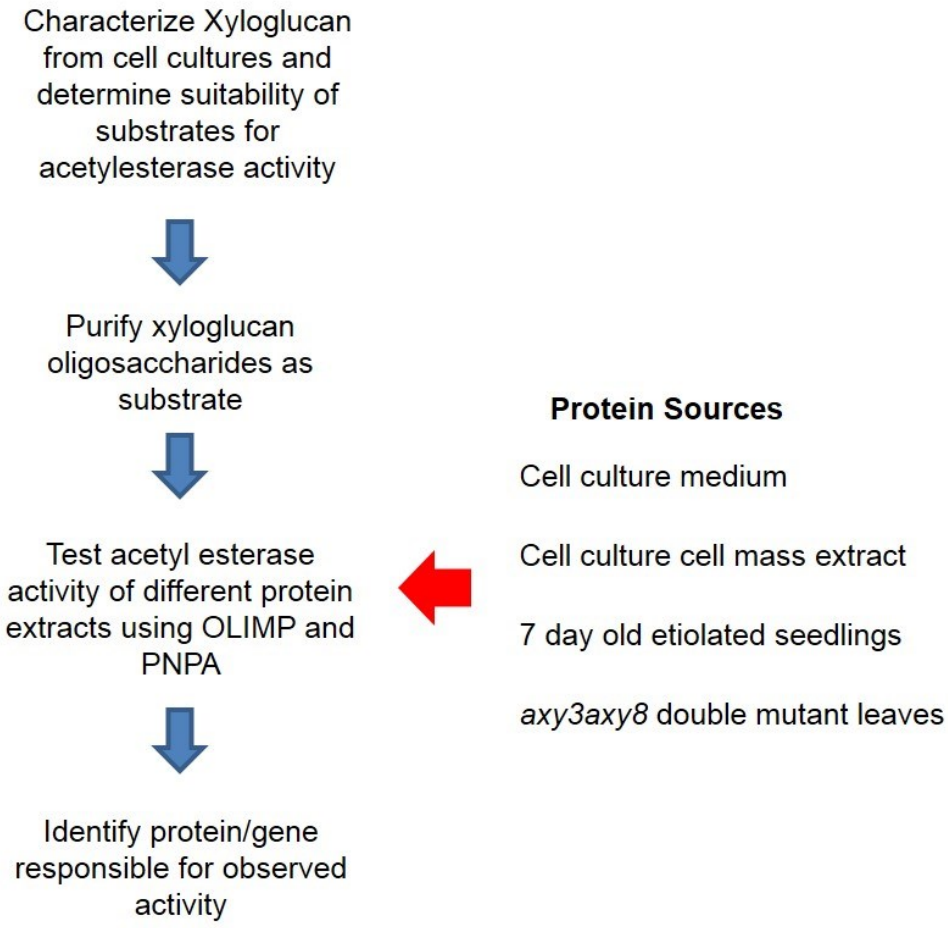

Figure 5.2.1-1 Overview of the approach used to identify a XyG acetylesterase.

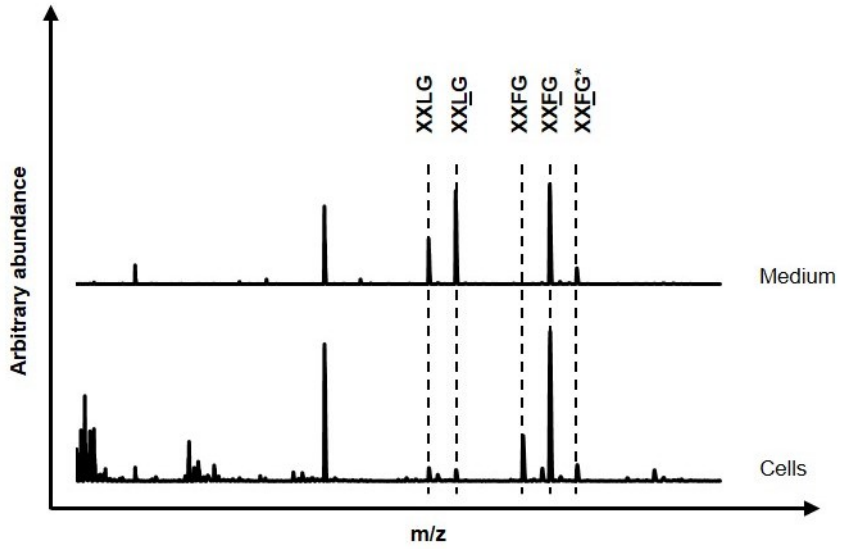

Figure 5.2.1-2 XyG mass spectra of *Arabidopsis* cell cultures. A) Mass spectra of XyG oligosaccharides released after XEG digest of the medium polysaccharides and cells mass of *Arabidopsis* cell cultures. The figure depicts the presence of the double acetylated XXFG*

Total protein was prepared by ball milling tissue followed by buffer extraction (7 day old etiolated seedlings and cell mass of cell cultures; 2.2.11) or concentrating protein in the medium using columns with size exclusion cut offs (2.2.11). Protein preparations were used in *in vitro* assays to test for acetylesterase activity against PNPA (4-nitrophenyl acetate; Figure 5.2.1-3). Upon hydrolysis of the acetyl group 4-nitrophenyl can be detected by absorbance at 410 nm. Protein extracts from cell mass and etiolated seedlings were able to de-esterify PNPA (Figure 5.2.1-3; 2.6) demonstrating that the protein extraction method yielded active acetylesterases.

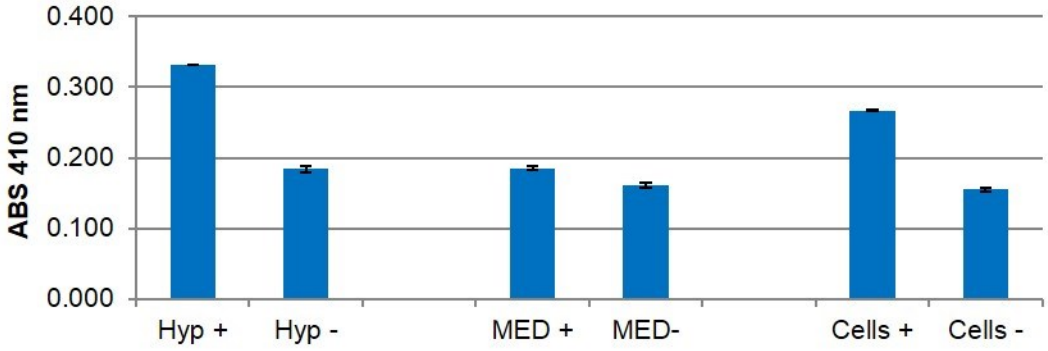

Figure 5.2.1-3 Esterase activity of crude protein extracts from different tissues. Activity (410nm absorbance) on the artificial substrate PNPA with different protein extracts (Hyp = 7 day old etiolated seedlings; MED = cell culture medium; Cells = Cell extracts; + native protein; - heat denatured protein). n=2

To test for specific XyG acetyl esterase activity an acetylated XyG substrate was necessary. Since there is no commercially available acetylated XyG, the cell culture cell mass was digested with XEG and the oligosaccharides obtained were further purified using 10 kDa size exclusion cut off membranes (2.5.7). This XyG substrate produced is composed in its majority by a mixture of: XXXG, XXLG, XXLG, XXFG and XXFG* (Figure 5.2.1-4). The various protein extracts were tested for acetylesterase activity against acetylated XyG oligosaccharides (Figure 5.2.1-4). After an overnight incubation at room temperature no acetylesterase activity could be observed based on analysis of the products by mass spectrometry (Figure 5.2.1-4). The absence of ion signals representing non-acetylated XXFG and the steady relative ratio between XXLG and XXLG indicate a lack of XyG acetylesterase activity with this substrate under these conditions. However, a reduction in the abundance of XXXG by the etiolated seedling protein extract can be observed (Figure 5.2.1-4).

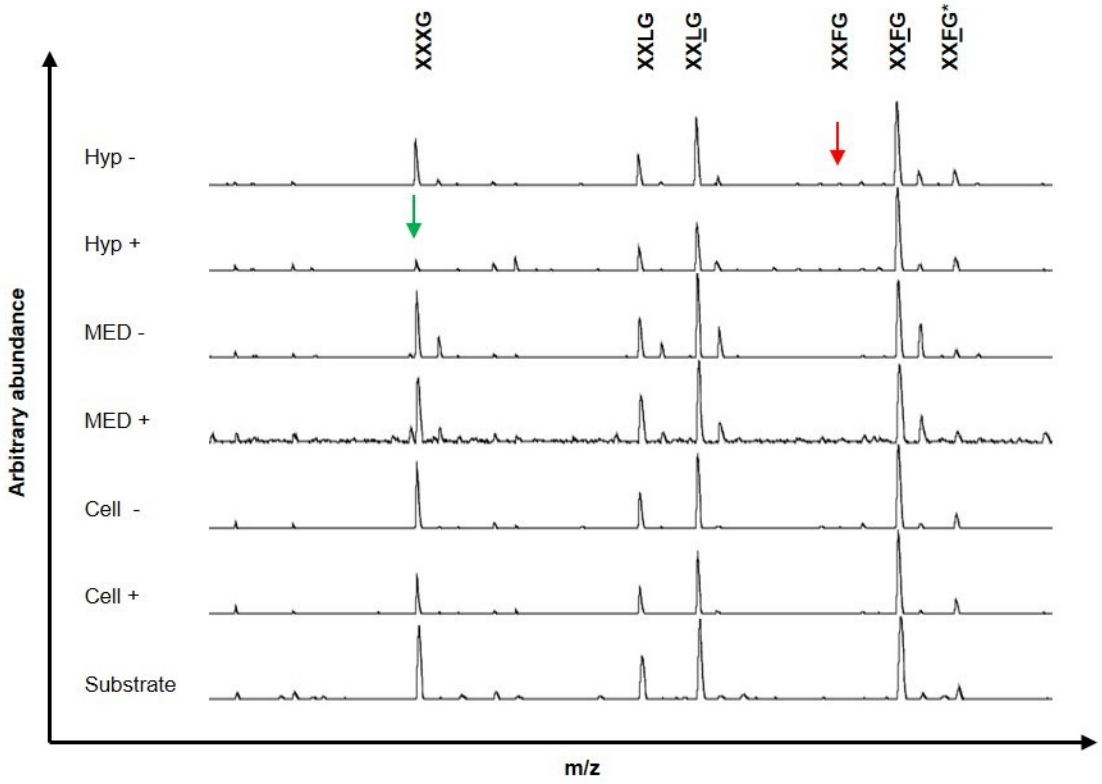

Figure 5.2.1-4 Activity of protein extracts on XyG oligosaccharides from cell culture medium. Mass spectra of XyG oligosaccharides incubated with various protein extracts. Green arrow indicates possible xylosidase activity against XXXG. MED = cell culture medium proteins; Hyp = 7 day old etiolated seedlings; Cell = Cell extracts; + = native protein; - = heat denatured protein; Substrate = purified oligosaccharides from cell cultures.

Activity against the XXXG oligosaccharide by 7 day old etiolated seedling protein (Hyp) was observed which suggests that active xylosidases were present in the protein extracts (Figure 5.2.1-4; green arrow). While this protein extract produces viable proteins for *in vitro* assays, it also suggests that other activities could be impacting the substrate. For this reason it was hypothesized that by using protein extracts (2.2.11) from the *axy3*/*axy8* double mutant, which lacks the predominant activities of a xylosidase (*AXY3*) and a fucosidase (*AXY8*) acting on XyG (Gunl et al. 2011), there could be less interference with the substrate, highlighting the activity of a possible XyG acetylesterase. In the *axy3*/*axy8* double mutant both genes are active in leaves and the mutant XyG is enriched in XXFG and also XXFG, reflecting the effect of the impaired xylosidase and fucosidase (Gunl et al. 2011; Sampedro et al. 2001). An impaired fucosidase would prevent the degradation of a de-acetylated XXFG oligosaccharide, causing this ion signal to accumulate in the mass spectrum of protein treated substrate. Protein extracts from the *axy3/axy8* double mutant leaves were incubated against the cell culture medium oligosaccharides (Figure 5.2.1-5). As can be observed in Figure 5.2.1-5 the protein preparation of the double mutant (Protein Pellet and Protein SUP) introduced additional ion signals in the mass spectra. Even though the precise nature of these ion signals was not determined they did not interfere with the XyG oligosaccharide signals (Figure 5.2.1-5). After incubation with the protein preparations some suppression of the XyG oligosaccharide signals could still be observed when using supernatant protein (SUP +, treated and not treated with protease; Figure 5.2.1-5), possibly due to some active hydrolases in this preparation other than the ones affected by the double mutation. However, again no acetylesterase activity could be observed due to the absence of ion signals representing non-acetylated XXFG and no obvious increase in XXLG ion abundance (Figure 5.2.1-5).

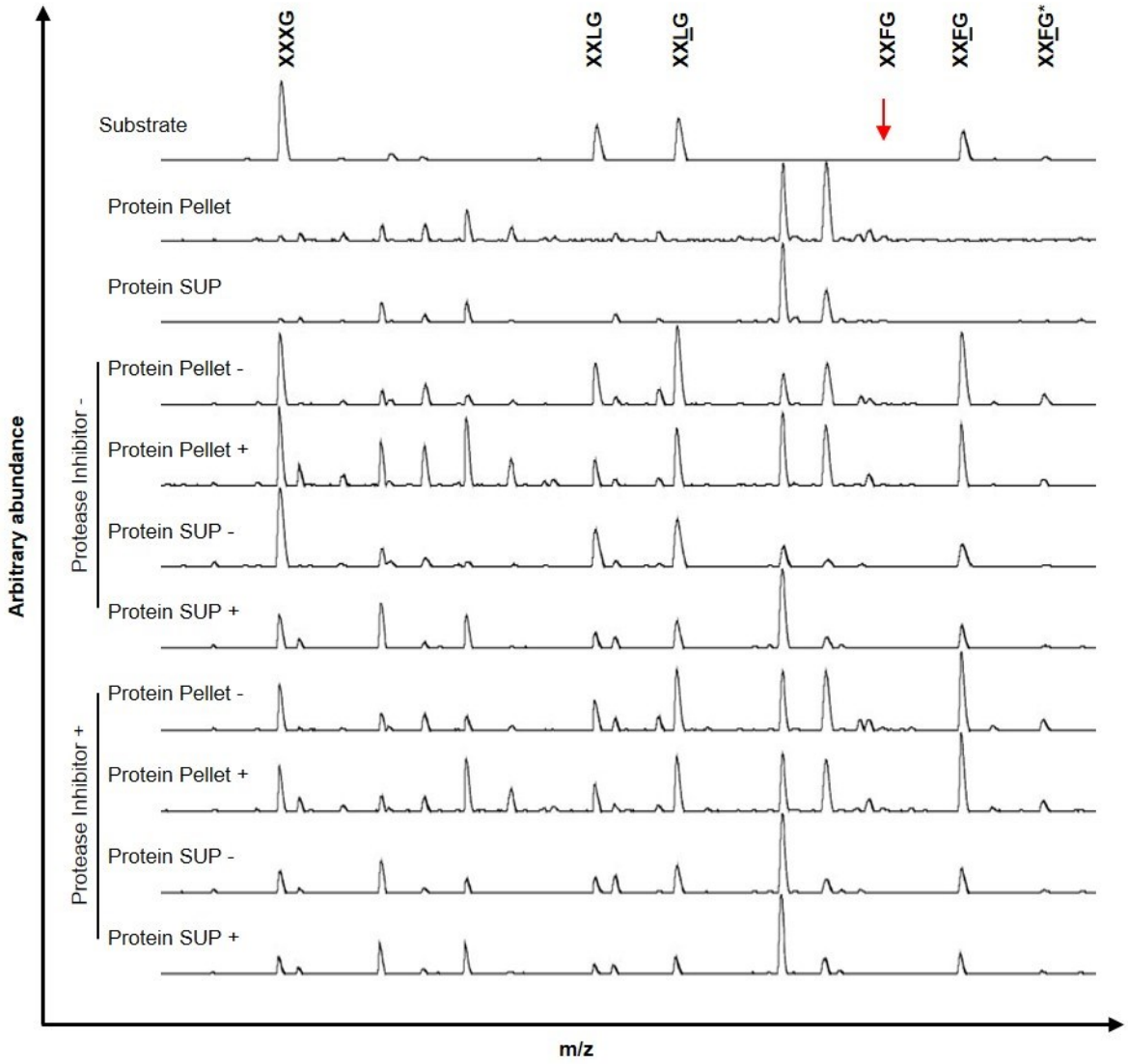

Figure 5.2.1-5 Activity of leaf protein extracts from the *axy3/axy8* double mutant on XyG oligosaccharides from cell culture mediumass spectra of XyG oligosaccharides incubated with protein extracts of 29 day old leaves from the *axy3axy8* double mutant. Protein SUP = protein from *axy3axy8* supernatant; Protein Pellet = protein from *axy3axy8* pellet; + = native protein; - = heat denatured protein; Substrate = purified oligosaccharides from cell cultures. Presence and absence of protease inhibitors in the extraction buffer is also indicated.

5.3 Discussion

5.3.1 It is unclear, if XyG acetylesterase activity exists in *Arabidopsis*

Under the experimental conditions used no XyG acetylesterase activity could be observed with protein extracts from Col-0 7 day old etiolated seedlings, cell culture cell mass, cell culture medium and leaves of the *axy3*/*axy8* double mutant (Figure 5.2.1-4; Figure 5.2.1-5) even though acetylesterase activity against the model substrate PNPA was present in the protein preparations (Figure 5.2.1-3).

There is some evidence supporting the existence of XyG acetylesterases in plants. In the AXY screen, performed by the Pauly Lab, increased XyG acetylation phenotypes were identified (*axy5*), which would be consistent with an impaired XyG acetylesterase, but the responsible gene is yet to be determined (Obel et al. 2006) and could also represent an acetylation regulatory gene. *Arabidopsis* ecotypes with increased acetate phenotypes have also been identified. The overexpression of the *AXY4* gene, a putative XyG acetyltransferase, does not result in a completely acetylated XyG and only leads to a mild increase in % XyG acetylation from 64.4 to 74.4% in *Arabidopsis* leaves (Gille et al. 2011b)], which would imply that XyG acetylesterase activity prevents further increase in acetylation. The high levels of XyG acetylation found in *Arabidopsis* cell suspension cultures (Figure 5.2.1-2) could suggest that under culturing conditions apoplastic acetylesterase activity could be dispersed and thus diluted by the medium. This is possible since these proteins are thought to be present in the cell wall (Gou et al. 2012; Orfila et al. 2012), which is constantly being washed by the medium.

The lack of an active acetylesterase could suggest that XyG acetylation is entirely controlled at synthesis. This idea finds some support in the observation that XyG isolated from microsomes are not fully acetylated (Gunl et al. 2011). If indeed acetylation is controlled exclusively at synthesis this would differ considerably from the pattern encountered for XyG post-deposition editing executed by apoplastic glycosyl hydrolases. In *A. thaliana* three major apoplastic hydrolase have been identified that act on XyG removing fucosyl-, galactosyl- and xylosyl residues from the polymer post deposition in the apoplast, resulting in modified polymer structure and biological phenotypes (Gunl et al. 2011; Gunl and Pauly 2011; Sampedro et al. 2012). If the fucosidase is knocked-out XyG cannot be completely degraded and accumulates aberrant structures (Gunl et al. 2011). Hence, an O-acetylesterase is expected to be present to ensure proper turnover of the polymer. In the future reverse genetics approaches based on selection of genes annotated as carbohydrate esterases from multiple families might shed some light into the existence of the elusive XyG acetylesterase. Forward genetics screens could also be utilized to identify this gene, as is the investigation of the *Arabidopsis* natural variation, which has revealed ecotypes with elevated XyG acetate content, a chemotype that would be associated with the loss of function of an acetylesterase gene.

6.0 The *A. thaliana* pectin acetylesterase (PAE) gene family and its role in plant cell wall acetylation

6.1 Background

With the completion of full plant genome sequences (Arabidopsis Genome 2000; Meinke et al. 1998) and advances in gene annotation the discovery of gene function expanded. The establishment of model plants like Arabidopsis with collections of gene knock-out mutants, generated by random insertion of T-DNA fragments (Alonso et al. 2003) or transposons (Kuromori et al. 2004) has enabled reverse genetics studies (Sessions et al. 2002; Somerville et al. 2004). The reverse genetics approach consists of the identification of candidate genes based on sequence similarity to already characterized genes, growth of the corresponding available knockout or overexpression lines followed by a phenotypic analysis. Such an approach can be coupled to complementary biochemical approaches such as the demonstration of *in vitro* enzymatic activities or biochemical properties (Jensen et al. 2008).

In the plant cell wall field this approach has benefited enormously from the structured annotation of carbohydrate active enzymes in the CAZy database (Lombard et al. 2014) including glycosyltransferases, glycoside hydrolases, polysaccharide lyases and carbohydrate esterases. The combination of available genomic and biochemical data by this initiative has allowed for the identification of many genes involved in cell wall biosynthesis. Genes involved in the biosynthesis and metabolism of xylogalacturonan (Jensen et al. 2008), arabinan (Harholt et al. 2006), xylan (Chiniquy et al. 2012), and XyG (Sampedro et al. 2012) have been identified using such a reverse genetics approach. The genes found to be involved in the biosynthesis of xylogalacturonan and arabinan are members of the glycosyltransferase family 47 which had its first plant gene described as a glucuronosyltransferase from *Nicotiana plumbaginifolia* (Harholt et al. 2006; Iwai et al. 2002). The grass xylan β-(1,2) xylosyltransferase, named XAX1, was identified from a GT61 group of genes which is associated with an α-(1,3)-arabinosyltransferase characterized in wheat (Anders et al. 2012; Chiniquy et al. 2012). The β-galactosidase, acting on XyG in *Arabidopsis*, was identified due to its close phylogenetic relationship with GH35 genes first shown to have the β-galactosidase activity in *Tropaeolum majus* (Sampedro et al. 2012).

The carbohydrate esterase family 13 [CE13, EC 3.1.1; (Lombard et al. 2014)] harbors putative plant pectin acetylesterases (PAEs) based on the biochemical characterization of proteins with this activity isolated from *Vigna radiata* var radiata Wilzeck [mung bean; (Bordenave et al. 1995; Breton et al. 1996)]. It was shown that the protein (43 kDa) extracted from the walls of mung bean hypocotyls was able to release acetate from sugar beet and flax pectin (Bordenave et al. 1995). In *A. thaliana* this family is composed of twelve members, none of which have been characterized to date. A PAE ortholog in *Populus trichocarpa* (Pt PAE1) was able to release acetate *in vitro* from artificially acetylated polygalacturonan, xylan, and arabinogalactan, when heterologously expressed in *E. coli*. The enzyme exhibited its highest activity towards pectic polymers [polygalacturonan; (Gou et al. 2012)]. The same protein, when overexpressed in *Nicotiana tabacum*, was able to reduce the acetate content of water soluble pectins by at least 13%. PAEs are thought to be localized to the apoplast acting

primarily on cell wall polymer post-deposition. The evidence for apoplast localization is based on the experimental observation that PAE activity can be extracted from wall preparations using buffers with high ionic strength (Christensen 1996; Orfila et al. 2012; Williamson 1991) or by fluorescent PAE protein fusions that localize to the apoplast in transgenic tobacco seedlings (Gou et al. 2012).

When the Poplar acetylesterase was overexpressed in tobacco the plants exhibited profound morphological aberrations in reproductive structures with shorter stamens, low pollen production and pollen grains with collapsed cell walls (Gou et al. 2012). When a mung bean acetylesterase (Bordenave et al. 1995; Breton et al. 1996) was overexpressed in potato tubers, walls exhibited as expected a reduced acetate content of 39% (Orfila et al. 2012). Hot water extracts from the potato tuber cell walls, which are enriched in HG, showed a 27% reduction in the acetate content. Reductions in acetate were also observed in the EPG/PME extracts (-8%; containing RGI and HG) and in the remaining cell wall residue (-68%; containing RGI and HG). An *A. thaliana* PAE ortholog in voodoo lily (*Amorphophallus konjac*) was recently identified as one of the top one hundred most highly expressed genes in the developing corm of this species (Gille et al. 2011a). The developing corm synthesizes acetylated glucomanan as a storage polymer (Gille et al. 2011a). This finding raised the possibility that the PAE family could also contain esterases that act on other polymers than pectin. To test this hypothesis a reverse genetics approach to characterize PAE genes in *A. thaliana* was pursued, where cell wall acetate phenotypes along with *in vitro* assays with recombinant proteins was explored.

6.2 Results

6.2.1 *A. thaliana* PAE mutants exhibit walls with increased acetate content

A reverse genetics approach was used to investigate the function of gene members in the *A. thaliana* PAE family (Figure 6.2.1-1). T-DNA insertion lines from all PAE genes (12) in *A. thaliana* were obtained from stock centers (Figure 6.2.1-2; Table 6.2.1-1). These lines were genotyped (2.2.1; 2.2.2) for homozygosity of the T-DNA insert (Figure 6.2.1-3).

It was possible to obtain RT-PCR data (2.2.10) for 9 out of the 12 genes in the *A. thaliana* PAE family [(*PAE3*, *PAE5*, *PAE6*, *PAE7, PAE8, PAE9, PAE10, PAE11 and PAE12*); Table 6.2.1-1; Figure 6.2.1-4]. In some lines (*pae3-2, pae5-2 and pae7-2*) a residual transcripts could still be detected rendering those knock-down mutants (Figure 6.2.1-4). In other cases the T-DNA insertions did not affect the expression of PAE gene (pae4-2, pae6-1, and pae7-1; Figure 6.2.1-4; Figure 6.2.1-5). Lines *pae3-1*, *pae5-1*, *pae6-2*, *pae8*, *pae9-1*, *pae9-2*, *pae10-1*, *pae10-2*, *pae11-1*, *pae11-2*, *pae12-1* and *pae12-2* were considered knockout lines since no transcript could be detected by RT-PCR. The coding sequence (cds) of all genes except for *PAE1* (due to failed cloning attempts) was overexpressed (2.2.4) in the Col-0 background under the control of the enTCUP2 tobacco promoter (Schultink 2013; Schultink et al. 2013). Three independent transgenic lines were generated for each PAE gene (Table 6.2.1-1).

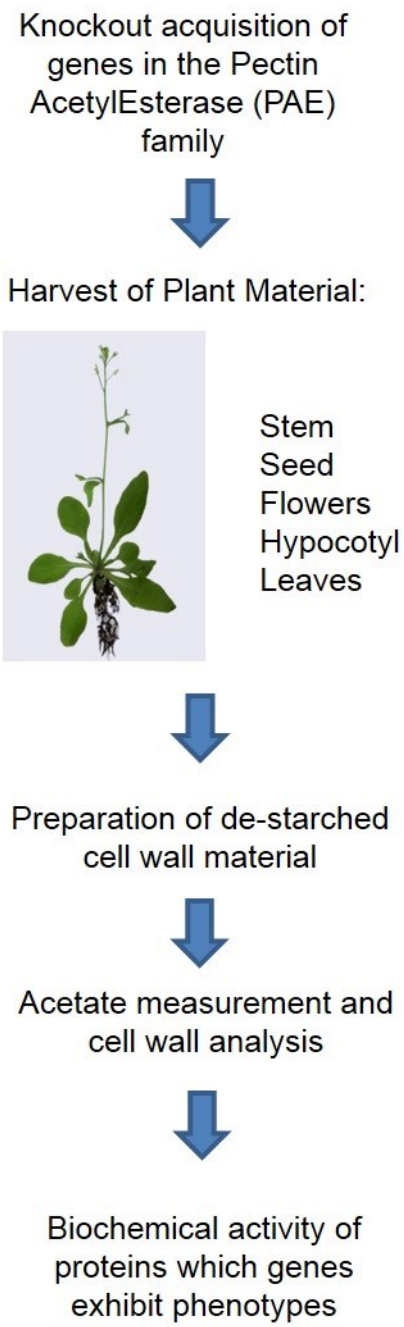

Figure 6.2.1-1 Overview of the reverse genetics approach used in the PAE family study.

A variety of plant tissues (seeds, flowers, stems, leaves and 7 day old etiolated seedlings), always accompanied by WT controls, were harvested for cell wall extractions (2.5.1.1; 2.5.2) based on gene expression patterns [Table 6.2.1-1; (Winter et al. 2007)]. Cell wall preparations were then analyzed for their total acetate (2.5.5) content and/or XyG acetylation levels (Figure 6.2.1-1; Table 6.2.1-1; 2.5.6). Acetate chemotypes were found in leaves for 3 genes in the *A. thaliana* PAE family: *PAE2*, *PAE8, and PAE9* (Table 6.2.1-1). When the *PAE2* cds was overexpressed in the Col-0 background, a reduction in total leaf wall acetate of approximately 10% was observed as well as a 6% reduction in leaf XyG acetylation (Table 6.2.1-1).

A PAE8 mutant line exhibited an increased total leaf (2.5.1.5; 2.5.2) acetate content of 20% (Table 6.2.1-2; Table 6.2.1-1). This knockout line exhibited a lesion in the 12th exon (Figure 6.2.1-5 A, B), hence 3 independent complementation lines consisting of the native *PAE8* promotor and genomic sequence (Hull 2012) transformed into the *pae8* background were generated (*pae8/comp*). These complementation lines had partially restored transcript levels (Figure 6.2.1-6; 2.2.10) and were able to complement the mutant wall acetate chemotype (Table 6.2.1-2), indicating that PAE8 modulates cell wall acetate levels.

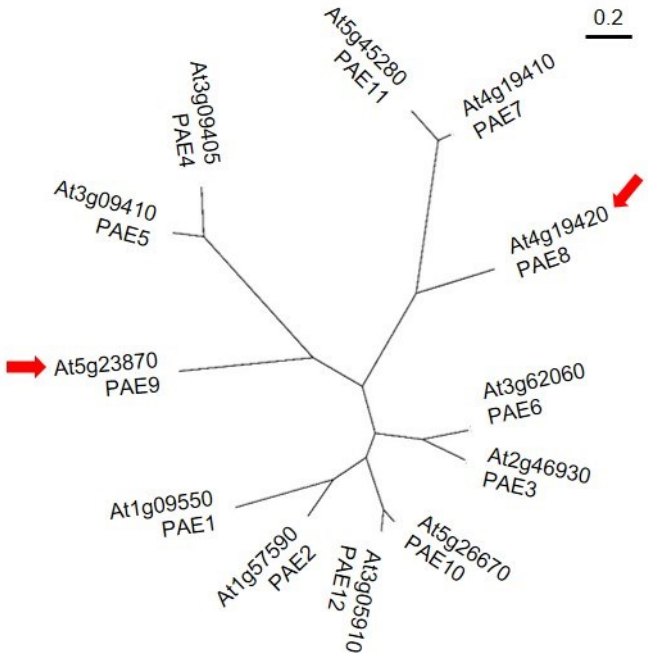

Figure 6.2.1-2 Maximum likelihood phylogenetic tree of the PAE family in *A. thaliana. PAE9* and *PAE8* are the only two genes without close paralogs (red arrows). Tree constructed using the Seaview software which used Muscle and PhyML to make the alignment and tree respectively

.

Table 6.2.1-1 Summary of PAE reverse genetics screen

gene	line	insert	insert position	RT PCR	tissue[a]	flower[a]	stem[a]	seed[a]	leaf[a]	hypocotyl[a]	seed[b]	flowers[b]	leaf[b]	stem[b]	hypocotyl[b]
At1g09550	*pae 1-1*	SALK_061326C	exon		seeds	91.8			105.5						
	pae1-2	GABI_627A02	exon		siliques	98.9			106.9				91.05		
At1g57590	*pae 2-1*	SALK_143273	exon		flowers	114.6	101.0	99.9			109.4	98.0		98.7	
	pae 2-2	SALK_102761C	exon		seeds	101.4	93.0	101.4			109.5	99.6		95.7	
	2oea1				stem				95.3				89.1		
	2oec1								90.8				86.3		
	2oed3								95.4				88.5		
At2g46930	*pae 3-1*	SALK_066524C	exon	KO	stem		93.4			100.0	91.4		103.6	99.5	
	pae 3-2	SALK_137505C	intron	K-down	leaves		99.2			101.3	96.7		106.5	94.1	
	pae 3-3	GABI_294C06	promotor		hypocotyl		100.5							99.3	
	pae 3-4	SAIL_906_F10	5 UTR				93.5							90.8	
	3oea2						101.1		91.7				86.8	95.1	
	3oeb1						100.2		95.4				99.8	100.8	
	3oec1						100.0		99.6				92.2	97.3	
At3g09405	*pae 4-1*	SALK_140726	exon		hypocotyl		95.2			97.6			104.0	106.4	103.1
	pae 4-2	SAIL_450_B07	5 UTR	WT+	stem		90.0			93.1			106.8	99.4	108.1
	4oeaa				leaves				96.4				97.3		
	4oebd								101.3				103.5		
	4oec1								88.1				104.3		
At3g09410	*pae 5-1*	SALK_140555	exon	KO	stem		94.3			94.7			104.4	96.0	103.3
	pae 5-2	SALK_052303C	exon	K-down	hypocotyl		99.1			96.5			104.0	99.0	108.1
	5oeb7				leaves				86.2				90.6		
	5oec10								90.7				92.2		
	5oea13								86.9				104.1		

continued

gene	line	insert	insert position	RT PCR	tissue[a]	flower[a]	stem[a]	seed[a]	leaf[a]	hypocotyl[a]	seed[b]	flowers[b]	leaf[b]	stem[b]	hypocotyl[b]
At3g62060	*pae6-1*	SALK_020618	promoter	WT	shoot apex		125.2			98.1			106.2	98.0	103.0
	pae6-2	SALK_134907	exon	KO	hypocotyl		102.2			95.0			105.0	103.0	103.0
	6oectt1				leaves				101.1				98.2		
	6oeap								98.1				95.1		
	6oeba								99.1				99.0		
At4g19410	*pae7-1*	SALK_093502C	intron	WT	uniform expression		95.1						113.3	109.4	95.5
	pae7-2	GABI_272B08	exon	K-down	leavesf	100.8	98.3	102.6					106.5	97.9	100.1
	pae7-3	SAIL_154_H11	intron		stem	101.5		83.1							
	pae7-4	SALK_091346C	5 UTR		hypocotyl	104.9		92.1							
	pae7-5	SALK_117590C	promoter			98.5		91.4							
	pae7-6	SALK_076487	5 UTR			99.2		84.0							
	7oea3								100.7				107.0		
	7oeb1								100.9				100.0		
	7oec3								98.8				110.0		
At4g19420	*pae8*	SALK_132026	exon	KO	stem leaves								120.0	110.0	
At5g23870	*pae9-1*	SALK_046973C	intron	KO	stem		98.1		105.8	121.9			120.3	97.5	
	pae9-2	GABI_803G08	exon	KO	leaves		97.0		115.6	112.6			121.6	100.6	
	pae9-3	SALK_058590	intron / exon										104.8		
	9oeb3								98.3				106.0		
	9oec1								100.4				101.0		
	9oea1								98.3				100.0		
At5g26670	*pae10-1*	SALK_043807	intron	KO	no data		100.3						94.1	97.0	
	pae10-2	SAIL_802_C05	exon	KO			98.7						104.1	104.0	
	10oea1								98.4				94.9		
	10oeb4								103.5				92.5		
	10oed9								102.3				96.6		

continued

gene	line	insert	insert position	RT PCR	tissue[a]	flower[a]	stem[a]	seed[a]	leaf[a]	hypocotyl[a]	seed[b]	flowers[b]	leaf[b]	stem[b]	hypocotyl[b]
At5g45280	*pae11-1*	SALK_049340.48.65.x	exon	KO	leaves		93.1			106.9			123.1	105.1	110.3
	pae11-2	GABI_505H02	exon	KO	stem		94.8			101.6			135.2	100.6	103.8
	11oea1				hypocotyl				107.5				105.0		
	11oeb3								103.8				114.0		
	11oec2								102.1				110.0		
At3g05910	*pae12-1*	GABI_018A02	exon	KO	uniform expression		100.3			102.4			100.4	90.6	96.0
	pae12-2	GABI_646F06	intron	KO	(weak)		112.2			102.7			105.7	104.8	95.9
	12oea1								94.4				94.4		
	12oeb1								98.6				88.2		
	12oec3								95.6				94.9		

oe = overexpression of the gene CDS under the enTCUP2 promoter.
[a] results from OLIMP, % XyG acetylation, WT= 100%
[b] results from acetic acid measurements, WT = 100%
Green cells indicate significant statistical differences to WT based on *T* test (P<0.05)

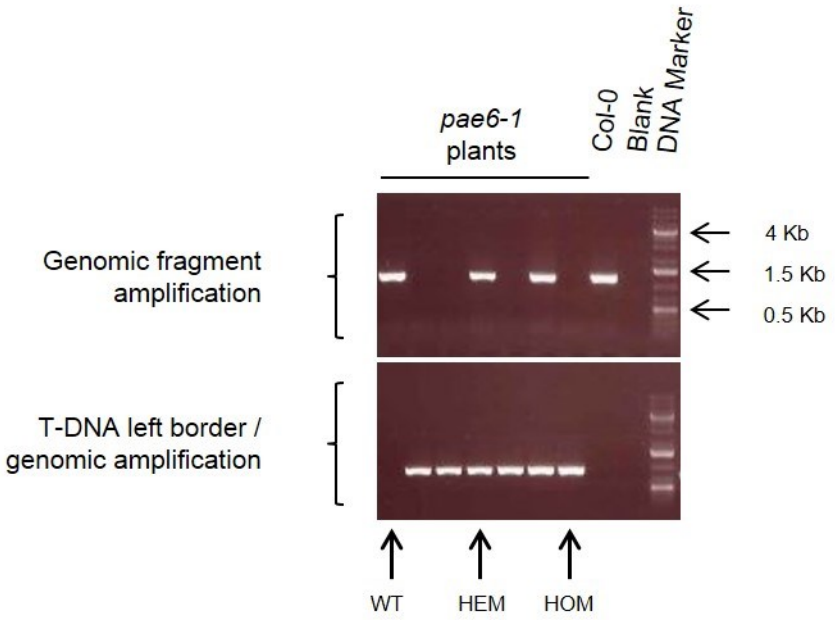

Figure 6.2.1-3 Example of genotyping PCR used to select homozygous T-DNA insertion lines. Agarose gels of PCR products amplifying a genomic fragment spanning the T-DNA insertion and a fragment from the T-DNA left border to a genomic position. WT = plant with no T-DNA insertion; HEM = plant hemizygous for the T-DNA insert; HOM = a plant homozygous for the T-DNA insert; Col-0 = PCR with Col-0 DNA; Blank = PCR mix without template; DNA marker = Gene Ruler™ 1 Kb plus DNA ladder Fermentas.

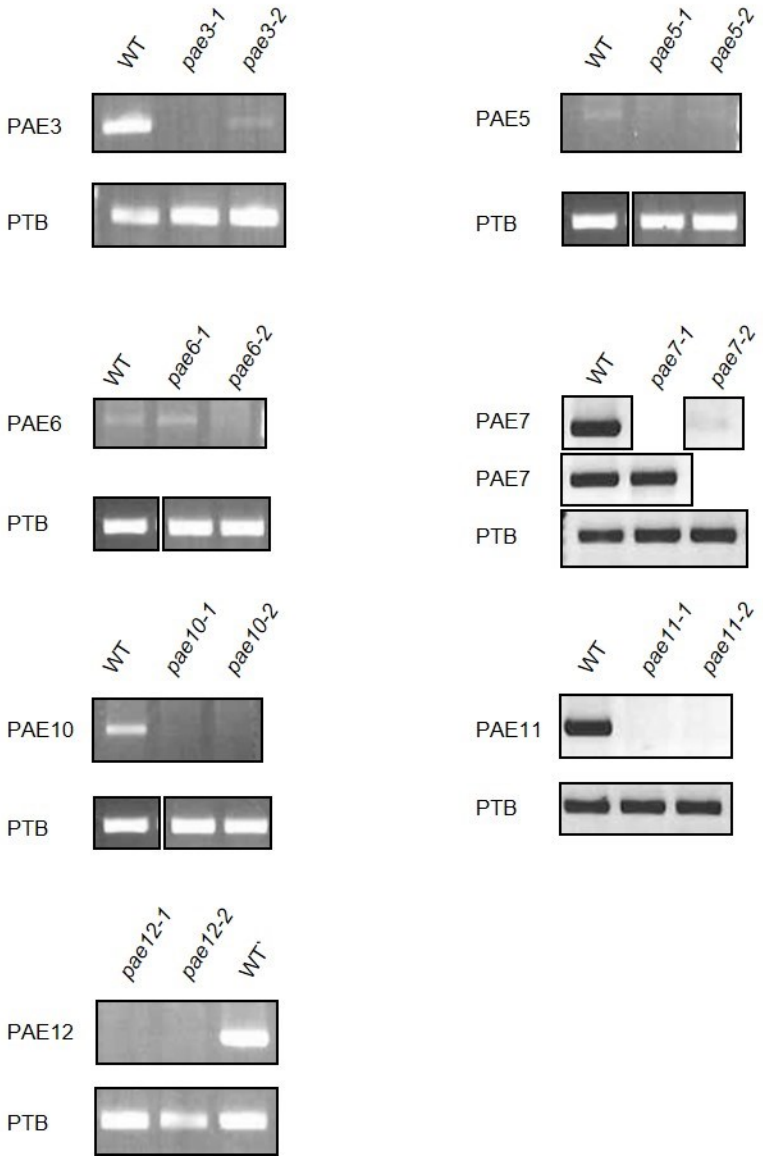

Figure 6.2.1-4 RT-PCR of T-DNA insertion lines in the *A. thaliana* PAE family. RT-PCR for PAE lines. PTB = expression of the *PTB1* gens as a control. WT = Col-0 plants of same age as insertion lines being tested. List of primers can be found in Appendix 1.

	Cell wall	
Set 1		
WT	12.39 ± 0.10	c
pae9-1	14.79 ± 0.34	b
pae9-2	15.04 ± 0.37	b
pae9-1/ox9-1	12.01 ± 0.28	c
pae9-1/ox9-2	11.85 ± 0.70	c
pae9-1/ox9-3	12.01 ± 0.35	c
pae8	15.15 ± 0.30	b
pae8/pae9-2	16.91 ± 0.24	a
Set 2		
WT	12.40± 0.75	b
pae8	14.87 ± 0.86	a
pae8/comp-1	12.03 ± 0.98	b
pae8/comp-2	12.41 ± 0.45	b
pae8/comp-3	12.58 ± 0.61	b

Table 6.2.1-2 Acetic acid content of cell walls (mg g^{-1} cell wall). ± indicates standard deviation; letters indicate statistical significant differences based on ANOVA (p-value < 0.05); n≥4.

Two different T-DNA insertion lines were available for *PAE9*, representing two independent alleles. The two insertion positions were located in the 3rd intron (*pae9-2*) and 7th (*pae9-1*) exon (Figure 6.2.1-5 C, D). The insertion in the *pae9-2* allele was accompanied by a 275 bp deletion, which removes exons 4 and 5. Both insertion lines were unable to produce transcripts (Figure 6.2.1-5 C, D) and both harbor a wall (2.5.1.5; 2.5.2) with an approximate 20% increase in the acetate content (2.5.5) in their leaves (Table 6.2.1-2). Three independent overexpression lines (2.2.4) were generated for the *PAE9* gene in the *pae9-1* background (*pae9-1/ox9*). Q-RT PCR analysis (2.2.10) of these lines demonstrated that the transcript levels was increased three times compared to expression in WT plants (Figure 6.2.1-6 B). The acetate chemotype in the overexpression lines is restored to WT levels (Table 6.2.1-2) but not exceeding it, providing genetic support that lesions in *PAE9* lead to the observed acetate increase in the *pae9* mutants.

A double mutant was generated between *pae8* and *pae9-2* (*pae8/pae9-2*), which resulted in a 37% increase in acetate levels in leaf tissues, enhancing the effect of the individual single mutants (Table 6.2.1-2).

Gene expression data from multiple microarray experiments in *Arabidopsis* indicate that *PAE8* and *PAE9* are expressed in multiple plant tissues (Figure 6.2.1-7). *PAE9* is expressed to a higher level in leaves than *PAE8.* However, each are sufficient to lead to enhanced wall acetate levels in leaf tissues (Table 6.2.1-2) The expression data shows a high expression of both genes in the second internode of the inflorescence stem (Figure 6.2.1-7). However, none of the knockout mutants exhibited an acetate chemotype in this tissue (Figure 6.2.1-8; 2.5.1.1; 2.5.2) suggesting the presence of other redundant PAEs.

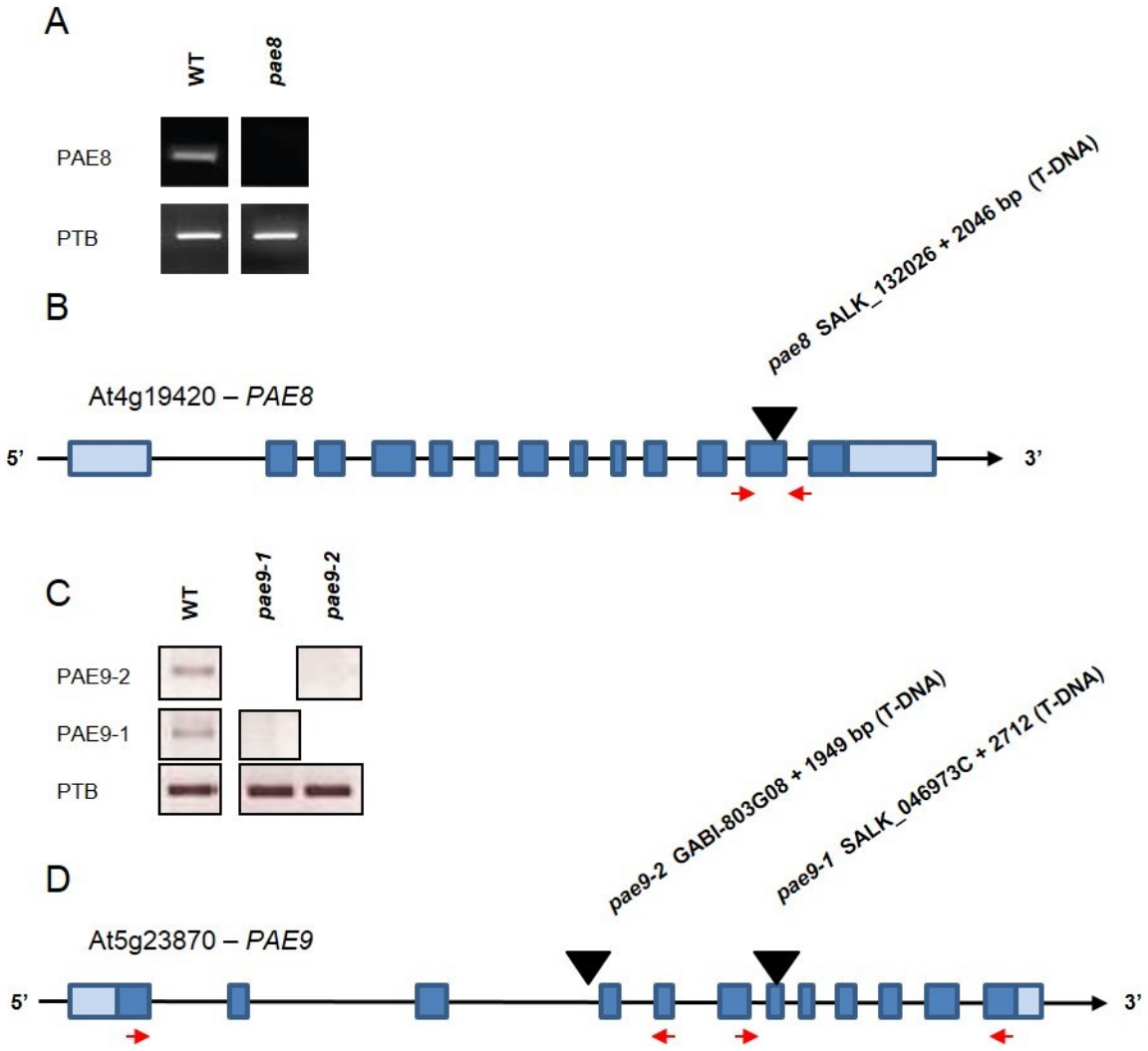

Figure 6.2.1-5 Gene models and RT-PCR for *PAE8* and *PAE9*. A) RT-PCR for *pae8* mutant, PTB = expression of the *PTB1* gens as a control. B) Gene model for *PAE8,* blue boxes indicate exons (dark blue = translated regions), black lines indicate introns. Black triangles - position of T-DNA insertions in relation to translation start site. C) RT-PCR for *pae9* mutants. D) Gene model for *PAE9,* blue boxes indicate exons (dark blue = translated regions) and black traces in between exons indicate introns. Black triangles position of T-DNA insertions in relation to translation start site. Red arrows indicate primers used for RT PCR. PAE8 data from Phillip A. M. Hull (Hull 2012).

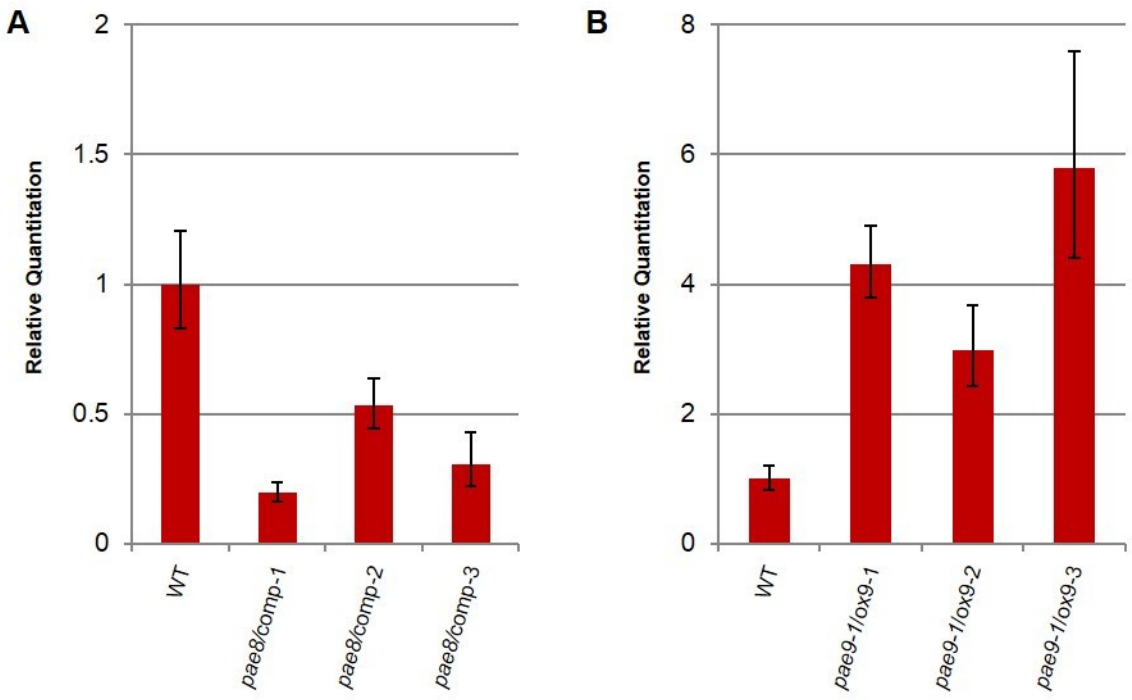

Figure 6.2.1-6 Q RT PCR of *pae8* complementation and *pae9* overexpression lines. Q-RT-PCR determination of the relative transcript abundance for PAE8/PAE9 in 35/30 day old leaves of T3 lines. *PTB1* gene expression was used as an internal normalization control. WT = Col-0 35/30 day old leaves. n=6

A

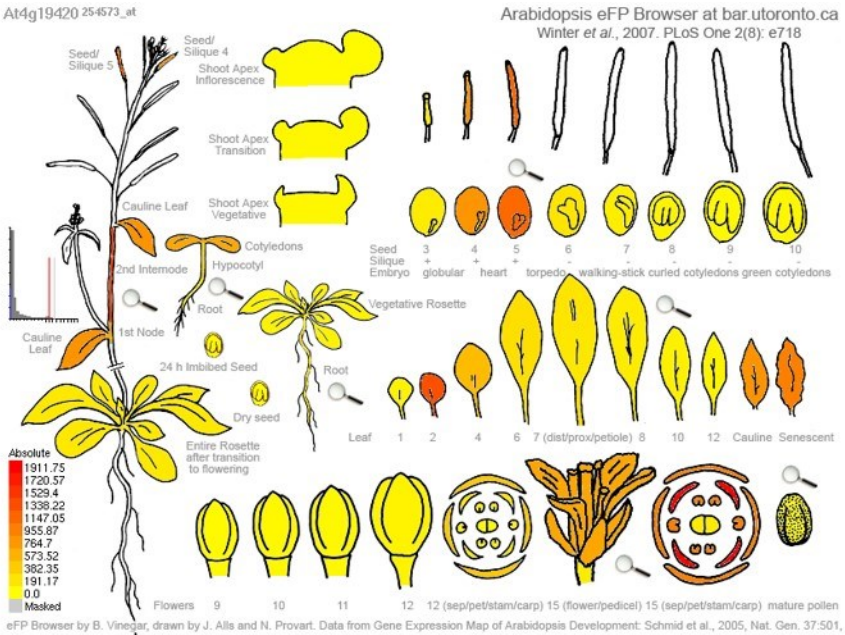

B

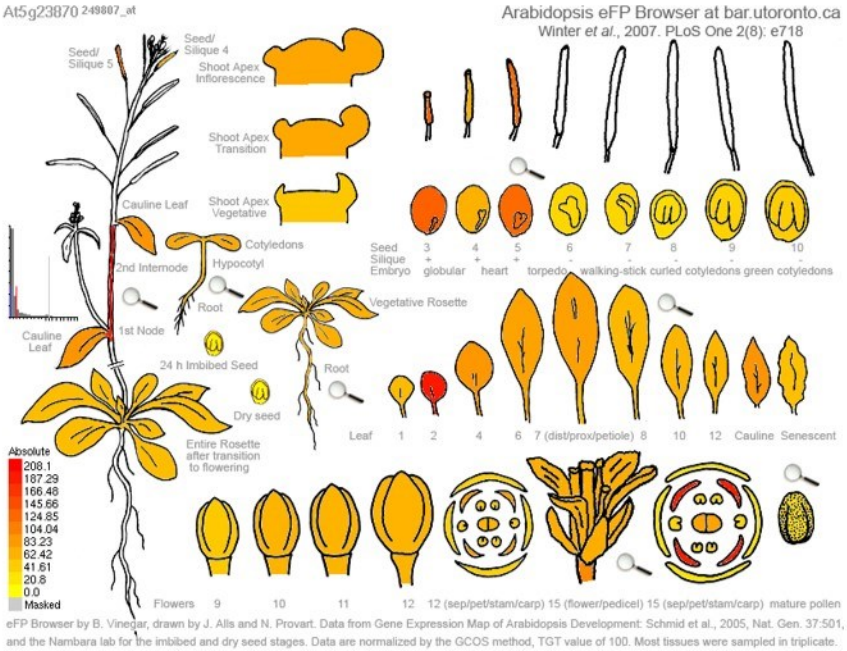

Figure 6.2.1-7 Expression patterns of *PAE8* and *PAE9*. Gene expression data in Arabidospsis thaliana according to the eFP-browser (http://bar.utoronto.ca/efp_arabidopsis/cgi-bin/efpWeb.cgi). A) expression of *PAE8* B) expression of *PAE9*. Data represents absolute values. Intensity scale of expression can be seen on the lower left corner of each section.

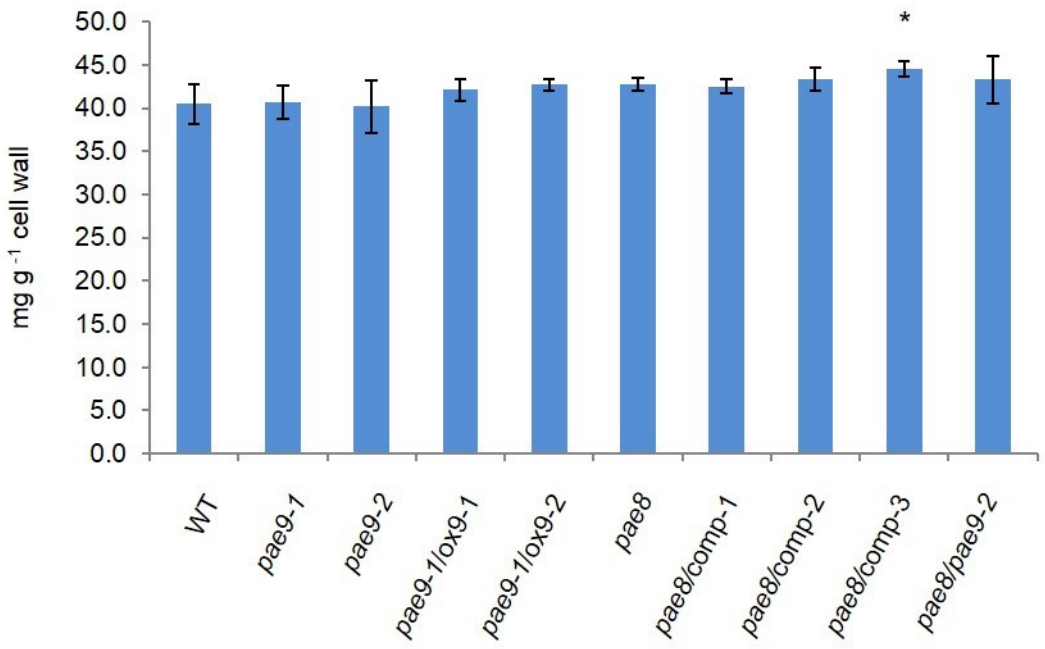

Figure 6.2.1-8 Stem acetate content in PAE mutants. Acetate content in mg g^{-1} cell wall. * indicates statistical significant differences based on *T* test (p-value < 0.01), n=6

To further investigate changes in the wall structure of the PAE mutants and overexpression and complementation lines, monosaccharide analysis of their de-starched walls was (2.5.1.5; 2.5.2) carried out by trifluoroacetic acid (TFA) hydrolysis and subsequent separation and quantification by high performance anion exchange chromatography (Xiong et al. 2013). No significant changes were observed in the sugar composition of these plants apart from a small reduction in the minor component fucose in the double mutant (Figure 6.2.1-9).

The crystalline cellulose content of 35 d old leaf material (2.5.1.5; 2.5.2) was also determined and while *pae9-1* exhibited a significant reduction in cellulose this could not be confirmed in the *pae9-2* mutant. Hence, no consistent changes in cellulose content were found (Figure 6.2.1-10).

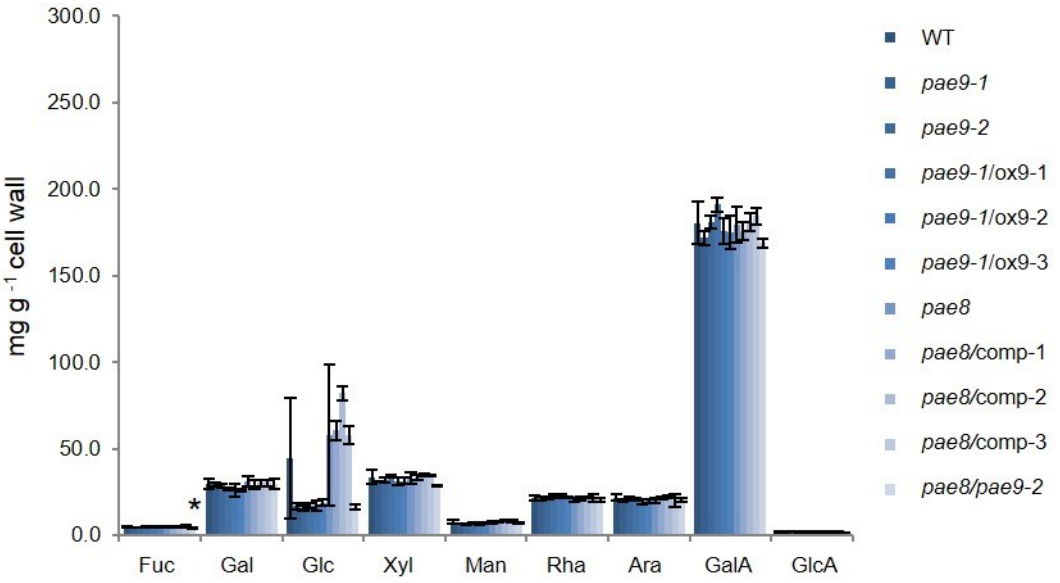

Figure 6.2.1-9 Monosacharide composition of de-starched cell walls. Monosaccharide content shown in mg g^{-1} DS-AIR. * indicates statistical significant differences based on T test (p-value < 0.01), n≥3.

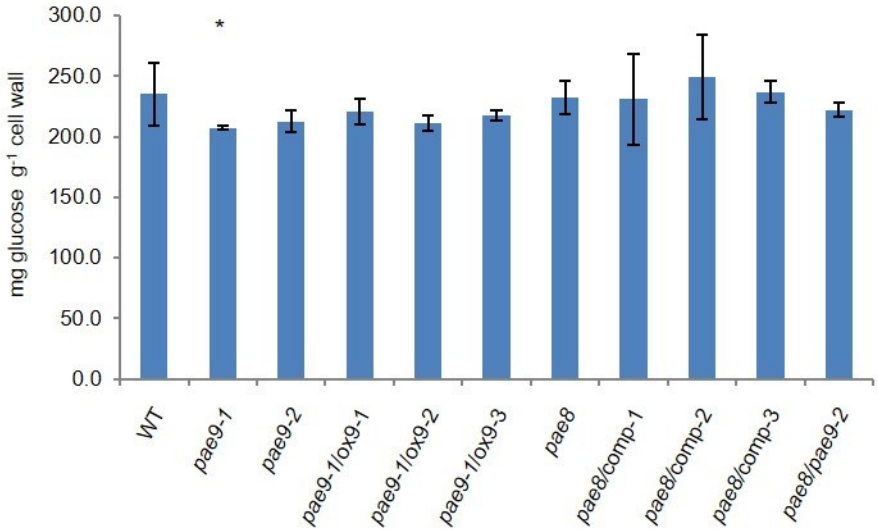

Figure 6.2.1-10 Crystalline cellulose content of 35 day old leaf de-starched cell walls in PAE lines. * indicates statistical significant differences based on T test (p-value < 0.05), n≥3.

6.2.2 Pectin fractions in *pae8* and *pae9* mutant lines have increased acetate content and reveal different modes of action towards pectin

Since the total amount of wall acetylation was increased in some of the PAE mutants, attempts were made to identify the polymeric origin of this acetate increase. Numerous polymers in the wall can be acetylated including XyG, heteromannans, heteroxylans and pectins (Harholt et al. 2010; Pauly et al. 2013). Based on OLIMP (2.5.1.3; 2.5.6) XyG acetylation levels were not altered in the *pae8* and *pae9* mutants (Figure 6.2.2-1). The acetylation status of pectic polysaccharides was also assessed since pectin is one of the most abundant acetylated polymers in the *Arabidopsis* leaf (Zablackis et al. 1995) and the gene family is annotated as PAE. A pectic digest (2.5.3) using a combination of endopolygalacturononase (EPG) and a pectin methylesterase (PME) was performed to solubilize pectic components from rosette leaves (2.5.1.5). This enzyme combination can solubilize HG and associated RGI and RGII (Oxenboll Sorensen et al. 2000). The monosaccharide analysis of this pectic extract was enriched in galactose, arabinose, xylose, rhamnose and galacturonic acid, all monosaccharides associated with pectic polymers (Figure 6.2.2-2). The acetate content of the pectic extract was determined (2.5.5). The mutants *pae8, pae9-1, pae9-2* and *pae8/pae9-2* exhibit increased acetate (16.5, 14, 14 and 27 %, respectively), when compared to WT (Table 6.2.2-1). Consistent with this result is a restoration to WT acetate levels in the *pae8* complementation lines (Table 6.2.2-1). The *PAE9* overexpression lines exceeded WT acetate levels by an additional 5.5% decrease (Table 6.2.2-1).

The remaining residue after the pectin extraction was analyzed for acetate content (2.5.5) as a control. Approximately 50 % of the total wall acetate was extracted with the pectolytic enzymes and the remaining residue exhibited similar chemotypic differences as the solubilized pectic extract (Table 6.2.2-1). The monosaccharide composition of the remaining pellet (2.5.8) suggests that the pectinase digest was incomplete since rhamnose and galacturonic acid were still present (Figure 6.2.2-2 B). Roughly half of the rhamnose was still accounted for in the residue suggesting that only half of the RGI structures were removed by the enzymatic digest (Figure 6.2.2-2 B). A much higher portion of the HG was extracted by the pectinases based on the monosaccharide analysis of the pectin extract and residue (Figure 6.2.2-2).

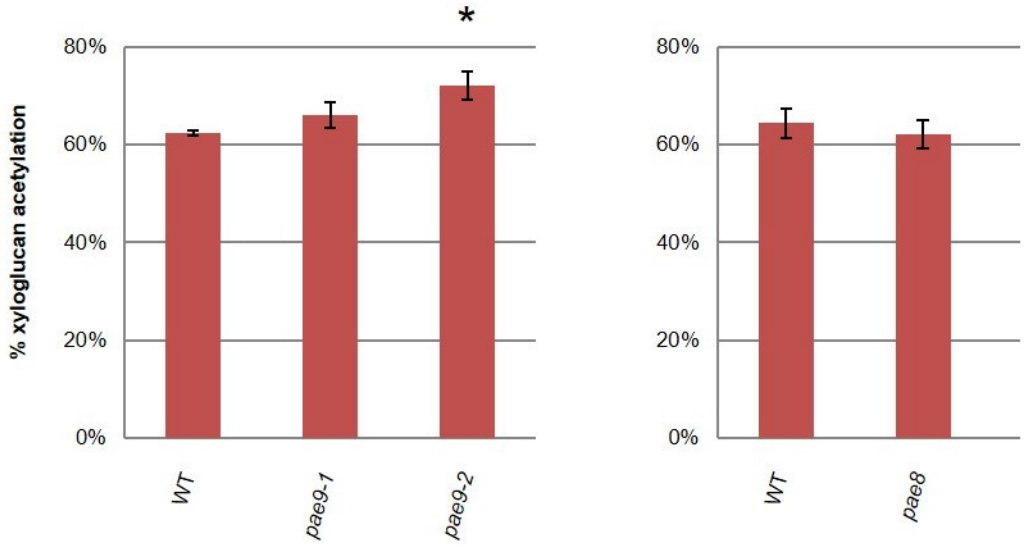

Figure 6.2.2-1 XyG acetylation in *pae8* and *pae9* mutants. % XyG acetylation as determined as in Figure 3.2.2-2. Tissues investigated - 5 week old rosette leaves for *pae9* and 6 week old rosette leaves for *pae8*). * indicates statistical significant differences based on T test (p-value < 0.01), n≥5. *pae8* data from Phillip Hull (Hull 2012).

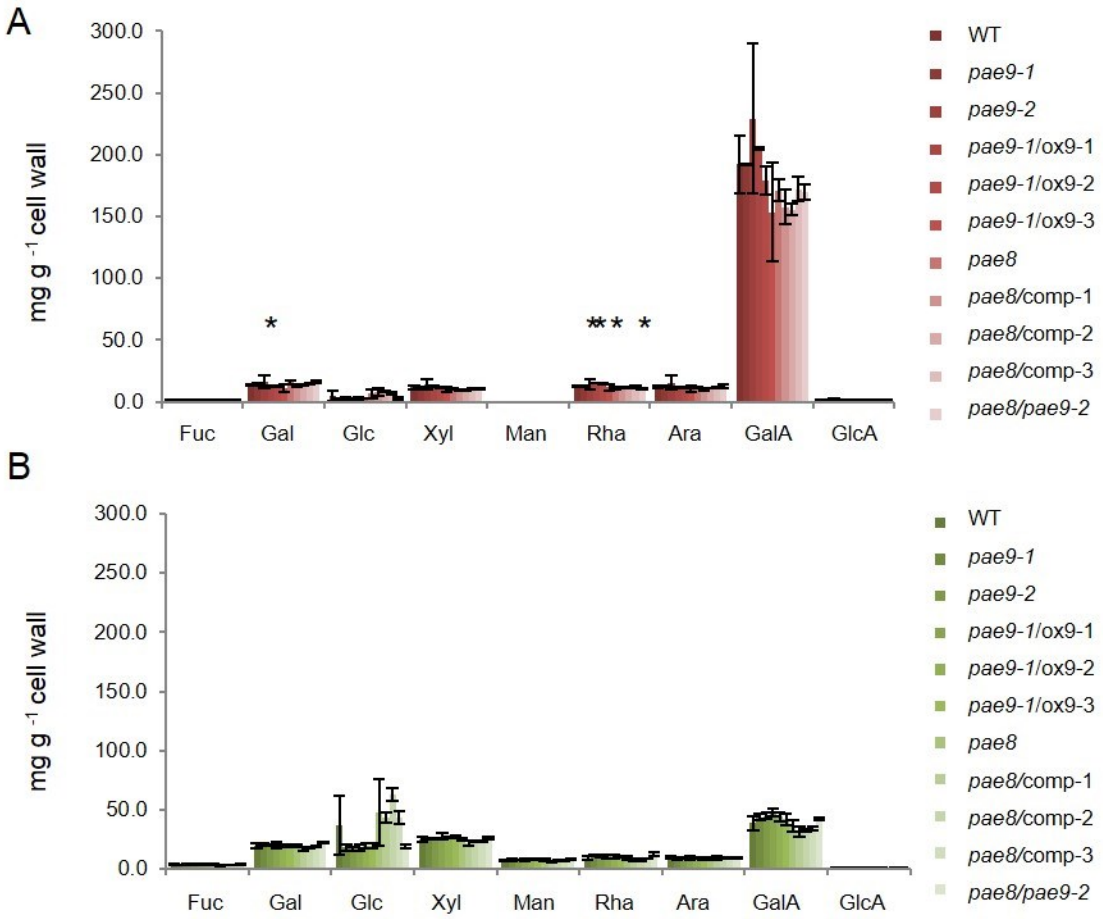

Figure 6.2.2-2 Monosaccharide composition of pectic digest and remaining residue. A) monosaccharide composition of pectic extract B) monosaccharide composition of pectin digest residue. Monosugar content shown in mg g^{-1} DS-AIR. * indicates statistical significant differences based on T test (p-value < 0.01), n≥3.

	Pectin extract		Pectin residue	
Set 1				
WT	6.33 ± 0.08	c	6.30 ± 0.29	c
pae9-1	7.22 ± 0.23	b	7.59 ± 0.17	b
pae9-2	7.24 ± 0.15	b	7.99 ± 0.26	b
pae9-1/ox9-1	5.96 ± 0.10	d	6.17 ± 0.27	c
pae9-1/ox9-2	6.08 ± 0.14	cd	6.02 ± 0.37	c
pae9-1/ox9-3	5.9 ± 0.11	d	6.13 ± 0.21	c
pae8	7.21 ± 0.16	b	8.02 ± 0.25	b
pae8/pae9-2	7.97 ± 0.20	a	9.17 ± 0.45	a
Set 2				
WT	5.80 ± 0.21	b	7.45 ± 0.26	bc
pae8	6.91 ± 0.18	a	8.52 ± 0.28	a
pae8/comp-1	5.85 ± 0.33	b	7.10 ± 0.76	c
pae8/comp-2	5.97 ± 0.28	b	7.79 ± 0.14	b
pae8/comp-3	6.16 ± 0.25	b	7.40 ± 0.17	b

Table 6.2.2-1 Acetate content of pectic extract and remaining residue (mg g^{-1} cell wall). ± indicate standard deviation; letters indicate statistical significant differences based on ANOVA test (p-value < 0.05); n≥4.

The pectin extract was subjected to fractionation by size exclusion chromatography (SEC; 2.5.4). The objective was to isolate different pectic fractions of different sizes and determine, if the acetate chemotype pertains to specific pectic fractions. The SEC chromatograms of the pectic extracts from the various mutants are shown in Figure 6.2.2-3. As previously shown (Oxenboll Sorensen et al. 2000), distinct peaks can be observed. These peaks were collected and pooled into distinct fractions (numerals I-V; Figure 6.2.2-3). The approximate size (Figure 6.2.2-3), acetate content (Table 6.2.2-2), and monosaccharide composition (Figure 6.2.2-4; Figure 6.2.2-5; 2.5.8) was determined for each fraction. Fractions I and II contained sugar molecules larger than 23 kDa and are enriched in monosaccharides present in RGI structures (galacturonic acid, rhamnose, arabinose and galactose). Fraction III contained molecules ranging between 23.2 and 4.6 kDa and has a higher content of galacturonic acid compared to fractions I and II suggesting the presence of RGII (Glushka et al. 2003; ONeill et al. 1996) and HG, respectively. Fractions IV and V contain an even higher percentage of galacturonic acid with small oligosaccharides between 0.6 - 4.6 kDa suggesting the abundance of HG fragments produced by the EPG/PME digest. Based on the chromatograms for the different mutant lines (Figure 6.2.2-3) no major differences could be found in the pectin digest profiles indicating that no major structural changes in the pectins in the mutants occurred.

The acetate measurements (2.5.5) of the different fractions reveal different chemotypic profiles for the two genes investigated (*PAE8* and *PAE9*). In *pae8*, an acetate increase can be found in all fractions with the exception of fraction III (Table 6.2.2-2). Genetic complementation of the *pae8* mutant successfully restores the acetate in these fractions back to WT levels (Table 6.2.2-2) indicating that PAE8 is responsible for the observed phenotype. The two mutants alleles of *PAE9* show increase in the acetate content exclusively in fractions I and II (Table 6.2.2-2). When *PAE9* is overexpressed in the *pae9-1* mutant background the acetate content in those fractions is restored to WT levels (Table 6.2.2-2). Taken together these results are consistent with the mode of action of PAEs.

The *pae8*/*pae9-2* double mutant shows an acetate increase in all fractions except in fraction III (Table 6.2.2-2). The double mutant also shows a reduction in the RGI monosaccharide rhamnose; pectin extract - 17% reduction; Figure 6.2.2-2 A, fraction II - 40% reduction; Figure 6.2.2-4 B, and fraction III - 13% reduction; Figure 6.2.2-4 C.

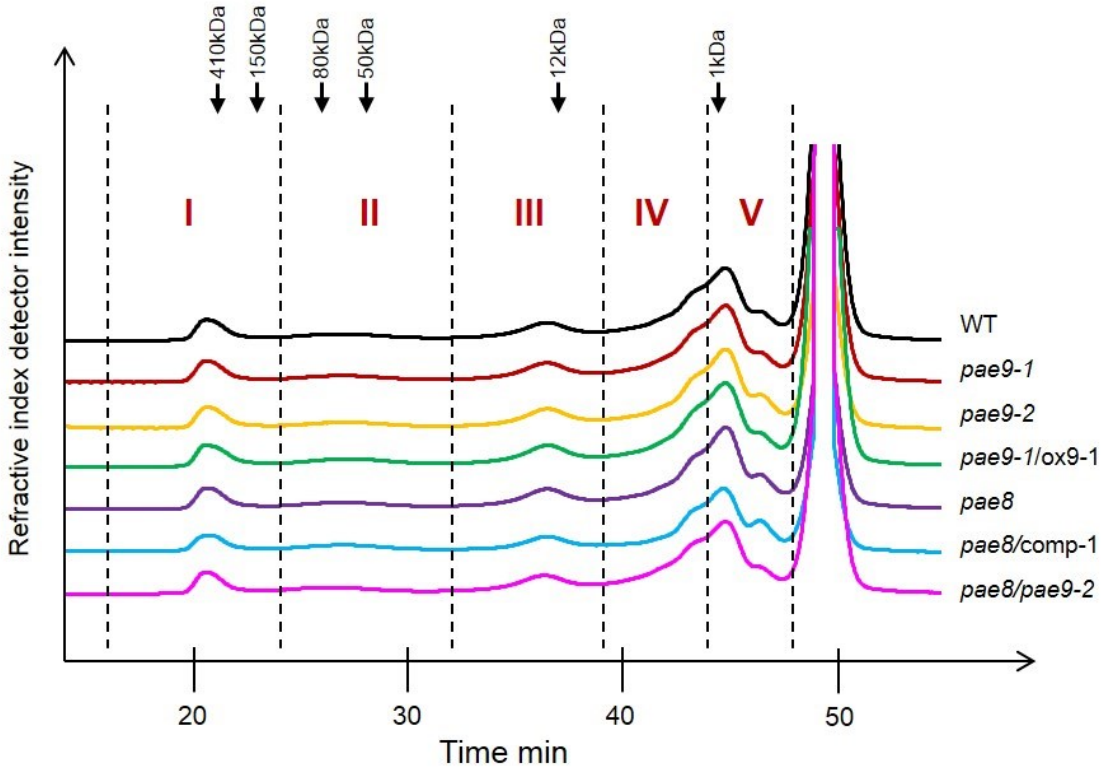

Figure 6.2.2-3 Size exclusion chromatograms of pectin extracts. Identity of applied samples are depicted on the right. Fractions were collected according to the depicted scheme with dashed bars indicating fraction borders. Fractions are labeled with roman numerals. Black arrows indicate elution time of dextran standards of known relative molecular weights.

	FI		FII		FIII		FIV		FV	
Set 1										
WT	1.20 ± 0.06	c	1.41 ± 0.08	d	0.78 ± 0.04	ae	1.24 ± 0.04	ce	0.77 ± 0.04	b
pae9-1	1.53 ± 0.12	ab	1.66 ± 0.04	ab	0.81 ± 0.03	a	1.26 ± 0.06	cd	0.78 ± 0.05	b
pae9-2	1.45 ± 0.12	b	1.56 ± 0.13	bc	0.77 ± 0.05	ag	1.29 ± 0.1	c	0.75 ± 0.06	b
pae9-1/ox9-1	1.14 ± 0.05	c	1.35 ± 0.05	d	0.78 ± 0.03	ad	1.15 ± 0.05	defg	0.74 ± 0.02	b
pae9-1/ox9-2	1.13 ± 0.08	c	1.34 ± 0.05	d	0.78 ± 0.03	af	1.19 ± 0.06	cf	0.73 ± 0.03	b
pae9-1/ox9-3	1.09 ± 0.05	c	1.3 ± 0.06	d	0.73 ± 0.05	bcdefg	1.16 ± 0.07	cg	0.72 ± 0.06	b
pae8	1.48 ± 0.08	b	1.62 ± 0.08	ac	0.8 ± 0.04	ac	1.48 ± 0.1	b	0.87 ± 0.05	a
pae8/pae9-2	1.65 ± 0.08	a	1.73 ± 0.09	a	0.81 ± 0.04	ab	1.63 ± 0.08	a	0.91 ± 0.02	a
Set 2										
WT	1.10 ± 0.05	b	1.45 ± 0.07	b	0.72 ± 0.03	ac	1.16 ± 0.08	b	0.77 ± 0.06	b
pae8	1.37 ± 0.03	a	1.74 ± 0.03	a	0.77 ± 0.01	a	1.38 ± 0.03	a	0.9 ± 0.05	a
pae8/comp-1	1.09 ± 0.05	b	1.43 ± 0.08	b	0.71 ± 0.05	bc	1.14 ± 0.08	b	0.77 ± 0.07	b
pae8/comp-2	1.13 ± 0.03	b	1.45 ± 0.09	b	0.72 ± 0.03	bc	1.12 ± 0.06	b	0.78 ± 0.04	b
pae8/comp-3	1.17 ± 0.07	b	1.52 ± 0.11	b	0.74 ± 0.02	ab	1.19 ± 0.04	b	0.81 ± 0.03	b

Table 6.2.2-2 Acetate content of pectic fractions (mg g^{-1} cell wall). ± indicate standard deviation; letters indicate statistical significant differences for each row based on ANOVA test (p-value < 0.05); n≥4.

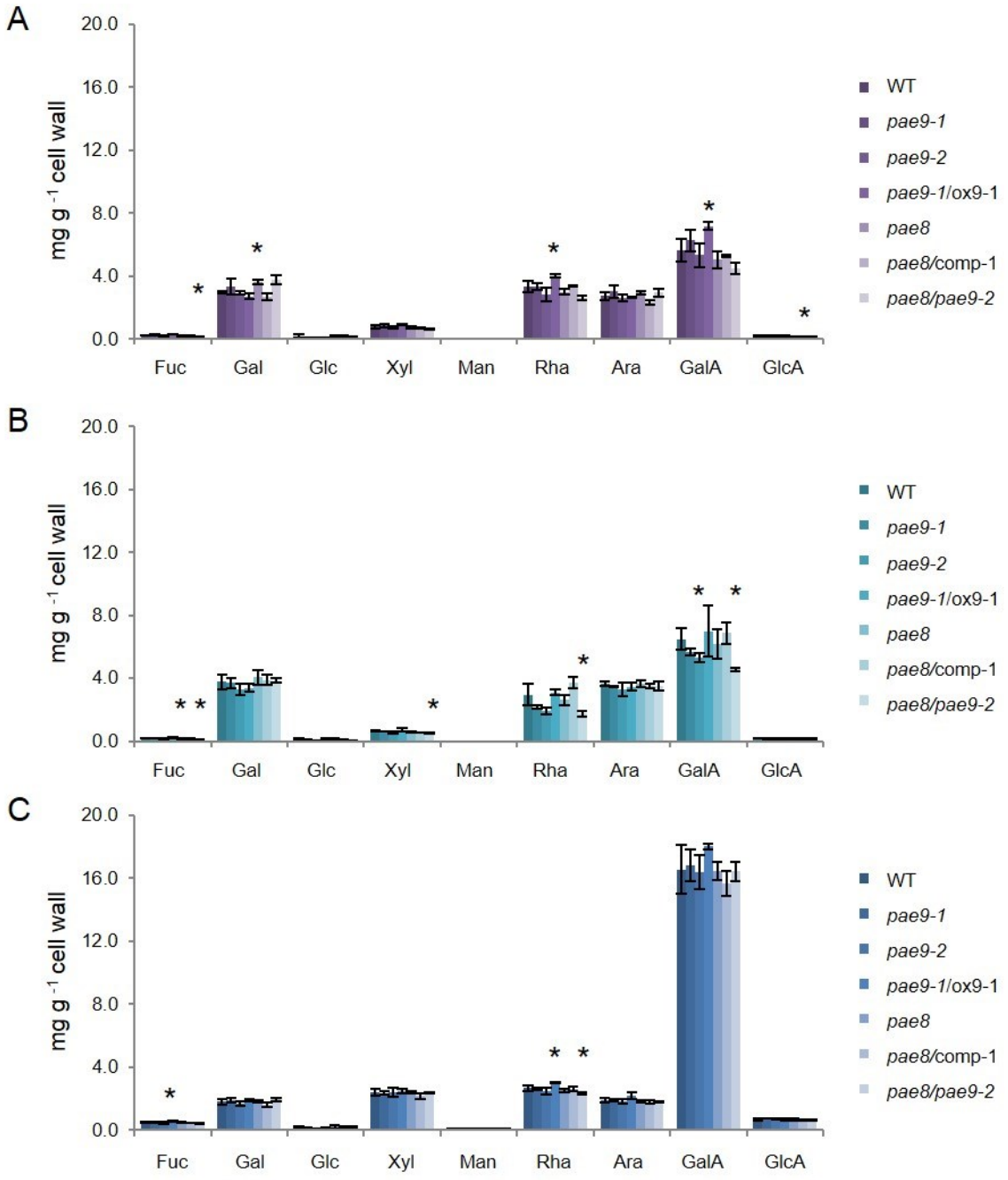

Figure 6.2.2-4 . Monosaccharide composition of fraction I (A), II (B) and III (C). Monosaccharide content shown in mg g^{-1} DS-AIR as detected by high performance anion exchange chromatography. * indicates statistical significant differences based on T test (p-value < 0.01) , n≥3.

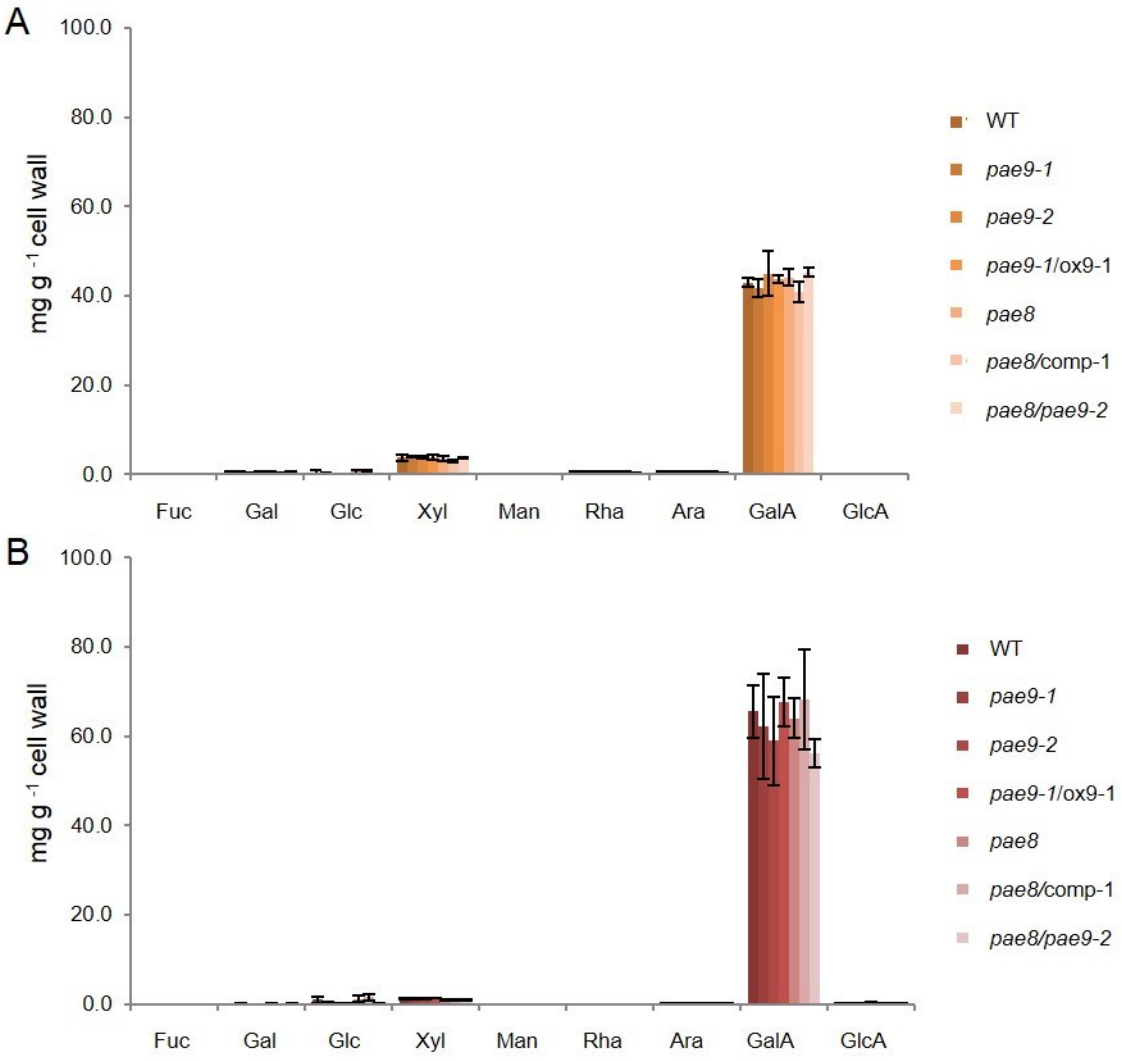

Figure 6.2.2-5 Monosacharide composition of fractions IV (A) and V (B). Monosaccharide content shown in mg g-1 DS-AIR as detected by high performance anion exchange chromatography. * indicates statistical significant differences based on T test (p-value < 0.01) , n≥3.

6.2.3 Subcellular localization studies for PAE9

The determination of the subcellular localization of the PAEs is relevant for the mode of action of these genes. To generate this data, different constructs containing the PAE9 cds fused C-terminally to GFP were used (2.2.4). In a first attempt *N. benthamiana* plants were transiently transformed (2.2.9) via agrobacterium infiltration with PAE9:GFP expressed under the control of the 35S promoter. Five days after infiltration, GFP fluorescence signals were observed by confocal microscopy (2.3) in areas that surround the cell (Figure 6.2.3-1). In order to ascertain from which subcellular compartments the GFP signal originated, two dyes were used: propidium iodide (PI), which stains cell walls (Gunl et al. 2011), and FM4-64, which stains membrane structures (Fischer-Parton et al. 2000). Plasmolysis conditions together with the mentioned dyes allow differentiating signals originating from the plasma membrane (FM4-64 stained receding structures during plasmolysis) or the cell wall (immobile structure during plasmolysis). When the PAE9:GFP transformed leaf material was infiltrated with PI (Figure 6.2.3-1 B, C, D; see Appendix for controls) the GFP signal co-localizes with the stain suggesting a localization in the cell wall. Under plasmolysis conditions the plasma membrane recedes, but a retention of the PI signal to the wall is observed, and partial diffusion of the GFP signal with structures interpreted as the plasma membrane (Figure 6.2.3-1 G, H). A similar experiment was performed using the FM-64 dye. Without plasmolysis the GFP signal partially co-localizes with the FM4-64 signal (Figure 6.2.3-1 L). When plasmolyzed these cells show that GFP signals can be found in wall structures but also at receding membranes together with FM4-64 (Figure 6.2.3-1 N, O, P). Taken together these experiments indicate that the PAE9:GFP fusion protein localizes to the plasma membrane and the wall.

In order to verify the physiological activity and thus relevance of the PAE9:GFP chimeric proteins the construct was used to complement the *pae9-2* mutant. The acetate measurements of 35 day old T2 leaf material (2.5.1.1; 2.5.5) reveal that the GFP fusion protein failed to complement the *pae9-2* mutant phenotype (Figure 6.2.3-2). Furthermore no GFP signal could be observed in *A. thaliana* leaves from either 35S:PAE9:GFP or empty vector controls (Figure 6.2.3-2 B). Due to the lack of GFP signal the native *PAE9* promoter (PAE9p) was used to drive PAE9:GFP expression. *pae9-1* plants were transformed with the PAE9p:cds:GFP construct as well as with the empty vector which consisted of the PAE9 promotor driving the GFP cds. As can be seen on Figure 6.2.3-3 none of the three independent complementation lines generated rescued the mutant phenotype. Again, no GFP signal could be detected from the PAE9p:cds:GFP or empty vector lines (Figure 6.2.3-3 B) indicating that the C-terminal GFP fusion seems to interfere with PAE9 activity.

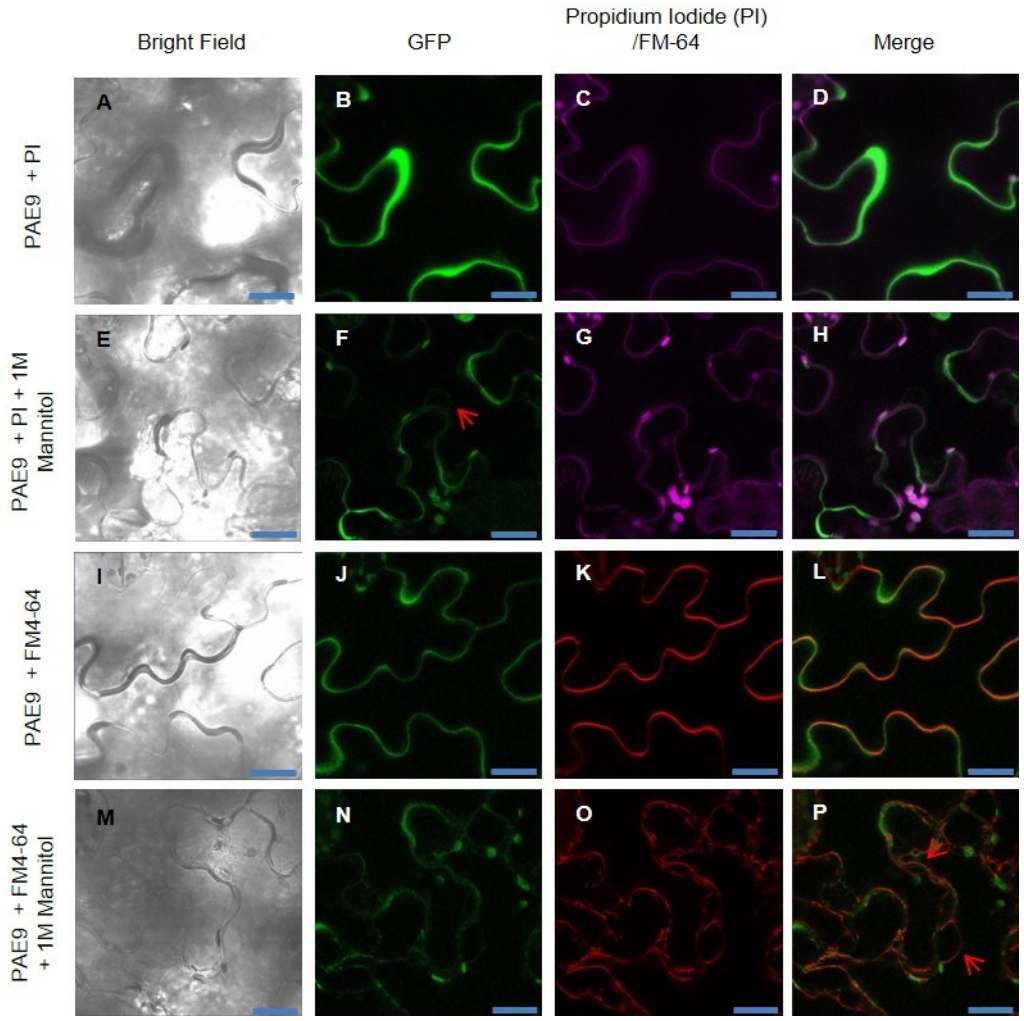

Figure 6.2.3-1 PAE9 subcellular localization. Subcellular localization of 35S:PAE9:GFP in *N benthamiana*. Columns indicate channels used for visualization: Bright field (A, E, I and M); GFP (B, F, J and N); Propidium iodide/FM4-64 (C and G for PI; K and O for FM4-64); Merge of GFP and Propidium iodide/FM4-64 (D, H, L and P). Rows exhibit treatment with dies (PI for cell wall staining and FM4-64 for plasma membrane staining) and plasmolizing agent (1M Mannitol). Red arrows highlight areas of interest showing membrane structures (F and P).

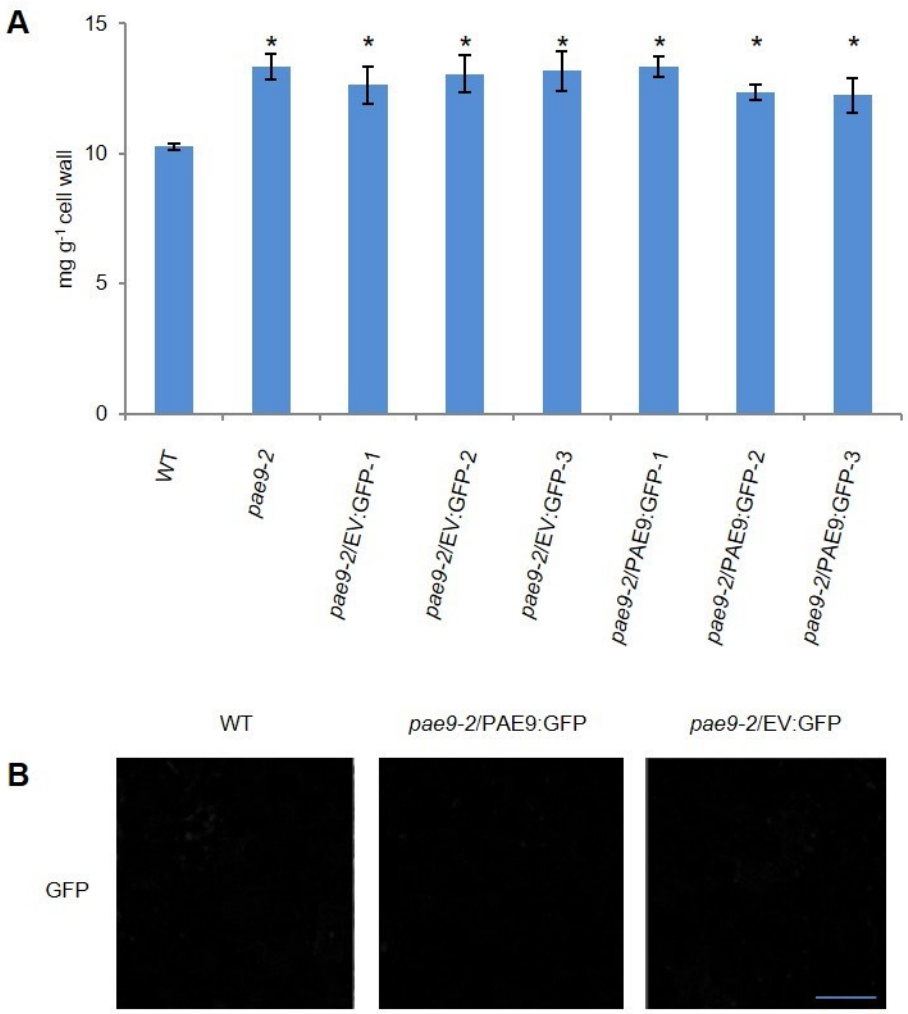

Figure 6.2.3-2 Acetate content and subcellular localization of PAE9:GFP expressed using the 35S promotor in the *pae9-2* background. A) Figure indicates acetate content of de-starched alcohol insoluble residue from 35 day old leaves. * indicates statistical significant differences based on T test (p-value < 0.01), n≥4. B) Sample images of confocal microscopy of 29 day old leaves of Col-0 (WT), *pae9-2*/PAE9:GFP and *pae9-2*/EV:GFP. Figures represent the GFP channel. Bar = 50µm. EV = 35S:GFP cds.

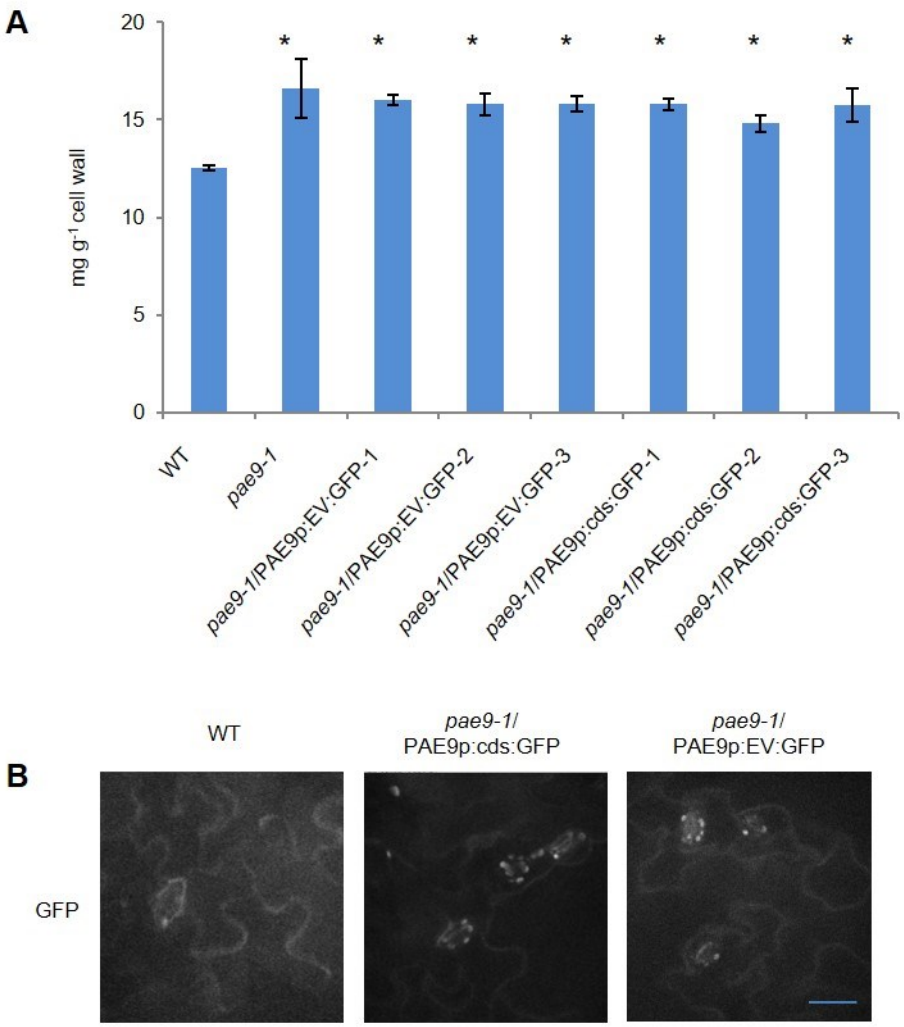

Figure 6.2.3-3 Acetate content and subcellular localization of PAE9cds:GFP under the control of the native PAE9 promotor in the pae9-1 background. Figure indicates acetate content of de-starched alcohol insoluble residue from 35 day old leaves. * indicates statistical significant differences based on T test (p-value < 0.01), n≥4. B) Sample images of confocal microscopy of 33 day old leaves of Col-0 (WT), pae9-1/PAE9p:cds:GFP and pae9-1/PAE9p:EV:GFP. Figures represent the GFP channel. Bar = 20 µm. EV = PAE9p:GFP cds.

6.2.4 PAE8 and PAE9 release acetate from mutant pectin fractions *in vitro*.

To obtain biochemical proof that PAE8 and PAE9 harbor indeed PAE activity, the proteins were heterologously expressed (2.2.9) and their activities determined in *in vitro* assays (2.2.11; 2.6). To facilitate purification, both proteins were C-terminally tagged with 6 x histidine and expressed transiently in *N. benthamiana.* PAE8 and PAE9 were partially purified via affinity chromatography and as a control empty vector protein extracts were processed in the same manner. The partially purified proteins expressed in *N. benthamiana* showed higher molecular weights (~ 55 kDa) than expected (45.3 kDa for PAE8 and 46.8 kDa for PAE9) based on the protein sequence derived from the clones open reading frame (Figure 6.2.4-1 A; Figure 6.2.4-2 A). A lower molecular weight band (~35 kDa) can be observed in western blots (2.2.12) of PAE8 preparations indicating partial degradation of the recombinant protein (Figure 6.2.4-1 A).

The protein preparations from tobacco leaves transiently expressing PAE8 or PAE9, and to a much lesser extent the empty vector controls, showed activity towards the substrate 4-nitrophenyl acetate that contains an acetyl-ester bond (Figure 6.2.4-1 B and Figure 6.2.4-1 B). This result is consistent with the acetylesterase activity proposed for these enzymes. To probe specific PAE activity, pectin fractions from the corresponding mutant walls (Figure 6.2.2-3.) were incubated with PAE8 or PAE9. Both proteins were capable of releasing acetate from fractions I and II of their corresponding mutant (Figure 6.2.4-1 C; Figure 6.2.4-2 C), which display enhanced acetate phenotypes in both single mutants (*pae8* and *pae9*). PAE8 releases less acetate than PAE9 in the *in vitro* assays (Figure 6.2.4-1 C; Figure 6.2.4-2 C). None of the other fractions tested (III-V; Figure 6.2.2-3.) served as substrates for these two enzymes under the conditions used. These observations are consistent with the mutant phenotype found in the *pae9* mutants. However, the enhanced acetate *pae8* mutant chemotype in fractions IV and V, cannot be explained by these *in vitro* data of purified PAE8.

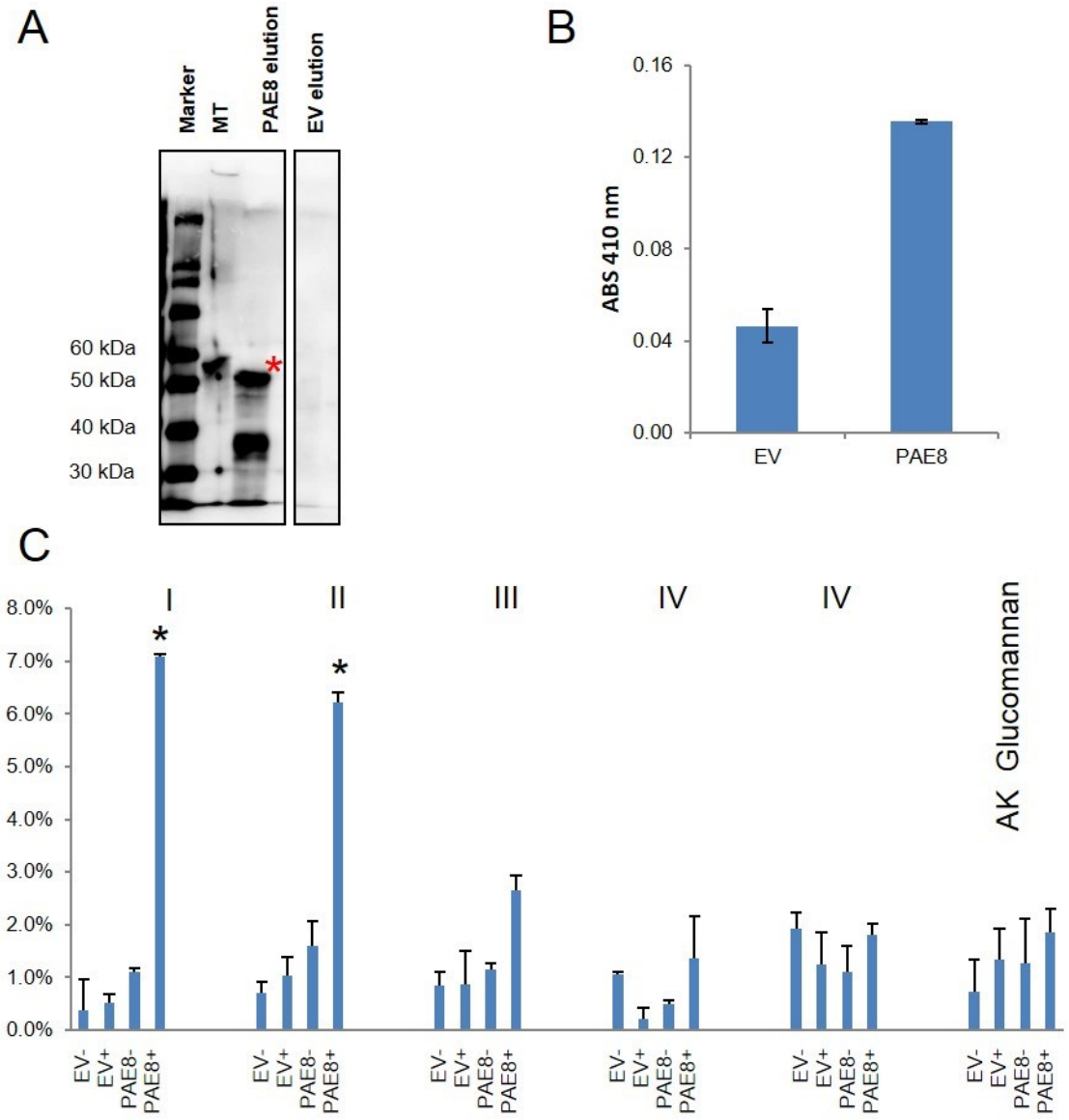

Figure 6.2.4-1 Partial protein purification and PAE8 activity. A) Western blot showing the presence of PAE8:6X HIS in the nickel column protein eluate (red asterix). No signal could be detected for the EV control (expression of the empty pART27 vector). Marker = Magic Marker; + control = multi-tag positive control (Life Technologies) B) activity of protein eluate on 4-nitrophenyl acetate; n=3. C) % labile acetate released from pectin fractions (I-V) and O-acetylated *Amorphophallus konjac* (AK) glucomannan. Alkali treatment would release 100% of the acetate from the substrate. Substrates for activity were purified from 3 independent *pae8* biological materials. Protein preparations were incubated with substrates for 18 h at room temperature. * indicates significant differences based on T-Test (p-value<0.015; n=3). EV = protein extract from a tobacco plant transformed with the empty vector control processed in the same manner as the

PAE8 construct; EV- = denatured EV protein; EV+ = native EV protein; PAE8 = purified protein extract from tobacco plants transformed with PAE8:6XHIS. PAE8- = denatured PAE8 protein; PAE8+ = PAE8 protein; n.d. = not detected.

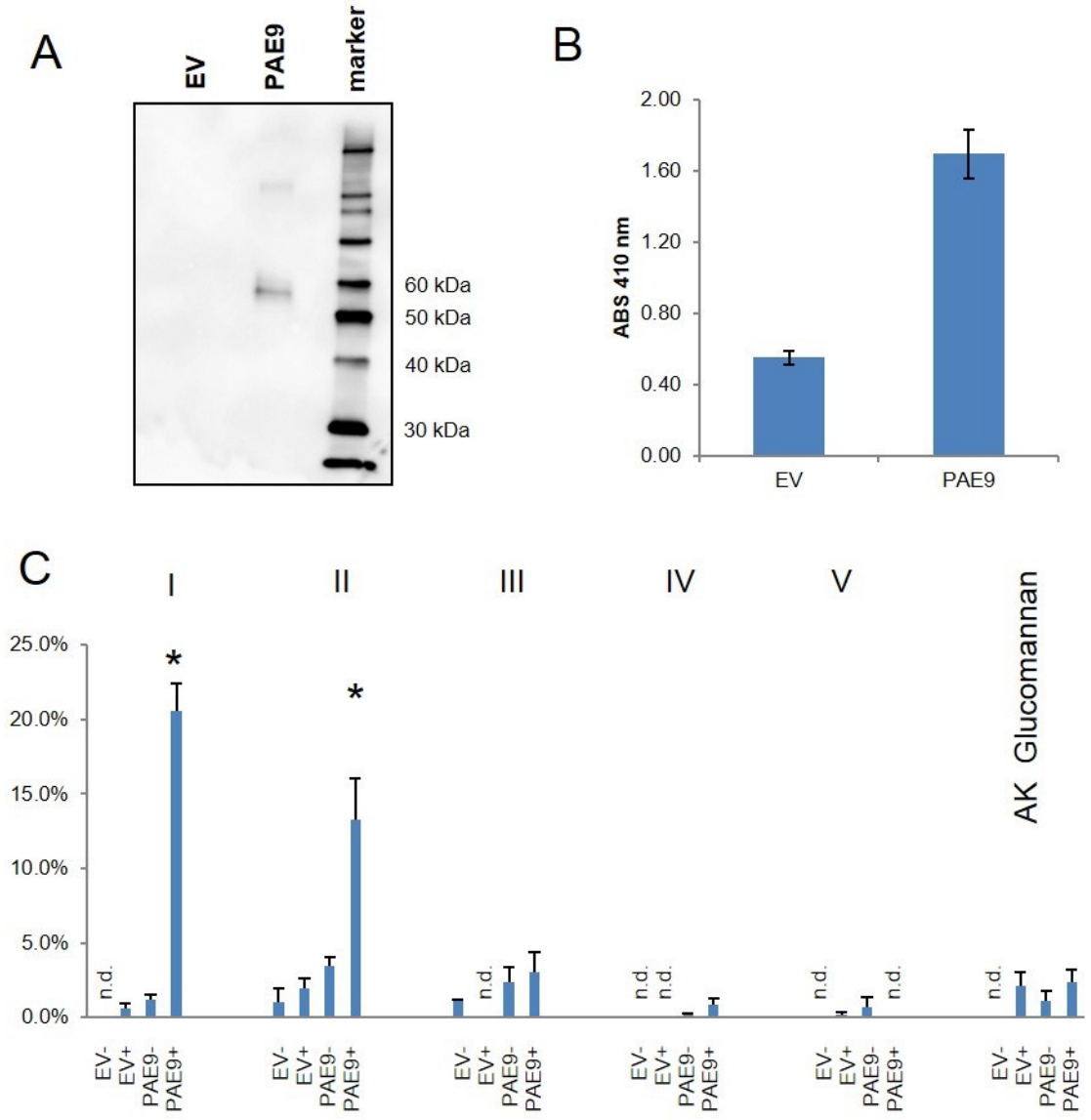

Figure 6.2.4-2 Partial protein purification and PAE9 activity. A) Western blot showing the presence of PAE9:6X HIS in the nickel column protein eluate. No signal could be detected for the EV control (expression of the empty pART27 vector). Marker = Magic Marker. B) activity of protein eluate on 4-nitrophenol acetate; n=3. C) % labile acetate released from pectin fractions (I-V) and *Amorphophallus konjac* glucomannan (acetylated), alkali treatment would release 100% of the substrate acetate. Substrates for activity were purified from 3 independent *pae9-1* biological materials. Protein preparations were incubated with substrates for 18 h at room temperature. * indicates significant differences based on T-Test (p-value<0.015; n=3). EV = protein extract from a tobacco plant transformed with the empty vector control processed in the same manner as the PAE9 construct; EV- = denatured EV protein; EV+ = native EV protein;

PAE9 = purified protein extract from tobacco plants transformed with PAE9:6XHIS. PAE9- = denatured PAE9 protein; PAE9+ = PAE9 protein; n.d. = not detected.

6.2.5 PAE mutant lines exhibit growth phenotypes and are susceptible to powdery mildew.

Some of the PAE mutant lines (*pae8*, *pae9-2*, *pae8*/*pae9-2* and *pae9-1*/*ox9-3*) exhibit reduced inflorescence growth (Figure 6.2.5-1; Figure 6.2.5-2; 2.7). The growth phenotypes found for *pae9-2* and *pae9-1*/*ox9-3* are not genetically consistent since the same reduction in growth cannot be found for the *pae9-1* mutant or the other *pae9-1*/*ox9* lines (Figure 6.2.5-1). However the growth reduction in *pae8* (9.6%) is genetically supported by the restoration of the growth phenotype observed in the *pae8* complementation lines (Figure 6.2.5-2). The *pae8*/*pae9-2* double mutant has a greater decrease in growth (26.6%) than *pae8* which suggests that *pae9-2* enhances the growth phenotype. *PAE8* and *PAE9* are highly expressed in stem tissue (Figure 6.2.1-7), despite the fact that the mutants do not exhibit stem acetate phenotypes (Figure 6.2.1-8) it is likely that these genes affect this tissue's development as is suggested by the stronger growth phenotype observed in the double mutant.

It has been reported that wall acetylation mutants can have increased resistance to pathogens (Manabe et al. 2011; Pogorelko et al. 2013; Vogel et al. 2004). Therefore, the *pae8* and *pae9* mutant lines were subjected to a plant pathogen, powdery mildew (2.8), to test for effects on pathogen resistance. As controls the *pmr5* [resistant; (Vogel et al. 2004)] and *sid2-1* [hypersensitive; (Wildermuth et al. 2001)] mutants were used. The powdery mildew growth was monitored visually on the leaf surface. No change in fungal growth was observed in any of those mutant lines compared to wild type plants (Figure **6.2.5-3**).

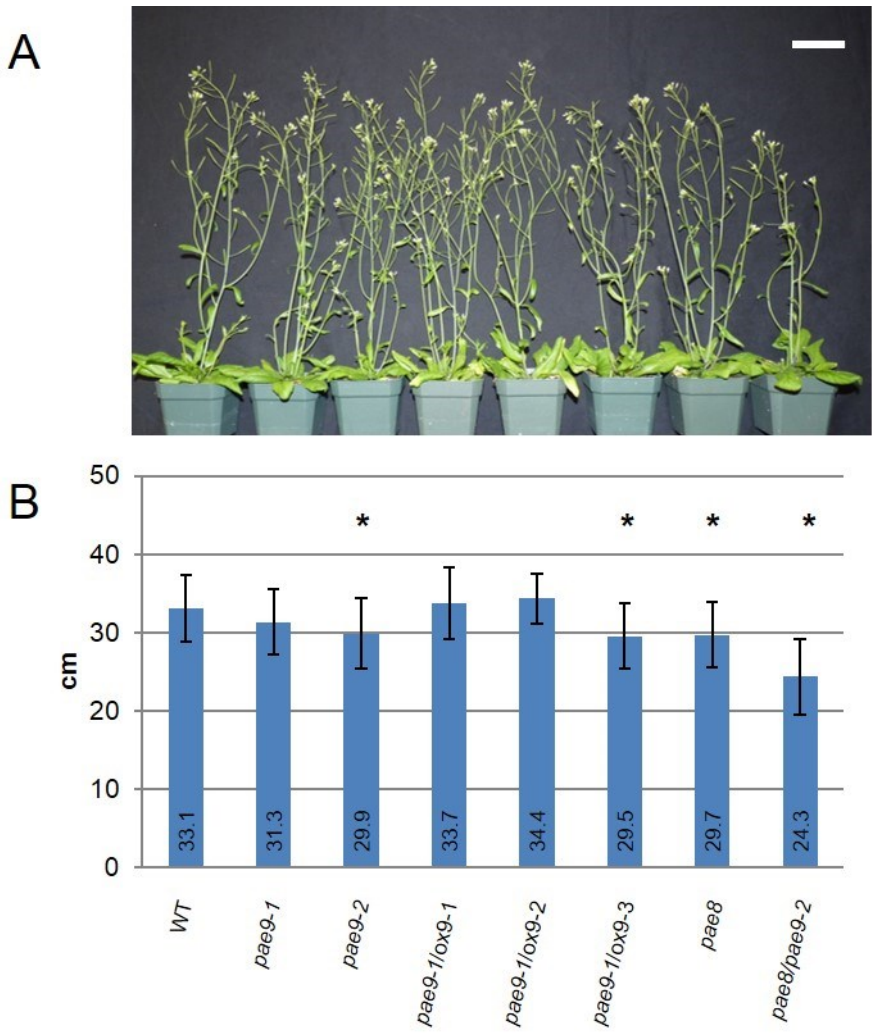

Figure 6.2.5-1 Length of inflorescence stems in 5 week old plants of PAE mutants (Set 1). A) Picture of representative plant. White bar = 4 cm. B) Inflorescence height in cm. * indicates statistical significant differences based on T test (p-value < 0.05).

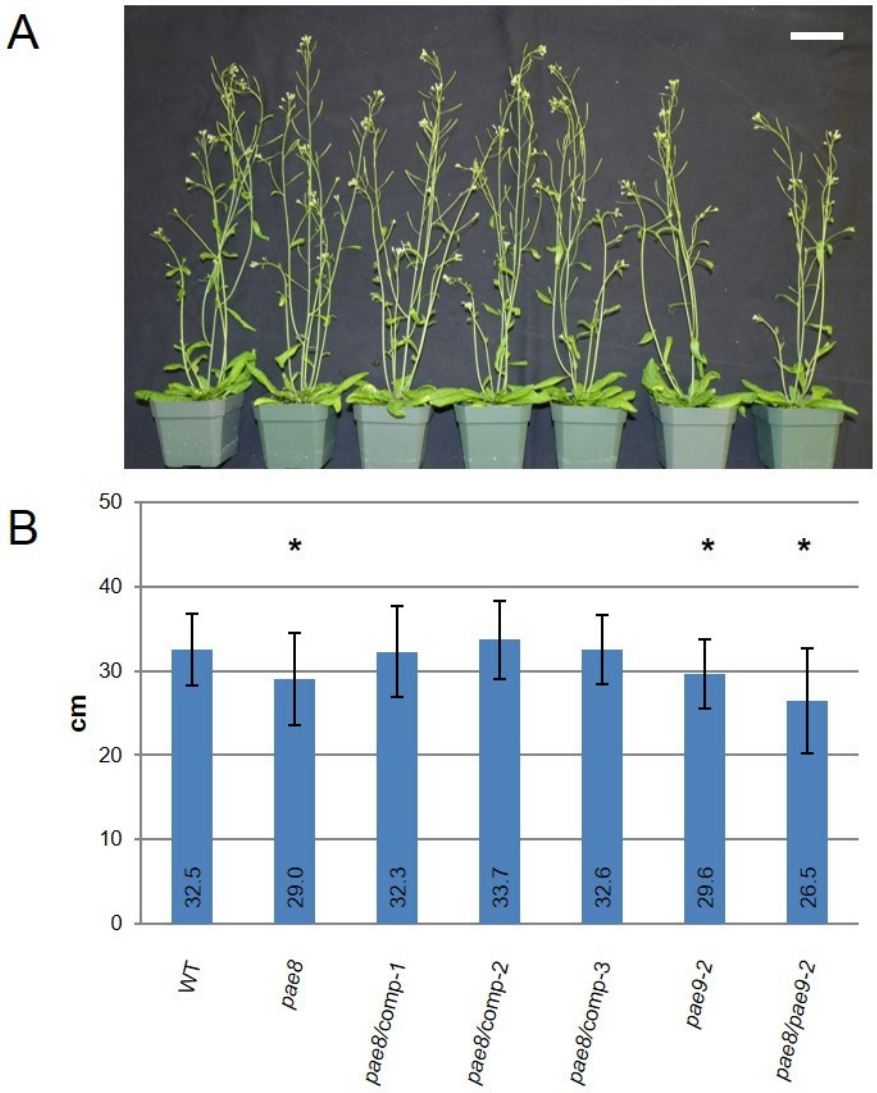

Figure 6.2.5-2 Length of inflorescence stems in 5 week old plants of PAE mutants (Set 2). A) picture of representative plant. White bar = 4 cm. B) Inflorescence height in cm. * indicates statistical significant differences based on T test (p-value < 0.01), n≥32.

Figure 6.2.5-3 Infection of powdery mildew in PAE lines. The figure depicts powdery mildew growth (white) in 3 week old *A. thaliana* plants. *pmr5* is resistant to the fungus and *sid2-1* is hypersensitive. White bar = 1 cm. Data from Dr. Heidi Szemenyei.

6.3 Discussion

6.3.1 PAE8 and PAE9 are PAEs acting on different substrates

The proposed reverse genetics approach to investigate gene function within the PAE gene family in *A. thaliana* proved to be successful. Out of the 12 genes investigated acetate chemotypes were found for three (PAE2; PAE8; PAE9; Table 6.2.1-1). Based on the phylogenetic tree of this gene family, *PAE8* and *PAE9* seem to be the only two members that lack close paralogs (Figure 6.2.1-2). This suggests genetic redundancy within the family, i.e. presence of close paralogs, prevented the observation of further acetate chemotypes. It is known that genome duplications in *Arabidopsis* have resulted in genetic redundancy in some traits (Vision et al. 2000). The generation of double mutants between two closely related paralogs could lead to the identification of novel acetate related phenotypes within the PAE family.

PAE8 and PAE9 were shown to modulate wall content in the leaves of *A. thaliana*. The single mutants of these genes contain walls with an increased acetate content of approximately 20% and a *pae8/pae9-2* double mutant with a 37% acetate increase (Table 6.2.1-2). The increased acetate content did not have any effect in the total cell wall monosaccharide composition (Figure 6.2.1-9) or influence its crystalline cellulose content (Figure 6.2.1-10). Through genetic means it was shown for the first time that is possible to increase the acetate content in the walls of plants. Previously, only the reduction in wall acetate had been achieved by the overexpression of acetylesterases and consequently the reduction in wall acetate (Gou et al. 2012; Orfila et al. 2012; Pogorelko et al. 2013).

Recently, it was proposed that members of the PAE family could be acting on wall polymers other than pectin (Gille et al. 2011a). This was suggested by the finding of a PAE ortholog expressed in the developing corm of the voodoo lily plant, which produces copious amounts of acetylated glucomannan as a storage polymer (Gille et al. 2011a). This hypothesis still stands, supported by the finding that *PAE2* when overexpressed affects the acetylation of a non-pectic polymer, reducing XyG acetylation by 6% (Table 6.2.1-1). *PAE8* and *PAE9* genes when mutated produce wall chemotypes associated with pectins and possibly other wall polymers. A pectic digest (Orfila et al. 2012; Oxenboll Sorensen et al. 2000) from the *pae8* and *pae9* mutants was prepared and indeed the increase in acetate was found in the pectic extract (Table 6.2.2-1). XyG analysis from leaf material of *PAE8* and *PAE9* mutants indicate that the acetylation status of this polymer is not affected (Figure 6.2.2-1). However, the analysis of the pectin residue after the digest revealed that only approximately half of the total acetate was extracted by the pectolytic enzymatic treatment (Table 6.2.2-1). The remaining pellets still exhibited acetate chemotypic differences similar to what was observed for total wall material and pectin (Table 6.2.1-2; Table 6.2.2-1). One possibility is that not all pectin was removed by the pectinase treatment, which is supported by the presence of pectin related monosaccharides (rhamnose and galacturonic acid) in the residue (Figure 6.2.2-2 B). However, the partially de-pectinated residue also contains other acetylated wall polymers such as heteroxylan and heteromannan [Figure 6.2.2-2 B; (Pettolino et al. 2012)]. It is therefore possible that PAE8 and PAE9 could act on these polymers.

Size-exclusion chromatography of the pectic extract resulted in pectic fractions with distinct sizes and compositions (Figure 6.2.2-3). An acetate phenotype was found in fractions I, II, IV and V for *pae8* and fractions I and II for *pae9* (Table 6.2.1-2). These results confirm that these PAEs act on pectic polysaccharides. Fractions I and II are enriched in RGI based on the monosaccharide analysis (Figure 6.2.2-4 A, B) and literature (Oxenboll Sorensen et al. 2000; Sengkhamparn et al. 2009). However, the ratio of rhamnose and galacturonic acid indicate that HG is also present in these fractions (I and II; Figure 6.2.2-4 A, B). Indeed, most pectin structural models show the covalent linkage between HG and RGI (Yapo 2011). Size profiles of the pectic extract (Figure 6.2.2-3) do not differ from WT and galacturonic acid content is not increased in fraction I and II suggesting that enhanced acetylation found in the mutants did not affect the EPG digest of HG covalently bound to RGI (Sengkhamparn et al. 2009). Soluble AGPs should have been eliminated from cell wall preparations during buffer washes [2.5.2; (Gille et al. 2013)]. However, there is still a possibility that AGP structures, which are large molecules enriched in arabinose and galactose (Albersheim et al. 2011; Gille et al. 2013; Nothnagel 1997), are covalently linked components of fraction I and II (Tan et al. 2013). These observations suggest that RGI in fractions I and II is the dominant molecule that exhibits a higher degree of acetylation in the *pae8* and *pae9* mutants. The RGI molecule with its complex structures could consist of structurally diverse substructures (Nakamura et al. 2002; Ridley et al. 2001; Yapo 2011) that act as independent substrates for PAE8 and PAE9. Fraction III lacks an acetate chemotype in the mutants and is likely to represent mostly RGII structures (ONeill et al. 1996). Fractions IV and V are enriched in galacturonic acid and therefore represent mainly HG oligomers. *pae8* exhibits acetate chemotypes in these fractions (Table 6.2.2-2) but not *pae9*, suggesting that PAE8 could be a more promiscuous enzyme, which acts on RGI and HG.

The *in vitro* activity studies for the two enzymes (PAE8 and PAE9) show that both proteins are active towards fraction I and II but not towards any other fraction (Figure 6.2.4-1 C; Figure 6.2.4-2 C). This observation suggests that the acetate phenotype found for *pae8* in fractions IV and V might be based on an indirect effect. Secondary effects caused by mutations in cell wall biosynthetic enzymes have been widely reported in the literature. In one case a rice xylan: xylosyltransferase, when functionally impaired, will produce plants that have reduced ferulic and coumaric acid esters in their walls (Chiniquy et al. 2012). In another case, the *xlt2* mutant impaired in a XyG: galactosyltransferase, exhibit plants with fucose enriched XyG (Jensen et al. 2012). It is possible that altered de-acetylation patterns in the *pae8* mutant could impact the action of other acetylesterases by altering the pool of available substrates in the wall generating indirect phenotypes. Because PAE8 is the closest ortholog to the recently identified voodoo lily PAE (Gille et al. 2011a) activity towards acetylated glucomannan was tested and both genes (PAE8 and PAE9) were unable to release acetate from that substrate *in vitro* (Figure 6.2.4-1 C; Figure 6.2.4-2 C). PAE8 and PAE9 were shown to have pectin acetyl esterase activity and are likely to act primarily on RGI substrates.

6.3.2 A non-functional PAE9:GFP fusion localizes to the cell apoplast

It is believed that PAEs act on cell wall polymers in the apoplast after polymer delivery to the wall via vesicle transport (Gou et al. 2012; Orfila et al. 2012). Synthesis of the matrix polymer in the Golgi-apparatus would thus be spatially separated from apoplastic editing by e.g. glycosyl hydrolases, *endo*-transglycosylases (de Silva et al. 1993) or pectin methylesterases (Micheli 2001). The function of apoplastic polymer editing is highlighted by PME35, which was shown to de-methylesterify HG and thereby controls the mechanical strength of *Arabidopsis* stems (Hongo et al. 2012). Other PMEs, when mutated, were shown to enhance the growth of the plant pathogen *Pseudomonas syringaea* implicating these proteins and thus apoplastic de-methylesterification in pathogen resistance (Bethke et al. 2014). In strawberries, fruit tissue softening and PME activity have been directly correlated (Draye and Van Cutsem 2008). In this study, the PAE9:GFP chimeric fusion under the control of the 35S promoter was found to localize to the wall and the plasma membrane (Figure 6.2.3-1). However, the construct failed to complement the mutant phenotype of *pae9-2* and is thus functionally inactive (Figure 6.2.3-2 A). Therefore, the apoplastic localization might constitute an experimental artifact with no physiological relevance. An attempt to localize the PAE9 protein and complement the *pae9-1* mutant phenotype with the PAE9:GFP fusion under its native promoter also failed (Figure 6.2.3-3). Since it was possible to overexpress the PAE9 cds (without GFP) with success and restore the mutant phenotypes with these constructs (Figure 6.2.1-6 B; Table 6.2.1-2) these observations point towards a loss of activity caused by the GFP attachment to the protein. The lack of GFP signal found when transformed with the 35S and native promoter constructs could have the following explanations: 1) the 35S promoter in the GFP fusion construct could have induced gene silencing in *Arabidopsis* (Elmayan and Vaucheret 1996); 2) The native promoter construct results in such a weak expression that the GFP-fluorescence cannot be observed. In agreement with the literature (Gou et al. 2012) it was shown that PAE9 occupies the apoplast and is likely to exert its activity in that space. The C-terminal GFP fusion proved to interfere with PAE9 activity suggesting that for future localization experiments GFP fusion to the N-terminus should be attempted. Other types of protein localization methods based on chemical interactions of small amino acid tags (6-12) to fluorescent compounds could be attempted (O'Hare et al. 2007). As an example, a tetracysteine tag, composed of 6 amino acids, which interacts with the biarsenical compound FlAsH producing a green fluorescent signal could be of advantage, since a small tag could potentially interfere less with the protein activity (O'Hare et al. 2007). Transmission electron microscopy coupled to immunogold labelling of proteins containing small tags could also be useful to localize PAEs (Hoh et al. 1995).

6.3.3 Reduced inflorescence growth and susceptibility to powdery mildew are features of PAE mutants

In general, the *pae8*, *pae9* and double mutant plants exhibit normal development and morphology with the exception of a consistent reduction in inflorescence height in the *pae8* and *pae8/pae9-2* mutants of 9.6% and 26.5%, respectively. Reduced inflorescence growth has been associated with pectin mutants such as QUASIMODO1, a putative galacturonic acid transferase, involved in HG synthesis. When mutated *qua1-*

1 exhibits inflorescences approximately 25% shorter than WT (Bouton et al. 2002). A mutation in an HG methyltransferase (*qua2*) results in dwarfed plants harboring developmental defects in 4-day-old dark-grown seedling (Mouille et al. 2007) linking defects in pectin structure to growth phenotypes. Expression profiles of *PAE8* and *PAE9* show increased activity in the secondary internode of the *Arabidopsis* inflorescence (Figure 6.2.1-7). However, the acetate content of this tissue is not altered (Figure 6.2.1-8). On one hand, the pectin content of the *A. thaliana* stem is at least ten times lower compared to leaf tissue [Figure 6.2.2-2 A; (Xiong et al. 2013)]. On the other hand, the acetate content of the stem is almost 4 times higher than the leaf acetate content (Figure 6.2.1-8; Table 6.2.1-2) due to the acetylation of hemicellulose xylan and mannan (Xiong et al. 2013). Therefore, a potential pectin acetate reduction in the stem could be below the detection limit. Genes involved in pectin biosynthesis have been shown to have high activity in stems (Orfila et al. 2005) or expression in the vasculature (Harholt et al. 2006), both tissues rich in secondary cell walls. The stem pectin acetylation status could play a critical role in tissue growth even if it represents a minor component. Alternatively, the stronger leaf acetate phenotype could lead to an interference with the normal time of flowering by delaying overall plant development but not compromising the normal stem wall composition. This possible pleiotropic effect for the delayed flowering phenotype for the *pae8* and *pae8*/*pae9-2* mutants parallels with delayed flowering times observed in some starch related mutants in *Arabidopsis*, which seem to exhibit also pleiotropic effects (Eimert et al. 1995). Experiments aiming at determining flowering time for mutant and WT as well as a detailed wall analysis of stems could help clarify, if the shorter inflorescences observed in the PAE mutants are a product of altered cell walls or a pleiotropic effect caused by the increased acetate in the leaf walls.

The first wall acetate mutant described, *rwa2*, was reported to have increased resistance to the necrotrophic fungal pathogen *Botrytis cinerea* (Manabe et al. 2011). In another case the *pmr5* mutant, identified in a screen for powdery mildew resistance (Vogel et al. 2004), is believed to have altered pectin acetylation levels (Lim 2013). *Arabidopsis* plants overexpressing fungal acetylesterases have also been reported to have increased resistance to the fungal pathogens *Botrytis cinerea* (Pogorelko et al. 2013). Due to the association of wall acetylation levels and pathogen resistance the PAE8 and PAE9 lines were tested for powdery mildew resistance or increased susceptibility. No phenotypes could be observed (Figure **6.2.5-3**).

The work presented here demonstrates that by manipulating the expression level of PAEs it is possible to engineer plant biomass with higher acetate levels. This capability could be useful in biorefinery processes and human health aspects. Biomass with increased acetyl-substitutions would result in a hydrolysate with a high acetate content, which could be beneficial in warding off microbial contaminants thus increasing the hygiene in the industrial fermentation processes increasing its overall efficiency (Wei et al. 2013). In clostridial ABE (acetone; butanol; ethanol) fermentation, elevated contents of acetate could increase the production of acetone (Martin et al. 1983), which is critical in driving the chemical synthesis of biofuels downstream of the fermentation process (Anbarasan et al. 2012). Concerning human health aspects it has been shown that acetate released in the colon is associated with the suppression of appetite and

obesity control (Frost et al. 2014). Increasing pectin acetylation could increase the amount of acetate released in the colon by bacteria acting on these polymers.

7.0 Concluding Remarks

Several approaches were used in this study to better understand the molecular mechanisms of plant cell wall acetylation. Genetics and biochemistry were utilized to identify new genes involved in various aspects of cell wall polymer acetylation.

Acetate chemotypes were identified within the natural diversity of *Arabidopsis* ecotypes demonstrating that this is a powerful resource for further genetic exploration of wall acetylation via QTL or single trait mapping. This could eventually lead to the discovery of new proteins involved in the biochemical pathway or regulation of cell wall acetate. It was shown in a specific case that an ecotype completely lacked acetylation in a wall polymer, an observation that opens new questions on the evolution and function of this trait. Are acetate moieties functionally redundant to other intra and inter wall polymer decorations, e.g. other sugar molecules? Does it represent an evolutionary strategy to save carbon (2 versus 5 or 6)? Does the acetylation of different polymers have different biological roles? Are these roles essential for the fitness of plants?

The significance of apoplastic acetylesterases in achieving appropriate wall acetylation levels was demonstrated. The extent to which plants remodel pectins ratifies the current view of the apoplast as a highly dynamic space essential for quantitative and qualitative polymer modifications. Similar to apoplastic hydrolases acetylesterases were shown here to participate in this process and their activities could represent a significant source for the polymer acetate variation encountered amongst different plant tissues and species. The precise biological role for this phenomena was not uncovered. However, some evidence suggests it could be related to tissue development. Utilizing acetylesterases as genetic tools it was possible to engineer plant cell walls with higher acetate content, which places acetylesterases as an immediately available resource for breeders aiming at producing tailored lignocellulosics for specific industrial applications in the food and biofuel sector. Future studies should attempt to determine the precise substrates for acetylesterases by using e.g. mass spectrometry techniques, and need to ascertain, if all genes in the pectin acetylesterase family (CE 13) act on pectin and are indeed pectin specific. Plant acetylesterases acting on other wall polymers are yet to be identified and their characterization will advance our knowledge of wall acetate dynamics. In *A. thaliana*, the elusive XyG acetylesterase might be among them or could be present in CE families 6, 8 or 11 based on the CAZY database.

8.0 References

Agrama HA, Moussa ME, Naser ME, Tarek MA, Ibrahim AH (1999) Mapping of QTL for downy mildew resistance in maize. Theoretical and applied genetics 99 (3-4):519-523. doi:10.1007/s001220051265

Albersheim P, Darvill A, Roberts K, Sederoff R, Staehelin A (2011) Plant cell walls : from chemistry to biology. Garland Science, New York, NY

Alejandro S, Lee Y, Tohge T, Sudre D, Osorio S, Park J, Bovet L, Lee Y, Geldner N, Fernie AR, Martinoia E (2012) AtABCG29 Is a Monolignol Transporter Involved in Lignin Biosynthesis. Current Biology 22 (13):1207-1212. doi:10.1016/j.cub.2012.04.064

Alonso-Blanco C, Bentsink L, Hanhart CJ, Blankestijn-de Vries H, Koornneef M (2003) Analysis of natural allelic variation at seed dormancy loci of *Arabidopsis thaliana*. Genetics 164 (2):711-729

Alonso-Blanco C, Koornneef M (2000) Naturally occurring variation in *Arabidopsis*: an underexploited resource for plant genetics. Trends in plant science 5 (1):22-29

Alonso JM, Stepanova AN, Leisse TJ, Kim CJ, Chen H, Shinn P, Stevenson DK, Zimmerman J, Barajas P, Cheuk R, Gadrinab C, Heller C, Jeske A, Koesema E, Meyers CC, Parker H, Prednis L, Ansari Y, Choy N, Deen H, Geralt M, Hazari N, Hom E, Karnes M, Mulholland C, Ndubaku R, Schmidt I, Guzman P, Aguilar-Henonin L, Schmid M, Weigel D, Carter DE, Marchand T, Risseeuw E, Brogden D, Zeko A, Crosby WL, Berry CC, Ecker JR (2003) Genome-wide insertional mutagenesis of *Arabidopsis thaliana*. Science 301 (5633):653-657. doi:10.1126/science.1086391

Anbarasan P, Baer ZC, Sreekumar S, Gross E, Binder JB, Blanch HW, Clark DS, Toste FD (2012) Integration of chemical catalysis with extractive fermentation to produce fuels. Nature 491 (7423):235-239. doi:10.1038/nature11594

Anders N, Wilkinson MD, Lovegrove A, Freeman J, Tryfona T, Pellny TK, Weimar T, Mortimer JC, Stott K, Baker JM, Defoin-Platel M, Shewry PR, Dupree P, Mitchell RA (2012) Glycosyl transferases in family 61 mediate arabinofuranosyl transfer onto xylan in grasses. Proc Natl Acad Sci U S A 109 (3):989-993. doi:10.1073/pnas.1115858109

Anderson CT, Wallace IS, Somerville CR (2012) Metabolic click-labeling with a fucose analog reveals pectin delivery, architecture, and dynamics in Arabidopsis cell walls. Proc Natl Acad Sci U S A 109 (4):1329-1334. doi:10.1073/pnas.1120429109

Arabidopsis Genome I (2000) Analysis of the genome sequence of the flowering plant *Arabidopsis thaliana*. Nature 408 (6814):796-815. doi:10.1038/35048692

Atmodjo MA, Hao Z, Mohnen D (2013) Evolving views of pectin biosynthesis. Annu Rev Plant Biol 64:747-779. doi:10.1146/annurev-arplant-042811-105534

Baronepel O, Gharyal PK, Schindler M (1988) Pectins as Mediators of Wall Porosity in Soybean Cells. Planta 175 (3):389-395. doi:10.1007/Bf00396345

Bethke G, Grundman RE, Sreekanta S, Truman W, Katagiri F, Glazebrook J (2014) Arabidopsis PECTIN METHYLESTERASEs contribute to immunity against Pseudomonas syringae. Plant Physiol 164 (2):1093-1107. doi:10.1104/pp.113.227637

Bischoff V, Nita S, Neumetzler L, Schindelasch D, Urbain A, Eshed R, Persson S, Delmer D, Scheible WR (2010a) TRICHOME BIREFRINGENCE and its homolog AT5G01360 encode plant-specific DUF231 proteins required for cellulose biosynthesis in Arabidopsis. Plant Physiol 153 (2):590-602. doi:10.1104/pp.110.153320

Bischoff V, Selbig J, Scheible WR (2010b) Involvement of TBL/DUF231 proteins into cell wall biology. Plant Signal Behav 5 (8):1057-1059

Blevins DG, Lukaszewski KM (1998) Boron in Plant Structure and Function. Annual review of plant physiology and plant molecular biology 49:481-500. doi:10.1146/annurev.arplant.49.1.481

Boerjan W, Ralph J, Baucher M (2003) Lignin biosynthesis. Annu Rev Plant Biol 54:519-546. doi:10.1146/annurev.arplant.54.031902.134938

Bordenave M, Goldberg R, Huet JC, Pernollet JC (1995) A novel protein from mung bean hypocotyl cell walls with acetyl esterase activity. Phytochemistry 38 (2):315-319

Bouchabke-Coussa O, Quashie ML, Seoane-Redondo J, Fortabat MN, Gery C, Yu A, Linderme D, Trouverie J, Granier F, Teoule E, Durand-Tardif M (2008) ESKIMO1 is a key gene involved in water economy as well as cold acclimation and salt tolerance. BMC plant biology 8. doi:10.1186/1471-2229-8-125

Bouton S, Leboeuf E, Mouille G, Leydecker MT, Talbotec J, Granier F, Lahaye M, Hofte H, Truong HN (2002) Quasimodo1 encodes a putative membrane-bound glycosyltransferase required for normal pectin synthesis and cell adhesion in Arabidopsis. Plant Cell 14 (10):2577-2590. doi:10.1105/Tpc.004259

Bradford MM (1976) A rapid and sensitive method for the quantitation of microgram quantities of protein utilizing the principle of protein-dye binding. Anal Biochem 72:248-254

Breton C, Bordenave M, Richard L, Pernollet JC, Huet JC, Perez S, Goldberg R (1996) PCR cloning and expression analysis of a cDNA encoding a pectinacetylesterase from *Vigna radiata* L. FEBS letters 388 (2-3):139-142

Brown DM, Goubet F, Vicky WWA, Goodacre R, Stephens E, Dupree P, Turner SR (2007) Comparison of five xylan synthesis mutants reveals new insight into the mechanisms of xylan synthesis. Plant J 52 (6):1154-1168. doi:10.1111/j.1365-313X.2007.03307.x

Brown DM, Zhang ZN, Stephens E, Dupree P, Turner SR (2009) Characterization of IRX10 and IRX10-like reveals an essential role in glucuronoxylan biosynthesis in Arabidopsis. Plant J 57 (4):732-746. doi:10.1111/j.1365-313X.2008.03729.x

Brumer H, Zhou Q, Baumann MJ, Carlsson K, Teeri TT (2004) Activation of crystalline cellulose surfaces through the chemoenzymatic modification of xyloglucan. J Am Chem Soc 126 (18):5715-5721. doi:10.1021/Ja0316770

Brutus A, Sicilia F, Macone A, Cervone F, De Lorenzo G (2010) A domain swap approach reveals a role of the plant wall-associated kinase 1 (WAK1) as a receptor of oligogalacturonides. Proc Natl Acad Sci U S A 107 (20):9452-9457. doi:10.1073/pnas.1000675107

Buckeridge MS (2010) Seed cell wall storage polysaccharides: models to understand cell wall biosynthesis and degradation. Plant Physiol 154 (3):1017-1023. doi:10.1104/pp.110.158642

Buckeridge MS, dos Santos HP, Tine MAS (2000) Mobilisation of storage cell wall polysaccharides in seeds. Plant Physiol Bioch 38 (1-2):141-156. doi:10.1016/S0981-9428(00)00162-5

Burton RA, Wilson SM, Hrmova M, Harvey AJ, Shirley NJ, Medhurst A, Stone BA, Newbigin EJ, Bacic A, Fincher GB (2006) Cellulose synthase-like CslF genes mediate the synthesis of cell wall (1,3;1,4)-beta-D-glucans. Science 311 (5769):1940-1942. doi:10.1126/science.1122975

Busse-Wicher M, Gomes TCF, Tryfona T, Nikolovski N, Stott K, Grantham NJ, Bolam DN, Skaf MS, dupree P (2014) The pattern of xylan acetylation suggests xylan may interact with cellulosemicrofibrils as a two-fold helical screw in the secondary plant cell wall of Arabidopsisthaliana. The Plant Journal. doi:10.1111/tpj.12575

Caffall KH, Pattathil S, Phillips SE, Hahn MG, Mohnen D (2009) *Arabidopsis thaliana* T-DNA mutants implicate GAUT genes in the biosynthesis of pectin and xylan in cell walls and seed testa. Mol Plant 2 (5):1000-1014. doi:10.1093/mp/ssp062

Carpita N, Sabularse D, Montezinos D, Delmer DP (1979) Determination of the Pore-Size of Cell-Walls of Living Plant-Cells. Science 205 (4411):1144-1147. doi:10.1126/science.205.4411.1144

Carpita NC (1996) Structure and Biogenesis of the Cell Walls of Grasses. Annual review of plant physiology and plant molecular biology 47:445-476. doi:10.1146/annurev.arplant.47.1.445

Carpita NC, Gibeaut DM (1993) Structural models of primary cell walls in flowering plants: consistency of molecular structure with the physical properties of the walls during growth. Plant J 3 (1):1-30

Carpita NC, McCann MC (2000) The Cell Wall. In: Buchanan BG, W.; Jones, R. (ed) Biochemistry & Molecular Biology of Plants American Society of Plant Physiologists, pp 52-51-58

Carroll A, Somerville C (2009) Cellulosic biofuels. Annu Rev Plant Biol 60:165-182. doi:10.1146/annurev.arplant.043008.092125

Cassab GI (1998) Plant Cell Wall Proteins. Annual review of plant physiology and plant molecular biology 49:281-309. doi:10.1146/annurev.arplant.49.1.281

Cavalier DM, Lerouxel O, Neumetzler L, Yamauchi K, Reinecke A, Freshour G, Zabotina OA, Hahn MG, Burgert I, Pauly M, Raikhel NV, Keegstra K (2008) Disrupting two *Arabidopsis thaliana* xylosyltransferase genes results in plants deficient in xyloglucan, a major primary cell wall component. Plant Cell 20 (6):1519-1537. doi:10.1105/tpc.108.059873

Chalfie M, Tu Y, Euskirchen G, Ward WW, Prasher DC (1994) Green Fluorescent Protein as a Marker for Gene-Expression. Science 263 (5148):802-805. doi:10.1126/science.8303295

Chiniquy D, Sharma V, Schultink A, Baidoo EE, Rautengarten C, Cheng K, Carroll A, Ulvskov P, Harholt J, Keasling JD, Pauly M, Scheller HV, Ronald PC (2012) XAX1 from glycosyltransferase family 61 mediates xylosyltransfer to rice xylan. Proc Natl Acad Sci U S A 109 (42):17117-17122. doi:10.1073/pnas.1202079109

Christensen TMIE, Nilsen JE, Mikkelsen JD (1996) Isolation, characterization and immuno localization of orange fruit acetyl esterase. In: Visser JV, Voragen AGJ (ed) Pectins and Pectinases. Elsevier Science B.V., Amsterdan, pp 723-730

Clarke JH, Mithen R, Brown JK, Dean C (1995) QTL analysis of flowering time in *Arabidopsis thaliana*. Molecular & general genetics 248 (3):278-286

Clough SJ, Bent AF (1998) Floral dip: a simplified method for Agrobacterium-mediated transformation of *Arabidopsis thaliana*. Plant J 16 (6):735-743

Cocuron JC, Lerouxel O, Drakakaki G, Alonso AP, Liepman AH, Keegstra K, Raikhel N, Wilkerson CG (2007) A gene from the cellulose synthase-like C family encodes a beta-1,4 glucan synthase. Proc Natl Acad Sci U S A 104 (20):8550-8555. doi:10.1073/pnas.0703133104

Condit CM, Meagher RB (1986) A Gene Encoding a Novel Glycine-Rich Structural Protein of Petunia. Nature 323 (6084):178-181. doi:10.1038/323178a0

Cooper JB, Varner JE (1984) Cross-linking of soluble extensin in isolated cell walls. Plant Physiol 76 (2):414-417

Cosgrove DJ (1998) Cell wall loosening by expansins. Plant Physiol 118 (2):333-339

Cosgrove DJ (2005) Growth of the plant cell wall. Nature reviews Molecular cell biology 6 (11):850-861. doi:10.1038/nrm1746

Cox PM, Betts RA, Jones CD, Spall SA, Totterdell IJ (2000) Acceleration of global warming due to carbon-cycle feedbacks in a coupled climate model. Nature 408 (6809):184-187. doi:10.1038/35041539

Curtis MD, Grossniklaus U (2003) A gateway cloning vector set for high-throughput functional analysis of genes in planta. Plant Physiol 133 (2):462-469. doi:10.1104/pp.103.027979

Dai XX, You CJ, Chen GX, Li XH, Zhang QF, Wu CY (2011) OsBC1L4 encodes a COBRA-like protein that affects cellulose synthesis in rice. Plant Mol Biol 75 (4-5):333-345. doi:10.1007/s11103-011-9730-z

Darvill A, Augur C, Bergmann C, Carlson RW, Cheong JJ, Eberhard S, Hahn MG, Lo VM, Marfa V, Meyer B, Mohnen D, Oneill MA, Spiro MD, Vanhalbeek H, York WS, Albersheim P (1992) Oligosaccharins - Oligosaccharides That Regulate Growth, Development and Defense Responses in Plants. Glycobiology 2 (3):181-198. doi:10.1093/glycob/2.3.181

de Silva J, Jarman CD, Arrowsmith DA, Stronach MS, Chengappa S, Sidebottom C, Reid JS (1993) Molecular characterization of a xyloglucan-specific endo-(1-->4)-beta-D-glucanase (xyloglucan endo-transglycosylase) from nasturtium seeds. Plant J 3 (5):701-711

Dean GH, Zheng H, Tewari J, Huang J, Young DS, Hwang YT, Western TL, Carpita NC, McCann MC, Mansfield SD, Haughn GW (2007) The Arabidopsis MUM2 gene encodes a beta-galactosidase required for the production of seed coat mucilage with correct hydration properties. Plant Cell 19 (12):4007-4021. doi:10.1105/tpc.107.050609

Delmer DP (1999) CELLULOSE BIOSYNTHESIS: Exciting Times for A Difficult Field of Study. Annual review of plant physiology and plant molecular biology 50:245-276. doi:10.1146/annurev.arplant.50.1.245

Deuschle K, Okumoto S, Fehr M, Looger LL, Kozhukh L, Frommer WB (2005) Construction and optimization of a family of genetically encoded metabolite sensors by semirational protein engineering. Protein science 14 (9):2304-2314. doi:10.1110/ps.051508105

Dhugga KS, Barreiro R, Whitten B, Stecca K, Hazebroek J, Randhawa GS, Dolan M, Kinney AJ, Tomes D, Nichols S, Anderson P (2004) Guar seed beta-mannan synthase is a member of the cellulose synthase super gene family. Science 303 (5656):363-366. doi:10.1126/science.1090908

Doblin MS, Pettolino FA, Wilson SM, Campbell R, Burton RA, Fincher GB, Newbigin E, Bacic A (2009) A barley cellulose synthase-like CSLH gene mediates (1,3;1,4)-beta-D-glucan synthesis in transgenic Arabidopsis. Proc Natl Acad Sci U S A 106 (14):5996-6001. doi:10.1073/pnas.0902019106

Dobson CM (2003) Protein folding and misfolding. Nature 426 (6968):884-890. doi:10.1038/nature02261

Domozych DS, Ciancia M, Fangel JU, Mikkelsen MD, Ulvskov P, Willats WG (2012) The Cell Walls of Green Algae: A Journey through Evolution and Diversity. Front Plant Sci 3:82. doi:10.3389/fpls.2012.00082

Draye M, Van Cutsem P (2008) Pectin methylesterases induce an abrupt increase of acidic pectin during strawberry fruit ripening. Journal of plant physiology 165 (11):1152-1160. doi:10.1016/j.jplph.2007.10.006

Dwivedi S, Perotti E, Ortiz R (2008) Towards molecular breeding of reproductive traits in cereal crops. Plant Biotechnol J 6 (6):529-559. doi:10.1111/j.1467-7652.2008.00343.x

Edwards K, Johnstone C, Thompson C (1991) A Simple and Rapid Method for the Preparation of Plant Genomic DNA for Pcr Analysis. Nucleic acids research 19 (6):1349-1349. doi:10.1093/nar/19.6.1349

Edwards M, Bowman YJ, Dea IC, Reid JS (1988) A beta-D-galactosidase from nasturtium (Tropaeolum majus L.) cotyledons. Purification, properties, and demonstration that xyloglucan is the natural substrate. J Biol Chem 263 (9):4333-4337

Edwards ME, Dickson CA, Chengappa S, Sidebottom C, Gidley MJ, Reid JSG (1999) Molecular characterisation of a membrane-bound galactosyltransferase of plant cell wall matrix polysaccharide biosynthesis. Plant J 19 (6):691-697. doi:10.1046/j.1365-313x.1999.00566.x

Egelund J, Petersen BL, Motawia MS, Damager I, Faik A, Olsen CE, Ishii T, Clausen H, Ulvskov P, Geshi N (2006) *Arabidopsis thaliana* RGXT1 and RGXT2 encode Golgi-localized (1,3)-alpha-D-xylosyltransferases involved in the synthesis of pectic rhamnogalacturonan-II. Plant Cell 18 (10):2593-2607. doi:10.1105/tpc.105.036566

Eimert K, Wang SM, Lue WL, Chen JC (1995) Monogenic Recessive Mutations Causing Both Late Floral Initiation and Excess Starch Accumulation in Arabidopsis. Plant Cell 7 (10):1703-1712

Elmayan T, Vaucheret H (1996) Expression of single copies of a strongly expressed 35S transgene can be silenced post-transcriptionally. Plant J 9 (6):787-797. doi:10.1046/j.1365-313X.1996.9060787.x

Engler C, Gruetzner R, Kandzia R, Marillonnet S (2009) Golden gate shuffling: a one-pot DNA shuffling method based on type IIs restriction enzymes. Plos One 4 (5):e5553. doi:10.1371/journal.pone.0005553

Faik A (2010) Xylan Biosynthesis: News from the Grass. Plant Physiol 153 (2):396-402. doi:10.1104/pp.110.154237

Faik A, Price NJ, Raikhel NV, Keegstra K (2002) An Arabidopsis gene encoding an alpha-xylosyltransferase involved in xyloglucan biosynthesis. P Natl Acad Sci USA 99 (11):7797-7802. doi:10.1073/pnas.102644799

Fanutti C, Gidley MJ, Reid JS (1993) Action of a pure xyloglucan endo-transglycosylase (formerly called xyloglucan-specific endo-(1-->4)-beta-D-glucanase) from the cotyledons of germinated nasturtium seeds. Plant J 3 (5):691-700

Fields S, Song O (1989) A novel genetic system to detect protein-protein interactions. Nature 340 (6230):245-246. doi:10.1038/340245a0

Fink H, Ahrenstedt L, Bodin A, Brumer H, Gatenholm P, Krettek A, Risberg B (2011) Bacterial cellulose modified with xyloglucan bearing the adhesion peptide RGD promotes endothelial cell adhesion and metabolism - a promising modification for vascular grafts. J Tissue Eng Regen M 5 (6):454-463. doi:10.1002/Term.334

Fischer-Parton S, Parton RM, Hickey PC, Dijksterhuis J, Atkinson HA, Read ND (2000) Confocal microscopy of FM4-64 as a tool for analysing endocytosis and vesicle trafficking in living fungal hyphae. J Microsc-Oxford 198:246-259. doi:10.1046/j.1365-2818.2000.00708.x

Fleischer A, O'Neill MA, Ehwald R (1999) The Pore Size of Non-Graminaceous Plant Cell Walls Is Rapidly Decreased by Borate Ester Cross-Linking of the Pectic Polysaccharide Rhamnogalacturonan II. Plant Physiol 121 (3):829-838

Frost G, Sleeth ML, Sahuri-Arisoylu M, Lizarbe B, Cerdan S, Brody L, Anastasovska J, Ghourab S, Hankir M, Zhang S, Carling D, Swann JR, Gibson G, Viardot A, Morrison D, Louise Thomas E, Bell JD (2014) The short-chain fatty acid acetate reduces appetite via a central homeostatic mechanism. Nature communications 5:3611. doi:10.1038/ncomms4611

Fry SC (2004) Primary cell wall metabolism: tracking the careers of wall polymers in living plant cells. New Phytol 161 (3):641-675. doi:10.1111/j.1469-8137.2003.00980.x

Fry SC, York WS, Albersheim P, Darvill A, Hayashi T, Joseleau JP, Kato Y, Lorences EP, Maclachlan GA, Mcneil M, Mort AJ, Reid JSG, Seitz HU, Selvendran RR, Voragen AGJ, White AR (1993) An Unambiguous Nomenclature for Xyloglucan-Derived Oligosaccharides. Physiol Plantarum 89 (1):1-3

Gibeaut DM, Pauly M, Bacic A, Fincher GB (2005) Changes in cell wall polysaccharides in developing barley (Hordeum vulgare) coleoptiles. Planta 221 (5):729-738. doi:10.1007/s00425-005-1481-0

Gibson DG, Young L, Chuang RY, Venter JC, Hutchison CA, Smith HO (2009) Enzymatic assembly of DNA molecules up to several hundred kilobases. Nat Methods 6 (5):343-U341. doi:10.1038/Nmeth.1318

Gille S, Cheng K, Skinner ME, Liepman AH, Wilkerson CG, Pauly M (2011a) Deep sequencing of voodoo lily (Amorphophallus konjac): an approach to identify relevant genes involved in the synthesis of the hemicellulose glucomannan. Planta 234 (3):515-526. doi:10.1007/s00425-011-1422-z

Gille S, de Souza A, Xiong G, Benz M, Cheng K, Schultink A, Reca IB, Pauly M (2011b) O-acetylation of *Arabidopsis* hemicellulose xyloglucan requires AXY4 or AXY4L, proteins with a TBL and DUF231 domain. Plant Cell 23 (11):4041-4053. doi:10.1105/tpc.111.091728

Gille S, Hansel U, Ziemann M, Pauly M (2009) Identification of plant cell wall mutants by means of a forward chemical genetic approach using hydrolases. Proc Natl Acad Sci U S A 106 (34):14699-14704. doi:10.1073/pnas.0905434106

Gille S, Pauly M (2012) O-acetylation of plant cell wall polysaccharides. Front Plant Sci 3:12. doi:10.3389/fpls.2012.00012

Gille S, Sharma V, Baidoo EE, Keasling JD, Scheller HV, Pauly M (2013) Arabinosylation of a Yariv-precipitable cell wall polymer impacts plant growth as exemplified by the Arabidopsis glycosyltransferase mutant ray1. Mol Plant 6 (4):1369-1372. doi:10.1093/mp/sst029

Gleave AP (1992) A Versatile Binary Vector System with a T-DNA Organizational-Structure Conducive to Efficient Integration of Cloned DNA into the Plant Genome. Plant Mol Biol 20 (6):1203-1207. doi:10.1007/Bf00028910

Glushka JN, Terrell M, York WS, O'Neill MA, Gucwa A, Darvill AG, Albersheim P, Prestegard JH (2003) Primary structure of the 2-O-methyl-alpha-L-fucose-containing side chain of the pectic polysaccharide, rhamnogalacturonan II. Carbohyd Res 338 (4):341-352. doi:10.1016/S0008-6215(02)00461-5

Gou JY, Miller LM, Hou G, Yu XH, Chen XY, Liu CJ (2012) Acetylesterase-mediated deacetylation of pectin impairs cell elongation, pollen germination, and plant reproduction. Plant Cell 24 (1):50-65. doi:10.1105/tpc.111.092411

Goubet F, Barton CJ, Mortimer JC, Yu XL, Zhang ZN, Miles GP, Richens J, Liepman AH, Seffen K, Dupree P (2009) Cell wall glucomannan in Arabidopsis is synthesised by CSLA glycosyltransferases, and influences the progression of embryogenesis. Plant J 60 (3):527-538. doi:10.1111/j.1365-313X.2009.03977.x

Goubet F, Jackson P, Deery MJ, Dupree P (2002) Polysaccharide analysis using carbohydrate gel electrophoresis: A method to study plant cell wall polysaccharides and polysaccharide hydrolases. Anal Biochem 300 (1):53-68. doi:10.1006/abio.2001.5444

Graham LE, Cook ME, Busse JS (2000) The origin of plants: body plan changes contributing to a major evolutionary radiation. Proc Natl Acad Sci U S A 97 (9):4535-4540

Guinee TP, Wilkinson MG (1992) Rennet Coagulation and Coagulants in Cheese Manufacture. J Soc Dairy Technol 45 (4):94-104

Gunl M, Neumetzler L, Kraemer F, de Souza A, Schultink A, Pena M, York WS, Pauly M (2011) AXY8 encodes an alpha-fucosidase, underscoring the importance of apoplastic metabolism on the fine structure of Arabidopsis cell wall polysaccharides. Plant Cell 23 (11):4025-4040. doi:10.1105/tpc.111.089193

Gunl M, Pauly M (2011) AXY3 encodes a alpha-xylosidase that impacts the structure and accessibility of the hemicellulose xyloglucan in *Arabidopsis* plant cell walls. Planta 233 (4):707-719. doi:10.1007/s00425-010-1330-7

Ha MA, Apperley DC, Evans BW, Huxham M, Jardine WG, Vietor RJ, Reis D, Vian B, Jarvis MC (1998) Fine structure in cellulose microfibrils: NMR evidence from onion and quince. Plant J 16 (2):183-190. doi:10.1046/j.1365-313x.1998.00291.x

Hadfield KA, Bennett AB (1998) Polygalacturonases: many genes in search of a function. Plant Physiol 117 (2):337-343

Harholt J, Jensen JK, Sorensen SO, Orfila C, Pauly M, Scheller HV (2006) ARABINAN DEFICIENT 1 is a putative arabinosyltransferase involved in biosynthesis of

pectic arabinan in *Arabidopsis*. Plant Physiol 140 (1):49-58. doi:10.1104/pp.105.072744
Harholt J, Suttangkakul A, Vibe Scheller H (2010) Biosynthesis of pectin. Plant Physiol 153 (2):384-395. doi:10.1104/pp.110.156588
Hayashi T (1989) Xyloglucans in the Primary-Cell Wall. Annual review of plant physiology and plant molecular biology 40:139-168
Hayashi T, Ogawa K, Mitsuishi Y (1994) Characterization of the Adsorption of Xyloglucan to Cellulose. Plant and Cell Physiology 35 (8):1199-1205
He Z, Wang ZY, Li J, Zhu Q, Lamb C, Ronald P, Chory J (2000) Perception of brassinosteroids by the extracellular domain of the receptor kinase BRI1. Science 288 (5475):2360-2363
Herth W (1983) Arrays of Plasma-Membrane Rosettes Involved in Cellulose Microfibril Formation of Spirogyra. Planta 159 (4):347-356. doi:10.1007/Bf00393174
Hilscher J, Schlotterer C, Hauser MT (2009) A single amino acid replacement in ETC2 shapes trichome patterning in natural *Arabidopsis* populations. Current biology 19 (20):1747-1751. doi:10.1016/j.cub.2009.08.057
Hoh B, Hinz G, Jeong BK, Robinson DG (1995) Protein storage vacuoles form de novo during pea cotyledon development. J Cell Sci 108 (Pt 1):299-310
Hongo S, Sato K, Yokoyama R, Nishitani K (2012) Demethylesterification of the primary wall by PECTIN METHYLESTERASE35 provides mechanical support to the *Arabidopsis* stem. Plant Cell 24 (6):2624-2634. doi:10.1105/tpc.112.099325
Hooke R (1665) Micrographia: or, Some physiological descriptions of minute bodies made by magnifying glasses. With observations and inquiries thereupon. Printed by J. Martyn and J. Allestry, London,
Hu CD, Chinenov Y, Kerppola TK (2002) Visualization of interactions among bZip and Rel family proteins in living cells using bimolecular fluorescence complementation. Mol Cell 9 (4):789-798. doi:10.1016/S1097-2765(02)00496-3
Hull PAM (2012) Insights into *O*-acetylation of the plant cell wall polysaccharide glucomannan. Master, Westfalische-Wilhelms Universitat Munster, Berkeley/Munster
Ishii T (1997) O-acetylated oligosaccharides from pectins of potato tuber cell walls. Plant Physiol 113 (4):1265-1272
Iwai H, Masaoka N, Ishii T, Satoh S (2002) A pectin glucuronyltransferase gene is essential for intercellular attachment in the plant meristem. P Natl Acad Sci USA 99 (25):16319-16324. doi:10.1073/pnas.252530499
Jarvis MC, Briggs SPH, Knox JP (2003) Intercellular adhesion and cell separation in plants. Plant Cell Environ 26 (7):977-989. doi:10.1046/j.1365-3040.2003.01034.x
Jensen JK, Schultink A, Keegstra K, Wilkerson CG, Pauly M (2012) RNA-Seq analysis of developing nasturtium seeds (Tropaeolum majus): identification and characterization of an additional galactosyltransferase involved in xyloglucan biosynthesis. Mol Plant 5 (5):984-992. doi:10.1093/mp/sss032
Jensen JK, Sorensen SO, Harholt J, Geshi N, Sakuragi Y, Moller I, Zandleven J, Bernal AJ, Jensen NB, Sorensen C, Pauly M, Beldman G, Willats WG, Scheller HV (2008) Identification of a xylogalacturonan xylosyltransferase involved in pectin biosynthesis in *Arabidopsis*. Plant Cell 20 (5):1289-1302. doi:10.1105/tpc.107.050906

Jia Z, Qin Q, Darvill AG, York WS (2003) Structure of the xyloglucan produced by suspension-cultured tomato cells. Carbohydr Res 338 (11):1197-1208
Johnsson N, Varshavsky A (1994) Split Ubiquitin as a Sensor of Protein Interactions in-Vivo. P Natl Acad Sci USA 91 (22):10340-10344. doi:10.1073/pnas.91.22.10340
Jolie RP, Duvetter T, Van Loey AM, Hendrickx ME (2010) Pectin methylesterase and its proteinaceous inhibitor: a review. Carbohydr Res 345 (18):2583-2595. doi:10.1016/j.carres.2010.10.002
Jones L, Milne JL, Ashford D, McQueen-Mason SJ (2003) Cell wall arabinan is essential for guard cell function. Proc Natl Acad Sci U S A 100 (20):11783-11788. doi:10.1073/pnas.1832434100
Kaiserli E, Sullivan S, Jones MA, Feeney KA, Christie JM (2009) Domain swapping to assess the mechanistic basis of *Arabidopsis* phototropin 1 receptor kinase activation and endocytosis by blue light. Plant Cell 21 (10):3226-3244. doi:10.1105/tpc.109.067876
Kaneko S, Ishii T, Matsunaga T (1997) A boron-rhamnogalacturonan-II complex from bamboo shoot cell walls. Phytochemistry 44 (2):243-248. doi:10.1016/S0031-9422(96)00539-0
Kasajima I, Ide Y, Ohkama-Ohtsu N, Hayashi H, Yoneyama T, Fujiwara T (2004) A protocol for rapid DNA extraction from *Arabidopsis thaliana* for PCR analysis. Plant Mol Biol Rep 22 (1):49-52. doi:10.1007/Bf02773348
Kato Y, Ito S, Mitsuishi Y (2004) Study on the structures of xyloglucans using xyloglucan specific enzymes. Trends Glycosci Glyc 16 (92):393-406
Keenan MHJ, Belton PS, Matthew JA, Howson SJ (1985) A C-13-Nmr Study of Sugar-Beet Pectin. Carbohyd Res 138 (1):168-170. doi:10.1016/0008-6215(85)85236-8
Keller B (1993) Structural Cell Wall Proteins. Plant Physiol 101 (4):1127-1130
Kiefer LL, York WS, Darvill AG, Albersheim P (1989) Xyloglucan Isolated from Suspension-Cultured Sycamore Cell-Walls Is O-Acetylated. Phytochemistry 28 (8):2105-2107. doi:10.1016/S0031-9422(00)97928-7
Kim JB, Olek AT, Carpita NC (2000) Cell wall and membrane-associated exo-beta-D-glucanases from developing maize seedlings. Plant Physiol 123 (2):471-485. doi:10.1104/Pp.123.2.471
Klein-Marcuschamer D, Oleskowicz-Popiel P, Simmons BA, Blanch HW (2010) Technoeconomic analysis of biofuels: A wiki-based platform for lignocellulosic biorefineries. Biomass Bioenerg 34 (12):1914-1921. doi:10.1016/j.biombioe.2010.07.033
Knox JP, Linstead PJ, King J, Cooper C, Roberts K (1990) Pectin Esterification Is Spatially Regulated Both within Cell-Walls and between Developing-Tissues of Root Apices. Planta 181 (4):512-521
Komalavilas P, Mort AJ (1989) The Acetylation at O-3 of Galacturonic Acid in the Rhamnose-Rich Portion of Pectins. Carbohyd Res 189:261-272. doi:10.1016/0008-6215(89)84102-3
Kong Y, Zhou G, Yin Y, Xu Y, Pattathil S, Hahn MG (2011) Molecular analysis of a family of *Arabidopsis* genes related to galacturonosyltransferases. Plant Physiol 155 (4):1791-1805. doi:10.1104/pp.110.163220
Kraemer F (2008) Characterization of *axy8*, an *Arabidopsis thaliana* mutant with altered xyloglucan structure. Diploma, University of Potsdam, East Lansing

Krupkova E, Immerzeel P, Pauly M, Schmulling T (2007) The TUMOROUS SHOOT DEVELOPMENT2 gene of *Arabidopsis* encoding a putative methyltransferase is required for cell adhesion and co-ordinated plant development. Plant J 50 (4):735-750. doi:10.1111/j.1365-313X.2007.03123.x

Kuromori T, Hirayama T, Kiyosue Y, Takabe H, Mizukado S, Sakurai T, Akiyama K, Kamiya A, Ito T, Shinozaki K (2004) A collection of 11 800 single-copy Ds transposon insertion lines in *Arabidopsis*. Plant J 37 (6):897-905

Laitinen RA, Schneeberger K, Jelly NS, Ossowski S, Weigel D (2010) Identification of a spontaneous frame shift mutation in a nonreference *Arabidopsis* accession using whole genome sequencing. Plant Physiol 153 (2):652-654. doi:10.1104/pp.110.156448

Langan KJ, Nothnagel EA (1997) Cell surface arabinogalactan-proteins and their relation to cell proliferation and viability. Protoplasma 196 (1-2):87-98. doi:10.1007/Bf01281062

Lee CH, O'Neill MA, Tsumuraya Y, Darvill AG, Ye ZH (2007a) The irregular xylem9 mutant is deficient in xylan xylosyltransferase activity. Plant and Cell Physiology 48 (11):1624-1634. doi:10.1093/Pcp/Pcm135

Lee CH, Zhong RQ, Richardson EA, Himmelsbach DS, McPhail BT, Ye ZH (2007b) The PARVUS gene is expressed in cells undergoing secondary wall thickening and is essential for glucuronoxylan biosynthesis. Plant and Cell Physiology 48 (12):1659-1672. doi:10.1093/Pcp/Pcm155

Lefebvre V, Fortabat MN, Ducamp A, North HM, Maia-Grondard A, Trouverie J, Boursiac Y, Mouille G, Durand-Tardif M (2011) ESKIMO1 Disruption in *Arabidopsis* Alters Vascular Tissue and Impairs Water Transport. Plos One 6 (2). doi: 10.1371/journal.pone.0016645

Lerouxel O, Choo TS, Seveno M, Usadel B, Faye L, Lerouge P, Pauly M (2002) Rapid structural phenotyping of plant cell wall mutants by enzymatic oligosaccharide fingerprinting. Plant Physiol 130 (4):1754-1763. doi:10.1104/pp.011965

Liepman AH, Wilkerson CG, Keegstra K (2005) Expression of cellulose synthase-like (Csl) genes in insect cells reveals that CslA family members encode mannan synthases. P Natl Acad Sci USA 102 (6):2221-2226. doi:10.1073/pnas.0409179102

Lim CC (2013) Roles of the plant cell wall in powdery mildew disease resistance in *Arabidopsis thaliana*:PMR5 (POWDERY MILDEW RESISTANT 5) affects the acetylation of cell wall pectin University of California at Berkeley, Berkeley

Lippincott-Schwartz J, Snapp E, Kenworthy A (2001) Studying protein dynamics in living cells. Nature reviews Molecular cell biology 2 (6):444-456. doi:10.1038/35073068

Liu LF, Shang-Guan KK, Zhang BC, Liu XL, Yan MX, Zhang LJ, Shi YY, Zhang M, Qian Q, Li JY, Zhou YH (2013) Brittle Culm1, a COBRA-Like Protein, Functions in Cellulose Assembly through Binding Cellulose Microfibrils. Plos Genet 9 (8). doi: 10.1371/journal.pgen.1003704

Liu XL, Liu L, Niu QK, Xia C, Yang KZ, Li R, Chen LQ, Zhang XQ, Zhou Y, Ye D (2011) Male gametophyte defective 4 encodes a rhamnogalacturonan II xylosyltransferase and is important for growth of pollen tubes and roots in *Arabidopsis*. Plant J 65 (4):647-660. doi:10.1111/j.1365-313X.2010.04452.x

Liwanag AJM, Ebert B, Verhertbruggen Y, Rennie EA, Rautengarten C, Oikawa A, Andersen MCF, Clausen MH, Scheller HV (2012) Pectin Biosynthesis: GALS1 in *Arabidopsis thaliana* Is a beta-1,4-Galactan beta-1,4-Galactosyltransferase. Plant Cell 24 (12):5024-5036. doi:10.1105/tpc.112.106625

Lombard V, Golaconda Ramulu H, Drula E, Coutinho PM, Henrissat B (2014) The carbohydrate-active enzymes database (CAZy) in 2013. Nucleic acids research 42 (Database issue):D490-495. doi:10.1093/nar/gkt1178

Luquez VM, Sasal Y, Medrano M, Martin MI, Mujica M, Guiamet JJ (2006) Quantitative trait loci analysis of leaf and plant longevity in *Arabidopsis thaliana*. J Exp Bot 57 (6):1363-1372. doi:10.1093/jxb/erj112

Manabe Y, Nafisi M, Verhertbruggen Y, Orfila C, Gille S, Rautengarten C, Cherk C, Marcus SE, Somerville S, Pauly M, Knox JP, Sakuragi Y, Scheller HV (2011) Loss-of-function mutation of REDUCED WALL ACETYLATION2 in *Arabidopsis* leads to reduced cell wall acetylation and increased resistance to Botrytis cinerea. Plant Physiol 155 (3):1068-1078. doi:10.1104/pp.110.168989

Manabe Y, Verhertbruggen Y, Gille S, Harholt J, Chong SL, Pawar PM, Mellerowicz EJ, Tenkanen M, Cheng K, Pauly M, Scheller HV (2013) Reduced Wall Acetylation proteins play vital and distinct roles in cell wall O-acetylation in *Arabidopsis*. Plant Physiol 163 (3):1107-1117. doi:10.1104/pp.113.225193

Marcus SE, Verhertbruggen Y, Herve C, Ordaz-Ortiz JJ, Farkas V, Pedersen HL, Willats WG, Knox JP (2008) Pectic homogalacturonan masks abundant sets of xyloglucan epitopes in plant cell walls. BMC plant biology 8:60. doi:10.1186/1471-2229-8-60

Marry M, Roberts K, Jopson SJ, Huxham IM, Jarvis MC, Corsar J, Robertson E, McCann MC (2006) Cell-cell adhesion in fresh sugar-beet root parenchyma requires both pectin esters and calcium cross-links. Physiol Plantarum 126 (2):243-256. doi:10.1111/j.1399-3054.2005.00591.x

Martin JR, Petitdemange H, Ballongue J, Gay R (1983) Effects of Acetic and Butyric Acids on Solvents Production by Clostridium-Acetobutylicum. Biotechnol Lett 5 (2):89-94. doi:10.1007/Bf00132165

Matsuyama T, Satoh H, Yamada Y, Hashimoto T (1999) A maize glycine-rich protein is synthesized in the lateral root cap and accumulates in the mucilage. Plant Physiol 120 (3):665-674. doi:10.1104/Pp.120.3.665

Matzke AJ, Matzke MA (1998) Position effects and epigenetic silencing of plant transgenes. Curr Opin Plant Biol 1 (2):142-148

Mccann MC, Wells B, Roberts K (1990) Direct Visualization of Cross-Links in the Primary Plant-Cell Wall. J Cell Sci 96:323-334

McDougall GJ, Fry SC (1990) Xyloglucan oligosaccharides promote growth and activate cellulase: evidence for a role of cellulase in cell expansion. Plant Physiol 93 (3):1042-1048

McNeil M, Darvill AG, Fry SC, Albersheim P (1984) Structure and function of the primary cell walls of plants. Annual review of biochemistry 53:625-663. doi:10.1146/annurev.bi.53.070184.003205

Meier H, Reid JSG (1982) Reserve polysaccharides other than starch in higher plants. In: Loewus F, Tanner W (eds) Plant carbohydrates I, vol 13/A. Encyclopedia of

plant physiology. Springer, Berlin, pp 418–471. doi:10.1007/978-3-642-68275-9_11
Meikle PJ, Hoogenraad NJ, Bonig I, Clarke AE, Stone BA (1994) A (1-]3,1-]4)-Beta-Glucan-Specific Monoclonal-Antibody and Its Use in the Quantitation and Immunocyto-Chemical Location of (1-]3,1-]4)-Beta-Glucans. Plant J 5 (1):1-9. doi:10.1046/j.1365-313X.1994.5010001.x
Meinke DW, Cherry JM, Dean C, Rounsley SD, Koornneef M (1998) *Arabidopsis thaliana*: a model plant for genome analysis. Science 282 (5389):662, 679-682
Miao YC, Liu CJ (2010) ATP-binding cassette-like transporters are involved in the transport of lignin precursors across plasma and vacuolar membranes. P Natl Acad Sci USA 107 (52):22728-22733. doi:10.1073/pnas.1007747108
Micheli F (2001) Pectin methylesterases: cell wall enzymes with important roles in plant physiology. Trends in plant science 6 (9):414-419
Mishra A, Malhotra AV (2009) Tamarind xyloglucan: a polysaccharide with versatile application potential. J Mater Chem 19 (45):8528-8536. doi:10.1039/B911150f
Mohnen D (2008) Pectin structure and biosynthesis. Curr Opin Plant Biol 11 (3):266-277. doi:10.1016/j.pbi.2008.03.006
Moir D, Mao J, Schumm JW, Vovis GF, Alford BL, Taunton-Rigby A (1982) Molecular cloning and characterization of double-stranded cDNA coding for bovine chymosin. Gene 19 (1):127-138
Mouille G, Ralet MC, Cavelier C, Eland C, Effroy D, Hematy K, McCartney L, Truong HN, Gaudon V, Thibault JF, Marchant A, Hofte H (2007) Homogalacturonan synthesis in *Arabidopsis thaliana* requires a Golgi-localized protein with a putative methyltransferase domain. Plant J 50 (4):605-614. doi:10.1111/j.1365-313X.2007.03086.x
Mueller SC, Brown RM, Jr. (1980) Evidence for an intramembrane component associated with a cellulose microfibril-synthesizing complex in higher plants. The Journal of cell biology 84 (2):315-326
Murray MG, Thompson WF (1980) Rapid isolation of high molecular weight plant DNA. Nucleic acids research 8 (19):4321-4325
Nakamura A, Furuta H, Maeda H, Takao T, Nagamatsu Y (2002) Structural studies by stepwise enzymatic degradation of the main backbone of soybean soluble polysaccharides consisting of galacturonan and rhamnogalacturonan. Bioscience, biotechnology, and biochemistry 66 (6):1301-1313
Neelakantan S, Mohanty AK, Kaushik JK (1999) Production and use of microbial enzymes for dairy processing. Curr Sci India 77 (1):143-148
Nicol F, His I, Jauneau A, Vernhettes S, Canut H, Hofte H (1998) A plasma membrane-bound putative endo-1,4-beta-D-glucanase is required for normal wall assembly and cell elongation in *Arabidopsis*. The EMBO journal 17 (19):5563-5576. doi:10.1093/emboj/17.19.5563
Nishitani K (1998) Construction and restructuring of the cellulose-xyloglucan framework in the apoplast as mediated by the xyloglucan related protein family - A hypothetical scheme. J Plant Res 111 (1101):159-166. doi:10.1007/Bf02507162
Nishitani K, Tominaga R (1992) Endoxyloglucan Transferase, a Novel Class of Glycosyltransferase That Catalyzes Transfer of a Segment of Xyloglucan Molecule to Another Xyloglucan Molecule. J Biol Chem 267 (29):21058-21064

Nothnagel EA (1997) Proteoglycans and related components in plant cells. International review of cytology 174:195-291

O'Hare HM, Johnsson K, Gautier A (2007) Chemical probes shed light on protein function. Curr Opin Struct Biol 17 (4):488-494. doi:10.1016/j.sbi.2007.07.005

Obel N, Neumetzler L, Immerzeel P, Kühnel S, Kraemer F, Zander K, Schwarz T, Andres D, Rädisch S, Kienast S, Rhaman S, Geisler K, Franke C, Krämer M, Seidel D, Rose A, Biedermann M, Fodor A, Pauly M (2006) Collection of *Arabidopsis* mutants with altered xyloglucan structures (axy-mutants). http://paulylab.berkeley.edu/axy-mutants.html. 2014

Obrien TP, Feder N, Mccully ME (1964) Polychromatic Staining of Plant Cell Walls by Toluidine Blue O. Protoplasma 59 (2):368-&. doi:10.1007/Bf01248568

Odriscoll D, Read SM, Steer MW (1993) Determination of Cell-Wall Porosity by Microscopy - Walls of Cultured-Cells and Pollen Tubes. Acta Bot Neerl 42 (2):237-244

Oikawa A, Lund CH, Sakuragi Y, Scheller HV (2013) Golgi-localized enzyme complexes for plant cell wall biosynthesis. Trends in plant science 18 (1):49-58. doi:10.1016/j.tplants.2012.07.002

ONeill MA, Warrenfeltz D, Kates K, Pellerin P, Doco T, Darvill AG, Albersheim P (1996) Rhamnogalacturonan-II, a pectic polysaccharide in the walls of growing plant cell, forms a dimer that is covalently cross-linked by a borate ester - In vitro conditions for the formation and hydrolysis of the dimer. J Biol Chem 271 (37):22923-22930

Orfila C, Dal Degan F, Jorgensen B, Scheller HV, Ray PM, Ulvskov P (2012) Expression of mung bean pectin acetyl esterase in potato tubers: effect on acetylation of cell wall polymers and tuber mechanical properties. Planta 236 (1):185-196. doi:10.1007/s00425-012-1596-z

Orfila C, Sorensen SO, Harholt J, Geshi N, Crombie H, Truong HN, Reid JS, Knox JP, Scheller HV (2005) QUASIMODO1 is expressed in vascular tissue of *Arabidopsis thaliana* inflorescence stems, and affects homogalacturonan and xylan biosynthesis. Planta 222 (4):613-622. doi:10.1007/s00425-005-0008-z

Ostergaard L, Teilum K, Mirza O, Mattsson O, Petersen M, Welinder KG, Mundy J, Gajhede M, Henriksen A (2000) *Arabidopsis* ATP A2 peroxidase. Expression and high-resolution structure of a plant peroxidase with implications for lignification. Plant Mol Biol 44 (2):231-243

Oxenboll Sorensen S, Pauly M, Bush M, Skjot M, McCann MC, Borkhardt B, Ulvskov P (2000) Pectin engineering: modification of potato pectin by in vivo expression of an endo-1,4-beta-D-galactanase. Proc Natl Acad Sci U S A 97 (13):7639-7644. doi:10.1073/pnas.130568297

Pagant S, Bichet A, Sugimoto K, Lerouxel O, Desprez T, McCann M, Lerouge P, Vernhettes S, Hofte H (2002) KOBITO1 encodes a novel plasma membrane protein necessary for normal synthesis of cellulose during cell expansion in *Arabidopsis*. Plant Cell 14 (9):2001-2013

Park YB, Cosgrove DJ (2012) Changes in cell wall biomechanical properties in the xyloglucan-deficient xxt1/xxt2 mutant of *Arabidopsis*. Plant Physiol 158 (1):465-475. doi:10.1104/pp.111.189779

Parsons HT, Christiansen K, Knierim B, Carroll A, Ito J, Batth TS, Smith-Moritz AM, Morrison S, McInerney P, Hadi MZ, Auer M, Mukhopadhyay A, Petzold CJ, Scheller HV, Loque D, Heazlewood JL (2012) Isolation and proteomic characterization of the *Arabidopsis* Golgi defines functional and novel components involved in plant cell wall biosynthesis. Plant Physiol 159 (1):12-26. doi:10.1104/pp.111.193151

Pauly M, Albersheim P, Darvill A, York WS (1999a) Molecular domains of the cellulose/xyloglucan network in the cell walls of higher plants. Plant J 20 (6):629-639

Pauly M, Andersen LN, Kauppinen S, Kofod LV, York WS, Albersheim P, Darvill A (1999b) A xyloglucan-specific endo-beta-1,4-glucanase from Aspergillus aculeatus: expression cloning in yeast, purification and characterization of the recombinant enzyme. Glycobiology 9 (1):93-100

Pauly M, Gille S, Liu L, Mansoori N, de Souza A, Schultink A, Xiong G (2013) Hemicellulose biosynthesis. Planta 238 (4):627-642. doi:10.1007/s00425-013-1921-1

Pauly M, Keegstra K (2008) Physiology and metabolism 'Tear down this wall'. Curr Opin Plant Biol 11 (3):233-235. doi:10.1016/j.pbi.2008.04.002

Pauly M, Scheller HV (2000) O-Acetylation of plant cell wall polysaccharides: identification and partial characterization of a rhamnogalacturonan O-acetyl-transferase from potato suspension-cultured cells. Planta 210 (4):659-667

Pena MJ, Darvill AG, Eberhard S, York WS, O'Neill MA (2008) Moss and liverwort xyloglucans contain galacturonic acid and are structurally distinct from the xyloglucans synthesized by hornworts and vascular plants. Glycobiology 18 (11):891-904. doi:10.1093/glycob/cwn078

Pena MJ, Kong YZ, York WS, O'Neill MA (2012) A Galacturonic Acid-Containing Xyloglucan Is Involved in *Arabidopsis* Root Hair Tip Growth. Plant Cell 24 (11):4511-4524. doi:10.1105/tpc.112.103390

Perrin RM, DeRocher AE, Bar-Peled M, Zeng W, Norambuena L, Orellana A, Raikhel NV, Keegstra K (1999) Xyloglucan fucosyltransferase, an enzyme involved in plant cell wall biosynthesis. Science 284 (5422):1976-1979

Persson S, Caffall KH, Freshour G, Hilley MT, Bauer S, Poindexter P, Hahn MG, Mohnen D, Somerville C (2007a) The *Arabidopsis* irregular xylem8 mutant is deficient in glucuronoxylan and homogalacturonan, which are essential for secondary cell wall integrity. Plant Cell 19 (1):237-255. doi:10.1105/tpc.106.047720

Persson S, Paredez A, Carroll A, Palsdottir H, Doblin M, Poindexter P, Khitrov N, Auer M, Somerville CR (2007b) Genetic evidence for three unique components in primary cell-wall cellulose synthase complexes in *Arabidopsis*. Proc Natl Acad Sci U S A 104 (39):15566-15571. doi:10.1073/pnas.0706592104

Pettolino FA, Walsh C, Fincher GB, Bacic A (2012) Determining the polysaccharide composition of plant cell walls. Nature protocols 7 (9):1590-1607. doi:10.1038/nprot.2012.081

Pogorelko G, Lionetti V, Fursova O, Sundaram RM, Qi M, Whitham SA, Bogdanove AJ, Bellincampi D, Zabotina OA (2013) *Arabidopsis* and Brachypodium distachyon transgenic plants expressing Aspergillus nidulans acetylesterases have

decreased degree of polysaccharide acetylation and increased resistance to pathogens. Plant Physiol 162 (1):9-23. doi:10.1104/pp.113.214460
Popper ZA, Fry SC (2003) Primary cell wall composition of bryophytes and charophytes. Ann Bot 91 (1):1-12
Popper ZA, Michel G, Herve C, Domozych DS, Willats WG, Tuohy MG, Kloareg B, Stengel DB (2011) Evolution and diversity of plant cell walls: from algae to flowering plants. Annu Rev Plant Biol 62:567-590. doi:10.1146/annurev-arplant-042110-103809
Puhlmann J, Bucheli E, Swain MJ, Dunning N, Albersheim P, Darvill AG, Hahn MG (1994) Generation of monoclonal antibodies against plant cell-wall polysaccharides. I. Characterization of a monoclonal antibody to a terminal alpha-(1-->2)-linked fucosyl-containing epitope. Plant Physiol 104 (2):699-710
Ralet MC, Crepeau MJ, Buchholt HC, Thibault JF (2003) Polyelectrolyte behaviour and calcium binding properties of sugar beet pectins differing in their degrees of methylation and acetylation. Biochem Eng J 16 (2):191-201. doi:10.1016/S1369-703x(03)00037-8
Ralet MC, Crepeau MJ, Lefebvre J, Mouille G, Hofte H, Thibault JF (2008) Reduced number of homogalacturonan domains in pectins of an *Arabidopsis* mutant enhances the flexibility of the polymer. Biomacromolecules 9 (5):1454-1460. doi:10.1021/Bm701321g
Reiter WD, Chapple C, Somerville CR (1997) Mutants of *Arabidopsis thaliana* with altered cell wall polysaccharide composition. Plant J 12 (2):335-345
Ridley BL, O'Neill MA, Mohnen D (2001) Pectins: structure, biosynthesis, and oligogalacturonide-related signaling. Phytochemistry 57 (6):929-967
Rodriguez-Gacio MDC, Iglesias-Fernandez R, Carbonero P, Matilla AJ (2012) Softening-up mannan-rich cell walls. J Exp Bot 63 (11):3975-3988. doi:10.1093/Jxb/Ers096
Roudier F, Fernandez AG, Fujita M, Himmelspach R, Borner GHH, Schindelman G, Song S, Baskin TI, Dupree P, Wasteneys GO, Benfey PN (2005) COBRA, an *Arabidopsis* extracellular glycosyl-phosphatidyl inositol-anchored protein, specifically controls highly anisotropic expansion through its involvement in cellulose microfibril orientation. Plant Cell 17 (6):1749-1763. doi:10.1105/tpc.105.031732.
Ryser U, Schorderet M, Zhao GF, Studer D, Ruel K, Hauf G, Keller B (1997) Structural cell-wall proteins in protoxylem development: Evidence for a repair process mediated by a glycine-rich protein. Plant J 12 (1):97-111. doi:10.1046/j.1365-313X.1997.12010097.x
Salk Arabidopsis 1001 Genomes. (2014). http://signal.salk.edu/atg1001/index.php.
Sampedro J, Gianzo C, Iglesias N, Guitian E, Revilla G, Zarra I (2012) AtBGAL10 is the main xyloglucan beta-galactosidase in *Arabidopsis*, and its absence results in unusual xyloglucan subunits and growth defects. Plant Physiol 158 (3):1146-1157. doi:10.1104/pp.111.192195
Sampedro J, Sieiro C, Revilla G, Gonzalez-Villa T, Zarra I (2001) Cloning and expression pattern of a gene encoding an alpha-xylosidase active against xyloglucan oligosaccharides from *Arabidopsis*. Plant Physiol 126 (2):910-920

Sandor F, Latz E, Re F, Mandell L, Repik G, Golenbock DT, Espevik T, Kurt-Jones EA, Finberg RW (2003) Importance of extra- and intracellular domains of TLR1 and TLR2 in NFkappa B signaling. The Journal of cell biology 162 (6):1099-1110. doi:10.1083/jcb.200304093

Scheller HV, Ulvskov P (2010) Hemicelluloses. Annu Rev Plant Biol 61:263-289. doi:10.1146/annurev-arplant-042809-112315

Schultink A (2013) Identification and characterization of genes involved in the biosynthesis of the plant cell wall polysaccharide xyloglucan PhD, UC Berkeley, Berkeley

Schultink A, Cheng K, Park YB, Cosgrove DJ, Pauly M (2013) The identification of two arabinosyltransferases from tomato reveals functional equivalency of xyloglucan side chain substituents. Plant Physiol 163 (1):86-94. doi:10.1104/pp.113.221788

Seifert GJ (2004) Nucleotide sugar interconversions and cell wall biosynthesis: how to bring the inside to the outside. Curr Opin Plant Biol 7 (3):277-284. doi:10.1016/j.pbi.2004.03.004

Seifert GJ, Roberts K (2007) The biology of arabinogalactan proteins. Annu Rev Plant Biol 58:137-161. doi:10.1146/annurev.arplant.58.032806.103801

Sengkhamparn N, Bakx EJ, Verhoef R, Schols HA, Sajjaanantakul T, Voragen AG (2009) Okra pectin contains an unusual substitution of its rhamnosyl residues with acetyl and alpha-linked galactosyl groups. Carbohydr Res 344 (14):1842-1851. doi:10.1016/j.carres.2008.11.022

Sessions A, Burke E, Presting G, Aux G, McElver J, Patton D, Dietrich B, Ho P, Bacwaden J, Ko C, Clarke JD, Cotton D, Bullis D, Snell J, Miguel T, Hutchison D, Kimmerly B, Mitzel T, Katagiri F, Glazebrook J, Law M, Goff SA (2002) A high-throughput *Arabidopsis* reverse genetics system. Plant Cell 14 (12):2985-2994

Showalter AM (1993) Structure and function of plant cell wall proteins. Plant Cell 5 (1):9-23. doi:10.1105/tpc.5.1.9

Smith RC, Fry SC (1991) Endotransglycosylation of Xyloglucans in Plant-Cell Suspension-Cultures. Biochem J 279:529-535

Somerville C (2006) Cellulose synthesis in higher plants. Annual review of cell and developmental biology 22:53-78. doi:10.1146/annurev.cellbio.22.022206.160206

Somerville C, Bauer S, Brininstool G, Facette M, Hamann T, Milne J, Osborne E, Paredez A, Persson S, Raab T, Vorwerk S, Youngs H (2004) Toward a systems approach to understanding plant cell walls. Science 306 (5705):2206-2211. doi:10.1126/science.1102765

SommerKnudsen J, Clarke AE, Bacic A (1997) Proline- and hydroxyproline-rich gene products in the sexual tissues of flowers. Sex Plant Reprod 10 (5):253-260. doi:10.1007/s004970050095

Sorensen I, Pettolino FA, Wilson SM, Doblin MS, Johansen B, Bacic A, Willats WGT (2008) Mixed-linkage (1 -> 3), (1 -> 4)-beta-D-glucan is not unique to the poales and is an abundant component of Equisetum arvense cell walls. Plant J 54 (3):510-521. doi:10.1111/j.1365-313X.2008.03453.x

Soukup A (2014) Selected Simple Methods of Plant Cell Wall Histochemistry and Staining for Light Microscopy. Methods Mol Biol 1080:25-40. doi:10.1007/978-1-62703-643-6_2

Sperry JS (2003) Evolution of water transport and xylem structure. Int J Plant Sci 164 (3):S115-S127. doi:10.1086/368398

Sterjiades R, Dean JF, Eriksson KE (1992) Laccase from Sycamore Maple (Acer pseudoplatanus) Polymerizes Monolignols. Plant Physiol 99 (3):1162-1168

Sterling JD, Atmodjo MA, Inwood SE, Kumar Kolli VS, Quigley HF, Hahn MG, Mohnen D (2006) Functional identification of an *Arabidopsis* pectin biosynthetic homogalacturonan galacturonosyltransferase. Proc Natl Acad Sci U S A 103 (13):5236-5241. doi:10.1073/pnas.0600120103

Suzuki S, Li LG, Sun YH, Chiang VL (2006) The cellulose synthase gene superfamily and biochemical functions of xylem-specific cellulose synthase-like genes in Populus trichocarpa. Plant Physiol 142 (3):1233-1245. doi:10.1104/pp.106.086678

Takeda T, Furuta Y, Awano T, Mizuno K, Mitsuishi Y, Hayashi T (2002) Suppression and acceleration of cell elongation by integration of xyloglucans in pea stem segments. P Natl Acad Sci USA 99 (13):9055-9060. doi:10.1073/pnas.132080299

Tan L, Eberhard S, Pattathil S, Warder C, Glushka J, Yuan C, Hao Z, Zhu X, Avci U, Miller JS, Baldwin D, Pham C, Orlando R, Darvill A, Hahn MG, Kieliszewski MJ, Mohnen D (2013) An *Arabidopsis* cell wall proteoglycan consists of pectin and arabinoxylan covalently linked to an arabinogalactan protein. Plant Cell 25 (1):270-287. doi:10.1105/tpc.112.107334

Tauszig S, Jouanguy E, Hoffmann JA, Imler JL (2000) Toll-related receptors and the control of antimicrobial peptide expression in Drosophila. Proc Natl Acad Sci U S A 97 (19):10520-10525. doi:10.1073/pnas.180130797

Taylor NG, Howells RM, Huttly AK, Vickers K, Turner SR (2003) Interactions among three distinct CesA proteins essential for cellulose synthesis. P Natl Acad Sci USA 100 (3):1450-1455. doi:10.1073/pnas.0337628100

Thakur BR, Singh RK, Handa AK (1997) Chemistry and uses of pectin--a review. Critical reviews in food science and nutrition 37 (1):47-73. doi:10.1080/10408399709527767

Thompson JE, Fry SC (2000) Evidence for covalent linkage between xyloglucan and acidic pectins in suspension-cultured rose cells. Planta 211 (2):275-286. doi:10.1007/s004250000287

Tierney ML, Varner JE (1987) The extensins. Plant Physiol 84 (1):1-2

Turner SR, Somerville CR (1997) Collapsed xylem phenotype of *Arabidopsis* identifies mutants deficient in cellulose deposition in the secondary cell wall. Plant Cell 9 (5):689-701. doi:10.1105/tpc.9.5.689

Ullmann A, Jacob F, Monod J (1967) Characterization by in vitro complementation of a peptide corresponding to an operator-proximal segment of the beta-galactosidase structural gene of Escherichia coli. Journal of molecular biology 24 (2):339-343

Ulvskov P, Wium H, Bruce D, Jorgensen B, Qvist KB, Skjot M, Hepworth D, Borkhardt B, Sorensen SO (2005) Biophysical consequences of remodeling the neutral side chains of rhamnogalacturonan I in tubers of transgenic potatoes. Planta 220 (4):609-620. doi:10.1007/s00425-004-1373-8

Urbanowicz BR, Pena MJ, Ratnaparkhe S, Avci U, Backe J, Steet HF, Foston M, Li HJ, O'Neill MA, Ragauskas AJ, Darvill AG, Wyman C, Gilbert HJ, York WS (2012) 4-O-methylation of glucuronic acid in *Arabidopsis* glucuronoxylan is catalyzed by a domain of unknown function family 579 protein. P Natl Acad Sci USA 109 (35):14253-14258. doi:10.1073/pnas.1208097109

Van Acker R, Leple JC, Aerts D, Storme V, Goeminne G, Ivens B, Legee F, Lapierre C, Piens K, Van Montagu MC, Santoro N, Foster CE, Ralph J, Soetaert W, Pilate G, Boerjan W (2014) Improved saccharification and ethanol yield from field-grown transgenic poplar deficient in cinnamoyl-CoA reductase. Proc Natl Acad Sci U S A 111 (2):845-850. doi:10.1073/pnas.1321673111

van Hengel AJ, Tadesse Z, Immerzeel P, Schols H, van Kammen A, de Vries SC (2001) N-acetylglucosamine and glucosamine-containing arabinogalactan proteins control somatic embryogenesis. Plant Physiol 125 (4):1880-1890. doi:10.1104/pp.125.4.1880

Vanholme R, Demedts B, Morreel K, Ralph J, Boerjan W (2010) Lignin biosynthesis and structure. Plant Physiol 153 (3):895-905. doi:10.1104/pp.110.155119

Vanzin GF, Madson M, Carpita NC, Raikhel NV, Keegstra K, Reiter WD (2002) The mur2 mutant of *Arabidopsis thaliana* lacks fucosylated xyloglucan because of a lesion in fucosyltransferase AtFUT1. P Natl Acad Sci USA 99 (5):3340-3345. doi:10.1073/pnas.052450699

Varner JE, Lin LS (1989) Plant cell wall architecture. Cell 56 (2):231-239

Verhertbruggen Y, Yin L, Oikawa A, Scheller HV (2011) Mannan synthase activity in the CSLD family. Plant Signal Behav 6 (10):1620-1623. doi:10.4161/psb.6.10.17989

Versailles Arabidopsis Stock Center. (2014). http://publiclines.versailles.inra.fr/rils/index.

Vignols F, Rigau J, Torres MA, Capellades M, Puigdomenech P (1995) The brown midrib3 (bm3) mutation in maize occurs in the gene encoding caffeic acid O-methyltransferase. Plant Cell 7 (4):407-416. doi:10.1105/tpc.7.4.407

Vision TJ, Brown DG, Tanksley SD (2000) The origins of genomic duplications in *Arabidopsis*. Science 290 (5499):2114-2117

Vogel C, Marcotte EM (2012) Insights into the regulation of protein abundance from proteomic and transcriptomic analyses. Nat Rev Genet 13 (4):227-232. doi:10.1038/Nrg3185

Vogel JP, Raab TK, Somerville CR, Somerville SC (2004) Mutations in PMR5 result in powdery mildew resistance and altered cell wall composition. Plant J 40 (6):968-978. doi:10.1111/j.1365-313X.2004.02264.x

Voinnet O, Rivas S, Mestre P, Baulcombe D (2003) An enhanced transient expression system in plants based on suppression of gene silencing by the p19 protein of tomato bushy stunt virus. Plant J 33 (5):949-956

Wang Y, Alonso AP, Wilkerson CG, Keegstra K (2012) Deep EST profiling of developing fenugreek endosperm to investigate galactomannan biosynthesis and its regulation. Plant Mol Biol 79 (3):243-258. doi:10.1007/s11103-012-9909-y

Wang Y, Mortimer JC, Davis J, Dupree P, Keegstra K (2013) Identification of an additional protein involved in mannan biosynthesis. Plant J 73 (1):105-117. doi:10.1111/Tpj.12019

Wei N, Quarterman J, Kim SR, Cate JH, Jin YS (2013) Enhanced biofuel production through coupled acetic acid and xylose consumption by engineered yeast. Nature communications 4:2580. doi:10.1038/ncomms3580

Weigel D (2012) Natural variation in *Arabidopsis*: from molecular genetics to ecological genomics. Plant Physiol 158 (1):2-22. doi:10.1104/pp.111.189845

Western TL, Skinner DJ, Haughn GW (2000) Differentiation of mucilage secretory cells of the *Arabidopsis* seed coat. Plant Physiol 122 (2):345-355. doi:10.1104/Pp.122.2.345

Wildermuth MC, Dewdney J, Wu G, Ausubel FM (2001) Isochorismate synthase is required to synthesize salicylic acid for plant defence. Nature 414 (6863):562-565. doi:10.1038/35107108

Wilkerson CG, Mansfield SD, Lu F, Withers S, Park JY, Karlen SD, Gonzales-Vigil E, Padmakshan D, Unda F, Rencoret J, Ralph J (2014) Monolignol Ferulate Transferase Introduces Chemically Labile Linkages into the Lignin Backbone. Science 344 (6179):90-93. doi:10.1126/science.1250161

Willats WGT, Knox P, Mikkelsen JD (2006) Pectin: new insights into an old polymer are starting to gel. Trends Food Sci Tech 17 (3):97-104. doi:10.1016/j.tifs.2005.10.008

Williamson G (1991) Purification and characterization of pectin acetylesterase from orange peel. Phytochemistry 30 (2):445-449

Winter D, Vinegar B, Nahal H, Ammar R, Wilson GV, Provart NJ (2007) An "Electronic Fluorescent Pictograph" browser for exploring and analyzing large-scale biological data sets. Plos One 2 (8):e718. doi:10.1371/journal.pone.0000718

Wolf S, Mouille G, Pelloux J (2009) Homogalacturonan methyl-esterification and plant development. Mol Plant 2 (5):851-860. doi:10.1093/mp/ssp066

Xin Z, Browse J (1998) Eskimo1 mutants of *Arabidopsis* are constitutively freezing-tolerant. Proc Natl Acad Sci U S A 95 (13):7799-7804

Xiong G, Cheng K, Pauly M (2013) Xylan O-acetylation impacts xylem development and enzymatic recalcitrance as indicated by the *Arabidopsis* mutant tbl29. Mol Plant 6 (4):1373-1375. doi:10.1093/mp/sst014

Yapo BM (2011) Pectic substances: From simple pectic polysaccharides to complex pectins-A new hypothetical model. Carbohyd Polym 86 (2):373-385. doi:10.1016/j.carbpol.2011.05.065

York WS, Darvill AG, Albersheim P (1984) Inhibition of 2,4-dichlorophenoxyacetic Acid-stimulated elongation of pea stem segments by a xyloglucan oligosaccharide. Plant Physiol 75 (2):295-297

Yoshida S, Ito M, Nishida I, Watanabe A (2001) Isolation and RNA gel blot analysis of genes that could serve as potential molecular markers for leaf senescence in *Arabidopsis thaliana*. Plant and Cell Physiology 42 (2):170-178. doi:10.1093/Pcp/Pce021

You A, Lu X, Jin H, Ren X, Liu K, Yang G, Yang H, Zhu L, He G (2006) Identification of quantitative trait loci across recombinant inbred lines and testcross populations for traits of agronomic importance in rice. Genetics 172 (2):1287-1300. doi:10.1534/genetics.105.047209

Yuan Y, Teng Q, Zhong R, Ye ZH (2013) The Arabidopsis DUF231 domain-containing protein ESK1 mediates 2-O- and 3-O-acetylation of xylosyl residues in xylan. Plant & cell physiology 54 (7):1186-1199. doi:10.1093/pcp/pct070

Zablackis E, Huang J, Muller B, Darvill AG, Albersheim P (1995) Characterization of the cell-wall polysaccharides of *Arabidopsis thaliana* leaves. Plant Physiol 107 (4):1129-1138

Zandleven J, Sorensen SO, Harholt J, Beldman G, Schols HA, Scheller HV, Voragen AJ (2007) Xylogalacturonan exists in cell walls from various tissues of *Arabidopsis thaliana*. Phytochemistry 68 (8):1219-1226. doi:10.1016/j.phytochem.2007.01.016

Zhang GF, Staehelin LA (1992) Functional Compartmentation of the Golgi-Apparatus of Plant-Cells - Immunocytochemical Analysis of High-Pressure Frozen-Substituted and Freeze-Substituted Sycamore Maple Suspension-Culture Cells. Plant Physiol 99 (3):1070-1083. doi:10.1104/Pp.99.3.1070

Zou G, Zhai G, Feng Q, Yan S, Wang A, Zhao Q, Shao J, Zhang Z, Zou J, Han B, Tao Y (2012) Identification of QTLs for eight agronomically important traits using an ultra-high-density map based on SNPs generated from high-throughput sequencing in sorghum under contrasting photoperiods. J Exp Bot 63 (15):5451-5462. doi:10.1093/jxb/ers205

9.0 Appendix 1

Primer Name	Purpose	SEQUENCE 5'-3'
Genotyping of PAE T-DNA lines		
PAE 2.1 LP	SALK_143273	CAACTTTTGCAAAGGCTTTTG
PAE 2.1 RP		TCCATTGAAAACTGTGAACCAC
PAE 2-8 LP	SALK_102761C	TTAGACGATTATACGCCGGTG
PAE 2-8 RP		TTCATTTCATTGTGTTGCCTG
PAE 3-2 LP	SALK_066524C	TCAAAGATTTGGTTCGTGACG
PAE 3-2 RP		TGTGTAAGTGCGCAGATTGTC
PAE 3.3 LP	SALK_137505C	GAAACCAAGTTCTGGGGAAAG
PAE 3.3 RP		TTGGCCTTCACTGGAATATTG
PAE 3-4 LP	GABI_294C06	CGAAAAGATCGATTTCTGTGG
PAE 3-4 RP		TAACATGCAAAAGAGGCCAAC
PAE 3.1 LP	SAIL_906_F10	TCCAGAACCAGGGTGTAGATG
PAE 3.1 RP		GCCCAGTGATTATAAAAGGCC
PAE 4-1 LP	SALK_140726	GACTCTATCCCCTCCGTTGAC
PAE 4-1 RP		AAGATCCCATTGTTGGGTTTC
PAE 4-3 LP	SAIL_450_B07	AATGACCTCACCTGTTTCGTG
PAE 4-3 RP		GTCAACGGAGGGGATAGAGTC
PAE 5.2 LP	SALK_140555	CGAAAAAGTCCACAAGCAGAG
PAE 5.2 RP		AACGGAGCCATCTAAGGTAGG
PAE 5.6 LP	SALK_052303C	ATGATATTCGGGGTCGAATTC
PAE 5.6 PR		GAACATGACGCAACTGTGTTG
PAE 6.1 LP	SALK_020618	CGCAGTCTCAGTATCTCTGGG
PAE 6.1 RP		TGATCAATGTGCAGGAAGTTG
PAE 6-4 LP	SALK_134907	ACACTATGTTACCACGCGTGC
PAE 6-4 RP		TATCTGGAAGGCATGCAAATC
PAE 7-4 LP	SALK_093502C	TTTGTTGCAAATTTCTGGACC
PAE 7-4 RP		GTATGGCACGGAAAGTGTCAC
PAE 7.8_LP	GABI_272B08	ATTACAGCAAAGTCGTCGCAC
PAE 7.8_RP		AACAAATCCAAAATGTTTGCG
PAE 7.3_LP	SAIL_154_H11	ATTACAGCAAAGTCGTCGCAC
PAE 7.3_RP		AACAAATCCAAAATGTTTGCG
PAE 7.7 LP	SALK_091346C	CATATGGTAACATGCGGACTG
PAE 7.6_RP		TCAAGGTCCGAGCATAATCTC
PAE 7.6_LP	SALK_117590C	AAAAGACATCCATCGTCCATG
PAE 7.6_RP		TCAAGGTCCGAGCATAATCTC
PAE 7.7 LP	SALK_076487	CATATGGTAACATGCGGACTG
PAE 7.6_RP		TCAAGGTCCGAGCATAATCTC
SALK_132026-LP	SALK_132026	ACCTCTCCGAAGAAACCTGAG
SALK_132026-RP		TCTGTTCATTCTTAATGCCGC
PAE 9-8 LP	SALK_046973C	AACCGGAAAATATACCGAACG
PAE 9-8 RP		AACCAGTCCATGATGGAACTG
PAE 9-9 LP	GABI_803G08	GGTTGTGGTCTCTCTTTCACG
PAE 9-9 RP		GGTTTGCTGCTACATCGATTC
PAE 9.5 LP	SALK_058590	GATCCCCTCAAGTCTTATGGC
PAE 9.5RP		AAACTCCGGTTTTGTTTTTGC
PAE 10.1 LP	SALK_043807	GACTGGTTCTTGGGAATGAGG
PAE 10.1 RP		CTAGACCACCTGCAGAGCAAC
PAE 10-7 LP	SAIL_802_C05	GTTGCTCTGCAGGTGGTCTAG
PAE 10-7 RP		TCCTATCACACGGGTATGGAC
PAE 11-4 LP	SALK_049340.48.65.x	TTATCAACAGAGGTTGGTGCC
PAE 11-4 RP		TGAGACTGAATCGGATTTTGG
PAE 11.6 LP	GABI_505H02	ACGATTGTAGAAGGGCAAAGG
PAE 11.6 RP		ACATCTCTCTTTTCCTTGGCC
PAE 12-1 LP	GABI_018A02	TGGACAGGGTTCAACTTCAAG
PAE 12-1 RP		GGCATGACTGCAGACTAAACC
PAE 12.2 LP	GABI_646F06	TTGCAACAGCATCAGAATGAG
PAE 12.2 RP		CAGGAAGACTACTCGACGTGG
Gabi LB	Left border primer for Gabi lines	ATATTGACCATCATACTCATTGC
SAIL-LB	Left border primer for Sail lines	GCCTTTTCAGAAATGGATAAATAGCCTTGCTTCC
LBb1.3	Left border primer for Salk lines	ATTTTGCCGATTTCGGAA

Genotyping: *axy4-3*; *rwa2-3* X *axy4-1*		
salk_044972-RP2	*axy4-3*	ATGCGTGTAAATGAATGATATCATAGGA
salk_044972-LP	*axy4-3*	TTATGCGATTATACGCAAGGG
axy4Dcaps-FW (EcoRV)	*axy4-1*	CGGTTATCTTTACTGGAAATGGATA
Axy4-REV (EcoRV)	*axy4-1*	CGAGATCAGGGCTAGAGACG
RWA2-3-FW	*rwa2-3*	CACCCTGAATTTCATCTCAGC
RWA2-3-REV	*rwa2-3*	TTG AAT AGG CAT CAA ACC GAG
DCAPS ECORI Markers for Genotyping of Ecotype Crosses		
ER4488648c1-FW	Er-0	GACTGGAATTAGTTAAAGCG
ER4488648c1-REV	Er-0	TTCTTCATCGTCTACCTTTC
RA15935489-FW	Ra-0	AGCTCCAAGACATGTAGAAG
RA15935489-REV	Ra-0	CAACTAATGCCAGAGGTAAT
Ta6825955c2-FW	Ta-0	CTTTGATTTGATCTCTCGTT
Ta6825955c2-REV	Ta-0	TTTGATATGCAAAGAGTTCA
TY7916310c3-FW	Ty-0	GGGGTATGTTTTCTTTGTAA
TY7916310c3-REV	Ty-0	AGAAGATGTGATGCCACTAT
Cloning, sequencing and genotyping of PAE overexpression lines		
ATTB_PAE2 FW	*PAE2* cloning	GGGGACAAGTTTGTACAAAAAAGCAGGCTATGCTCTTAAGTCACTCTCG
ATTB_PAE2 REV	*PAE2* cloning	GGGGACCACTTTGTACAAGAAAGCTGGGTTTATCTTCTAAAGACCAAAT
PAE2_C_F	*PAE2* cloning	ATGCTCTTAAGTCACTCTCGT
PAE2_C_R	*PAE2* cloning	TTATCTTCTAAAGACCAAATTGT
PAE2seq3	*PAE2* cloning/genotyping	GCGTCAAGCTAAGCAGGCTC
PAE2seq4	*PAE2* cloning	TCACTCTGGTGGAAGGAGGAAAC
ATTB_PAE3 FW	*PAE3* cloning	GGGGACAAGTTTGTACAAAAAAGCAGGCTATGAAGAGTGTGTTGCGTAT
ATTB_PAE3 REV	*PAE3* cloning	GGGGACCACTTTGTACAAGAAAGCTGGGTTCACTTGAAGATGAGATTGT
PAE 3 SEQ3	*PAE3* cloning/genotyping	CCGGCGATAGTCAGGATGAGAG
PAE4_C_F	*PAE4* cloning	ATGGTGATTCGCTCTCTGCT
PAE4_C_R	*PAE4* cloning	TCAACAAGAGGCATTGCACG
PAE4_ATTB_F	*PAE4* cloning	GGGGACAAGTTTGTACAAAAAAGCAGGCTATGGTGATTCGCTCTCTGCT
PAE4_ATTB_R	*PAE4* cloning	GGGGACCACTTTGTACAAGAAAGCTGGGTTCAACAAGAGGCATTGCACG
PAE4seq3	*PAE4* cloning/genotyping	ATGCGAAACGTGCCATGCTC
ATTB_PAE5 FW	*PAE5* cloning	GGGGACAAGTTTGTACAAAAAAGCAGGCTATGGCGATTCCAAGGTTTAG
ATTB_PAE5 REV	*PAE5* cloning	GGGGACCACTTTGTACAAGAAAGCTGGGTTCATGTGAAATTCATGTTGT
PAE5seq3	*PAE5* cloning/genotyping	CTTTCTCAACGTGCCTGATGTCC
ATTB_PAE6 FW	*PAE6* cloning	GGGGACAAGTTTGTACAAAAAAGCAGGCTATGAGGAGCTTGTTGTTGTG
ATTB_PAE6 REV	*PAE6* cloning	GGGGACCACTTTGTACAAGAAAGCTGGGTTCACTCGAAAATCAGATTGT
PAE6seq3	*PAE6* cloning/genotyping	TGTTTCTGGACTCAGTGGATGTCTC
attB1_PAE 7.4	*PAE7* cloning	GGGGACAAGTTTGTACAAAAAAGCAGGCTATGGGGAGGCTTAAGCAA
attB2_PAE 7.4	*PAE7* cloning	GGGGACCACTTTGTACAAGAAAGCTGGGTCTAGTCTTCAGTAGAGAT
Seq_PAE 7.4	*PAE7* cloning/genotyping	TGCGGTGGTTGATGATCTTATGG
ATTB_PAE9 FW	*PAE9* cloning	GGGGACAAGTTTGTACAAAAAAGCAGGCTATGAAGACGACGACTCGGCT
ATTB_PAE9 REV	*PAE9* cloning	GGGGACCACTTTGTACAAGAAAGCTGGGTTTAAATATCTAGATTTACCA
PAE9_seq3	*PAE9* cloning/genotyping	CGATGTAGCAGCAAACCGGAC
ATTB_PAE10 FW	*PAE10* cloning	GGGGACAAGTTTGTACAAAAAAGCAGGCTATGAGGAAGCTTTTCTTGTT
ATTB_PAE10 REV	*PAE10* cloning	GGGGACCACTTTGTACAAGAAAGCTGGGTTCATCTGAAGACCAGATTGT
PAE 10 SEQ3	*PAE10* cloning/genotyping	GCCGCAATGGACGATTTGAAGG
ATTB_PAE11 FW	*PAE11* cloning	GGGGACAAGTTTGTACAAAAAAGCAGGCTATGACGTGGCTAAAACAAAT
ATTB_PAE11 REV	*PAE11* cloning	GGGGACCACTTTGTACAAGAAAGCTGGGTCTACGTTCTGAAACGTACTC
PAE 11 SEQ3	*PAE11* cloning/genotyping	CATTGCGACCAGTTCAAGTCCAC
AT3G05910_GTW_fw	*PAE12* Cloning	GGGGACAAGTTTGTACAAAAAAGCAGGCTATGGTGAAGCTTTTGTTA
AT3G05910_GTW_rev	*PAE12* Cloning	GGGGACCACTTTGTACAAGAAAGCTGGGTTCATCTGAACACCAAGTT
PAE12 Seq P-3	*PAE12* cloning/genotyping	TCGTTACTGCGATGGCGCTTC

AS-208	Sequencing of overexpression constructs	GGGAGAATTCGTCGACTTTG
AS-209	Sequencing of overexpression constructs / genotyping	CGTAGCGGATAACAATTTCAC

Sequencing AXY4 in Ty-0 background	
AS-166	ATTATTGGAAGCTGGTGAGC
AS-167	GTGTAGACTAGCATTTCACTG
AS-168	AGCAAAGCCAGAAAGAATGT
AS-169	AAAACCATTGAACCACTCGTC
AS-170	GCAGTCCGTTATACAACTGG
AS-172	AACGAATGCGATATACCGAG

Sequencing of PAE8 locus in *A. thaliana*	
AtAEseq1	ACTGCTCTTTGAGTCTGCTTCTTTG
AtAEseq3	AGCTCCATAAGAGATTTGACAATAACT
AtAEseq5	GATATGAAAACCTGTCCACCAATCGT
AtAEseq7	TCTCTATGATTTTTATTATGCCAATAGT
AtAEseq9	AAAATCTACTAAAAACACTGAAAGTATCGT
AtAEseq11	TGGAAGCTTTTGACTAACTTGTTGATCA
AtAEseq13	GCACATCAAGATTAACTCCTGCAATG
AtAEseq2	TCATCAGATCGACCTTGTTCATTTG
AtAEseq4	GTCTTATGTAAATATATGGTCCCATCA
AtAEseq6	TACCCCTATTAGCATTTCTGAACTCAA
AtAEseq10	GTTTAGATGGAAGTCCACCAGCTTATCA
AtAEseq12	GGCTGTTTTGTCTGGCTGTTCTGCT
ATAEseq17rev	AGCTGGCGGAGAAGTAGTATAGTTG

Cloning of PAE9 Native promotor in PMDC107		
PAE9promg2-FW	cloning	CGGCCAGTGCCAAGCTCTAGTTAATTAAGAAGAAGAAGCCACCG
PAE9promg2-rev	cloning/sequencing	GAGTCGTCGTCTTCATTGTTACAGTTTTGGACGC
PAE9cdsg2-fw	cloning	CAAAACTGTAACAATGAAGACGACGACTCGG
PAE9promEV-rev	cloning/sequencing	ACCGGTACCGGGCCCCCCCTCGAGGCGCGCCACATTGTTACAGTTTTGGACGC
PAE9promseq1-rev	sequencing	AAATGGGCATTATCGGTTCCTCTG
PAE9promseq21-fw	sequencing	GGTGCAACCAGAAGACCATTACAAG
PAE9promseq22-rev	sequencing	TGGAGATGGGTCTTGATGGGTGG
PAE9promseq23-fw	sequencing	GCCTTATCTACGCCCTATGCTGTC
PAE9promseq24-fw	sequencing	AGGACCCGTGAGGACCAAAC
PAE9promseq25-rev	sequencing	GGACTCACCATCTATGTTTCACTGC
M13F	sequencing	TGTAAAACGACGGCCAGT
RT_PAE9-1_FW	sequencing	TCGATCTAACAGCGGCTATGG
RT_PAE9-1_REV	sequencing	CCGGTTAGAAGAGCCTTGTGG
RT_PAE9-8_FW	sequencing	GCGTTAAGTGCATGAGCGATGCTG

Cloning of PAE9 for Tobacco overexpression	
PAE9tobOExhoI FW	CTCGAGATGAAGACGACGACTCGG
PAE9tobOEBamhI REV	GGATCCTCAATGATGATGATGATGATGAATATCTAGATTTACCAA

Cloning of PAE8 in pART7		
PAE8cdsg-fw	cloning/sequencing	TTCATTTCATTTGGAGAGGACACGCTCGAGATGTTCAAGTTGAAGCAATG
PAE8cdsg1-rev	cloning	GATCCTCAATGATGATGATGATGATGAATTGGAGGAGCATCTAGAG
PAE8cdsg2-rev	cloning	ATCTCATTAAAGCAGGACTCTAGAGGATCCTCAATGATGATGATGATGATG
PAE8seq4-rev	sequencing	CAGGGTTCACTGCTTCTACATCTC
SALK_132026-RP	sequencing	TCTGTTCATTCTTAATGCCGC

Genotyping of PAE8 complementation lines	
SALK_132026-RP	TCTGTTCATTCTTAATGCCGC
M13F	TGTAAAACGACGGCCAGT

RT PCR primers for PAEs		
PAE3_RT_FW	*pae3-1, pae3-2* - RT-PCR	GCGGCGATATTCTGGCTTTGG
PAE3_RT_REV		CCCAGAGACATCCACTGCATCC
PAE4_C_F	*PAE4s* RT PCR	ATGGTGATTCGCTCTCTGCT
PAE4_C_R		TCAACAAGAGGCATTGCACG
PAE5_RT-FW	*pae5-1, pae5-2* - RT-PCR	ATGGCGATTCCAAGGTTTAGC
PAE5_RT_Rev		TCATGTGAAATTCATGTTGTAAC
PAE6_RT_FW	*pae6-1, pae6-2* - RT-PCR	ATGAGGAGCTTGTTGTTGTGG
PAE6_RT_REV		TCACTCGAAAATCAGATTGTG
RT_PAE7-4_FW	*pae7-1* - RT-PCR	ACTTATCTCCAAAGCGCCGTC
RT_PAE7-4_REV		GGCACGGAAAGTGTCACAATG
RT_PAE7-8_FW	*pae7-2* - RT-PCR	TCCACGGATCTGCAAAGAGTC
RT_PAE7-8_REV		TAGGATTACAAGTCGGCGACG
	pae8 - RT-PCR	ATTAGAACTCCTCTGTTCATTC
		CAGCACACAAGACAAGTGCTGAAG
RT_PAE9-8_FW	*pae9-1; pae9-3* - RT-PCR	GCGTTAAGTGCATGAGCGATGCTG
RT_PAE9-8_REV		ACCGCGAGAGTTATGGCCTG
RT_PAE9-1_FW	*pae9-2* - RT-PCR	TCGATCTAACAGCGGCTATGG
RT_PAE9-1_REV		CCGGTTAGAAGAGCCTTGTGG
PAE 10.1 LP	*pae10-1, pae10-2* - RT-PCR	GACTGGTTCTTGGGAATGAGG
PAE 10-7 RP		TCCTATCACACGGGTATGGAC
RT_PAE11_FW	*pae11-1, pae11-2* - RT-PCR	ACGCTATACTCTCCGGTTGTTC
RT_PAE11_REV		TTCGTCGTCGCGGATCGAAC
PAE12_RT_FW	*pae12-1, pae12-2*- RT-PCR	TCGTTACTGCGATGGCGCTTC
PAE12_RT_REV		AATGAGGCATTGGTTACTACC
PTB-FW	PTB control for RT-PCR	GCGAATGTCTTATTCAGCTCATACTGATC
PTB-REV		CATTGCTGCTGTTGGTATATCAGAGT

Q- RT PCR primers for PAEs		
	pae9-1/ox9 lines Q-RT-PCR	CTGGATTCTTTCTTGACGCAAT
		TCGAGGTTTTTTTGTATACCCTGTAGA
	pae8/comp lines Q-RT-PCR	TCTTGCTACACTCACTGCCAAA
		CAACAGCTTTTGCTATTGTCGTT
	PTB control for Q-RT-PCR	ACAACAATGATCGATCTAGGGATTATAC
		ATGTGTTTGCCATCTGAGGAT

Q-RT PCR for TBL swaps		
swap3end-FW		TGCATTGGTGTCTACCTGGTC
swap3end-REV		CGTCATCCTTGTAGTCGCTGT
swapTDNA-FW		TGAGAGCGGTTGCTGGAAGT
swapTDNA-REV		GCCGAGACTGTCCCAAGG

Cloning TBL swaps		
For TBL3/AXY4 swaps cloning, fragments:		
TBL3A1FW	A1	GGGGACAAGTTTGTACAAAAAAGCAGGCTATGAGCTTCTTGATTCCT
TBL3A1REV		TTTGGTCTCATAGACACCAAACACACGAACGA
TBL3A2FW	A2	TTTGGTCTCATCTACCGTCTCTAGCCCT
7TBL3B3newREV		GGGGACCACTTTGTACAAGAAAGCTGGGTCAACCTTCCATCGCCGCA
1TBL3B1FW	B1	GGGGACAAGTTTGTACAAAAAAGCAGGCTATGGGATTAAACGAGCAA
2TBL3B1REV		TTTGGTCTCAGAGCAAGCATAAAAGAGA
3TBL3B2FW	B2	TTTGGTCTCAGCTCGAATCAATAATACCCGAA

4TBL3B2REV		TTTGGTCTCATATCAGCTCCTTCCCAAAACTT
5TBL3B3FW	B3	TTTGGTCTCAGATACGGTCGTAGTCTCT
7TBL3B3newREV		GGGGACCACTTTGTACAAGAAAGCTGGGTCAACCTTCCATCGCCGCA
1TBL3B1FW	C1	GGGGACAAGTTTGTACAAAAAAGCAGGCTATGGGATTAAACGAGCAA
TBL3C1REV		TTTGGTCTCAAAAACGTTCTAAATCATTGCCCCA
TBL3c2FW	C2	TTTGGTCTCATTTTGATATTTTGGTTTTCAAC
TBL3c2REV		TTTGGTCTCATACACTTCGTGCCGTTTGGCTT
TBL3_C2newFW		AATGATTTAGAACGTTTTGATATTTTGGTTTTCAACAC
TBL3_C2newREV		TACGGCTTGGTCATGTTACACTTCGTGCCGTTTGGCTTTC
TBL3c3FW	C3	TTTGGTCTCATGTAACATGACCAAGCCG
TBL3_C3newFW		TGTAACATGACCAAGCCGTAC
7TBL3B3newREV	D1	GGGGACCACTTTGTACAAGAAAGCTGGGTCAACCTTCCATCGCCGCA
TBL3D1REV		TTTGGTCTCATGCGCCGAGACTGTCCCAA
TBL3D2FW	D2	TTTGGTCTCACGCATGTTTCAACGAGACGAAACCGATA
TBL3D2REV		GGGGACCACTTTGTACAAGAAAGCTGGGTCCAAATGAGCCAATAGGAT
TBL3_c_FW	re-cloning into TOPO vectors for proper LR reaction	ATGAGCTTCTTGATTCCTAATAGA
TBL3_c_REV		CAAATGAGCCAATAGGATCCGA
axy4_c_FW		ATGGGATTAAACGAGCAACA
axy4_c_REV		AACCTTCCATCGCCGCAACA

For TBL26/AXY4 swaps cloning, fragments:

1TBL26A1FW	A1	ATGGAACAACAATTAACCTTAGT
2TBL26A1REV		TTTGGTCTCATAGAGAGAATGCAGATGAGAGACT
TBL3A2FW	A2	TTTGGTCTCATCTACCGTCTCTAGCCCT
axy4_c_REV		AACCTTCCATCGCCGCAACA
axy4_c_FW	B1	ATGGGATTAAACGAGCAACA
2TBL3B1REV		TTTGGTCTCAGAGCAAGCATAAAAGAGA
3TBL26B2FW	B2	TTTGGTCTCAGCTCTCTCAGGTGGAAGAAGTGGA
4TBL26B2REV		TTTGGTCTCATATCGAATTTCGGGTATTGGACA
5TBL3B3FW	B3	TTTGGTCTCAGATACGGTCGTAGTCTCT
axy4_c_REV		AACCTTCCATCGCCGCAACA
axy4_c_FW	C1	ATGGGATTAAACGAGCAACA
TBL3C1REV		TTTGGTCTCAAAAACGTTCTAAATCATTGCCCCA
5TBL26C2FW	C2	TTTGGTCTCATTTTGACTACGTTGTTATCTCT
6TBL26C2REV		TTTGGTCTCATACAATACCCACCAGTGTTCCA
TBL3c3FW	C3	TTTGGTCTCATGTAACATGACCAAGCCG
axy4_c_REV		AACCTTCCATCGCCGCAACA
axy4_c_FW	D1	ATGGGATTAAACGAGCAACA
TBL3D1REV		TTTGGTCTCATGCGCCGAGACTGTCCCAA
7TBL26D2FW	D2	TTTGGTCTCACGCATGCAACAGAACGATGCCGT
8TBL26D2REV		ACCGGTTAAATCGTATAGTTC

For sequencing of TBL3 and TBL26/AXY4 swaps

M13F	sequencing	TGTAAAACGACGGCCAGT
M13R	sequencing	GGAAACAGCTATGACCATG
prom_cDNAseq1	sequencing	CATTGAACCACTCGTCTCGTCTCTTC
prom_cDNAseq2	sequencing	TGGAATCACCGATAAAAGCTAGATGC
prom_cDNAseq3	sequencing	CTTCGTACGGCTTGGTCATGTTACA
prom_cDNAseq4	sequencing	GTGAGGTTAGAGGTGTTGGACGTGA
prom_cDNAseq5	sequencing	TCCTGTTGCCGGTCTTGCGATGAT

10.0 Appendix 2

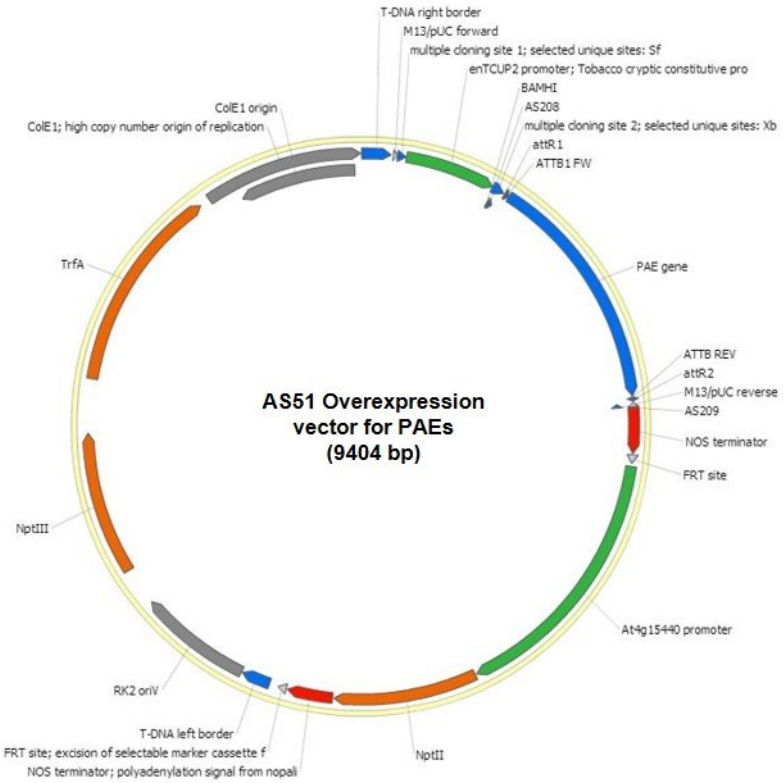

Figure 10-1 Vector used in overexpression of PAE genes. (2.2.4).

11.0 Appendix 3

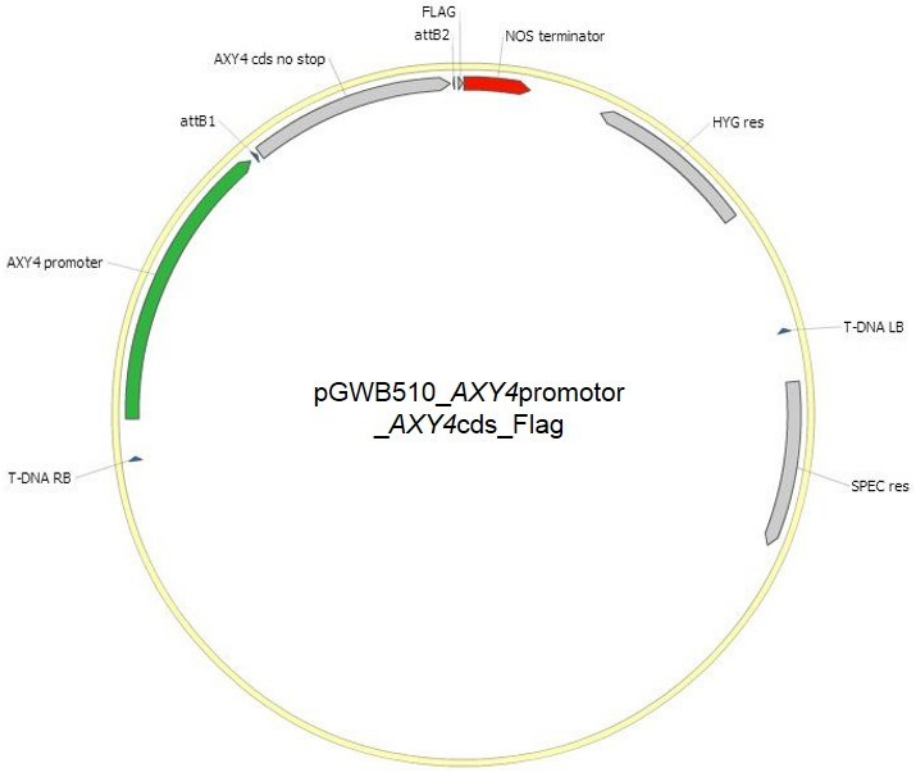

Figure 11-1 Vector used in chimeric TBL constructs. (2.2.4).

12.0 Appendix 4

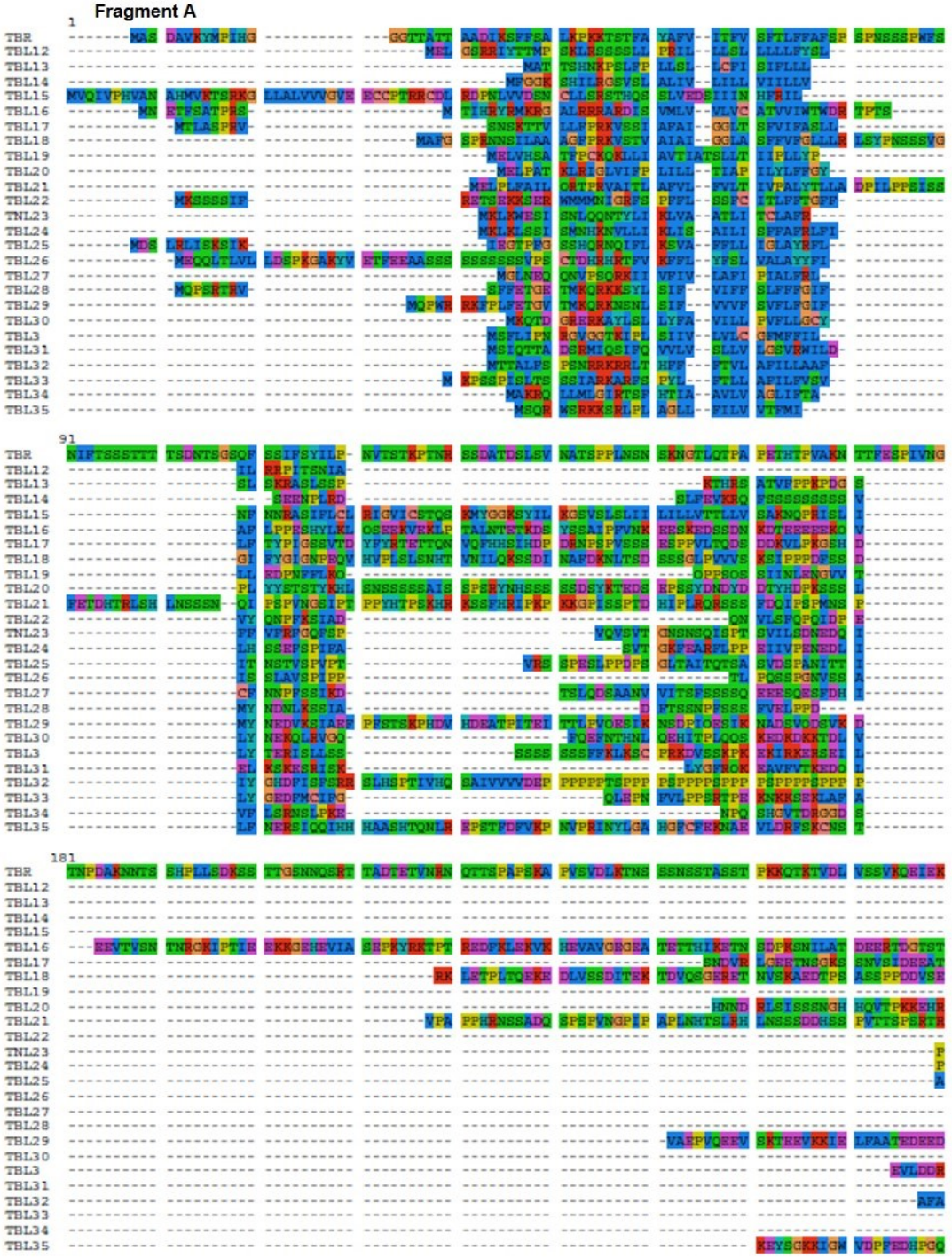

Continued…

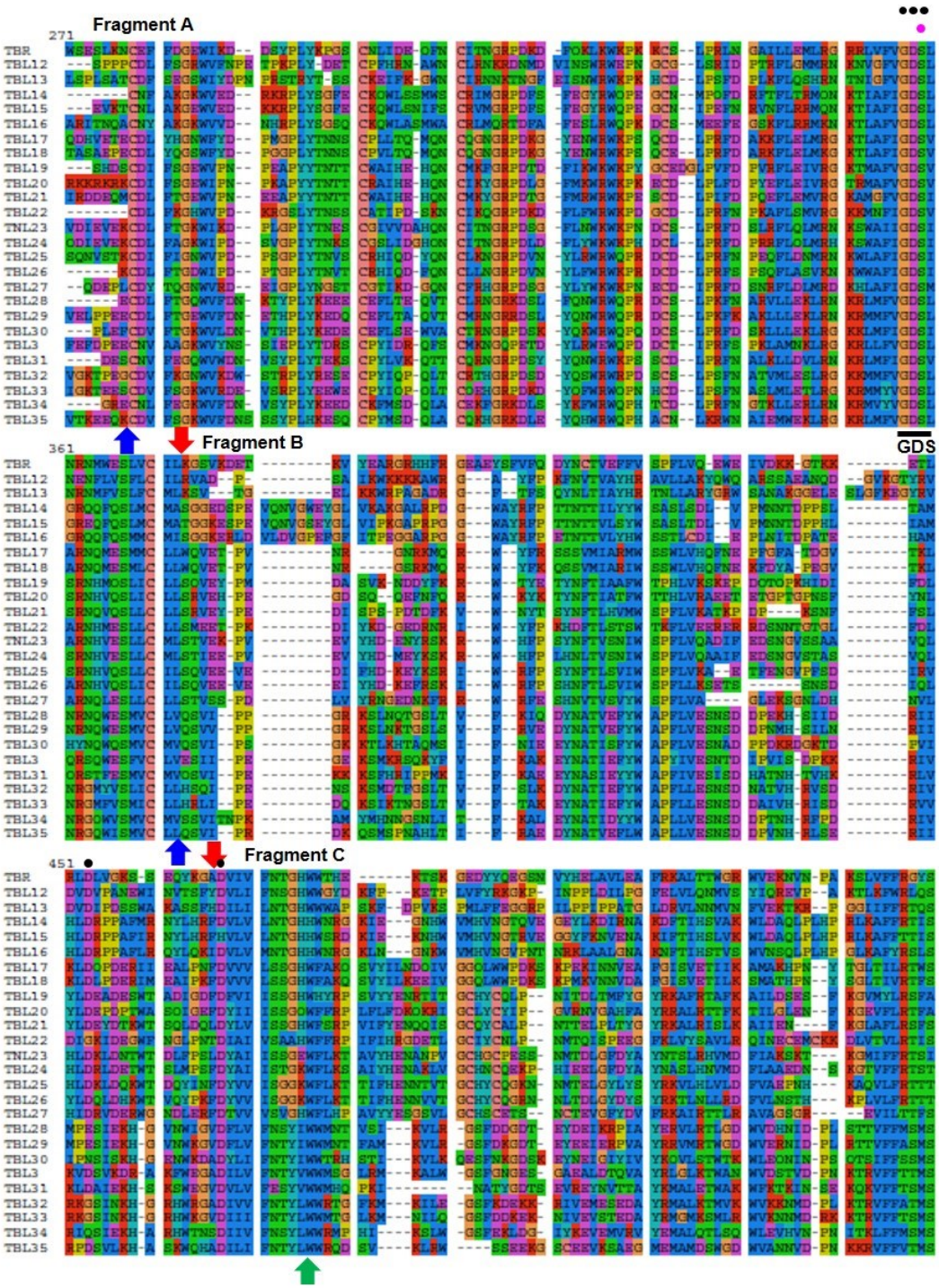

Continued…

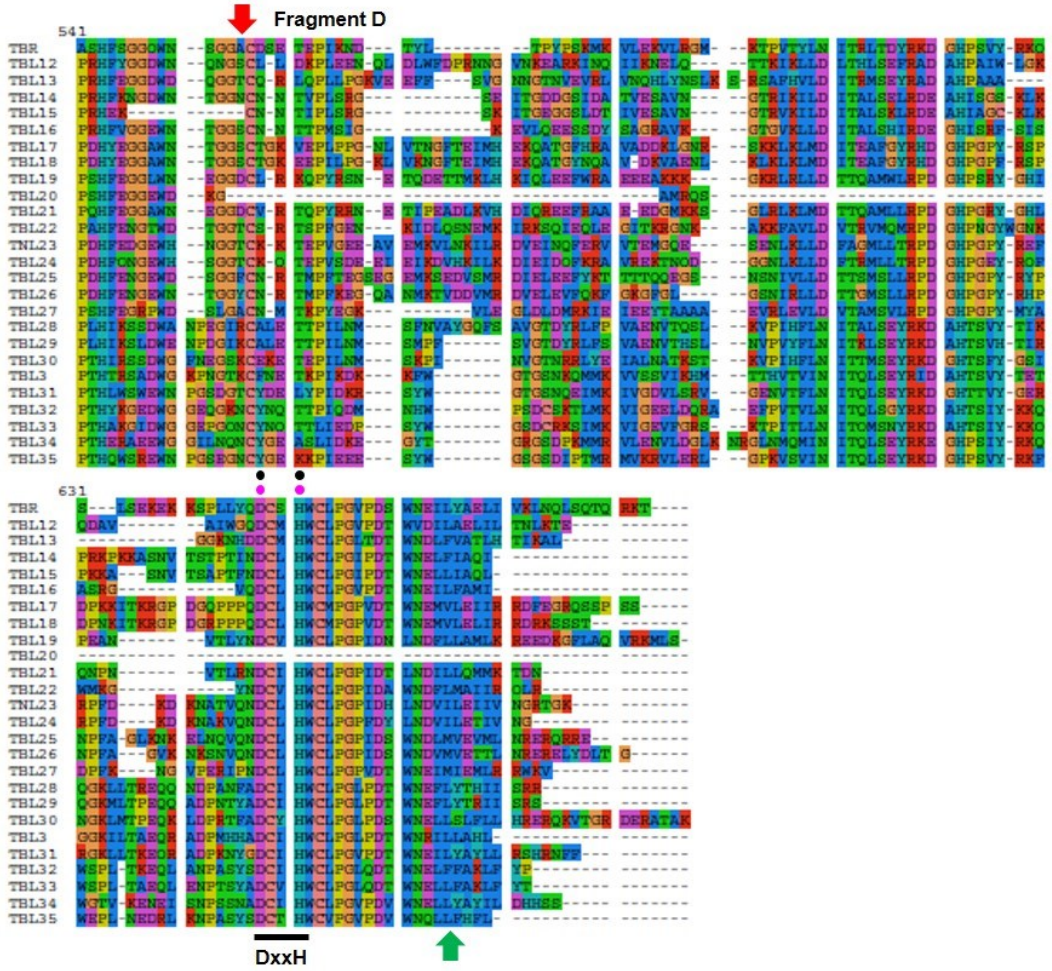

Figure 12-1. Sequence alignment of TBL family members 12-35, 3 and TBR. Alignments used for determining cut sights for domain swap experiments. Red arrows above sequence indicate cut sites for fragments A, B, C and D. Blue arrows below sequence delimit TBL domain. Green arrows below sequence delimit DUF231 domain. Black dots above sequence indicate directed mutagenesis sites. Pink dots above sequence indicate sites putatively involved in the catalytic site of TBL proteins. GDS and DxxH motifs are indicated with a black bar bellow sequences.

13.0 Appendix 5

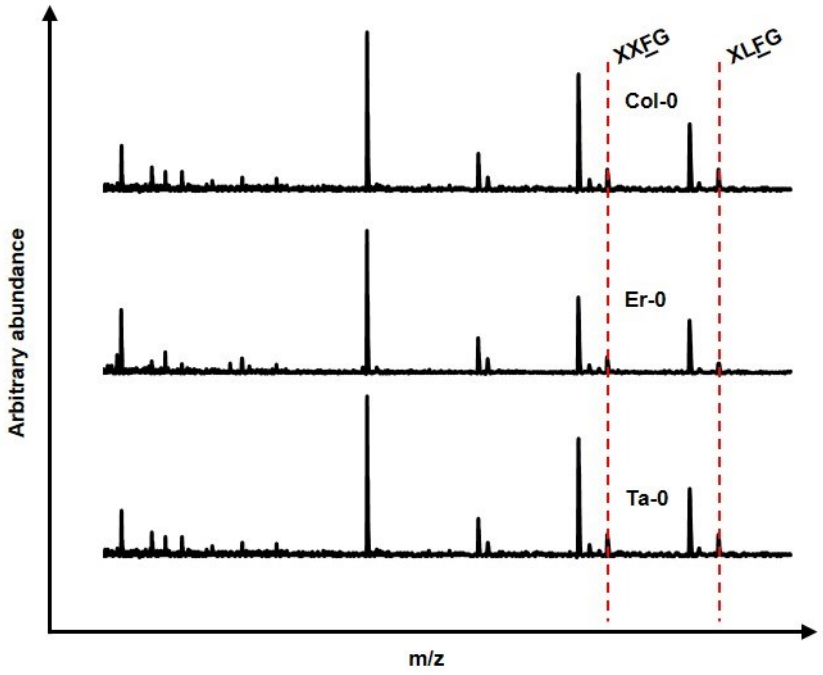

Figure 13-1 Mass spectra of XyG oligosacharides from flowers in Er-0, Ta-0 and Col-0. The figure depicts mass spectra obtained by MALDI-TOF after XEG digest (OLIMP) of *Arabidopsis* flowers (5-7 week old). Dashed red bars indicate acetylated mass peaks. Overall quantity of acetylated oligosaccharides is reduced in flowers, increasing the mapping difficulties in mapping this trait.

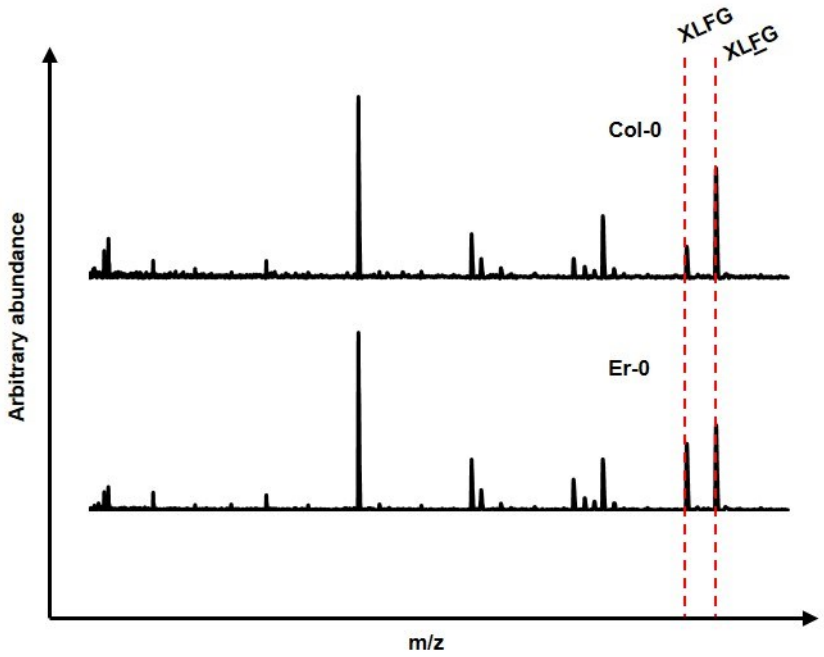

Figure 13-2Mass spectra of XyG oligosacharides from leaves in Er-0 and Col-0. The figure depicts mass spectra obtained by MALDI-TOF after XEG digest of *Arabidopsis* leaves (27 day old). A significant difference can be observed between the ratio of XLFG / XLFG between Er-0 and Col-0 (dashed bars).

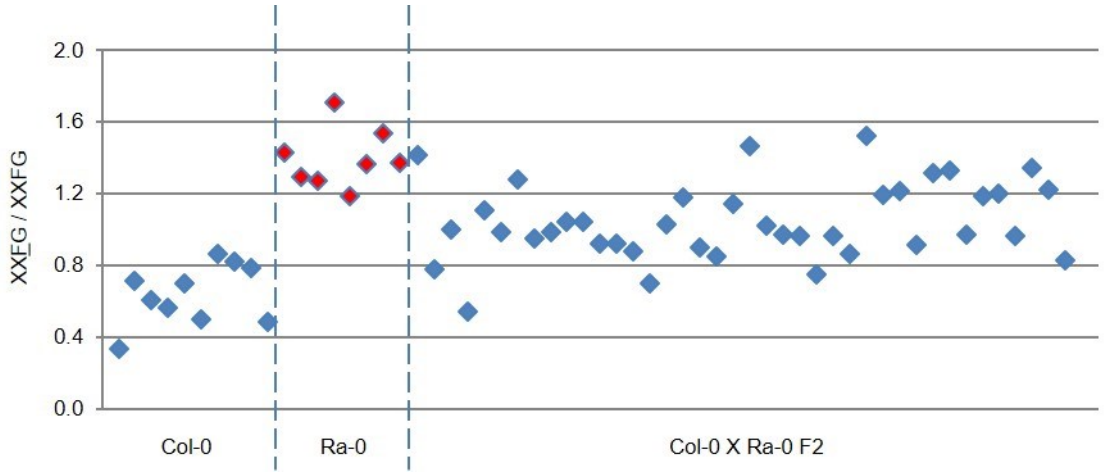

Figure 13-3 Phenotypic analysis of Col-0 X to Ra-0 F2 plants. The figure depicts the ratio between the XXFG / XXFG oligosaccharides intensity based on mass spectra obtained by MALDI-TOF after XEG digest (OLIMP) of 7 day old etiolated *Arabidopsis* seedlings. Each polygon represents an individual plant. The phenotype observed in the F2 does not reveal a clear recessive monogenic segregation.

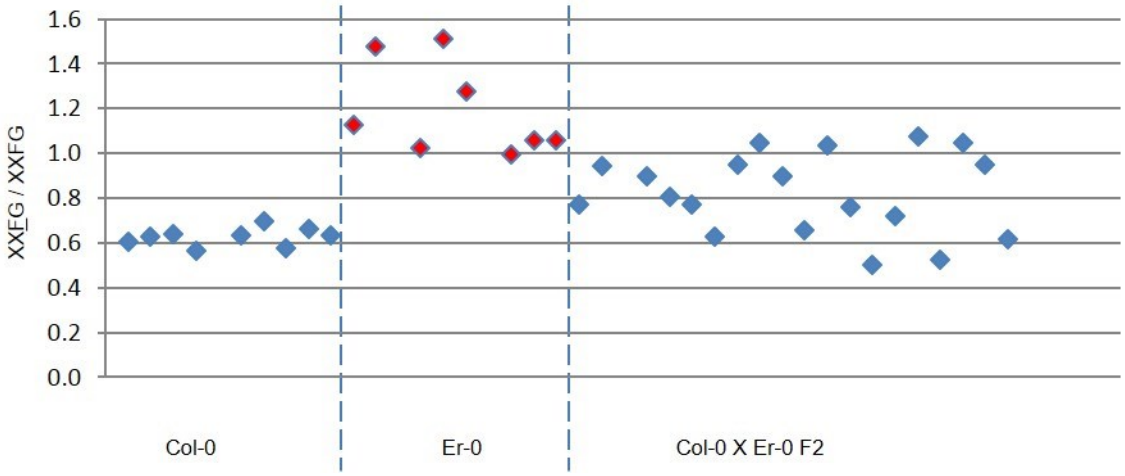

Figure 13-4 Phenotypic analysis of Col-0 X to Er-0 F2 plants. The figure depicts the ratio between the XXFG / XXFG oligosaccharides based on mass spectra obtained by MALDI-TOF after XEG digest (OLIMP) of 7 day old etiolated *Arabidopsis* seedlings. Each polygon represents an individual plant. The phenotype observed in the F2 does not reveal a clear recessive monogenic segregation.

14.0 Appendix 6

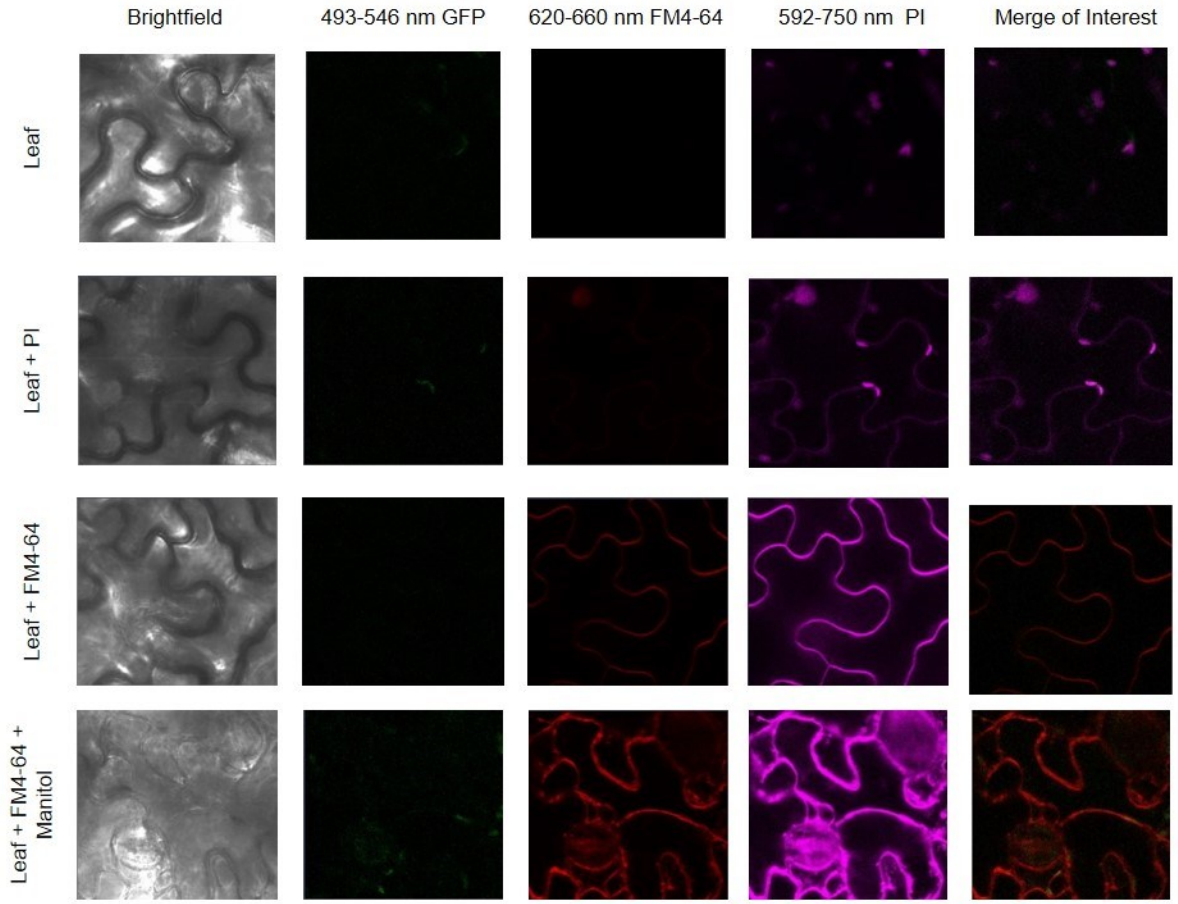

Figure 14-1 *N. benthamiana* leaf controls for 35S:PAE9:GFP subcellular localization experiments. Confocal images of WT leaf. Columns indicate channels used for visualization. Rows exhibit treatment with dies (PI, propidium iodide for cell wall staining; FM4-64 for plasma membrane staining) and plasmolizing agent (1M Mannitol). Data shows that the GFP channel is not affected by the treatments used and that its possible to stain and plasmolyze the plasma membrane with FM4-64.

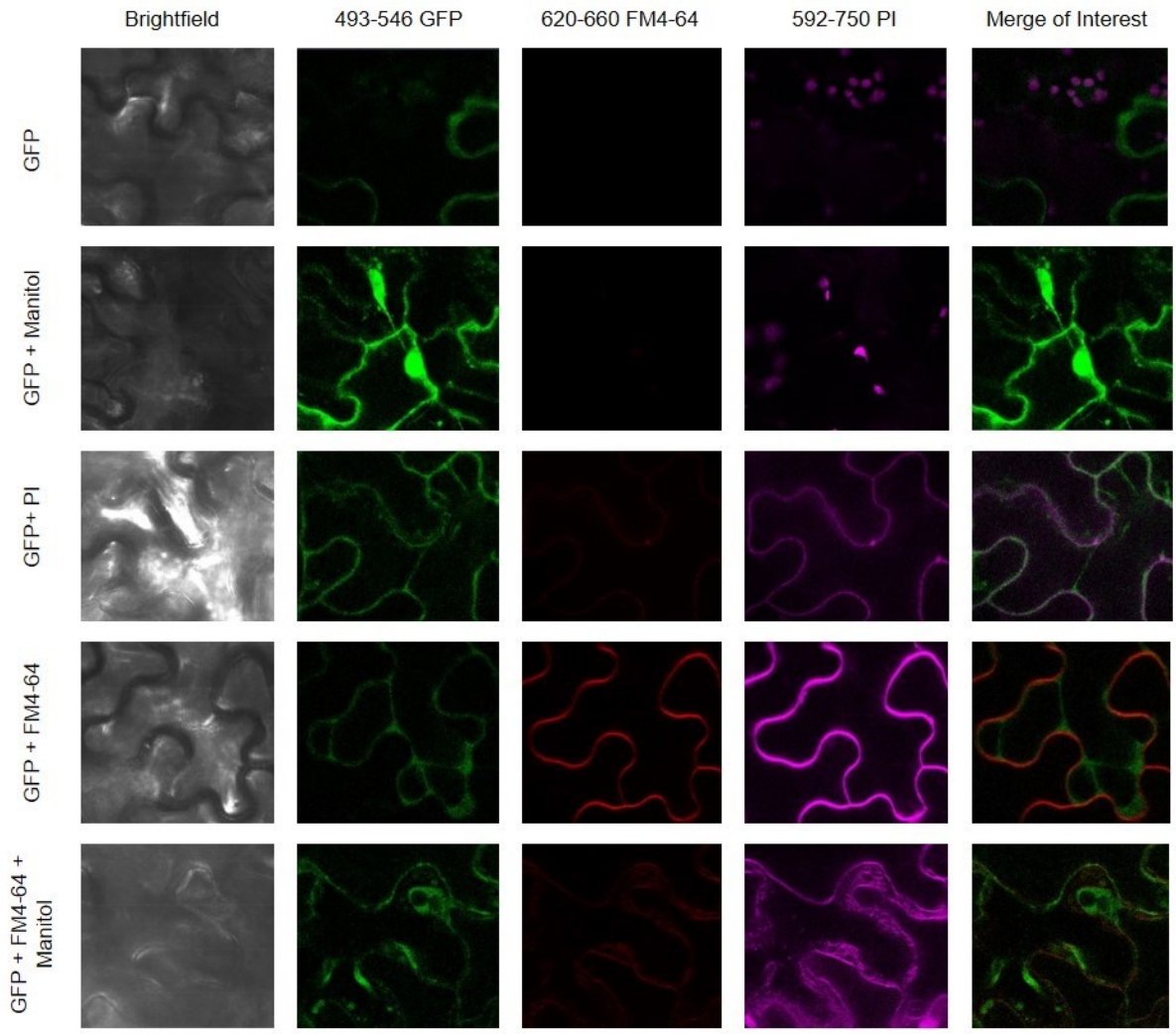

Figure 14-2 Soluble GFP (35S:GFP) controls for 35S:PAE9:GFP subcellular localization experiments. Subcellular localization of leaf transformed with 35S:GFP. Columns indicate channels used for visualization. Rows exhibit treatment with dies (PI, propidium iodide for cell wall staining; FM4-64 for plasma membrane staining) and plasmolyzing agent (1M Mannitol). Data shows that soluble GFP is expressed and localizes to the cytosol.